



Trinity College Dublin
Coláiste na Tríonóide, Baile Átha Cliath
The University of Dublin

**Investigating the Neural Correlates of Cervical Dystonia
and Temporal Discrimination using Neuroimaging
based Computational Modelling and
Multimodal Pattern Recognition**

Shruti Narasimham, B.Tech., M.Sc.

Under the supervision of Professor Richard B. Reilly

A dissertation submitted to the

University of Dublin, Trinity College

In fulfilment of the requirements for the degree of

Doctor of Philosophy

February 2020



Department of Electronic and Electrical Engineering,
University of Dublin, Trinity College

Declaration

I, Shruti Narasimham, confirm that this thesis has not been submitted as an exercise for a degree at this or any other university and is entirely my own work.

I agree to deposit this thesis in the University's open access institutional repository or allow the Library to do so on my behalf, subject to Irish Copyright Legislation and Trinity College Library conditions of use and acknowledgement.

I do not consent to the examiner retaining a copy of the thesis beyond the examining period, should they so wish (EU GDPR May 2018).

Signed,

Shruti Narasimham

September 24, 2019

Summary

Movement disorders, such as Parkinson's disease and Dystonia, have traditionally been considered as disorders of impaired motor control resulting predominantly from dysfunction of the Basal Ganglia. However, there has been increased recognition lately of associated behavioural, psychiatric, autonomic, and other non-motor symptoms. The sensory aspects include fundamental sensory abnormalities and the effects of external sensory input on the underlying motor abnormality. The Basal Ganglia, Cerebellum, Thalamus, and their connections, coupled with altered sensory input, seem to play a role in abnormal sensorimotor integration. However, the physiological basis of sensory abnormalities, the role of the Basal Ganglia, Cerebellum, and related structures on sensory processing, and their effects on movement disorders is poorly understood.

Dystonia is the third most common movement disorder characterized by sustained muscle contractions and sometimes painful postures. Although an exact prevalence remains a challenge, Primary Dystonia has been estimated with a prevalence of 16.43 per 100,000. In Ireland, it affects 592 individuals, of which 410 are Cervical Dystonia patients. Cervical Dystonia involves muscles of the head, neck and shoulders, with no precise cause attributed to date. A dysfunction in the midbrain network for covert attention has been recently implicated in Cervical Dystonia with the Superior Colliculus as a significant node in this process. Concurrently, the paucity of genetic discovery has stimulated the search for endophenotypes, of which the temporal discrimination threshold has been proposed as a potential mediational endophenotype. However, the neural substrates of abnormal temporal discrimination are poorly understood.

The primary aim of this research was to localize specific regions in the subcortical midbrain network that play a crucial role in the pathomechanisms of Cervical Dystonia, via novel neuroimaging based computational methods. Furthermore, since first-degree relatives harbour sensory abnormalities similar to patients, the objective was to probe the neural substrates of abnormal temporal discrimination in a cohort of unaffected relatives of dystonia patients.

The main findings of this thesis are as follows:

- Subjects with an abnormal temporal discrimination threshold (patients and unaffected relatives) have a significantly reduced superior collicular activation to looming visual stimuli. As TDT Z-score worsens, superior collicular activation diminishes, indicating the crucial role of this node in the shared pathomechanisms of both Cervical Dystonia and abnormal temporal discrimination.
- The intrinsic connectivity within the Superior Colliculus as well as between the Substantia Nigra and the Superior Colliculus is significantly altered under the influence of the loom visual stimulus, in subjects with an abnormal temporal discrimination threshold (patients and unaffected relatives). The bottom-up attentional network is dysfunctional, providing evidence for involvement of the midbrain network for covert attention.
- Local, regional as well as global resting-state connectivity properties are altered in relatives with abnormal temporal discrimination when compared to relatives with normal temporal discrimination threshold. The existence of differences along with similarities in large-scale network architecture and topology, suggests that these discrepancies may be indicative of a subclinical pre-symptomatic phase due to the expression of an abnormal gene or a protective neuroplastic response to that gene.
- Multivoxel pattern analysis and multimodal combination of abnormalities in adult-onset idiopathic focal dystonia, facilitate a more sensitive, robust and comprehensive approach towards analyzing this network disorder. An increase in classification performance using a multivariate approach in comparison to the previously employed univariate and unimodal analysis cautiously suggests the need for the existence of both structural as well as functional abnormalities for disorder manifestation.

In conclusion, key insights about Cervical Dystonia pathomechanisms have been uncovered by designing, developing and deploying novel neuroimaging based experimental paradigms, computational models and multimodal pattern analysis. The incorporation of a cohort of unaffected relatives of Cervical Dystonia patients in the investigation has resulted in a more comprehensive assessment of the mediational endophenotype concept in this disorder. Additionally, there is potential in an improved

automated diagnosis of dystonia patients via multivoxel and multimodal neuroimaging analysis.

Acknowledgements

I would like to take this opportunity to give a special mention to people without whom this thesis, and these four years would not have been possible.

I would like to thank Professor Richard Reilly for his patient supervision and motivation, professional guidance, and priceless advice on research and beyond. His positive attitude has helped raise my confidence and belief on more occasions than I can count. I have learnt and grown both professionally as well as personally under his mentorship, for which I will always be immensely grateful.

I also owe a big thanks to Professor Michael Hutchinson for his clinical insight, expertise and profound knowledge without which my research would have been incomplete. His dedication and relentless spirit, coupled with an energizing and warm humour on an early Tuesday morning meeting, has enthused me throughout my research.

Sean O’Riordan for his invaluable feedback and inputs on my research and manuscripts. Eavan, my clinical partner-in-crime, for her dedication and domain knowledge. Her methodical and meticulous qualities, enabled vigorous recruitment of participants during the research, and inspire me.

Students whom I had the pleasure of working with: Owen, Alexander and Oisin, for the brain-storming sessions, enthusiasm and hard work while comparing countless methodologies and approaches.

I feel lucky to have undertaken my research in such a conducive environment; a friendly, cheerful and supportive lab and Dystonia team. Thank you to all members, past and present, of the Reilly Lab (Isabelle, John, Celine, Rebecca, Terence, Alejandro, Brendan, Saskia, Tudor, Clodagh, Ciara, Surbhi, Vikram, Helena, Laura, Isadora, Manuel, Oisin, Jack, Sarah, Marta, Luca and Eugene), the Lalor Lab (Giovanni, Denis, Emily, Adam, Nate, Michael and Joyce), and the Dystonia team. Kristina Simonyan and team, for welcoming me into their lab in Boston, and sharing their data and expertise.

I am deeply indebted to the patients, their families and Dystonia Ireland who were so generous with their time, patience and support in making this research possible. The Irish Research Council who funded this research.

All my friends in Ireland and around the world, whose company has helped in maintaining a healthy body and happy mind via travel, food, recreational activities and engaging conversations.

Last but certainly not the least, I am grateful to my family (grandparents, mother, sisters, aunts and uncles) for their unconditional love and for the qualities they have instilled in me. Their continued support towards my education, in the face of all odds, has kept me focussed and dedicated, always striving for excellence. My sister, my guiding light who is always there for me. And, a big thank you to Gaurav, who has been a pillar of strength and support, always facilitating my ambitions and aspirations.

Shruti Narasimham

September 24, 2019

Publications Arising from this Thesis

Peer Reviewed Journal Articles

- **Narasimham S.**, McGovern E. M., Quinlivan B., Killian O., Beck R., O’Riordan S., Hutchinson M. and Reilly R. B. (2019). Neural Correlates of Abnormal Temporal Discrimination in Unaffected Relatives of Cervical Dystonia Patients. *Frontiers in Integrative Neuroscience*, 13, 8. doi: 10.3389/fnint.2019.00008.
- **Narasimham S.**, Meulemans A., Beck R., O’Riordan S., Hutchinson M., Reilly R. B. (2019). Investigating Ensemble Learning and Multidimensional Pattern Analysis for Multimodal Neuroimaging Insights into Cervical Dystonia. *Journal of Neuroscience Methods*, Under Review - JNEUMETH-D-19-00467.
- McGovern E. M., Killian O., **Narasimham S.**, Quinlivan B., Butler J. B., Beck R., Beiser I., Williams L. W., Killeen R. P., Farrell M., O’Riordan S., Reilly, R. B., Hutchinson M. (2017). Disrupted superior collicular activity may reveal cervical dystonia disease pathomechanisms. *Scientific Reports*, 7(1), 16753. doi: 10.1038/s41598-017-17074-x.
- Beck R., Kneafsey S. L., **Narasimham S.**, O’Riordan S., Isa T., Hutchinson M. and Reilly R. B. (2018). Reduced Frequency of Ipsilateral Express Saccades in Cervical Dystonia: Probing the Nigro-Tectal Pathway. *Tremor and Other Hyperkinetic Movements*, 8. doi: 10.7916/D8864094.
- Beck R., McGovern E. M., Butler J. S., Birsanu D., Quinlivan B., Beiser I., **Narasimham S.**, O’Riordan S., Hutchinson M. and Reilly, R. B. (2018). Measurement and Analysis of the Temporal Discrimination Threshold Applied to Cervical Dystonia. *Journal of Visualized Experiments*, (131), e56310. doi: 10.3791/56310.
- Hutchinson M., McGovern E. M., **Narasimham S.**, Beck R., Reilly R. B., Cathal B Walsh, Kevin Malone, Marina A. J. T., O’Riordan S. (2018). The pre-motor syndrome of cervical dystonia: disordered processing of salient environmental stimuli. *Movement Disorders*, 33(2), 232. doi: 10.1002/mds.27229.

- Killian O., McGovern E. M., Beck R., Beiser I., **Narasimham S.**, Quinlivan B., O’Riordan S., Simonyan K., Hutchinson M., and Reilly R. B. (2017). Practice does not make perfect: Temporal discrimination in musicians with and without dystonia. *Movement Disorders*, 32(12), 1791. doi: 10.1002/mds.27185.
- Conte A., McGovern E. M., **Narasimham S.**, Beck R., Killian O., O’Riordan S., Reilly R. B., Hutchinson M. (2017). Temporal discrimination: mechanisms and relevance to adult onset dystonia. *Frontiers in Neurology*, 8, 625. doi: 10.3389/fneur.2017.00625.
- McGovern E. M., O’Connor E., Beiser I., Williams L., Butler J. S., Quinlivan B, **Narasimham S.**, Beck R., Reilly R.B, O’Riordan S., Hutchinson M. (2017). Menstrual cycle and the temporal discrimination threshold. *Physiological Measurements*, 38(2), N65. doi: 10.1088/1361-6579/38/2/N65.
- McGovern E. M., Butler J. S., Beiser I., Quinlivan B., **Narasimham S.**, Beck R., Reilly R. B., O’Riordan S. and Hutchinson M. (2017). A comparison of stimulus presentation methods in temporal discrimination testing. *Physiological Measurements*, 38(2), N57. doi: 10.1088/1361-6579/38/2/N57.

Peer Reviewed Conference Papers

- **Narasimham S.**, Vikram Sundarajan, McGovern E. M., Quinlivan B., Killian O., O’Riordan S., Hutchinson M., Reilly R. B. 2019 Characterizing Brain Network Topology in Cervical Dystonia Patients and Unaffected Relatives using Graph Theory. *41st Annual International Conference of the IEEE Engineering in Medicine and Biology Society*, Berlin, Germany.
- Duggan O., **Narasimham S.**, McGovern E. M., Killian O., O’Riordan S., Hutchinson M., R. B. Reilly, 2019. A Study of the Midbrain Network for Covert Attentional Orienting in Cervical Dystonia Patients using Dynamic Causal Modelling. *41st Annual International Conference of the IEEE Engineering in Medicine and Biology Society*, Berlin, Germany.

Conference Poster Presentations

- **Narasimham S.**, McGovern E. M., O. Killian, Beck R., Farrell M., O’Riordan S., Hutchinson M. and Reilly R. B. Optimization of Region of Interest Analysis of the Superior Colliculus for Improved Activation Detection in Cervical Dystonia. *Proceedings of the 21st International Congress of Parkinson’s disease and Movement Disorders. Movement Disorders Society Congress*, Hong Kong, 2018.
- **Narasimham S.**, A. Meulemans, Beck R., O’Riordan S., Hutchinson M. and Reilly R. B. Integration of Multi-Modal Data via Ensemble Learning for Improved Pattern Classification in Cervical Dystonia Patients and Unaffected Relatives. *Proceedings of the 18th International Workshop on Pattern Recognition in Neuroimaging*, National University of Singapore (NUS), Singapore, June 2018.
- **Narasimham S.**, Meulemans A., Beck R., O’Riordan S., Hutchinson M. and Reilly R. B. Investigating Ensemble Learning for Multi-Modal Data Fusion and Classification with Application to Cervical Dystonia. *Proceedings of The Organization of Human Brain Mapping 2018 Annual Meeting*, Singapore, June 2018.
- **Narasimham S.**, Vikram Sundarajan, McGovern E. M., Quinlivan B., Beck R., O’Riordan S., Hutchinson M. and Reilly R. B. Altered Resting State Connectivity in Unaffected Relatives of Cervical Dystonia Patients – A Graph Theory and Dual Regression Study. *Proceedings of the 21st International Congress of Parkinson’s disease and Movement Disorders. Movement Disorders Society Congress*, Vancouver, Canada, 2017.
- Sundararajan V., **Narasimham S.**, McGovern E. M., Quinlivan B., Beck R., O’Riordan S., Hutchinson M. and Reilly R. B. Graph Theoretical Analysis of Resting-State fMRI Data from Cervical Dystonia Patients and Unaffected Relatives. *Brain Research in Ireland*. Dublin, Ireland, 2017.
- **Narasimham S.**, McGovern E. M., Quinlivan B., Beck R., O’Riordan S., Hutchinson M. and Reilly R. B. Rs-fMRI in cervical dystonia – Associations between functional networks and temporal discrimination thresholds. *45th Annual Meeting of the Society for Neuroscience*, San Diego, California, 2016.

- McGovern E. M., **Narasimham S.**, Killian O., Quinlivan B., Beiser I., Williams L., Beck R., Butler J. S., Killeen R., Farrell M., O’Riordan S., Reilly R. B. and Hutchinson M. Responses to looming stimuli: a functional magnetic resonance imaging study in cervical dystonia relatives with normal and abnormal temporal discrimination. *Proceedings of the 20th International Congress of Parkinson’s disease and Movement Disorders*, Berlin, Germany, 2016.
- Killian O., **Narasimham S.**, McGovern E. M., Quinlivan B., Butler J. S., Hutchinson M. and Reilly R. B. Optimization of Region of Interest Analysis for Activation Detection in Functional Magnetic Resonance Imaging of the Superior Colliculus. *Proceedings of the 22nd Bioengineering in Ireland Conference*, Galway, Ireland, 2016.
- Beiser I., Quinlivan B., McGovern E. M., **Narasimham S.**, Williams L., Killian O., Beck R., O’Riordan S., Butler J. S., Reilly R. B. and Hutchinson M. Investigation of head tremor in cervical dystonia: Novel application of virtual reality head mounted display, the oculus rift. *Proceedings of the 20th International Congress of Parkinson’s disease and Movement Disorders*, Berlin, Germany, 2016.
- **Narasimham S.**, Butler J. S., Quinlivan B., McGovern E. M., Hutchinson M. and Reilly R. B. Understanding Dystonia: Behavioural and fMRI Studies with Looming Stimuli on Controls and Patients. *Proceedings of the 21st Annual Bioengineering in Ireland Conference*, Galway, Ireland, 2015.
- McGovern E. M., Butler J. S., **Narasimham S.**, Williams L.J., Beiser I., Reilly R. B., O’Riordan S. and Hutchinson M. A functional magnetic imaging study of the response in the superior colliculus to looming stimuli in cervical dystonia patients and their relatives. *Proceedings of the 19th International Congress of Parkinson’s disease and Movement Disorders*, San Diego, California, 2015.

Contents

Declaration	i
Summary	iii
Acknowledgements	vii
Publications Arising from this Thesis	ix
Table of Contents	xiii
List of Figures	xix
List of Tables	xxiii
Glossary of Abbreviations	xxv
1 Introduction	1
1.1 Dystonia Overview	1
1.1.1 General	1
1.1.2 Genetics	5
1.1.3 Adult-Onset Isolated Focal Dystonia (AOIFD)	6
1.1.4 Cervical Dystonia (CD)	8
1.1.5 Endophenotypes and Temporal Discrimination	9
1.1.6 The Superior Colliculus and its role in AOIFD	11
1.2 Chapter Conclusion	12
2 Literature Review	15
2.1 Background	15
2.2 Methodology	16
2.3 Imaging in AOIFD with a focus on CD	17
2.3.1 Metabolic Imaging	17
2.3.2 Structural Imaging	21

2.3.3	Functional MRI in AOIFD and CD	28
2.3.4	Multimodal and Multivoxel Pattern Analysis	29
2.4	Sensory Motor Abnormalities in Dystonia	31
2.4.1	The Role of Unaffected Relatives	33
2.5	Head Movement and Oculomotor Control in CD	34
2.6	Imaging of the Midbrain and SC	38
2.7	Neural correlates of AOIFD and CD	45
2.7.1	Major Regions Implicated	45
2.7.2	The Network Concept	47
2.8	Chapter Conclusion	48
3	Research Questions	51
3.1	Examining the Role of the Superior Colliculus and the Covert Attention Network	51
3.2	Investigating the Neural Correlates of TDT in Unaffected Relatives of CD Patients	53
3.3	Exploring the contribution (and combination) of structure and function in the manifestation and automated diagnosis of CD	55
3.4	Conclusion	57
4	General Methodology	59
4.1	Ethical Approval from Research Ethics Review Board	59
4.2	Subject Recruitment	59
4.3	Temporal Discrimination Threshold (TDT) Testing	60
4.3.1	Sensory Testing	60
4.3.2	TDT Analysis	61
4.3.3	Subject Stratification	62
4.4	MRI Acquisition	63
4.4.1	Structural MRI	63
4.4.2	Functional MRI	64
4.4.3	Resting-fMRI	64
4.4.4	Pre-processing	65
4.5	Chapter Conclusion	68

5	Heading for the Hills: A Study of the Response of the Superior Colliculus to a Looming Event in Patients, Unaffected Relatives and Controls	69
5.1	Introduction	70
5.2	Methods	72
5.2.1	Ethics, Participants and Data Acquisition	72
5.2.2	Task - Visual Paradigm	72
5.2.3	Pre-processing	74
5.2.4	Whole-brain Analysis	74
5.2.5	Optimization of ROI Analysis of the SC for Improved Activation Detection in CD	75
5.2.6	Region of Interest Analysis	78
5.3	Results	79
5.3.1	TDT Testing	79
5.3.2	Whole-brain Analysis	79
5.3.3	Optimization of ROI Analysis for the SC	81
5.3.4	ROI Analysis	82
5.4	Discussion	85
5.5	Chapter Conclusion	88
6	Atop the Hill, as Far as ‘Eye’ Can See: Examining the Midbrain Network for Covert Attentional Orienting in Cervical Dystonia using Dynamic Causal Modelling	89
6.1	Introduction	90
6.1.1	Dynamic Causal Modelling	91
6.2	Methods	93
6.2.1	Participants, Data Acquisition and Pre-processing	93
6.2.2	Dynamic Causal Modelling (DCM)	93
6.2.3	Study 1 – Striatum, Thalamus, SC Circuit in Patients vs. Controls	97
6.2.4	Study 2 – Striatum, Thalamus, SC, Substantia Nigra Circuit in Patients, Relatives and Controls	100
6.3	Results	102
6.3.1	GLM analysis	102
6.3.2	Study 1 analysis	102

6.3.3	Study 2 analysis	104
6.4	Discussion	107
6.5	Chapter Conclusion	111
7	It's a Small World: Probing Resting State Connectivity and Brain Network Topology in Unaffected Relatives of Cervical Dystonia Patients	113
7.1	Introduction	114
7.1.1	ICA, ReHo and ALFF	116
7.1.2	Graph Theory	116
7.2	Methods	117
7.2.1	Ethics, Participants and Pre-processing	117
7.2.2	Data Analysis	117
7.3	Results	120
7.3.1	Study A - ICA, ReHo and ALFF	120
7.3.2	Study B - Graph Theory Analysis	126
7.4	Discussion	128
7.4.1	Study A - ICA, ReHo and ALFF	128
7.4.2	Study B - Graph Theory	133
7.5	Chapter Conclusion	134
8	A Bird's Eye View: Investigating Mutlimodal Multivoxel Pattern Analysis and Ensemble Learning in Dystonia	137
8.1	Introduction	138
8.2	Methods	141
8.2.1	Participants, Ethics, Data Acquisition and Pre-processing	141
8.2.2	Feature Extraction	142
8.2.3	Masks	143
8.2.4	Feature Extraction and Selection	143
8.2.5	Classifiers and Ensemble Classification	146
8.3	Results	147
8.3.1	Feature Extraction and Selection	147
8.4	Discussion	153
8.5	Validation Study	156
8.5.1	Methods	156

8.5.2	Results	160
8.5.3	Discussion	163
8.6	Conclusion	163
9	Discussion	165
9.1	Main Findings	165
9.1.1	Midbrain structures and the network for covert attentional orienting may be implicated in Cervical Dystonia and abnormal temporal discrimination (addressing Research Questions 1, 2 and 6)	165
9.1.2	Functional activation of the SC may be reliably captured in CD patients, their unaffected relatives and controls via the loom-recede visual paradigm (addressing Research Questions 3, 4 and 5)	166
9.1.3	ROI analysis of the SC and other midbrain structures requires optimization for improved activation detection in Cervical Dystonia patients (addressing Research Question 4)	167
9.1.4	Dynamic causal modelling may be used to probe effective connectivity in the covert attention network with the loom-recede visual stimulus driving SC activity (Research Questions 6 and 7)	168
9.1.5	Unaffected relatives (of CD patients) with an abnormal TDT harbour resting-state abnormalities consistent with CD pathophysiology (Research Questions 8-10 and 12)	168
9.1.6	Resting-state fMRI may be used to uncover local, regional and network-related connectivity patterns in unaffected relatives (addressing Research Questions 11 and 12)	169
9.1.7	Abnormalities detected across rs-fMRI, s-MRI and t-fMRI may be combined to improve automatic classification of CD Patients and healthy controls (addressing Research Questions 13-15)	170
9.1.8	PCA and ensemble learning are powerful tools for multivoxel pattern analysis and multimodal data integration in AOIFD (addressing Research Questions 16-19)	171

9.2	Limitations and Challenges	172
9.2.1	Common Challenges	172
9.2.2	Study 1 – Looming Responses in the SC	173
9.2.3	Study 2 – Dynamic Causal Modelling in the Covert Attention Network	174
9.2.4	Study 3 – Neural Correlates of Abnormal Temporal Discrimination	175
9.2.5	Study 4 – Multimodal MVPA in Cervical Dystonia and AOIFD	176
9.3	Future Research Directions	177
9.3.1	Magnetic Resonance Imaging of GABA in Patients and Unaffected Relatives	177
9.3.2	Dynamic Causal Modelling in Cervical Dystonia and AOIFD .	179
9.3.3	Longitudinal Neuroimaging Studies with Unaffected Relatives and other Movement Disorder Cohorts	180
9.3.4	Tractography of the Cerebello-Thalamo-Cortical (CbTC) and SC-Fastigial Nucleus Pathways in Unaffected Relatives	181
9.3.5	Multi-centre Data Integration along with Genetic Data via MVPA	183
9.4	Conclusion	185
	References	186
	A Appendix - Ethics	211
	B Appendix - Graph Theory Metrics	213

List of Figures

1.1	Different types of dystonia	2
1.2	Forms of adult-onset idiopathic focal dystonia	7
1.3	Neck postures in cervical dystonia	8
1.4	The mediational endophenotype concept in AOIFD	10
1.5	The location of the Superior Colliculus in the brain	11
2.1	A proposed model of the dysfunction in dystonia	18
2.2	Motor circuit abnormalities associated with DYT1 genotype	21
2.3	DTI tractography differences in CD patients vs. controls	24
2.4	Global network topology differences in task-specific and non-task specific focal dystonias	29
2.5	Multivoxel pattern analysis in fMRI	31
2.6	VBM abnormalities in unaffected relatives of AOIFD patients	33
2.7	The role of the SC in oculomotor and cephalomotor control	37
2.8	Direct, indirect and hyperdirect pathways of the Basal Ganglia	46
4.1	TDT setup for temporal discrimination testing in patients, relatives and controls	61
4.2	TDT z-scores of all patients, relatives and controls used in all the studies	63
4.3	MRI scanner employed for data acquisition	64
4.4	Pre-processing pipeline followed for all studies	65
5.1	Saccades: Connections among the SC, brainstem, Cerebellum and Basal Ganglia	70
5.2	Loom-Recede-Random visual paradigm employed in the study of the SC	73
5.3	ROI boundary delineating for the Superior Colliculus	76
5.4	Region of Interest Definition on Structural MRI of an Exemplary Subject	77
5.5	Whole-brain GLM analysis of SC activation with task fMRI data	80
5.6	Whole-brain 2 nd level GLM analysis of SC activation with task fMRI data	81
5.7	Different ROI processing pipelines compared for SC activation detection	82

5.8	Event-related time courses and percentage signal change plots of SC activity	84
5.9	Correlation analysis of SC activation with TDT Z-scores	85
6.1	Linear and Non-linear DCMs	92
6.2	Workflow of DCM implementation undertaken with the task-fMRI data	94
6.3	Saliency detection network as proposed by Redgrave et al. (2010) . . .	94
6.4	Circuit of the DCM study undertaken in patients and controls	98
6.5	Model design of the DCM study undertaken in patients and controls . .	99
6.6	Circuit of the DCM study undertaken in patients, unaffected relatives and controls	100
6.7	Model design of the DCM study undertaken in patients, unaffected relatives and controls	101
6.8	GLM whole-brain results	102
6.9	BMS results of the models tested in Study 1	103
6.10	PEB results of the models tested in Study 1	104
6.11	BMS results of the models tested in Study 2 in patients and controls . .	105
6.12	BMS results of the models tested in Study 2 in relatives	106
6.13	PEB results of the connectivity differences in Study 2	107
6.14	PEB results of the connectivity differences between patients and controls	108
6.15	PEB results of the connectivity differences in CD patients, relatives and controls	109
7.1	ICA and Dual Regression analysis	118
7.2	Graph Theory analysis	120
7.3	Exploratory and hypothesis based ICA analysis in unaffected relatives .	122
7.4	ReHo abnormalities in unaffected relatives	122
7.5	ALFF abnormalities in unaffected relatives	124
7.6	Topographic circular plots of brain functional architecture in relatives with normal and abnormal TDT	127
7.7	Clustering coefficient and local efficiency plots of unaffected relatives .	127
7.8	Global efficiency plot	128
7.9	Characteristic path length plots of patients, unaffected relatives and controls	128

7.10	Summary of resting-state abnormalities observed in relatives in comparison to previous CD rs-fMRI studies	130
7.11	Topographic circular plots of brain functional architecture in patients, relatives and controls	133
8.1	Univariate vs. multivariate analysis	139
8.2	Ensemble learning	141
8.3	Early feature integration, late feature integration, decision integration ensemble learning	146
8.4	Classifier performance metrics	147
8.5	Feature extraction and selection	148
8.6	ROC curves of the unimodal analysis with the VPSC mask	149
8.7	ROC curves of the unimodal analysis with the a-priori Combination mask	150
8.8	ROC curves of the unimodal analysis with the Wholebrain mask	151
8.9	ROC curves of the multimodal MVPA analysis	153
8.10	Early feature integration, late feature integration, decision integration ensemble learning in AOIFD	159
8.11	Cross-Validation and Test Accuracy Approach	159
8.12	Feature extraction and selection	160
8.13	ROC curves of the unimodal and multimodal MVPA ensemble with the a-priori Combination mask	161
8.14	ROC curves of the unimodal and multimodal MVPA ensemble with the Wholebrain mask	162
9.1	A pilot MRS-GABA study with the Putamen	178
9.2	DTI study of the CbTC tract in manifesting and non-manifesting dystonia gene carriers	182

List of Tables

1.1	Evolution of dystonia classification	3
2.1	VBM studies undertaken in CD to date	26
2.2	DTI studies undertaken in CD to date	27
2.3	Literature Review of fMRI Region of Interest Analysis Studies undertaken with the SC	41
7.1	Coordinates of brain regions where ReHo abnormalities were detected .	123
7.2	Coordinates of brain regions where ALFF abnormalities were detected .	125
8.1	Unimodal classification results with the Vermis, Putamen, SC mask . .	149
8.2	Unimodal classification results with the Combination mask	150
8.3	Unimodal classification results with the Wholebrain mask	151
8.4	Multimodal classification results with the Vermis, Putamen, SC mask .	152
8.5	Multimodal classification results with the Combination mask	152
8.6	Multimodal classification results with the Wholebrain mask	153
8.7	Demographics of the AOIFD Cohort in the Multimodal MVPA Validation Study	157
8.8	Unimodal and multimodal MVPA results with the AOIFD cohort . . .	161

Glossary of Abbreviations

3D	3-Dimensional
ALFF	Amplitude of Low Frequency Fluctuations
ANO3	Anoctamin 3
ANOVA	Analysis of Variance
AOIFD	Adult-Onset Idiopathic Focal Dystonia
AOPTD	Adult-Onset Primary Torsion Dystonia
AR	Relatives with Abnormal TDT
AUC	Area-under-the-Curve
BA	Broadmann Area
BMS	Bayesian Model Selection
BOLD	Blood Oxygen Level Dependent
BoNT	Botulinum Toxin
BSP	Blephrospasm
CAO	Covert Attentional Orienting
CbTC	Cebrello-Thalamo-Cortical
CD	Cervical Dystonia
CSF	Cerebro-Spinal-Fluid
DBS	Deep Brain Stimulation
DCM	Dynamic Causal Modelling
DTI	Diffusion Tensor Imaging
DYT1/6	Dystonia genes
ECG	ElectroCardioGraphy
EEG	ElectroEncephaloGraphy
EMBC	Engineering in Medicine and Biology Conference
ERD	Event Related Design
ESDE	Epidemiological Study of Dystonia in Europe
FA	Fractional Anisotropy
FDG	2-fluoro-2-deoxy-glucose

FEF	Frontal Eye Fields
FFX	Fixed Effects
FHD	Focal Hand Dystonia
fMRI	Functional MRI
FN	False Negative
FN	Fastigial Nucleus
FP	False Positive
FWE	Family Wise Error
FWHM	Full Width Half Maximum
GABA	Gama-Amino-Butyric-Acid
GAG	Group-specific Antigen
GAT	Graph Analysis Toolbox
GE	General Electric
GLM	General Linear Modelling
GNAL	G-Protein Subunit Alpha
GP	Global Pallidus
GPi/e	Global Pallidus externa/interna
GPC	Gaussian Process Classifier
HC	Healthy Controls
HRF	Hemodynamic Response Function
ICA	Independent Component Analysis
INC	Interstitial Nucleus of Cajal
ISIs	Inter-Stimulus-Intervals
KCC	Kendall Coefficient of Concordance
LEDs	Light Emitting Diodes
LOOCV	Leave-One-Out-Cross-Validation
MAN	Manifesting
MEG	MagnetoEncephaloGraphy
MD	Mean Diffusivity
MNI	Montreal Neurological Institute
MR	Magnetic Resonance
MRI	Magnetic Resonance Imaging
MRS	Magnetic Resonance Spectroscopy

ms/s	Milliseconds / seconds
MSNs	Medium Spiny Neurons
MVPA	Multi-Voxel Pattern Analysis
NL	Normal (Controls)
NM	Non-manifesting
NR	Relatives with Normal TDT
OMD	Oromandibular Dystonia
PAT	Patients
PCA	Principal Component Analysis
PEB	Parametric Empirical Bayes
PET	Positron Emission Tomography
PPU	Photo-Plethysmographer Unit
PSC	Percentage Signal Change
rCBF	Regional Cerebral Blood Flow
ReHo	Regional Homogeneity
RETROICOR	Retrospective Correction
RF	Random Forest
RFE	Recursive Feature Elimination
RFX	Random Effects
ROC	Receiver Operating Characteristic
ROI	Region of Interest
Rs-fMRI	Resting-state functional MRI
RSNs	Resting State Networks
SC	Superior Colliculus
SD	Spasmodic Dysphonia
SD	Standard Deviation
SDT	Somatosensory Discrimination Threshold
SLSC	Superficial Layers of the SC
DLSC	Deep Layers of the SC
SMA	Sensorimotor Area
s-MRI	Structural MRI
SN	Substantia Nigra
SNpr	Substantia Nigra Pars Reticula

SNpc	Substantia Nigra Pars Compacta
SNR	Signal-to-Noise Ratio
SPECT	Spectral Positron Emission Computed Tomography
SPM	Statistical Parametric Mapping
SPSS	Statistical Processing Software System
STN	Subthalamic Nucleus
SVM	Support Vector Machine
T	Tesla
TDT	Temporal Discrimination Threshold
TE	Echo Time
TFCE	Threshold Free Cluster Enhancement
t-fMRI	Task MRI
THAP1	Thanatos-Associated domain-containing apoptosis-associated Protein
TN	True Negative
TOR1A	Torsin-1A: Dystonia 1 protein
TP	True Positive
TPM	Tissue Probability Maps
TR	Repetition Time
TTC	Time-to-Collision
TWSTRS	Toronto Western Spasmodic Torticollis Rating Scale
VBM	Voxel Based Morphometry
VOI	Volume of Interest
VPSC	Vermis-Putamen-Superior-Colliculus
WC	Writer's Cramp
WFU	Wake Forest University

1 Introduction

1.1 Dystonia Overview

1.1.1 General

The neurological disorder dystonia arose from the term "dystonia musculorum deformans", which was first reported by Hermann Oppenheim, a prominent neurologist in Germany, in 1911. He used this term to describe a condition he observed in four children (unrelated but all of Jewish decent) who came to consult him from Galicia and Russia (Klein and Fahn, 2013). The common characteristics observed were: (1) muscle spasms affecting limbs and trunk resulting in warped postures; (2) deteriorating upon walking, sometimes with a noticeably flexed spine; (3) rapid and also rhythmic movements; (4) the symptoms which progressed eventually led to continued postural deformities; (5) muscle tone switched from hypotonic at one occasion to tonic at another; (6) the absence of weakness, significant psychological abnormalities, impaired perception, sensory loss, atrophy, or alteration of electrical excitability. Other physicians across the world observed similar patterns in patients, and there was soon increasing number of cases documented by Davison (Davison and Goodhart, 1938), Zeman (Zeman and Dyken, 1967), Elridge (Eldridge and Gottlieb, 1976), Korzcyn (Korzyn et al., 1980) and Risch (Risch et al., 1995).

From then to now, great progress has been made to comprehend the symptoms and heterogeneity of this disorder. While the different forms of dystonia (Figure 1.1) were often categorized earlier as cramps, task-specific or occupational spasms in the 19th century. It was in June 1975 at the 1st International Dystonia Symposium that the clinical features of focal forms of dystonia, such as blepharospasm, spasmodic dysphonia, and writer's cramp were re-evaluated. One of the leading neuroscientist at the time, David Marsden reassessed the then poorly understood field of movement disorders. Marsden proposed (Waddy et al., 1991) pooling together the different focal forms that were previously considered independent entities of dystonia. In 1984, the Dystonia Medical Research Foundation affirmed the first unanimous

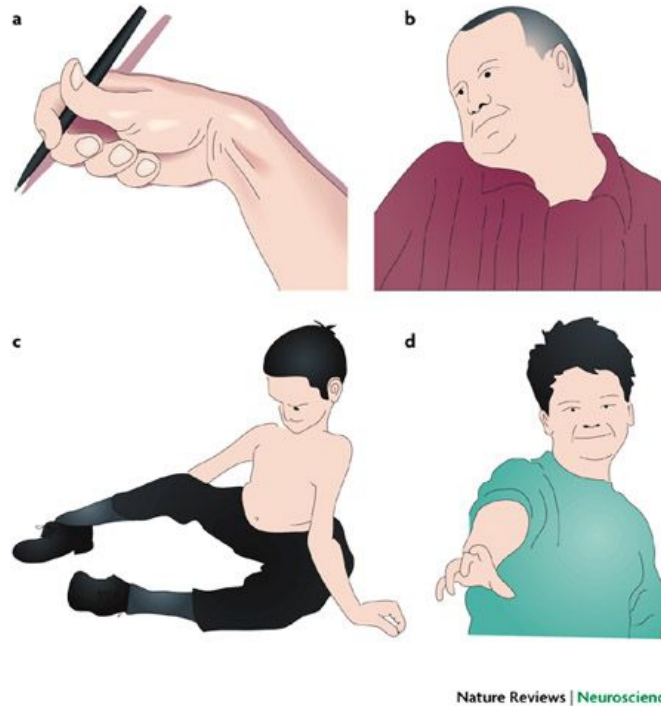


Figure 1.1: Different forms of dystonia: a) Writer's Cramp b) Cervical c) Generalized d) Limb dystonia. Adapted from (Breakefield et al., 2008).

definition of dystonia as a syndrome consisting “of sustained muscle contractions, frequently causing twisting and repetitive movements, or abnormal postures” (Balint and Bhatia, 2014; Fahn, 1984). The classification of dystonia evolved with new knowledge and understanding of its different forms. As shown in Table 1.1, this evolution ranged from Fahn and Eldridge’s first distinction between primary dystonia (with or without a hereditary pattern) and secondary dystonia (with other hereditary neurological conditions or due to known environmental cause) in 1998 (Fahn and Eldridge, 1976), to Fahn and Hallet’s grouping in 2011 (Fahn, 2011), to Albanese’s 2013 categorization based on (1) clinical utility for diagnosis and treatment and; (2) existing knowledge concerning biological mechanisms in order to guide future scientific research (Albanese et al., 2013). The revised definition provided in 2013 was: “Dystonia is a movement disorder characterized by sustained or intermittent muscle contractions causing abnormal, often repetitive, movements, postures, or both. Dystonic movements are typically patterned, twisting, and may be tremulous. Dystonia is often initiated or worsened by voluntary action and associated with overflow muscle activation.”

Table 1.1: The evolution of the classification of dystonia from Fahn (1998) to the 2013 consensus. Adapted from (Albanese et al., 2013).

	Fahn (1998)	Fahn (2011)	EFNS (2011)	Consensus (2013)
Age at Onset	Childhood	Young-onset (years)	(<26 Early-onset (years)	Infancy (<2 years)
	Adolescence	Adult-onset (years)	(>26 Late-onset	Childhood (3-12 years)
	Adulthood			Adolescence (13-20 years)
				Early adulthood (21-40 years)
			Late adulthood (>40 years)	
Distribution	Focal	Focal	Focal	Focal
	Segmental	Segmental	Segmental	Segmental
	Multifocal	Multifocal	Multifocal	Multifocal
	Generalized Hemidystonia	Generalized Hemidystonia	Generalized Hemidystonia	Generalized Hemidystonia
Temporal Pattern	N.A.	N.A.	N.A.	Disease occurrence (Static, Progressive, Variability, Persistent, Action-specific, Diurnal, Paroxysmal)
Associated Features	N.A.	N.A.	N.A.	Isolated or combined
				Occurrence of other neurological or systemic manifestation
Aetiology	Primary (Focal, Sporadic)	Primary	Primary (Pure, Paroxysmal, Plus)	Axis I (Age, Body distribution, Temporal pattern, Associated features)
	Dystonia-plus	Dystonia-plus		Axis II (Nervous system pathology, Inherited or acquired, Idiopathic)
	Secondary	Secondary	Secondary	
	Heredo-degenerative	Heredo-degenerative	Heredo-degenerative	
		Feature of another neurologic disease		

Based on this definition, the current classification of dystonia rests on two main axes:

1) Axis 1: Clinical Characteristics

(a) Age at Onset

- Infancy (birth to 2 years)
- Childhood (3–12 years)
- Adolescence (13–20 years)
- Early adulthood (21–40 years)
- Late adulthood (>40 years)

(b) Body Distribution

- Focal - Only one body region is affected. For example: blephrospasm, oro-mandibular dystonia, cervical dystonia, laryngeal dystonia, writer's cramp.
- Segmental - Two or more contiguous body regions are affected. For example: cranial dystonia (blephrospasm with lower facial and jaw or tongue involvement) or bi-brachial dystonia.
- Multifocal – Involvement of two non-contiguous or more (contiguous or not) body regions.
- Generalized – Trunk and at least two other sites are involved.
- Hemi dystonia – Involvement of more body regions restricted to one body side.

(c) Temporal Pattern

- Persistent – Persists to roughly the same degree all day.
- Action-specific – Occurs only during a particular activity or task.
- Diurnal fluctuations - Fluctuates during the day, with recognizable circadian variations in occurrence, severity and phenomenology.
- Paroxysmal – Sudden self-limited episodes of dystonia usually induced by a trigger with return to pre-existing neurological state.

(d) Associated Features

- Isolated dystonia – Dystonia is the only motor feature, with the exception of tremor.
- Combined dystonia – Dystonia combined with other movement disorders, such as myoclonus, parkinsonism, etc.

2) Axis 2: Aetiology

- (a) Nervous system pathology – Dystonia due to degeneration, lesions or neurodevelopmental anomalies
- (b) Inherited or acquired – Dystonia due to a known specific cause
- (c) Idiopathic – Dystonia due to an unknown cause

1.1.2 Genetics

The first dystonia causative gene, TOR1A¹, was discovered owing to the recurrence of a dominantly inherited mutation (a GAG¹ deletion) in an Ashkenazi Jewish population (Kramer et al., 1990). In this population, this mutation is found in 80% of patients with early-onset isolated dystonia, and TOR1A-related dystonia has an estimated prevalence of between 1 in 3,000 individuals and 1 in 9,000 individuals (Risch et al., 1995). Subsequent studies have identified over 100 distinct mutations in THAP1¹ in patients with familial and sporadic, mostly early-onset isolated dystonia. The detection of the first two gene mutations causing primary generalized dystonia (DYT1/TOR1A and DYT6/THAP1) has facilitated studies on pathogenesis and pathophysiology of primary dystonias (Ozelius et al., 1997). The advent of next-generation sequencing techniques enabled the identification of several candidate genes for autosomal dominant isolated dystonia. Mutations in some genes, such as GNAL24,25¹ and ANO3¹ were identified in several independent patients, and their causative roles have been conclusively established (Klein, 2014). Penetrance has also been shown to vary among the distinct genetic forms. For example, it is high (up to 90%) in GNAL¹ associated dystonia and up to 20–30% in individuals with TOR1A GAG deletions (Bressman et al., 1989; Kramer et al., 1994). Studies investigating the genetic cause of isolated dystonia have been hindered due to the paucity of families with multiple members manifesting dystonia as well as the extensive phenotypic variability of this disorder in terms of age and site at

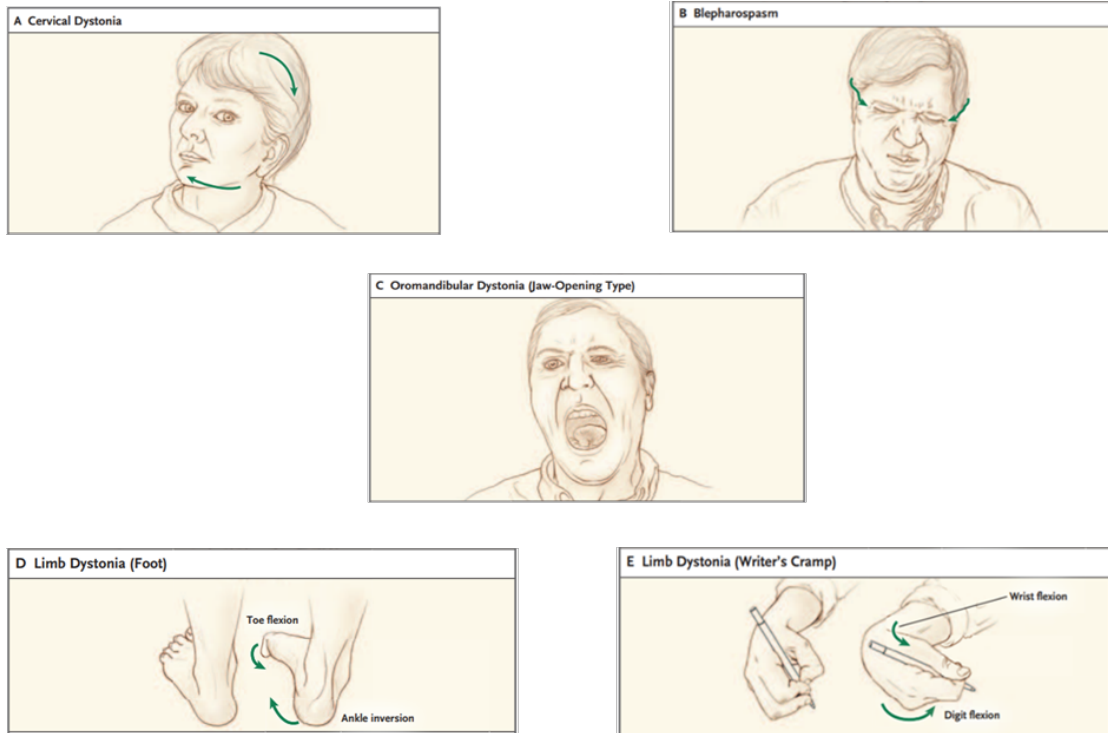
onset (Balint and Bhatia, 2014; Klein, 2014; Zeman and Dyken, 1967).

1.1.3 Adult-Onset Isolated Focal Dystonia (AOIFD)

As described above, primary or idiopathic (both terms used interchangeably in literature) dystonia represents dystonia with no accompanying neurological signs other than tremor. Adult onset isolated focal dystonia (AOIFD) is the most common form of primary dystonia (Bressman, 2004). While it is predominantly sporadic in nature, up to 25% of AOIFD patients have a family member affected (Leube et al., 1997; Stojanovic et al., 1995). Therefore, it is considered autosomal dominant in inheritance with considerably low penetrance of 12-15% (Waddy et al., 1991). This, coupled with the existence of the sporadic as well as familial forms in AOIFD, suggests that its aetiology results from a combination of environmental and heritable factors (Williams et al., 2017; Balint and Bhatia, 2014). The low penetrance entails challenges in effective genotyping of this disorder due to relatively few multiplex AOIFD families.

AOIFD has variable clinical expression (Figure 1.2) including cervical dystonia (CD), focal hand dystonia (FHD), blepharospasm (BSP), spasmodic dysphonia (SD), oromandibular dystonia (OMD) and writer's cramp (WC). Prevalence estimates of AOIFD range from 20 to 137 cases per million (Nutt et al., 1988; Steeves et al., 2012; Fukuda et al., 2006; ESDE, 2000; Pekmezovic et al., 2003). As of April 2016, Kimmich et al. documented 592 individuals with adult onset idiopathic isolated focal dystonia in Ireland, a point prevalence of 17.8 per 100 000 (Williams et al., 2017).

¹Gene names, please refer to glossary of abbreviations for full forms



Type of Dystonia	Main Clinical Features	Common Misdiagnoses
Cervical dystonia (spasmodic torticollis)	Abnormal head posture Head tremor Neck pain	Muscle strain Cervical disk disease Osteoarthritis
Blepharospasm	Increased blink rate Forced eye closure Difficulty opening eyes	Myasthenia gravis Dry eyes
Oromandibular dystonia	Jaw clenching (bruxism) Jaw in open position Lateral jaw shift	Temporomandibular joint syndrome Myasthenia gravis Dental malocclusion Edentulous movements
Orofacial dystonia	Action dystonias involving lips, tongue, or pharynx	Tic disorders
Spasmodic dysphonia		Chronic laryngitis, vocal-cord polyps, voice tremor, psychogenic causes
Adductor type	Voice breaks and strain	
Abductor type	Breathy voice	
Mixed type	Features of both	
Limb dystonia	Action dystonias affecting writing, playing musical instruments, handling tools, walking	Nerve entrapment Overuse syndromes Muscle cramps
Axial dystonia	Movements of shoulders, back, or abdomen	Myoclonus Motor tics Psychogenic causes

Figure 1.2: Different forms of adult-onset idiopathic focal dystonia along with their primary clinical features and the misdiagnosis associated with this disorder phenotype. Adapted from (Tarsy and Simon, 2006).

1.1.4 Cervical Dystonia (CD)

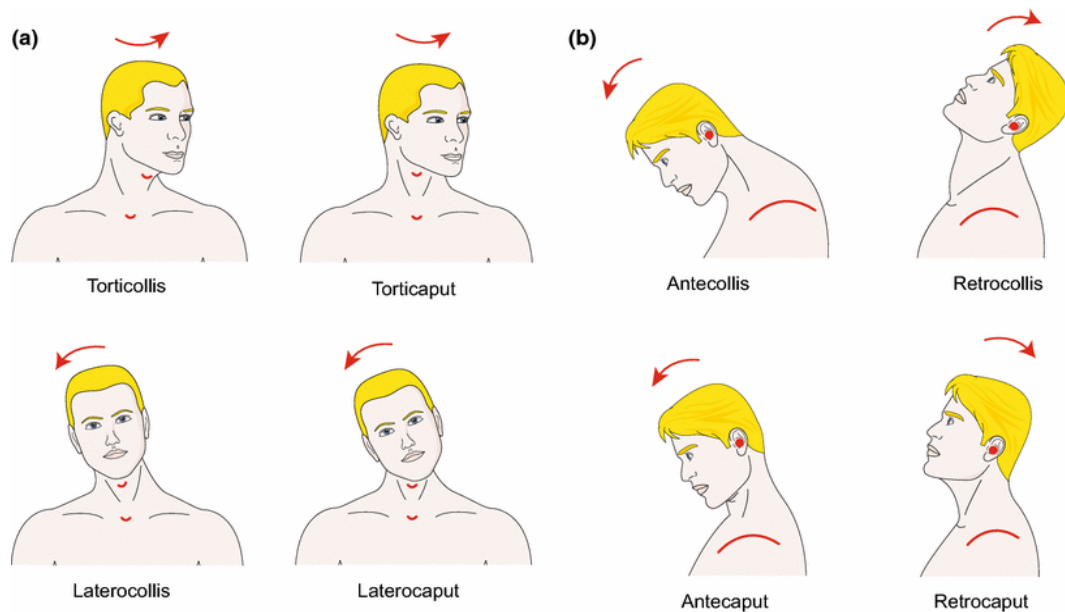


Figure 1.3: Different neck postures in Cervical Dystonia based upon the muscles affected in this disorder. Adapted from (Tatu and Jost, 2017).

Cervical dystonia is the most common form of AOIFD (Nutt et al., 1988; Crowner, 2007) and was the focus of the current research study due to its prevalence in Ireland (Williams et al., 2017). It is characterized by involuntary twisting and turning of the neck due to abnormal unintentional muscle contractions (Albanese et al., 2013). Although this condition also is commonly referred to as “torticollis” or “spasmodic torticollis”, such terms are misrepresentative of CD, as “torticollis” entails an impairment that is only rotatory, while patients with CD often have combined postures associated with flexion, extension, or side bending (Crowner, 2007). Common to all cases are the age at onset, higher incidence in women, characteristics of the dystonic posture and associated neurological abnormalities (Dauer et al., 1998). It typically presents between the ages of 30 and 50 years, initially with neck stiffness and restricted head mobility, followed by abnormal head postures, occasionally along with irregular head tremor. Neck and shoulder pain occur in 75% of the cases (Tarsy and Simon, 2006). Common misdiagnosis includes muscle strain, osteoarthritis and cervical disc disease. Dystonic malposture may affect only the cervical spine (collis: 20%) or only the head (caput: 19%) or a combination (61%) (Albanese et al., 2015). Figure 1.3 demonstrates the different forms of cervical dystonia that exists among

patients, based on the dimensions of movement and the associated muscles involved. The sternocleidomastoid, splenius capitis, splenius cervix, levator scapulae, trapezius, scalene complex are some of the main muscles of the head and neck. Understanding the anatomy and physiology of the neck and head system has garnered interest not only for treatment of symptoms, but also in order to comprehend signals in the form of relay loops in this possible head neural integrator disorder (Hutchinson et al., 2014; Shaikh et al., 2016; Tatu and Jost, 2017).

Botulinum toxin (BoNT) is the most common treatment for the symptoms of cervical dystonia; effective in reducing both abnormal movements and pain (Bhidayasiri and Tarsy, 2006; Brin et al., 1987; Jinnah and Factor, 2015; Jost and Tatu, 2015). Treatment is essentially provided every 3-6 months, depending on the patient's response. The effects of treatment take 5 to 10 days to manifest and can last anywhere from 10 weeks to 6 months. The use of deep brain stimulation (DBS) for treatment of cervical dystonia is also increasingly popular (Volkman et al., 2012; Skogseid, 2014; Moro et al., 2017). It is mostly recommended to patients who have exhausted all other treatment options due to the inherent risks involved and the requirement for relatively frequent reviews to monitor and control settings. DBS is well established as a therapy in the management of movement disorders, most commonly in Parkinson's disease (Lozano, 2001; Volkman, 2012). In general, the target for deep brain stimulation in dystonia is the bilateral Globus Pallidus (Lettieri et al., 2015; Volkman et al., 2012; Volkman, 2012).

1.1.5 Endophenotypes and Temporal Discrimination

The paucity of genetic discovery and causal knowledge on the pathomechanisms of dystonia has stimulated a search for endophenotypes in the past decade. Endophenotypes are measurable components along the pathway between disease and distal genotype, emerging as an important concept in movement disorders such as CD, with poorly penetrant genes. The endophenotype approach is an alternative route for measuring phenotypic variation to facilitate the identification of susceptibility genes for heterogeneously inherited traits. Endophenotypes thus offer simpler clues to genetic underpinnings than the disease syndrome itself (Gottesman and Gould, 2003). In psychiatry research, the accepted criteria (Beauchaine, 2009) which a biomarker must

fulfill to be called an endophenotype is:

- 1) An endophenotype must segregate with illness in the population.
- 2) An endophenotype must be heritable.
- 3) An endophenotype must not be state-dependent (i.e., manifests whether illness is active or in remission).
- 4) An endophenotype must co-segregate with illness within families.
- 5) An endophenotype must be present at a higher rate within affected families than in the population.
- 6) An endophenotype must be amenable to reliable measurement, and be specific to the illness of interest.

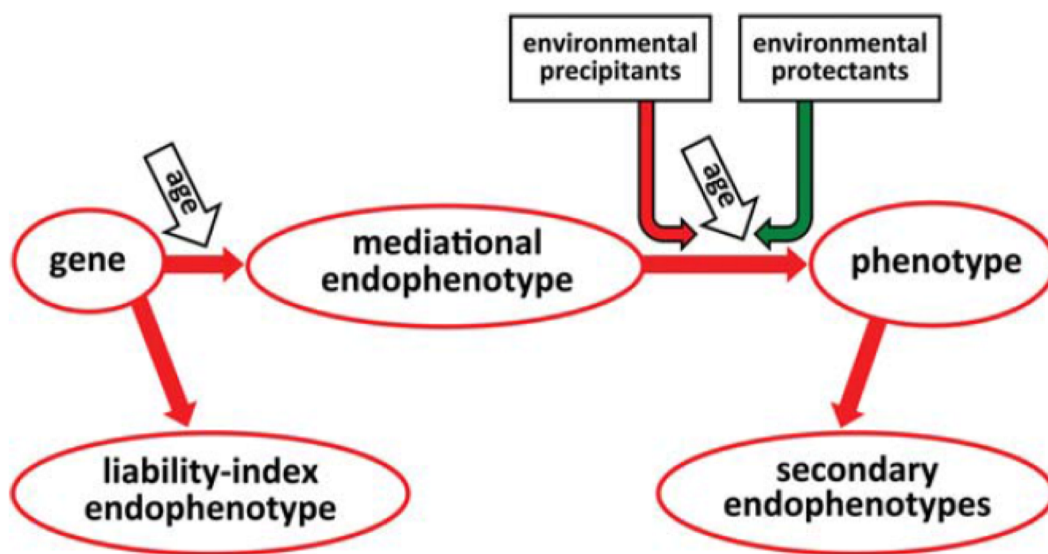


Figure 1.4: The concept of the phenotype, mediational phenotype and endophenotype in relation to gene carriage, environmental precipitants and protectors and other contributors such as age and gender. Adapted from (Hutchinson et al., 2013).

In this context, the Temporal Discrimination Threshold (TDT) has arisen as a possible mediational endophenotype candidate for adult-onset primary torsion dystonia (AOPTD) (Fiorio et al., 2006a; Bradley et al., 2009, 2012; Kimmich et al., 2014). The TDT is the shortest interval at which two stimuli can be detected as asynchronous. The mediational endophenotype model implies that the endophenotype and the disease

are both caused by a genetic disorder and that the pathway from gene to disease passes through the endophenotype; one cannot acquire the disease without first having the endophenotype (Hutchinson et al., 2013). Figure 1.4 illustrates this concept. Distinguishing between mediational and secondary endophenotypes is critical as secondary endophenotypes are not useful for tracking the genetics of the disease (Hutchinson et al., 2013).

There have been various studies exploring the visual and tactile (somatosensory) forms of the TDT in AOPTD cohorts, which will be discussed in further detail in the next chapter. The TDT is abnormal in more than 80% to 90% of patients with various AOPTD phenotypes, and sensitivity is highest (97%) in the most common phenotype, cervical dystonia. Further, an age- and gender-related penetrance has been shown to influence TDT (Butler et al., 2015). Little is known about the neural correlates underlying temporal discrimination. Various timing related mechanisms and duration interval studies have investigated possible regions involved, however, little can be said about the precise neural circuitry of this mediational endophenotype with respect to CD. Recent research has emphasized the study of an endophenotype along with its phenotype in order to draw more accurate conclusions regarding the interplay of the two and better understand the influence and relationship between the two (Battistella et al., 2015).

1.1.6 The Superior Colliculus and its role in AOPTD

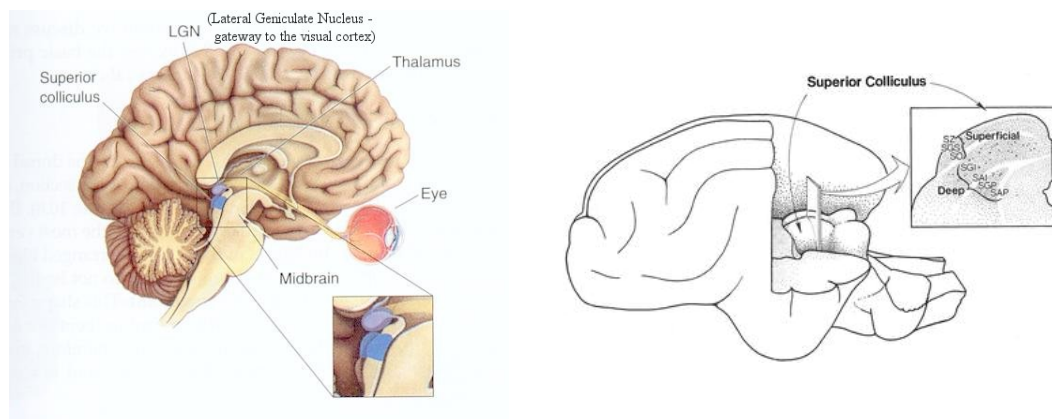


Figure 1.5: The location of the Superior Colliculus in the brain (blue) and a magnified view of the superficial and deep layers of this structure.

The Superior Colliculus (SC) is a part of the mid-brain (Figure 1.5) and plays a part in visual information processing, motor movement and integration of multi-sensory information. It is a multi-layer laminated structure of alternating gray and white matter. The superficial layers of the SC (SLSC) receive direct visual input from the retina and indirect visual input from many cortical structures. The deep layers (DLSC) contain sensory cells responsive to multiple sources and premotor neurons with outputs to a number of structures such as eye and neck muscles (Sprague and Meikle, 1965). Gamma-Amino-Butyric-Acid (GABA)ergic inter-neurons modulate the activity of both the visual sensory receptive cells in the superficial layers and the premotor neurons in the deep layers (Mize, 1992; Di Chiara et al., 1979).

The SC has been shown to be responsible for detecting looming stimuli and plays a central role in covert attentional orienting (CAO) (Dean et al., 1989; Liu et al., 2011). The midbrain CAO network detects sudden changes in the environment and alerts the individual to a salient stimulus, which requires inspection and action that may be important for survival (Vagnoni et al., 2015; Yilmaz and Meister, 2013). The SC transforms spatial information about a target location into orienting eye and head movements via projections to brain stem saccadic eye movement centres and the cervical spinal cord (Isa, 2002). Looming-sensitive neurons have been identified in the superficial layer of the optic tectum in early vertebrates and in the SC in mammals (Wu et al., 2005; Liu et al., 2011). In humans, a functional magnetic resonance imaging (fMRI) study revealed that looming stimuli (but not random stimuli) activated the SC (Billington et al., 2010). The defensive behaviours associated with a looming stimulus are known to be modulated by GABA inputs to the SC (Appell and Behan, 1990; Mize, 1992; Born and Schmidt, 2004; Kaneda et al., 2008) and by intrinsic inhibitory interneurons within the SC (Okada, 1992; Kardamakis et al., 2015).

Animal models of cervical dystonia suggest that the abnormal twisting postures and movements result from disruption of this inhibitory control (Holmes et al., 2012). Due to its chief function in controlling eye and neck movements (Hassler et al., 1981; Kardamakis et al., 2015), it is hypothesized to play a central role in cervical dystonia. Current evidence postulates that both, the mediational endophenotype, abnormal temporal discrimination and the phenotype, cervical dystonia, are caused by defective inhibition of sensory and motor neurons in the SC (Hutchinson et al., 2014). This disinhibition is due to the effects of reduced GABA activity, both from

the Substantia Nigra pars reticulata (SNpr) and GABAergic interneurons within the SC. Abnormal temporal discrimination, a subclinical marker of this disinhibition, results from prolonged duration firing of visual sensory neurons in the SLSC. The abnormal involuntary movement characteristic of cervical dystonia results from subsequent secondary disinhibition of cephalomotor neurons in the DLSC (Hutchinson et al., 2014). Further research is needed to ratify this hypothesis. Besides the SC, the midbrain Interstitial Nucleus of Cajal (Hassler et al., 1981; Klier et al., 2002) and midbrain neural integrator circuit have also been implicated in cervical dystonia (Shaikh et al., 2016).

1.2 Chapter Conclusion

Emerging from the above indications linking cervical dystonia, with an abnormal TDT observed in patients and unaffected relatives, along with possible deficits in the covert attention network due to a defective SC, the primary goal of this research was to address the hypothesis that core functionality of the SC is disrupted in individuals with abnormal TDTs. The focus is on CD patients and individuals with sensory abnormalities, in order to understand the interplay between the two. Based on this central theme, the following chapter presents a literature review that was undertaken of the most pertinent studies, which enabled the formation of relevant research questions followed by experiments designed to address them.

2 Literature Review

2.1 Background

As outlined in Chapter 1, the current hypothesis in CD revolves around dysfunction in the midbrain network for covert attentional orienting in patients and possibly their unaffected relatives who are gene carriers of this disorder. Concurrently, a plethora of concepts, hypothesis and evidence exists in dystonia, due to the heterogeneity of phenotypes and paucity in gene discovery. Therefore, in order to distillate efforts on topics related to the current hypothesis in CD, a literature review was carried out to specifically focus on neuroimaging studies in AOIFD, CD, temporal discrimination, covert attentional orienting and the superior colliculus. The search was divided into the following themes in order to assimilate the state of the art that is pertinent to improving our understanding of CD pathophysiology:

- What may be understood about the pathophysiology of AOIFD and Cervical Dystonia from the research carried out to date?
- What neuroimaging methods have already been applied to the study of AOIFD and Cervical Dystonia?
- Where do the findings of sensory abnormalities in AOIFD lead to?
- What may be deduced from head movement and eye movement research undertaken in AOIFD and CD?
- What is the current state of the art with respect to Temporal Discrimination, Covert Attentional Orienting, the Superior Colliculus and the regions involved in AOIFD and CD specifically?
- What is the network concept that is gaining importance in this disorder?

This review enabled the formation of coherent and targeted research questions detailed in Chapter 3, and laid the foundations of the research undertaken and the methodologies employed to probe the neural correlates of CD and abnormal temporal discrimination.

2.2 Methodology

A literature search and review was undertaken from September to November 2015. It was periodically updated from December 2015 - March 2019 as the studies, its scope and methodologies evolved. The review comprised of searches on PubMed, from the US National Library of Medicine National Institutes of Health. In order to target the most relevant literature, the review was divided into several themes:

- Structural, Functional and Metabolic Imaging in AOIFD and CD
- Sensory Motor Abnormalities in Dystonia
- Head Movement and Oculomotor Control in CD
- Imaging of the Midbrain and SC
- Major Regions Implicated and the Emerging Network Concept

The keyword search method using Boolean operators to connect search terms was carried out due to the excessive number (>800) of results generated by simpler searches. The results were then restricted to peer-reviewed English language publications using filters provided by the database. Often, the ensuing number of publications was excessively large for abstract review. Thus, the most relevant articles were identified by screening the results of the database searches in order of relevance and the best match criteria, as determined by the search function. If less than 100 articles were mined, their abstracts were then screened for relevance to the review. Common inclusion criteria across all the themes analysed were as follows:

- English-language publication
- Peer-Reviewed publication
- Journal and Review articles (clinical case studies with <5 subjects excluded)
- Human subjects

Following this, the articles which passed the manual abstract screening were again screened for relevance by appraising the full-text article. Only those articles with complete relevance to the topic of interest have been summarized in this chapter.

2.3 Imaging in AOIFD with a focus on CD

Rapid progress in neuroimaging has positively impacted our understanding of dystonia via advancements in higher resolution and high density acquisition as well as analysis routines coupled with computational power. It has been historically considered a cortical and later on a Basal Ganglia disorder due its role in amplifying activity in motor cortex areas that control the agonist muscles while simultaneously silencing the areas that control the antagonist muscles (Marsden et al., 1985; Vitek, 2002; Mink, 2003). Neuroimaging studies have been transformative in challenging traditional views restricting causes to a single node, and addressing altered neural organization underlying this disorder.

Several structural, functional and molecular imaging studies have utilized the advances in neuroimaging methods in order to identify and characterize abnormalities in patients with primary focal dystonias. This has augmented our understanding of the pathophysiology of its idiopathic form in particular (Simonyan, 2018). The diversity of clinical phenotypes of dystonia is believed to run parallel with the multivariate pathophysiology, which is linked not only to genetic mutations but also to alterations of neural organization and environmental stressors. This has motivated imaging studies in dystonia; some focussed on a specific dystonia phenotype cohort to enable unambiguous associations between type and abnormalities detected, while some focussed on a dystonia sub-group (primary vs. secondary, adult vs. early-onset, idiopathic vs. genetic, focal vs. generalized) in order to interpret patterns encompassing a comprehensive pathophysiology of the disorder. In the current literature review, the focus is on imaging studies in AOIFD, particularly highlighting those involving CD.

2.3.1 Metabolic Imaging

Two major pathways lead from the Striatum to the main output nucleus in the Basal Ganglia: 1) the direct pathway via inhibitory GABAergic fibres, and 2) the indirect pathway via inhibitory GABAergic neurons to the GPe (external segment of GP), inhibitory neurons projecting from the GPe to the subthalamic nucleus (STN), and excitatory glutamatergic neurons projecting from STN to the internal segment of GP (GPi)/Substantia Nigra (Alexander et al., 1990). Evidence from these studies suggests that the direct pathway selects the desired movement (facilitation), while the indirect

pathway suppresses unwanted surrounding movement (inhibition). Studies advocate that dystonia may represent a defect in surround inhibition due to abnormal functioning of the indirect pathway (Figure 2.1), along with excessive facilitation of the intended movement due to over activation of the direct pathway (Fujita and Eidelberg, 2017). Dopamine is believed to play an important role in the pathophysiology of dystonia (Karimi and Perlmutter, 2015) as dopaminergic nigrostriatal input plays a regulatory role in the activity of the direct and indirect pathways. Molecular activity imaging studies with positron emission tomography (PET), single-photon emission computed tomography (SPECT) and magnetic resonance spectroscopy (MRS) have helped lay the foundations of potential network dysfunction via aberrations of dopaminergic and GABA-ergic neurotransmission across different forms of dystonia.

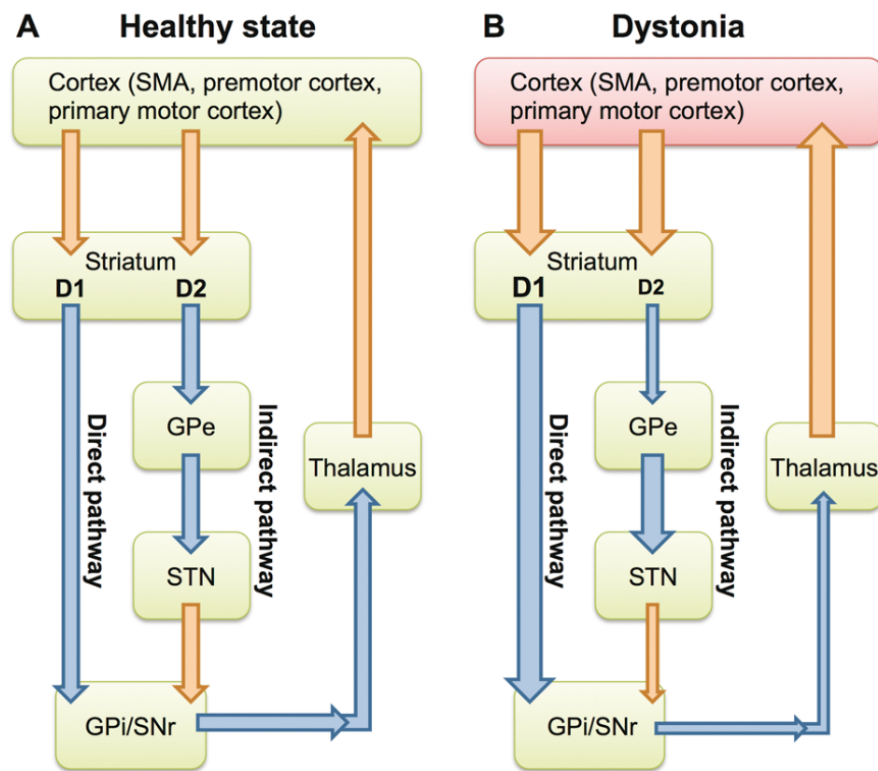


Figure 2.1: A simplified model of the motor circuit (adapted from Eidelberg, 2017). In dystonia, hyperactivity of the direct pathway and hypoactivity of the indirect pathway may together add to the hyperexcitability of the cortical regions. The wide and thin arrows indicate increased and decreased output, respectively.

PET studies in dystonia have focussed on tracing glucose metabolism (Otsuka et al., 1992; Magyar-Lehmann et al., 1997), regional cerebral blood flow (rCBF) (Tempel and Perlmutter, 1990; Feiwell et al., 1999) and dopamine receptor availability (Karimi et al., 2011; Karimi and Perlmutter, 2015). Using 2-fluoro-2-deoxy-glucose (FDG)

as an indicator of metabolic activity, increases and decreases in FDG uptake have been detected in the Basal Ganglia, Cerebellum and sensorimotor cortex of focal dystonia patients. Otsuka et al. (1992) studied striatal dopamine uptake and glucose metabolism using PET in 8 patients with idiopathic dystonia (torsion dystonia in three patients, focal dystonia limited in the arm in three and cervical dystonia in two). They reported increased uptake in the Putamen and in the Caudate head in patients with idiopathic dystonia compared to the normal controls. Galardi et al. (1996) employed FDG and PET to study the neural functional correlates of primary dystonia in 10 clinically homogeneous patients with idiopathic spasmodic torticollis. This was one of the first studies to demonstrate a consistent pattern of regional metabolic hyperactivity in a homogeneous group of patients with focal dystonia. They reported significant hypermetabolism in the Basal Ganglia, Thalamus, premotor-motor cortex and Cerebellum in the patients compared with normal controls. Bilateral increase in glucose metabolism in the lentiform nucleus in CD patients (Magyar-Lehmann et al., 1997), in the Striatum and Thalamus of patients with blepharospasm (Esmaeli-Gutstein et al., 1999) and in the Cerebellum and the pons in patients with BLS (Hutchinson et al., 2000; Nagata et al., 2007) were detected consistently across various glucose hypermetabolic studies. Kerrison et al. (2003) reported a complex network of cortical and subcortical regions with increased and decreased glucose metabolism in patients with BLS. There was increased metabolism in the inferior frontal gyri, right posterior cingulate gyrus, left middle occipital gyrus, fusiform gyrus of the right temporal lobe, left anterior cingulate gyrus and the Caudate nucleus. Decreased glucose metabolism was observed in the inferior frontal gyri, left cerebellar hemisphere, and Thalamus. Carbon et al. (2004b) performed a comprehensive and systematic evaluation of glucose metabolic assessment in idiopathic torsion dystonia patients and discovered that the disorder was characterized by relative metabolic overactivity of the lentiform nucleus and premotor cortices.

SPECT is an imaging methodology where a radiopharmaceutical is injected and binds to specific receptors or transporters in the brain and therefore reflects activity (Accorsi, 2008). Most studies reported in patients with focal dystonia made use of radiopharmaceuticals that image the dopamine system. Hierholzer et al. (1994) detected in 10 patients with CD that although the average specific striatal binding was not significantly different from a control group, patients exhibited a more asymmetric

striatal binding. 50% of the patient group showed a significantly higher receptor binding in the Striatum contralateral to the direction of head rotation. This is in accordance with the increased dopamine receptor binding in the contralateral Striatum reported in the PET study in patients with CD mentioned above and has also been found in other SPECT studies (Leenders et al., 1993). In a study evaluating 10 patients with writer's cramp (Horstink et al., 1997), the authors reported that the striatal D2/3R binding was bilaterally decreased in patients compared to controls. Albin et al. (2003) performed the only study that evaluated the integrity of cholinergic nerve terminals in 13 patients with CD. They reported reduced binding in the Putamen as well as in the whole Striatum in patients with CD compared to controls. In summary, the findings in SPECT studies implicate a role for the striatal dopaminergic system and the Basal Ganglia in the pathophysiology of focal dystonia.

Additionally, MRS has helped reveal the aberrations of GABAergic neurotransmission across different forms of dystonia as one of the potential underlying causes of altered network function (Levy and Hallett, 2002; Garibotto et al., 2011; Herath et al., 2010). Transcranial magnetic stimulation studies also suggest that decreased intracortical inhibition by GABAergic neurons in focal dystonia could lead to increased primary motor cortex excitability (Lozeron et al., 2016). Dysfunction of GABA-A receptor binding in motor cortical areas has been described recently in patients with primary dystonia, and findings were discussed as a possible cause of sensorimotor disinhibition leading to the generation of dystonic movements. In focal hand dystonia patients, conflicting data regarding local sensorimotor cortical and Basal Ganglia GABA have been published, Some reported unchanged and some abnormally decreased GABA levels as measured with magnetic resonance spectroscopy (Hinkley et al., 2009; Gallea et al., 2018). Abnormal GABA levels in the SC have been postulated as playing a central role in CD and AOIFD (Hutchinson et al., 2014; Butler et al., 2015). Hence, there is a need for future research to investigate the GABAergic contributions to different clinical manifestations of dystonia in further detail.

Altogether, the literature indicates dysfunction in key metabolic pathways (Figure 2.2) involving dopamine, GABA and glutamate in dystonia (Levy and Hallett, 2002; Tanabe et al., 2009; Alongi et al., 2014).

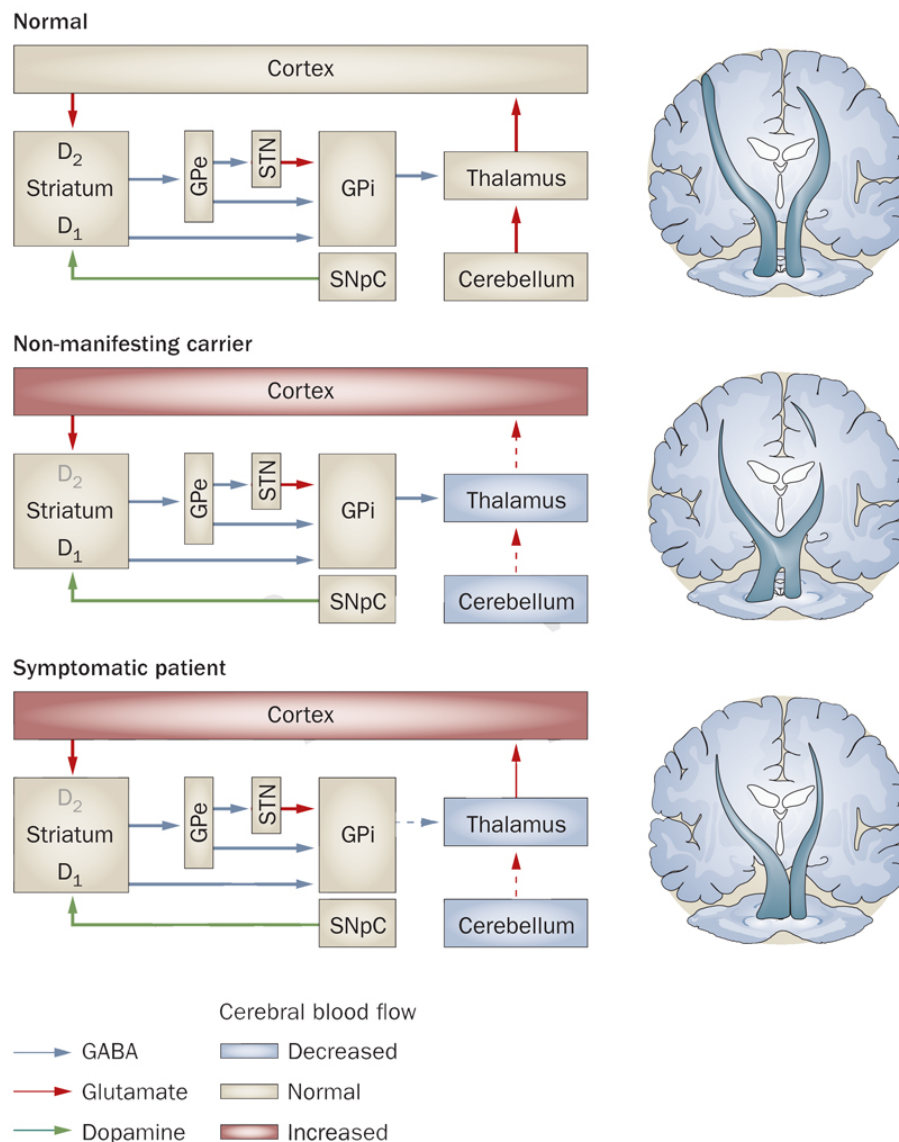


Figure 2.2: The DYT1-genotype is characterized by reduced dopamine D2 receptor availability and cerebellothalamocortical tract abnormalities, regardless of the existence of symptoms. Manifesting and non-manifesting DYT1 carriers exhibit similar abnormalities of cerebellothalamic tract microstructure (indicated by broken arrows connecting these structures). GPe=globus pallidus externa, GPi=globus pallidus interna, SNpC=substantia nigra pars compacta, STN=subthalamic nucleus. Adapted from Tanabe et al. (2009).

2.3.2 Structural Imaging

One of the clinical hallmarks of dystonia is the absence of gross structural abnormalities on conventional MRI scans. This was once considered misleading, but is now often a differential diagnosis criterion in dystonia. Nevertheless, detailed assessments of high-resolution T1-weighted and diffusion-weighted MR sequences in numerous

neuroimaging studies have led to the identification of microstructural cortical and subcortical alterations across all forms of isolated dystonia.

There is a growing body of evidence that patients with idiopathic focal dystonia exhibit subtle changes in brain area volume, cortical thickness and brain tissue microstructure. Structural studies in AOIFD have primarily utilized volume-based morphometry (VBM) and diffusion tensor imaging (DTI). These two imaging methodologies which have proven useful in detecting changes in grey/white matter volume as well as white matter tract integrity and microstructural connectivity (respectively).

Of research which has reported studies incorporating VBM analysis in AOIFD, grey matter changes have been identified in the Putamen, Basal Ganglia, Thalamus, sensorimotor cortex, Cerebellum, prefrontal cortex, and the inferior parietal cortex (Draganski et al., 2003; Obermann et al., 2007; Egger et al., 2007; Pantano et al., 2011; Prell et al., 2013; Ramdhani et al., 2014; Waugh et al., 2016). Grey matter abnormalities in SD patients compared with healthy controls have been reported to involve bilateral primary sensorimotor and premotor cortex, superior/middle temporal, supramarginal, inferior frontal gyri, inferior parietal lobule, insula, Putamen, Thalamus, and Cerebellum (Bianchi et al., 2017; Simonyan and Kristina, 2013; Kirke et al., 2017). While a change in putaminal volume has been recognised as one of the hallmarks of the pathophysiology of idiopathic focal dystonia (Walsh et al., 2009), there have been contradictory findings regarding the interpretations of a decrease / an increase in regional volumes in CD patients across the studies (Ramdhani and Simonyan, 2013). The cause for this discrepancy is unknown, but may be attributed to low subject numbers in the studies implemented, low field strength MRI technology and lower scan resolution (majority employed 1.5T), different smoothing kernels employed in the preprocessing stage. Some results reflect uncorrected biases in statistical analysis. Table 2.1 summarizes the VBM studies reported in CD to date up to 2015. In most of these studies, subjects were scanned at a single time point and in a small cohort. Therefore it could not be established whether increases/decreases in volume and density were static or progressed with age, and to what extent these effects would be observed in a larger cohort. VBM studies also show considerable variability across different phenotypes of dystonia (Ramdhani and Simonyan, 2013). It is, therefore, reasonable to conclude that we are yet to ascertain an absolute alteration in grey/white matter that links its

occurrence to a specific phenotype of the disorder. Nevertheless, these VBM studies have been instrumental in illuminating key areas in the pathophysiology in primary focal dystonia such as the Putamen, Cerebellum and sensory-motor areas, which would not have been possible to identify otherwise.

Most of the knowledge surrounding white matter organization in isolated dystonia comes from the use of diffusion tensor imaging (DTI), which is an imaging method that analyzes the microstructural integrity of white matter by examining axonal organization in brain tissue (Alexander et al., 2007). Diffusion imaging quantifies the directionality of water diffusivity and the magnitude of water movement independent of the direction, thus reflecting axonal integrity, tissue coherence, providing information regarding the organization of the extracellular space and the intracellular water content. One of the earliest studies applying DTI to dystonia was carried out by Carbon et al. (2004a), to assess the microstructure of white matter pathways in mutation carriers and control subjects. Their subjects included DYT1 mutation carriers (4 clinically affected/manifesting carriers and 8 non-manifesting carriers) and healthy controls. They reported reduced Fractional Anisotropy (FA - a measure of axonal integrity and coherence) values ($p < 0.005$) in the subgyral white matter of the sensorimotor cortex of DYT1 carriers. Thus, it was suggested that abnormal anatomical connectivity of the supplementary motor area may contribute to the susceptibility of DYT1 carriers to develop clinical manifestations of dystonia. Colosimo and colleagues were the first to study primary cervical dystonia patients (Colosimo et al., 2005). When they compared DTI results in 15 CD patients vs. 10 healthy controls, they found higher FA values in patients in both putamina and lower FA values in the genu and in the body of the corpus callosum. They also demonstrated that patients also had lower mean diffusivity (MD) values in the left pallidum, the left Putamen, and both Caudate. Following this, there have been studies applying DTI in CD (Figure 2.3) to investigate white matter connectivity in CD patients vs. controls (Fabbrini et al., 2008; Pinheiro et al., 2015); the results are summarized in Table 2.2. Blood et al. (2006) studied the effect of botulinum toxin on white matter connectivity and tracked changes before and after treatment. Their findings of abnormal hemispheric asymmetry in a focal region between the pallidum and the Thalamus in patients, which was absent four weeks after being treated with intramuscular botulinum toxin injections, led to conclusions about crucial central nervous system changes following peripheral reductions in muscle activity. This

opened the debate on activity-dependent white matter plasticity in adults. Besides CD, a number of studies demonstrated altered microstructural white matter connectivity in SD, FHD, BSP, HD across different regions of the brain, including a findings about a positive correlation between the diffusivity changes and clinical symptoms in SD (Carbon et al., 2008a; Fabbrini et al., 2008; Bonilha et al., 2009; Ramdhani et al., 2014). However, a study by Pinheiro et al. (2015) contradicted previous findings about white matter changes by reporting no primary or major involvement of white matter differences in cranio-cervical dystonia. Pinheiro et al. (2015) cited the reasons for the discrepancies in the results as the small sample sizes employed in previous DTI-Dystonia studies, the use of an ROI-based analysis rather than a whole-brain approach which probably enhanced the possibility of finding statistical differences and increased the chance of a Type II error, and the different softwares platforms employed for DTI imaging processing, including traditional methods in comparison to the more refined and improved data processing softwares and methods they employed in their study in 2015. Table 2.2 summarizes the DTI studies undertaken in CD with number of subjects, specifications of data acquisition and key findings.

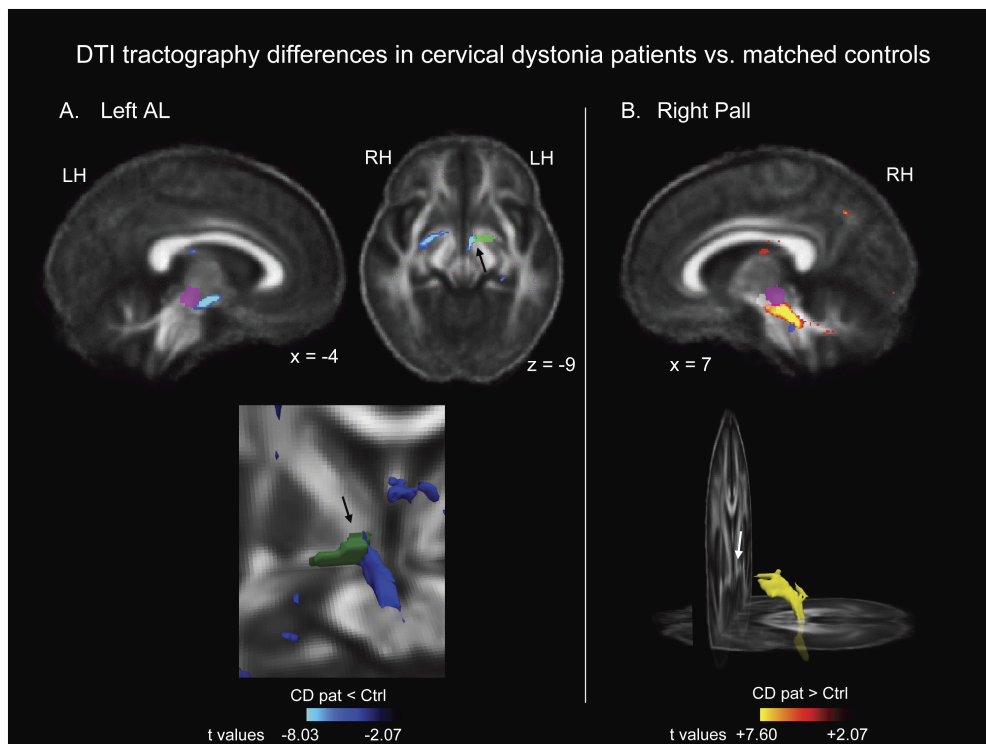


Figure 2.3: DTI tractography differences in CD patients vs. healthy controls. (A) reduced tractography from the left AL seed region, (B) elevated tractography from the right pallidal seed region. Pink = red nucleus, White = Substantia Nigra, Blue = pedunculopontine nucleus. Adapted from Blood et al. (2012b).

Table 2.1: VBM studies undertaken in CD to date

Study	No. of subjects	Mean Age	MRI	Pre-processing	Results (increase)	Results (decrease)
Draganski et al., 2002	10 CD, 10 HC	67.4 ± 4.3	1.5T Siemens Symphony	SPM99, MATLAB, 10mm FWHM	motor cortex, cerebellar flocculus, GPi	caudal supplementary motor area, dorsal lateral prefrontal and visual cortex
Obermann et al., 2007	9 CD, 14 HC	57.6 ± 7.2	1.5T Siemens Symphony	SPM2, MATLAB 6.5, 12mm FWHM	thalamus, caudate head, superior temporal lobe, left cerebellum	putamen
Egger et al., 2007	11 CD, 31 HC	49.1 ± 9.3	1.5T Siemens Symphony	SPM2, MATLAB 6.5, 12mm FWHM	globus pallidus internus, orbitofrontal cortex, medial frontal gyrus, sma, cingulate gyrus	-
Pantano et al., 2011	19 CD, 28 HC	53.2 ± 11.2	1.5T Philips Healthcare	SPM5, MATLAB 7.0, 12mm FWHM	-	caudate head, putamen, premotor and primary sensorimotor cortex
Prell et al., 2013 (p<0.001 uncorrected)	24 CD, 24 HC	53	1.5T GE Signa Horizon	SPM2, MATLAB, 8mm FWHM	globus pallidus, claustrum, putamen, frontal eye field (BA 8), the visual cortex (BA 17)	precentral gyrus, supplementary motor area (BA 6), somatosensory association cortex (BA 7), medial temporal gyrus
Delnooz et al., 2015	23 CD, 22 HC	57.3 ± 9.8	3T Siemens Magnetom Allegra	SPM8, MATLAB 7.9, DARTEL method, 10mm FWHM	-	ventral premotor cortex (BA 45)
Piccinin et al., 2015	27 CCD, 54 HC	54.2 ± 11.7	3T Philips Achieva Intera	-	premotor cortex, somatosensory integration area, anterior cingulate/paracingulate, cerebellum	-
Waugh et al., 2015	17 CD, 17 HC	52 ± 2.3	3T Siemens Allegra	FSL-VBM, 12mm FWHM	-	posterior cingulate

Table 2.2: DTI studies undertaken in CD to date

Study	No. of subjects	Mean Age	MRI	Pre-processing	Results (increase)	Results (decrease)
Colismo et al., 2005	15 CD, 10 HC	51.9 ± 11.0	1.5 T Philips Gyroscan NT	b-value: 0 and 1000, SPSS 10.0	bilateral putamen	genu, body of the corpus callosum, left pallidum, the left putamen, and both caudati
Blood et al., 2006	4 CD	Pre and Post-BoNT	3.0 T Siemens Allegra	b-value: 0 and 700		white matter hemispheric asymmetry
Bonihla et al., 2007	7 CD, 10 HC	58 ± 18	3.0 T Philips Intera	b-value: 0 and 1000, FSL-FDT	basal nuclei (right and left pallidum, right and left putamen, and left caudate)	right thalamus, right middle frontal gyrus
Fabrini et al., 2008	18 CD, 35 HC	55.5 ± 13.4	1.5 T Philips Gyroscan NT	b-value: 0 and 1000, SPSS 10.0	Bilateral putame, pre-frontal cortex bilaterally, left SMA	corpus callosum, right caudate nucleus, left putamen
Bonihla et al., 2009	7 CD, 7 HC	58 ± 18	3.0 T Philips Intera	b-value: 0 and 1000, FSL-FDT	none	Fiber tracts from the right thalamus - right prefrontal cortex
Blood et al., 2012	12 CD, 12 HC	49.17 ± 8.27	3.0 T Siemens Tim Trio	b-value: 0 and 700, FMRIB v4.1.4 and FDT v2.0	right pallidum-brainstem	hemisphere: left hemisphere: pallidum-brainstem
Pinheiro et al., 2015	18 CD	52.8 ± 12.2	3.0 T Philips Intera Achieva	b-value: 0 and 1000, FMRIB v4.1.4 and FDT v2.0		no significant differences

2.3.3 Functional MRI in AOIFD and CD

Functional MRI (fMRI) studies are based on the analysis of hemodynamic response functions (HRFs) reflecting dynamic blood-oxygen-level-dependent (BOLD) contrasts, which captures neuronal activity (Matthews and Jezzard, 2004). Several task based paradigms have been employed to study dystonia, such as writing, drawing or hand movements (WC and FHD) and blinking (BLS), through visual and tactile stimulation (Simonyan, 2018). Task-based fMRI studies have demonstrated variations in regional functional activity in the Basal Ganglia, Thalamus, Cerebellum and sensorimotor cortex across different forms of isolated dystonia. Some have suggested abnormal integration of sensorimotor information within the Basal Ganglia-thalamo-cortical and cerebello-thalamo-cortical circuits (Pujol et al., 2000; Baker et al., 2003; Butterworth et al., 2003; Islam et al., 2009; Haslinger et al., 2010; Dresel et al., 2014). A study by Oga et al. (2002) supported the view that an impairment of the excitatory as well as inhibitory motor control mechanism may be an underlying mechanism inducing dystonia. They reported decreased activity of the sensorimotor cortex and supplementary motor area associated with voluntary muscle contraction and also with muscle relaxation in WC patients compared to controls. Additionally, the results from a growing body of evidence advocate abnormal sensory processing in the primary somatosensory cortex potentially contributing to the pathophysiology of dystonia (Hallett, 1995; Dresel et al., 2006; Simonyan and Ludlow, 2010; Konczak and Abbruzzese, 2013; Lokkegaard et al., 2016). Subclinical abnormalities in sensory discrimination were described as a mediational endophenotype of dystonia (Hutchinson et al., 2013) and linked to alterations in primary somatosensory and middle frontal cortices (Termsarasab et al., 2016). Simultaneously, studies examining the effects of botulinum toxin injections on neural activity in patients with focal dystonia provides inconclusive results. Studies have reported either modulated or unmodulated neural activity following injection (Valls-Sole et al., 1991; Ce, 2000; Opavsky et al., 2012). Some other valuable findings include the activation of the Basal Ganglia during tactile stimulation (Peller et al., 2006). In one of the very few fMRI studies in patients with CD, de Vries et al. (2008) compared patients to healthy controls during execution and imagination of hand movements; they reported that CD was associated with impaired cerebral activation of the parietal cortices, cingulate cortex/SMA and ipsilateral

Putamen during both execution and imagining of non-dystonic right-hand movements.

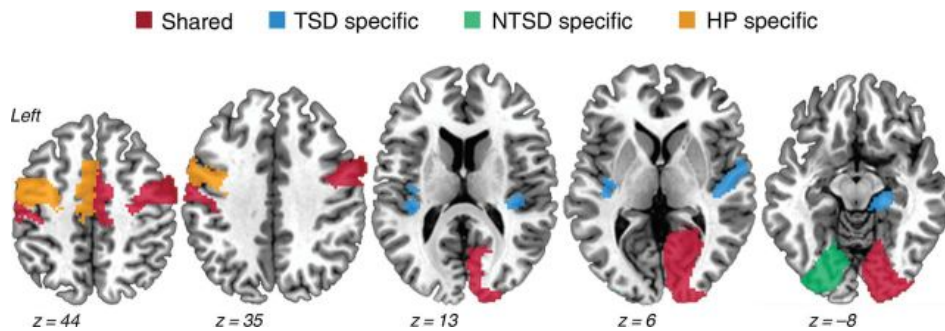


Figure 2.4: Alterations in topology, global and local features of large-scale functional brain networks across different forms of isolated focal dystonia, including patients with task-specific and nontask-specific dystonias. All patients showed altered network architecture, such as breakdown of basal ganglia-cerebellar community, loss of a hub node in the premotor cortex, and connectivity reduction within the sensorimotor and frontoparietal regions. HP=Healthy participants, TSD=task-specific dystonia patients, NTSD=non-task-specific dystonia patients. Adapted from Battistella et al. (2015).

Resting-state fMRI (rs-fMRI) has also proven to be instrumental in aiding the comprehension of the pathophysiology of dystonia. This method circumvents the challenges associated with the execution of task-related designs across different forms of dystonia (which exhibit differing symptoms). It also overcomes the disadvantage of task-based fMRI which may confound task-dependent activation with pathophysiological alterations (Lee et al., 2013a). Furthermore, an examination of resting-state activity and neural connectivity may help resolve the ambiguity arising from the diversity of dystonia phenotypes and genotypes associated with a combination of motor and sensory components (Figure 2.4). Applying rs-fMRI analysis in cervical dystonia cohorts, alterations were reported not only in sensorimotor but also in visual and executive control networks (Delnooz et al., 2013, 2015) as well as altered striatal and pallidal connectivity in the resting brain of patients vs. controls. Studies in focal hand dystonia reported decreased connectivity in primary somatosensory region, increased connectivity in the Putamen along with functional decoupling of the premotor cortex from the parietal cortex (Delnooz et al., 2012; Mohammadi et al., 2012). Changes in blepharospasm were linked to the default-mode network as well as alterations in the cortico-striato-pallido-thalamic loop (Zhou et al., 2013; Yang et al., 2013; Jochim et al., 2018).

2.3.4 Multimodal and Multivoxel Pattern Analysis

Almost all of the neuroimaging research undertaken in dystonia to date has applied univariate methods of analysis. This method involves studying a single dependent variable along with one or more independent variables. Multivoxel pattern analysis (MVPA) approaches (e.g.: multivariate regression, multivariate analysis of variance, machine learning etc.) are sophisticated pattern recognition, statistical and computational tools to evaluate multiple variables/measurements simultaneously. While univariate approaches are excellent for localizing activations in individual voxels, multivoxel and multivariate approaches may be employed to examine responses that are jointly encoded across multiple voxels.

MVPA is gaining increasing interest in the neuroimaging community because it enables the detection of differences between conditions with higher sensitivity than conventional univariate analysis by focusing on the analysis and comparison of distributed patterns of activity. Two variables, may discriminate poorly between the groups, but perfect separability exists when they are considered jointly. Therefore, within the last decade, there has been a substantial shift in the use of MVPA from voxel-wise statistics to analyze fMRI data (Figure 2.5). Machine learning (Carbonell et al., 1983) is an associated type of analysis that overlaps substantially with multivariate statistical approaches. Machine learning methods have become popular in neuroscience as they do not require many of the challenging assumptions that plague univariate analyses (Vu et al., 2018; Vogt, 2018). The combination of large datasets and comparatively fewer assumptions lend machine learning methods an air of objectivity. From now on, the terms MVPA and machine learning will be employed to represent the same multivariate analysis method, interchangeably.

Research undertaken in dystonia and reported in the literature has focussed on identifying and localizing features (to neuroanatomical correlations) using different measures, paradigms and acquisition modes. However, few have utilized these features in a machine learning paradigm. For any machine learning algorithm, the greater the number of distinguishable feature sets, the better its performance. Thus, while there are many diverse modalities and features per modality, combining multiple significant features from these individual data sets may not only inform better on the pathomechanisms of dystonia but also aid in the diagnosis and future prognosis to

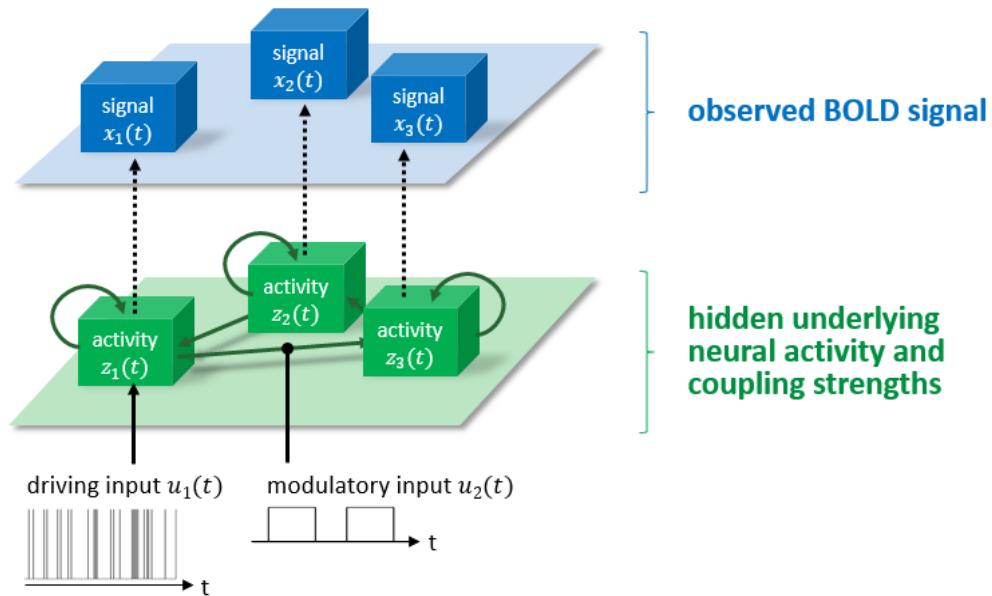


Figure 2.5: Multivariate approaches may utilize ‘hidden’ quantities such as coupling strengths. Adapted from Friston, Harrison Penny (2003) NeuroImage; Stephan Friston (2007) Handbook of Brain Connectivity; Stephan et al. (2008) NeuroImage.

differentiate cervical dystonia patients from controls. One of the most recent studies in this context was the resting state study on cervical dystonia that demonstrated a classification accuracy of 90% when using functional connectivity measures along with detected regional homogeneity abnormalities (Li et al., 2017). Further, the usage of combined measures offers insight into the underlying pathophysiology of the disorder in relation to network dysfunction and somatosensory disturbances in cortical and sub-cortical regions. A similar multi-measure study was carried out in patients with musician’s dystonia, where combinations of variables measured in this study, were employed to perform supervised machine learning analyses (Van Der Steen et al., 2014). An overview of past literature sheds light upon the fact that i) there are a plethora of research findings suggesting neural regions involved using different modalities ii) only a few dystonia studies have employed machine learning for detection of features and classification of patients and controls, and iii) feature selection has only been performed using one modality (data acquired). This warrants the further exploration of a multimodal feature approach to better inform on the pathophysiology of this disorder.

2.4 Sensory Motor Abnormalities in Dystonia

The sensory trick is a prevalent clinical feature in dystonia (Naumann et al., 2000; Schramm et al., 2004; Loyola et al., 2013; Patel et al., 2014). In spasmodic torticollis, a finger placed gently on the face neutralizes the spasm. While in blephrospasm, pressure on the eyelids tends to improve it in some sufferers. Although dystonia is considered a movement disorder, the arbitrary nature of the segregation between the motor and sensory functions in the central nervous system has led many to consider dystonia as a sensory disorder (Bradley et al., 2012; Hutchinson et al., 2013; Walsh et al., 2009; Hallett, 1995). This theory emanated from a series of somatosensory studies undertaken in dystonia patients and controls, as well as from animal models.

Byl and colleagues undertook studies that required owl monkeys to perform repetitive hand movements to receive rewards, and observed a change in hand representation in the somatosensory cortex that accompanied hand dystonia in these monkeys. Based on the theory that somatosensory representations in cortex are plastic and based on their animal models, Byl and colleagues proposed the “sensorimotor learning” hypothesis of focal hand dystonia (Sanger and Merzenich, 2000; Blake et al., 2002; Byl, 2003, 2004). In another study to model the origin of blephrospasm, two mild alterations to the rat trigeminal reflex blink system reproduced the symptoms of benign essential blepharospasm (Schicatano et al., 1997). It resulted in/from dysfunctional sensorimotor integration where the nervous system either misinterpreted sensory signals or misrepresented the desired movement.

Tempel and Perlmutter (1990) reported a diminished response to somatosensory input in the primary sensory cortex region and the supplementary motor area region in patients with idiopathic dystonia and writer’s cramp compared to controls by examining regional cerebral blood flow. A change in the amplitude of the median nerve somatosensory-evoked potential (N30) was detected as enhanced in patients by Reilly et al. (1992), though others failed to replicate this finding later (Mazzini et al., 1994). Tinazzi et al. (2000) assessed somatosensory discrimination threshold (SDT) (the capability to perceive as separate two successive stimuli applied to the index finger) in seven patients with idiopathic dystonia (involving at least one upper limb) and nine sex- and age-matched healthy controls. They reported higher SDT threshold in dystonic patients than in normal subjects, no significant correlation to motor control

impairment severity, and the presence of these SDT abnormalities were also observed at the clinically normal hand in the same patient. In another study, dystonic subjects had diminished ability to distinguish between stimuli closely related spatially, with higher spatial localization errors along with an amplified threshold for spatial frequency discrimination (Bara-Jimenez et al., 2000). Further research into probing sensory abnormalities in dystonia included employing uni-modal and cross-modal stimuli (Aglioti et al., 2003), the Grating Orientation Task (Molloy et al., 2003) and assessing kinesthetic deficits (which involves relying on intact peripheral sensory input involving muscle spindles) (Putzki et al., 2006) in patients compared to controls. All these studies demonstrated that abnormal sensory input may be a trigger for dystonia or conversely, the brain response to sensory input may be abnormal in dystonia patients. Additionally, there is also evidence for a more global disruption in central timing mechanisms in dystonia, besides the impairment of temporal discrimination. A study by Filip et al. (2013a) revealed that when asked to intercept a moving target on a screen by launching a virtual projectile, CD patients were impaired compared to controls. This led to the postulation that predictive central timing mechanisms are defective in CD. Furthermore, in addition to impairments of sensation or perception, several studies have demonstrated the lack of appropriate integration of afferent proprioceptive information by the sensorimotor system in focal dystonia (Frima et al., 2003; Yoneda et al., 2000; Frima et al., 2008; Avanzino and Fiorio, 2014).

2.4.1 The Role of Unaffected Relatives

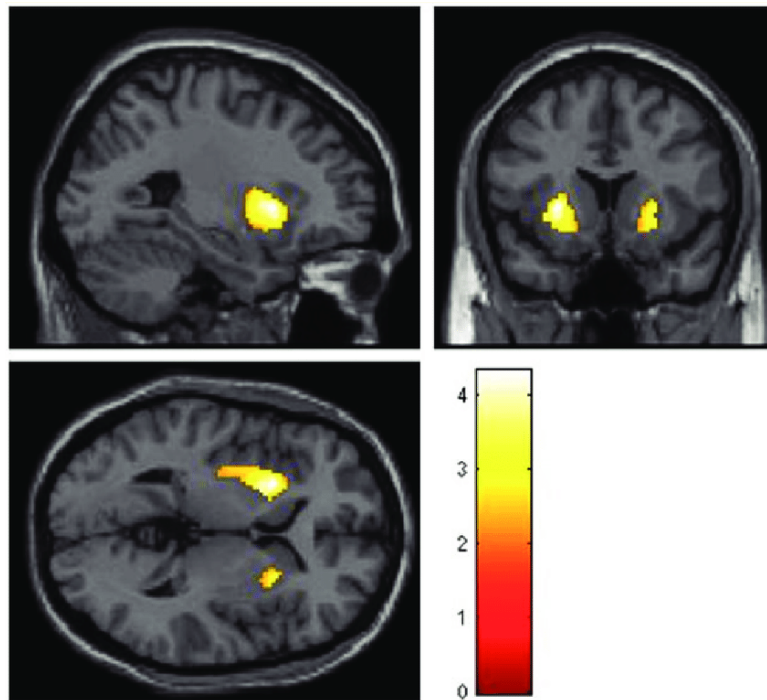


Figure 2.6: Results of the voxel-based morphometry analysis showing increased volume of the anterior and posterior putamen on the left side and right side in unaffected AOPTD relatives with abnormal TDTs in comparison with relatives with normal TDTs. Adapted from Bradley et al. (2012).

Despite advances in the possible regions and pathomechanisms involved in primary torsion dystonia, its genetic aetiology remains largely unknown. Following initial findings of somatosensory abnormalities in 12 of 49 unaffected relatives of familial primary torsion dystonia patients (O'Dwyer et al., 2005), Walsh et al. (2007) were among the first to recognize that unaffected siblings and offspring of patients with sporadic adult-onset primary torsion dystonia (AOPTD) also demonstrate abnormalities of spatial acuity. This led them to suggest that sensory abnormalities may be an endophenotype, conceivably expressed later as AOPTD. This was further supported by Bradley et al. (2009), who investigated the utility of temporal discrimination threshold as a possible endophenotype in AOPTD. They measured TDT using visual and tactile stimuli on age- and gender-matched cohort of 35 AOPTD patients, 42 unaffected first-degree relatives of the patients, 32 unaffected second-degree relatives of the patients and 43 control subjects. Furthermore, voxel-based morphometry was also employed in order to compare putaminal volumes between relatives with

abnormal and normal TDTs. The VBM analysis comparing 13 unaffected relatives with abnormal TDTs and 20 with normal TDTs demonstrated a bilateral increase in putaminal grey matter in unaffected relatives with abnormal TDTs. 86% AOPTD patients had abnormal TDTs, 52% of first-degree unaffected relatives demonstrated abnormal TDTs and 50% of second-degree relatives had abnormal TDTs, compared with controls. In another study by Walsh et al. (2009), it was postulated that unaffected relatives with abnormal spatial acuity, and a correlated reduction in striatal volume (Figure 2.6), are non-penetrant gene carriers. Temporal discrimination threshold results were also found to be comparable across common adult-onset primary torsion dystonia phenotypes (Bradley et al., 2012). The above findings propound that patients with cervical dystonia, in conjunction with their first-degree unaffected relatives harbouring the possible endophenotype, make for a comprehensive cohort to study this movement disorder. By enhancing our understanding of the neural networks involved in temporal discrimination, we may unveil disease pathomechanisms distinct from the clinical phenotype.

2.5 Head Movement and Oculomotor Control in CD

Given the findings from the previously discussed studies and the loss of motor control in the head-neck region in CD, probing the head-neck circuitry is central to developing a deeper understanding of the pathophysiology of this disorder.

In addition to abnormal movement patterns in the head and neck muscles, previous kinematic studies have shown that swift voluntary redirections of the head from one target to another (head saccades) in CD patients are slower than in healthy controls (Curra et al., 1998; Carpaneto et al., 2004; Gregori et al., 2008). In 2009, a study demonstrated, in a comprehensive assessment that, patients with CD have abnormal neck movement patterns, characterized by reduced peak movement velocities, increased coupled movements out of the attempted movement plane and reduced range of movements (De Beyl and Salvia, 2009a). These ranges and velocities of movements (for flexion-extension and lateral bending) correlated with the TWSTRS¹total score (severity, disability, and pain). Hotson and Boman (1991) found that the latency of saccades differed significantly in cranial dystonia and blephrospasm patients. With neuroimaging evidence suggesting a possible pathophysiological role of cerebellar

dysfunction in dystonia, Hubsch et al. (2011) analysed saccade adaptation in a genetically homogeneous group of DYT11 dystonia patients. Upon studying 14 patients and controls, they identified that saccade adaptation was significantly lower in DYT11 patients than in healthy controls, which supported the role of cerebellar dysfunction. Eye movements and saccades, in particular, may therefore be employed to probe the functions of many other areas within the brain including within the Thalamus, Basal Ganglia, and cerebral cortex (Sedov et al., 2017). Furthermore, a study published in 2017, demonstrated that saccadic acceleration and latency were abnormal in WC patients compared to controls while performing eye-hand coordination tasks (Jhunjhunwala et al., 2017), corroborating the Cerebellum's role in the pathophysiology.

A fascinating feature of the head-movement control system is that it shares properties of both the eye and arm-movement control systems. Like the eye, the head is used to control the direction of gaze. It thus requires mechanisms to keep its orientation steady in the face of external perturbations (Monteon et al., 2005). The head congruently participates in gaze shifts that align the optic axes with an object to be viewed (Guitton and Volle, 1987; Peterson et al., 2004). Therefore, an integral part of studying CD involves probing eye-head-neck gaze shifts, due to the complexity of integration involved in the control system and execution of movements. The kinematics of oculomotor (eye) movement and cephalomotor (head-neck) movement differ in their complexities due to the number of muscles involved. In the oculomotor system, three pairs of muscles control the three rotational degrees of freedom of the eye (yaw, pitch and roll) (Robinson, 1986; Fukushima et al., 1992). Head movements are more complex than eye movements as they are controlled by numerous neck muscles; any given neck muscle can be activated during movements in more than one plane, and movements can be around more than one joint (Peterson et al., 2004). Nevertheless, animal model studies have implicated similar evolved mechanisms for head control as to those for the eyes (Freedman and Sparks, 1997; Corneil et al., 2002; Gandhi and Sparks, 2007; Gandhi et al., 2008; Klier et al., 2002).

Malouin and Bédard (1983) revealed that in cats, unilateral electrolytic lesions of the lateral substantia nigra pars reticulata evoked a sustained contralateral head turn. In another study, microinjection of receptor ligands into the red nucleus of alert rats, produced a marked rotation of the head about the saggital axis and led to dystonic

¹Toronto Western Spasmodic Torticollis Rating Scale

head postures within 10 minutes of the injection (Okumura et al., 1996; Nakazawa et al., 1999; Matsumoto and Pouw, 2000). These studies in animals demonstrated that alterations in the activity of one of the cerebellum's interfaces with the rest of the brain, could cause torticollis-like head postures. Klier et al. (2002) concluded that the inter-stitial nucleus of Cajal may function as a neural integrator for both oculomotor and cephalomotor control after they studied the results of injecting muscimol in the midbrain of subhuman primates to inactivate the INC and surrounding structures. They also proposed that the postural symptoms of cervical dystonia in humans may be explained by an imbalance in activity within such an integrator. This neural integrator hypothesis was further supported by a study on human subjects, where the investigators demonstrated the possibility of deficits in a neural integrator for cephalomotor control that may predict complicated patterns of head movements in patients with cervical dystonia (Sedov et al., 2017; Jinnah et al., 2017a). The investigators further advocated the role of proprioception in enhancing the performance of the head control neural integrator mechanism (Avanzino and Fiorio, 2014).

Vision assists in proprioception and sensory feedback as it enables us to interact with our environment (Figliozzi et al., 2005; Shaikh et al., 2013). The environment is dynamic and is abundant with information that may be utilized to guide behaviours necessary for survival. The extraction of pertinent information from the environment is facilitated by our ability to align specialized sensory apparatus with select objects of interest. For example, in order to extract visual information, primates can search their surroundings using rapid eye movements (saccades) to focus the high-resolution portion of the retina (the fovea) on a relevant object (e.g., a potential food source) for further examination (Cecala, 2016). Orienting spatial attention in response to head-turn and eye-movement is one of the most primary ways in which we process external stimuli (Posner et al., 1982; Corbetta, 1998; Corbetta et al., 1998). Overt and covert attention are terms that describe the ways in which the oculomotor system perceives attention. Spatial selective attention occurs independent of gaze-direction, i.e. objects in peripheral vision may be selected for processing similar to those in foveal vision (Von Helmholtz, 1867). The term covert attention is thus used to describe attentional selection of regions outside the central foveal region. The midbrain covert attentional network plays a key role in the detection of salient stimuli in our environment (Fecteau and Munoz, 2005; Bell et al., 2005; Fecteau and Munoz, 2006; Redgrave et al., 2010).

The superior colliculus (SC) is a key node involved in this process (Dean et al., 1989; Furigo et al., 2010). Detection of rapid changes in the environment confers survival advantage amongst species and relies on the accurate detection of approaching objects (Terry et al., 2008; Yilmaz and Meister, 2013; Vagnoni et al., 2015). Looming-sensitive neurons have been identified in the superficial layer of the optic tectum in early vertebrates and in the superior colliculus in mammals (Wu et al., 2005; Liu et al., 2011). In man, a functional magnetic resonance imaging (fMRI) study revealed that looming stimuli (but not random stimuli) activated the superior colliculus (Billington et al., 2010).

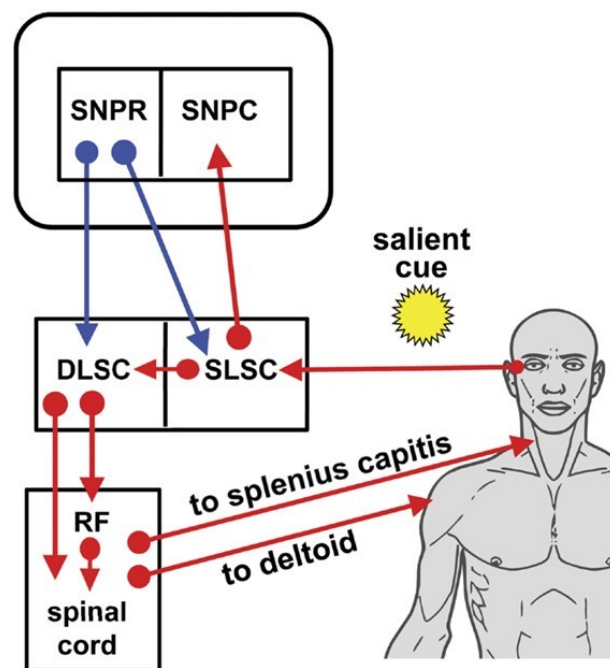


Figure 2.7: Reflexive covert orienting: the visual grasp reflex. The postulated basal ganglia and brainstem pathway involved in oculomotor and cephalomotor control. Blue arrows indicated inhibition; red arrows indicate excitation. DLSC=intermediate and deep laminae of the superior colliculus, RF=reticular formation, SLSC=superficial laminae of superior colliculus, SNPR=substantia nigra pars reticulata, SNPC=substantia nigra pars compacta. Adapted from Boehnke and Munoz (2008).

The superior colliculi are a pair of bumps on the dorsum of the midbrain. There are three superficial layers (SLSC) and four inner layers (Wurtz and Albano, 1980). The SLSC receive direct retinal input and contain visual neurons with retinotopically

organized receptive fields (Feldon and Kruger, 1970; Cynader and Berman, 1972; Gitelman et al., 2002; King, 2004; May, 2006). The two intermediate layers contain motor output neurons that control eye movements (Robinson and Keller, 1972), whereas the two DLSC contain multisensory integration neurons (Sprague and Meikle, 1965; Meredith and Stein, 1990). The outputs originating in the DLSC control eye movements and saccades through the oculomotor nucleus, head and neck movements through the cephalomotor nucleus, as well as reaching gestures of the upper limb (Goldberg and Wurtz, 1972; Corneil et al., 2002; King, 2004; May, 2006). The striato-nigro-collicular pathway forms a key connection between the Basal Ganglia and the SC. Thus, besides integrating multimodal sensory information from visual, auditory, and tactile sources (Wurtz and Albano, 1980; King, 2004; May, 2006), it also produces outputs for gaze, head, and arm movement; and is involved in target selection (Harris, 1980; Krauzlis et al., 2004; Boehnke and Munoz, 2008; Krauzlis et al., 2013) by directing priority signals to the Substantia Nigra pars compacta (SNpc) and the intralaminar nucleus of the Thalamus. As described previously, it has been hypothesized that cervical dystonia is a disorder of this midbrain network for covert attentional orienting (Hutchinson et al., 2014), caused by reduced GABA inhibition which sub-clinically manifests as abnormal temporal discrimination and clinically manifests as cervical dystonia.

2.6 Imaging of the Midbrain and SC

Up until 1998, the functional architecture of selective attention had been inferred largely on the basis of anatomical labelling (Morecraft et al., 1993) and lesion studies (Mesulam, 1981). One of the earliest studies to capture superior collicular activation was in 1998 when a team undertook a comprehensive study of the functional anatomy of attention to visual motion using fMRI (Büchel et al., 1998). They reported significant subcortical activations in the medial Thalamus and the right SC besides in the cortical areas such as the frontal eye fields, frontal, parietal and occipital cortex. On similar lines, although the organization of the visual cortex had been studied via noninvasive functional imaging methods such as PET (Fox et al., 1987) and fMRI (Sereno et al., 1995; Engel et al., 1997), the organization of the human SC had not been studied with fMRI until 2000. This was due to its location at the rear of the midbrain, rendering it inaccessible to electrophysiological probes, and its small size and movement with

blood pulsation in the brainstem, resulting in its observation with noninvasive imaging methods difficult (Poncelet et al., 1992). However, with the advent of 3T MRI technology, DuBois and Cohen (2000) made use of a cardiac triggering and novel intensity correction method (Guimaraes and Santos, 1998) to image the SC. The SC was specifically targeted by using oblique coronal slices include a plane passing through the superior and inferior colliculi, 3.0 mm thick with no spacing, covering the entire volume of the superior colliculi and with an in-plane resolution of 1.56 mm. With these improved parameters, they were able to successfully map the spatiotopic organization of the SC and provide evidence that the SC is an important hub for visuospatial perception (DuBois and Cohen, 2000).

One of the most interesting and earliest studies investigating the neural basis of visually guided head movements was carried out by Petit and Beauchamp (2003) via an event-related fMRI paradigm with human subjects. Using a 3T GE MRI scanner with a slice thickness of 1.2mm and an in-plane resolution of 0.94mm for the structural scan, and a slice thickness of 5mm and an in-plane resolution of 3.75mm for the functional scan, they analysed brain activation regions for eye, head, and gaze movements. A volume-of-interest (VOI) approach was employed to delineate the regions of the SC. Although they identified consistent activity in the SC, they emphasized the need for a higher signal-to-noise-ratio (SNR) to allow detection of BOLD signal change in brain stem structures, along with physiological noise correction, particularly during heartbeat and respiration. Furthermore, most of their preprocessing description rested on motion correction particularly for the head-movement paradigm, with no indication for the standard procedures for fMRI preprocessing such as coregistration, normalization and smoothing.

The findings of the literature search process for the review of imaging, MRI and particularly fMRI analysis concerning the SC is described as follows. Most of the articles from 1998 to 2007 made use of 1.5T imaging technology along with varied pre-processing approaches and software. Sylvester and colleagues were one of the first to use a 3T scanner along with a region of analysis (ROI) approach for the SC by identification of landmarks on each subject's T1 image and studying the resulting percentage signal change (PSC) in the SC. They also engaged a more rigorous motion correction procedure that included cardiac noise correction with pulse oximetry data. The task fMRI paradigms were diverse and depended on the hypothesis being probed

but Limbrick-Oldfield et al. (2012a) utilised a paradigm quite similar to the Billington et al. (2010) article. 22 out of the 33 articles utilised 3T imaging technology. Recent studies have reported the midbrain structures and the SC with high-field imaging technology such as 7T (Jorge et al., 2018) and 9.4T (Loureiro et al., 2017, 2018) due to enhancements in acquisition scanners and image processing methods. Markedly, most articles utilize whole-brain functional scans, with some aligning with the Pons to include the midbrain and part of the brainstem. Slice thickness has ranged from 1.5 mm to 6.6 mm, the latter rendering exact recording of midbrain activity more challenging. The most commonly employed software for pre-processing in the literature has been SPM (n=21/33) along with FSL and AFNI. The articles reviewed varied in their pre-processing approaches probably due to the lack of a gold standard for pre-processing. All articles reviewed performed realignment/motion correction in addition to some form of co-registration and/or normalization. The choice of smoothing parameters (kernels and degree) were vastly different across the studies. While many employed the standard Gaussian kernel for smoothing, one employed Hanning (n=1) and another a Boxcar version (n=1), with two articles mentioning nothing about this procedure. Five articles employed no smoothing for ROI analysis. These variations are likely due to the fact that smoothing tends to bias the data to detect results on the same scale as that of the kernel employed. While this may be useful for detecting activations on the scale of the SC, the potential for signal pollution from surrounding structures such as blood vessels and CSF may, however, offset the gain in SNR (Reimold et al., 2006).

Out of the 33 articles, 12 carried out a region of interest analysis with the SC that included extracting beta-weights, values and calculating percent signal change (Table 2.3). While a few others also traced ROI's in the SC, they continued to use wholebrain statistics for the analysis and made use of the defined ROI for performing procedures such as voxel-wise correction rather than extracting signals/time series from the region. There was a mix of functional ROIs and structural ROIs for the SC but most of the ROI studies (n=7) applied manual tracing on individual T1 as a means of ROI definition. Other ways included using standard templates (these ranged from atlas-definition to semi- individual definitions where the ROI centre coordinates were averaged from individual scans and a sphere with a set radius was seeded at this point). Physiological modelling and cardiac gating (DuBois and Cohen, 2000)

were undertaken in very few studies to correct signals resulting from noise in the SC. Verstynen and Deshpande (2011) modelled electro-cardiogram recordings with the RETROICOR algorithm (Glover et al., 2000a) as part of their GLM whereas, Bellot et al. (2016) utilised a photo-plethysmographer to record the R-peaks in the cardiac cycle and modelled heart rate variability as part of their GLM. Physiological recording has been considered to improve the SNR and produce better results except in the case of the study from Verstynen and Deshpande (2011) where it had no effect. Along with a canonical HRF being accepted for modelling BOLD responses in midbrain structures, Wall et al. (2009) identified that an HRF with a 4s peak as being superior in detecting SC activation, due to its proximity to large vasculature which rapidly responds to increased metabolic demand.

Table 2.3: Functional MRI studies undertaken with a region of interest analysis of the SC. PSC = Percentage Signal Change, SC = Superior Colliculus, HC = Healthy Controls, PAT = Patients, β = beta, HRF = Hemodynamic Response Function, STC = Slice Timing Correction.

Study	No. of subjects	Pre-processing	ROI Definition	ROI Analysis	Results	
Almeida et al., 2015	20 HC	STC, Temporal filtering, Motion correction, Smoothing: 6mm, Normalization: Talairach	N/A for SC (ROI only for Amygdala)	None for SC (β for Amygdala)	Increased SC activation implying it is involved in processing implicit emotional content	
Coullon et al., 2015	7 PAT, 8 HC	Motion correction, BET, Coregistration, Normalization: MNI, Smoothing: None	Anatomically based on subject's T1	PSC	The SC is recruited for auditory processing in both anophthalmic and early blind individuals	
Zhang et al., 2015	13 HC	Realignment, Coregistration, Normalisation, Smoothing: None	Drawn on individual's T1	β -value	SC strongly responded to iso-luminant stimulus defined by chromatic contrast, suggesting that the SC is not colour-blind	
Zhang et al., 2015	18 PAT, 18 HC	Realignment, Normalisation: None	Coregistration, MNI, Smoothing: None	Manually traced from 0mm to different depths on individual's T1	β -value	Compared to controls, early glaucoma patients showed more reduction of response to transient achromatic stimuli than to sustained chromatic stimuli in the superficial layer of the SC.
Olive et al., 2015	7 + 18 HC	Realignment, Normalisation: MNI, Smoothing: 6mm	Coregistration, Segmentation, Anatomically derived in agreement with Martin et al., 2003	Activation detection with volume correction	First experimental evidence of the implication of the SC in bodily self-consciousness	
Furlan et al., 2015	15 HC	STC, High-pass filtration, Coregistration,	Functional and anatomical definition (4.5s HRF)	Normalized PSC	Besides saccade execution, saccade preparation also produced an increase in the hemodynamic activity of the SC	

Study	No. of subjects	Pre-processing	ROI Definition	ROI Analysis	Results
Katyal et al., 2014	5 HC	STC, Motion correction, Normalization, Smoothing: None, Segmentation	Using the localizer sessions, 4.5 mm ² surrounding peak depth-averaged amplitude	BOLD amplitude modelled via two approaches	The SC has a reliably lateralized detection response, a putative correlate of endogenous attention.
Steuwe et al., 2014	16 PAT, 16 HC	Motion correction, Smoothing: 8mm	Normalization, N/A	None	Post-traumatic stress disorder patients showed increased activation within the SC compared to controls
Himmelbach et al., 2012	16 HC	Motion correction, Coregistration, Smoothing: 3mm	Realignment, Normalisation,	Functional ROI β value (4s HRF) and PSC	Ventral SC is involved in arm movement execution
Thompson et al., 2012	72 HC	STC, Motion correction, Coregistration, Normalization: ICBM152, Smoothing: 6mm	Functional ROI – peak – 27-voxel mask – EPI space	Average of time series from voxels	SC one of the regions that was activated for face selectivity
Limbrick-Oldfield et al., 2012	16 HC	Realignment, Normalisation, Smoothing: 2mm	Coregistration, Hand-drawn on MNI template	β value	Physiological noise regressors increases number of supra-threshold voxels in left and right SC
Billington et al., 2011	10 HC	Realignment, STC, Talairach, Smoothing: None for ROI analysis, 5mm for wholebrain	Normalisation: 27mm ³ drawn on individual scans using landmarks from a brain atlas	PSC	Significant difference between Loom and Recede activation in SC.
Deshpande et al., 2011	10 HC	Realignment, STC, Smoothing: 4mm	Normalisation: MNI, Functional ROI	Voxel-wise correlation	Weak effect of the inclusion of physiological noise terms, but improvement in overall estimates of task-related activity in the SC

Study	No. of subjects	Pre-processing	ROI Definition	ROI Analysis	Results
Krebs et al., 2010	10 HC	Motion Correction, Coregistration, Smoothing: 4- mm	Realignment, Normalization, MRICron and 3mm radius on each individual's T1	PSC and PE with 4.5s HRF for the SC	Contralateral functional representation of the generation of saccades in the human SC
Kleinhans et al., 2010	31 PAT, 25 HC	Motion Correction, Coregistration, Smoothing: 5- mm	N/A Cluster location of SC by visual inspection and Tal. atlas	Mean Z-score within ROI	Lesser activation in the SC in patients vs controls
Katyal et al., 2010	5 HC	Motion Correction, Normalization, Smoothing: 3-5 frame boxcar on time series	Realignment, 3 mm dia. Covering activated regions for Laminar Profile Analysis	Phase, BOLD amplitude, BOLD response	Topographic representation of signals corresponding to visual stimulation in the SC
Wall et al., 2009	6 HC	Realignment, STC, Smoothing: None	Coregistration, Drawn on individual's T1 with reference to brain atlas (Duvernoy, 1991)	β -value (multiple HRFs)	4-5s HRF peak optimally models SC activation
Himmelbach et al., 2007	13 HC	Realignment, Coregistration, Smoothing: None	Unwarping, Normalisation, MRICro and individual's T1	PSC	Significant changes in SC between free visual exploration and saccades with/without irrelevant stimuli
Das et al., 2007	14 PAT, 14 HC	Motion correction, coregistration, normalization: MNI, smoothing: 8mm	realignment, WFU PickAtlas	Subtraction analysis and ReML	SC-Amygdala correlation during nonconscious fear processing
Sylvester et al., 2006	8 HC	Realignment, Coregistration, Smoothing: 2mm, Cardiac noise correction	Identification of anatomical landmarks on T1	PSC	SC showed temporal-nasal differences while LGN and visual cortex did not show the same

Study	No. of subjects	Pre-processing	ROI Definition	ROI Analysis	Results
Watkins et al., 2006	17 HC	Realignment, STC, Coregistration, Normalisation, Smoothing: 9mm	sphere of diam. 4 mm centered on anatomical location of SC (defined by Calvert et al., 2001)	small volume correction	SC activated by multisensory illusory perception
Schneider et al., 2005	11 HC	Motion correction, coregistration, Smoothing: 5-point moving average for time series	Voxels with significant correlation of time series with frequency	Time-series	SC responded to visual motion stimuli, feasibility of studying subcortical structures using high-resolution fMRI
Schmitz et al., 2004	16 PAT, 15 HC	Realignment, STC, Coregistration, Normalisation, Smoothing: 8mm	Extracted from activated clusters	β -value	Activations of the SC in patients
Petit et al., 2003	6 HC	Motion correction, Normalization	Manually traced on individual's T1	Activation within the volume	SC active during eye, head, and gaze movements
DuBois and Cohen, 2000	6 HC	Realignment, Coregistration, Smoothing: 3mm	Drawn on individual scans (EPI)	Voxel count > 0.25 R^2 with GLM	SC active, Cardiac gating can compensate for pulsatile motion in midbrain

2.7 Neural correlates of AOIFD and CD

2.7.1 Major Regions Implicated

a The Basal Ganglia

The Basal Ganglia has been one of the major regions implicated in movement disorders due to its circuitry that controls voluntary movement (Albin et al., 1989; Cui et al., 2013; Fujita and Eidelberg, 2017). The structures that form the Basal Ganglia, i.e. the Striatum (Caudate and Putamen), Globus Pallidus (internal and external segments), Subthalamic Nuclei and Substantia Nigra (pars reticulata and pars compacta), together with other brain regions like the Thalamus and brainstem, are involved in two main pathways for movement – the direct and indirect pathway (Alexander et al., 1990; Cui et al., 2013; Lanciego et al., 2012; Freeze et al., 2013). While the direct pathway is responsible for promoting movement, the indirect pathway inhibits movement (Sano et al., 2013). Both of these pathways originate in the Striatum which mainly consists of GABAergic neurons (Kita, 1993; Tepper et al., 2010; Girault, 2012a). The Basal Ganglia receives excitatory projections from multiple cortical and sub-cortical regions (Redgrave et al., 2010) and the Thalamus (Smith et al., 2004). A combination of excitatory and inhibitory connections control movement. Glutaminergic neurons from the cortex activate different groups of Medium Spiny Neurons (MSNs) in the Striatum projecting to i) the (GPi) and the SNpr via monosynaptic connections. This is the direct pathway. The GPi and SNpr indirectly via a polysynaptic relay involving the GPe and the STN. This is the indirect pathway. Dopamine activates the direct pathway and inhibits indirect pathway (Lanciego et al., 2012). iii) the GPi and SNpr via the STN. This is the hyper direct pathway (Nambu et al., 2002).

Motor function in humans has been associated with the Basal Ganglia - Brainstem pathway (Takakusaki et al., 2004). The role of the Basal Ganglia in dystonia originated with studies showing neuropathological defects in the Basal Ganglia and brainstem of individuals with various secondary forms of dystonia (Zweig et al., 1988; Standaert, 2011; Prudente et al., 2013). The Basal Ganglia has been further implicated by studies involving neurosurgical interventions showing that dystonia improves in patients following thermolytic lesions of the internal segment of the Globus Pallidus. The role of the Globus Pallidus has been reviewed previously (Berardelli et al., 1985; Hallett, 2006).

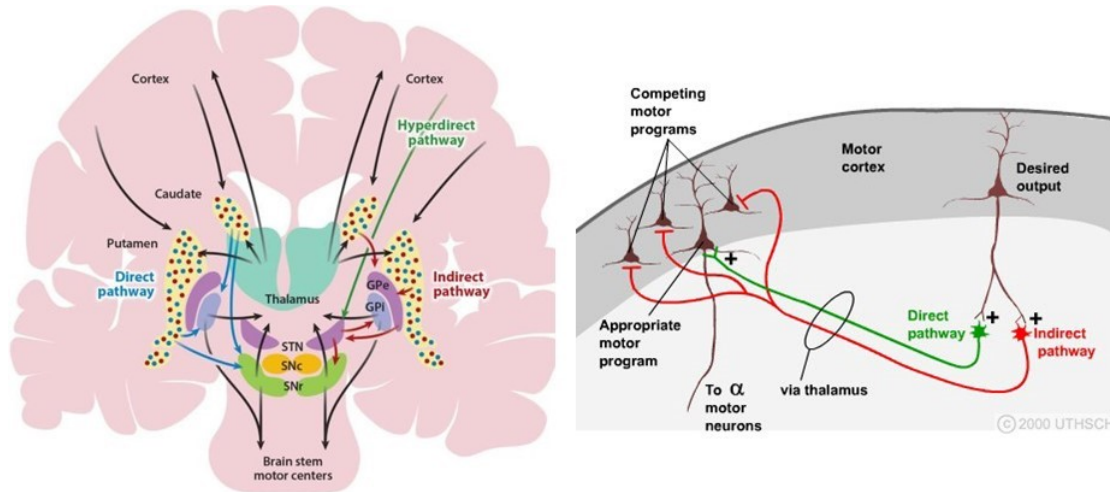


Figure 2.8: The direct, indirect and hyper direct pathways of the Basal Ganglia that cause varying motor outputs (Adapted from Nelson and Kreitzer, 2014 (left) and James Knierim, The Johns Hopkins University (right).)

Despite the strengths of the associations between dystonia and the Basal Ganglia, the correlations between dystonia and Basal Ganglia dysfunction are not clear. For example, there are many patients with dystonia who also have lesions but these do not affect do not affect the Basal Ganglia or its connections (Pettigrew and Jankovic, 1985; Bhatia and Marsden, 1994; Neychev et al., 2008). This observation implies that other regions may also play a role and further understanding of the Basal Ganglia circuitry with relevance to dystonia is needed.

b The Cerebellum

The Cerebellum is located behind the top part of the brainstem (where the spinal cord meets the brain) and is made of two hemispheres. It receives information from the sensory systems, the spinal cord, and other parts of the brain and then regulates motor movements (Avanzino et al., 2015a; Hardwick et al., 2013). The Cerebellum coordinates voluntary movements such as posture, balance, coordination, and speech, resulting in smooth and balanced muscular activity. There has been abundant evidence from animal studies indicating its pivotal contribution to different dystonias (LeDoux et al., 1998; Pizoli et al., 2002; Raike et al., 2005). This anatomical structure has been extensively reviewed in recent dystonia literature (Pong et al., 2008; Hardwick et al., 2013; Prudente et al., 2014; Bologna and Berardelli, 2017a). However, due to contradictory reports (Neychev et al., 2008; Sadnicka et al., 2012),

it is important to identify specific areas in the Cerebellum as well as its interplay with the dystonia macro-circuit to elucidate its role in this disorder. The cerebellar vermis has recently been identified as one such node in the Cerebellum contributing to dystonic pathophysiology (Alarcon et al., 2001; Pizoli et al., 2002; Usmani et al., 2011; Alvarez-Fischer et al., 2012), due to its projections to the motor areas (Coffman et al., 2011) as well as its visual inputs from the superior colliculus (Roldan and Reinoso-Suarez, 1981). However, there remains an ongoing debate concerning dystonia being classified as a cerebellar or basal-ganglia disorder (Kaji et al., 2018).

2.7.2 The Network Concept

The multifariousness of etiology, therapeutic responsiveness, penetrance, genetics and clinical manifestation complicates disease diagnosis and treatment of dystonia. Furthermore, the anatomical and functional heterogeneity underlying dystonia remains incompletely understood. This raises the question of whether there is one unifying model that underlies all forms of dystonia or whether dystonia symptoms manifest as a result of physiological changes in multiple circuits or locations across the peripheral and central nervous system. Several hypotheses regarding the pathophysiology of dystonia emphasize alterations in the Basal Ganglia Thalamo-Cortical motor circuit (Hendrix and Vitek, 2015), that stemmed from the initial Basal Ganglia dysfunction hypothesis. Neychev et al. (2011) discussed flaws in the Basal Ganglia hypothesis at length in their review. The hypothesis surrounding dystonia has evolved to include the Cerebellum (Sadnicka et al., 2012). Due to several questions that arise concerning the Cerebellum, such as the lack of ataxia and ocular nystagmus (common signs of cerebellar damage), its central role in the disorder is still in debate (Prudente et al., 2014).

More recently, mounting evidence from neuroimaging, behavioural and neurophysiological studies suggest multi-regional involvement and this has led to a system-level malfunctioning network concept of this movement disorder (Fuertinger and Simonyan, 2017; Jinnah et al., 2017b; DeSimone et al., 2019). Cerebellar and Basal Ganglia dysfunction are usually studied in isolation. However, in the network model of dystonia, their dysfunctions are relayed via separate subcortical pathways to the cerebral cortex, resulting in a final expression of dystonia (Akkal et al., 2007). Symptomatic animal models indicate that these anatomical structures are nodes in an

integrated network that is dysfunctional in dystonia (Wilson and Hess, 2013).

A review carried out by Jinnah et al. (2017b) collates evidence supporting the motor network model in dystonia and argues that different regions may play important roles in different subtypes of dystonia. To date, precisely how the motor network is disrupted in different types of dystonia remains ambiguous. Patients with dystonia display not only motor symptoms, but also a number of disturbances in the sensory domain and in cognitive processing of movements, such as movement simulation and prediction (Butterworth et al., 2003; Simonyan and Ludlow, 2010; Opavsky et al., 2012; Konczak and Abbruzzese, 2013; Avanzino et al., 2015b; Dresel et al., 2006). Thus, the network model of dystonia implicates a network level dysfunction comprising of Basal Ganglia–thalamic–frontal regions, as well as the somatosensory cortex and Cerebellum.

Impaired reaching movements, indicative of alterations in proprioceptive sensory input (Himmelbach, Linzenbold, Ilg, 2013), have been found in Cervical Dystonia (Marinelli et al., 2011). This cephalomotor disorder has subsequently been linked to the SC, a midbrain structure which has roles in orienting towards visual stimuli, saccade control and reach-related movements (Hikosaka et al., 2000; Linzenbold and Himmelbach, 2012; Himmelbach et al., 2013). The current hypothesis underlying CD suggests reduced GABA inhibition in the SC resulting in a subclinical manifestation as an abnormal temporal discrimination due to prolonged duration firing of the visual sensory neurons in the superficial laminae of the superior colliculus and clinically manifested by cervical dystonia due to disinhibited burst activity of the cephalomotor neurons of the intermediate and deep laminae of the superior colliculus. Abnormal temporal discrimination in unaffected first-degree relatives of patients with cervical dystonia represents a subclinical manifestation of defective GABA activity both within the superior colliculus and from the SNpr (Hutchinson et al., 2014). While the neural integrator hypothesis further illuminates possible mechanisms at play (Shaikh et al., 2016), a number of experiments are required to test the hypothesis surrounding the role of the SC and GABA in cervical dystonia.

2.8 Chapter Conclusion

This review of the literature was based upon the central premises that i) a dysfunction in the SC and subsequently the covert attentional orienting network is responsible for

both the clinical manifestation of CD as well as the subclinical manifestation of its endophenotype, an abnormal TDT and, ii) unaffected relatives with an abnormal TDT may/may not manifest the disorder at a later stage. Additional studies are required to authenticate these postulations and augment dystonia research. To conclude, the key outcomes identified are summarized as follows:

- Although the SC has been shown to play a key role in CD in primates, no study has been undertaken to date in humans which explores the role of the SC and the CAO network in CD patients, relatives with normal and abnormal TDT and healthy controls.
- Multifarious pre-processing pipelines currently exist for BOLD signal detection in the SC. However, reliable and robust imaging of the SC remains a challenge. Feasibility of imaging the SC via a task-fMRI paradigm in CD patients is unknown.
- Despite temporal discrimination being a reliable indicator for the existence of sensory abnormalities in CD, and abnormal TDT being a strong endophenotype candidate in CD, little is known about its circuitry and the neural correlates of an abnormal TDT in CD patients and unaffected relatives.
- The multitude of neuroimaging research undertaken to date in AOIFD and CD has involved employing univariate analysis on unimodal data. While this approach has greatly helped to shed light on abnormalities in specific regions, it does not explore the joint encoding of information across brain structure and function and does not combine information from multiple voxels/regions/modalities simultaneously.

3 Research Questions

A number of research questions emerged from the gaps identified in the review of the literature, as discussed in Chapter 2. While the present premise implicates the midbrain network for covert attentional orienting in the disorder, as well as in the endophenotype, there exists a clinical as well as a scientific need to validate these theories. This enabled the formation of the following principal research themes and a number of definitive research questions within each theme.

3.1 Examining the Role of the Superior Colliculus and the Covert Attention Network

- 1) Is superior collicular activity abnormal in patients with cervical dystonia and their unaffected relatives with abnormal temporal discrimination?

While animal models suggest a role of the SC in cervical dystonia pathophysiology, this link has yet to be established in patients. It is hypothesized that both abnormal TDT and CD arise from a dysfunction in the SC, possibly due to abnormal GABA levels in this structure, and that this will reflect as a difference in SC activity in the patient and relative cohorts when compared to healthy controls.

- 2) Is there any correlation between temporal discrimination threshold values and superior collicular levels of activation?

Evidence suggests that abnormal GABA levels in the SC is responsible for a clinical manifestation of the disorder - cervical dystonia, and a sub-clinical manifestation of the endophenotype - abnormal TDT. Therefore, it is hypothesized that there exists a correlation between TDT values and SC activity.

- 3) Is it possible to capture a difference in SC activity via neuroimaging, considering its challenges?

Imaging the SC is a challenge due to its small size and location in the brain, proximity to vasculature and anatomical variability across subjects. These

complications get amplified in case of subjects with a movement disorder such as dystonia, due to motion artifacts that are detrimental to image acquisition and analysis. It is hypothesized that by the design and employment of an accurate fMRI paradigm, combined with the optimization of an fMRI analysis pipeline, SC activation may be reliably captured with neuroimaging data, even in movement disorder studies such as CD.

- 4) Can a 2nd level GLM and ROI approach be employed to reliably detect BOLD changes within the SC?

Imaging the SC is a challenge due to its size and location in the brain. Previous fMRI work investigating midbrain structures (including the SC) have employed different processing pipelines and smoothing kernels. It is hypothesized that study-tailored ROI definition and analysis of the SC may yield reliable BOLD activity detection from the SC, and thus enable a robust analysis in CD patients.

- 5) Does the response of humans to visual looming stimuli vary when compared to their response to receding and random stimuli?

Previous research suggests the SC is a central node in the fight/flight pathways and consists of looming sensitive neurons. Billington et al. (2010) demonstrated SC activity in human subjects for looming vs. receding visual stimuli. However, this study did not carry out a 2nd level GLM and reported results from only eight subjects. This warrants the need for a replication study with a higher subject number, which will subsequently aid in comparing the SC response in CD patients vs. healthy controls. It is hypothesized that the SC responds differently to looming visual stimulus compared to receding visual stimulus.

- 6) Do hypothesized GABAergic abnormalities lead to downstream/upstream effects in other associated structures?

Putaminal abnormalities (structural and functional) have been observed in CD patients and unaffected relatives with an abnormal TDT. Structures such as the Thalamus and Caudate (which have been implicated in CD) also form an important network in the covert attention circuit. It is hypothesized that the observed putaminal differences are a result of connectivity abnormalities in the bottom-up network for covert attention, resulting from disrupted activity in the

SC.

- 7) Can the loom-recede visual paradigm's influence on the SC be instrumental in detecting the connectivity changes across the covert attentional orienting network?

The loom-recede-random paradigm has been proven to elicit a BOLD response in the SC (Billington et al., 2010). However, it is yet to be demonstrated if this response in the SC translates to ripple connectivity effects in other associated structures. It is hypothesized that possible defective processing of looming visual stimulus in the SC will have an impact on other associated structures in the covert attention network.

3.2 Investigating the Neural Correlates of TDT in Unaffected Relatives of CD Patients

- 8) What regions of the brain are involved in disordered sensory processing and share common patterns with the dystonia circuit?

Despite the potential importance of temporal discrimination as a marker of disordered sensory processing in the pathophysiology of CD, the neural network underlying abnormal temporal discrimination in CD is poorly understood. To date, only a few studies have identified structures such as the putamen linking abnormal temporal discrimination and CD. The heterogeneity of phenotypes makes it imperative to study each phenotype and its associated endophenotype in patients as well as unaffected relatives. It is hypothesized that neural substrates of abnormal temporal discrimination will be reflected in first-degree relatives of CD patients, who may be possible gene-carriers of the disorder.

- 9) How might a study on unaffected relatives help to understand the dystonia circuit?

Unaffected relatives (of CD patients) with an abnormal TDT are hypothesized to be as yet unidentified gene carriers, with TDT attributed as a mediational endophenotype in the disorder. Abnormal putaminal structure (hypertrophy by VBM analysis) and function (reduced activation by fMRI during a temporal discrimination task) have been reported in unaffected relatives with abnormal TDTs. It is hypothesized that neural correlates of abnormal temporal

discrimination will exist in unaffected relatives and this may aid in understanding the role of sensory abnormalities, as well as TDT as an endophenotype in this disorder.

- 10) Are there statistically significant differences in connectivity in relatives with normal TDT vs. abnormal TDT?

Previous research implicates the putamen and the SC in abnormal temporal discrimination as well as CD. Few studies have investigated unaffected relatives with normal vs. abnormal TDT. Since CD is postulated to be a network disorder, it is unlikely that neural correlates of its endophenotype are limited to one specific region in the brain. If abnormal TDT is indeed a heritable marker, it is hypothesized that gene carriage may translate to alterations in connectivity and brain network topology in unaffected relatives harbouring this endophenotype.

- 11) Will resting-state functional connectivity help illuminate possible connectivity changes in unaffected relatives of CD patients?

While task-specific neuroimaging studies have great potential to explore the regions and networks underlying an abnormal TDT, differences found with task-fMRI may reflect compensatory effects of the task, thus confounding the primary pathophysiological mechanisms involved. It is hypothesized that rs-fMRI will be sensitive and offer an unbiased medium, for detecting possible alterations in resting functional connectivity architecture in unaffected relatives of CD patients.

- 12) If functional connectivity alterations exist in unaffected relatives with abnormal TDT, do they manifest as local, regional, network or as compensatory mechanism changes?

To date, structural and functional connectivity changes have been identified in CD patients when compared to controls. These have ranged from micro-structural white matter abnormalities to widespread system-level network changes. While CD is considered to be a sensory-motor and neural integrator disorder, micro and macro changes have not yet been probed in unaffected relatives that are postulated to be non-penetrant gene carriers if they have an abnormal TDT. It is hypothesized that local, regional as well as global neural network connectivity differences will

exist in unaffected relatives who manifest sensory abnormalities such as abnormal TDT.

3.3 Exploring the contribution (and combination) of structure and function in the manifestation and automated diagnosis of CD

- 13) Do both structural and functional differences need to exist in CD patients for disorder manifestation?

Neuroimaging evidence suggests the existence of structural abnormalities in the Thalamus, striatum and cerebellum. In addition, independent studies have also demonstrated functional (activation and connectivity) differences in the sensory-motor, parietal, frontal and occipital areas of the brain. Yet, there has been no study linking these discoveries together. It is hypothesized that the combination of information from different modalities during the analysis will help to link (apparently) disconnected findings in the past and provide more conclusive evidence for the network dysfunction concept in CD.

- 14) Can structural and functional abnormalities detected be employed to automatically and accurately identify the manifestation of CD?

Only one study recently employed the abnormalities detected in rs-fMRI for automatic classification of CD patients and healthy controls (Li et al., 2017). They achieved an accuracy of 90.6% on a study with 14 patients and 14 controls. It is hypothesized that the deployment of structural and functional abnormalities together in a combined analysis will aid in the automated diagnosis of CD.

- 15) Can abnormalities detected from data across multiple modalities be combined to enhance the classification of patients and controls?

Due to cost, time and practical constraints, the preferred method for clinicians would be to use one modality, acquisition paradigm and/or data analysis method to aid in identification of the disorder. However, recent evidence points towards multi-regional network concept of dystonia. Therefore, it is hypothesized that abnormalities detected across different neuroimaging modalities may be combined to reveal the dependencies of one over the other as well as enhance

classification accuracies due to the enriched information available from the combined multimodal feature set.

- 16) How does multivoxel pattern analysis (MVPA) compare to a univariate analysis method in neuroimaging and with respect to CD?

Research in AOIFD and CD to date has predominantly followed a univariate approach of analysis. A univariate analysis focusses on decoding voxel-level differences across cohorts. Furthermore, conventional group-level neuroimaging data analysis techniques have only been able to identify average between-group differences and haven't been able to make predictions on individual subjects. No study to date has employed MVPA in cervical dystonia. It is hypothesized that an MVPA methodology will help decode individual subjects' brain states using neuroimaging scan data, and with greater sensitivity.

- 17) What is the best approach to combine feature sets/data from multiple modalities in cervical dystonia?

Data from multiple modalities can be simultaneously or separately acquired as well as analysed. Due to CD being a rare disorder, subject availability is a major issue in many studies, and therefore separate acquisition followed by data fusion at a later stage seems the most practical scenario. It is hypothesized that features from each modality may be combined at different stages of the pipeline, and have an impact on the final classification results. Few studies have investigated neuroimaging data fusion methods, with none undertaken to date in dystonia.

- 18) Do sample sizes vs. the rich feature sets pose a problem in neuroimaging? What is the solution for this with respect to data from CD patients and controls?

In many neuroimaging studies, the sample size (number of subjects) is very often <100. In comparison, pre-processed brain scans usually contain (>100,000) non-zero voxels. Consequently, the numbers of features (voxels) critically outnumber the number of observations (sample size). Various dimensionality reduction methods exist and vary according to the dataset. This warrants the need for an investigation into the most appropriate method specific to the current dataset as well as for future studies in dystonia.

19) Is it possible to use ensemble learning for data fusion and classification accuracy enhancement in a multimodal MVPA of acquired neuroimaging data in dystonia?

In statistics and machine learning, ensembles use multiple learning algorithms to generate a better predictive model than could have been obtained from any of the constituent learning algorithms independently. If unimodal as well as multimodal data are not powerful with the traditional pattern analysis methods, it is hypothesized that ensemble learning will aid in pattern recognition with neuroimaging data in dystonia.

3.4 Conclusion

In light of the literature review, the central premise established as well as the subsequent research questions discussed, the overarching goal of this thesis was to investigate irregularities in neurological structure and function in cervical dystonia, via novel and sophisticated computational modelling methods with neuroimaging data, in order to ascertain: i) the role of the SC in CD and temporal discrimination ii) neural correlates of sensory abnormalities such as abnormal temporal discrimination due to potential gene carriage in unaffected relatives, and iii) the contribution (and combination) of brain structural and functional alterations that lead to the manifestation of CD and aid in the automated diagnosis of this disorder. This resulted in the design of the following studies with a cohort that consisted of **CD patients, unaffected relatives and healthy controls**, in order to address the above research questions:

- **Study 1 - Studying the role of the Superior Colliculus.**
- **Study 2 - Examining the mid-brain network for covert attentional orienting.**
- **Study 3 - Probing neural correlates of abnormal temporal discrimination.**
- **Study 4 - Investigating multivoxel pattern analysis with resting-state, functional and structural MRI data.**

4 General Methodology

Based on the literature review discussed in Chapter 2, the research questions and central hypotheses discussed in Chapter 3, a systematic recruitment of participants, comprising of CD patients, their unaffected first-degree relatives and healthy controls, was undertaken. TDT testing and neuroimaging data were acquired in order to address: i) the role of the SC in CD and temporal discrimination, ii) neural correlates of TDT in unaffected relatives, and iii) the contribution (and combination) of brain structural and functional alterations leading to CD manifestation. This chapter outlines the general methodology that was followed for data acquisition across all studies. It has been divided into two main parts; a) the TDT task, data acquisition and subsequent data analysis, followed by b) MRI data acquisition and data pre-processing. Each study henceforth will refer to the data acquired as described in this chapter.

4.1 Ethical Approval from Research Ethics Review Board

Ethical approval for the research studies was granted by the Ethics and Medical Research Committee, St. Vincent's University Hospital, Elm Park, Dublin 4, Ireland. All experiments were performed in accordance with relevant guidelines and regulations. Written informed consent was obtained from all participants for study participation and publication. A copy of the approval letter is provided in Appendix A.

4.2 Subject Recruitment

Recruitment consisted of enrolling CD patients, their unaffected first degree relatives and healthy age-matched control subjects. CD patients were recruited from the Out Patients Clinic at the Department of Neurology, at St. Vincent's University Hospital. Recruitment also included age and gender-matching relatives and healthy controls to form the corresponding cohorts.

4.3 Temporal Discrimination Threshold (TDT) Testing

Temporal discrimination testing was carried out and TDT scores were acquired from patients, unaffected relatives and healthy controls. This method is similar to the one described in (Bradley et al., 2009; Kimmich et al., 2011) and has been described below. It consisted of a) Sensory Testing b) TDT analysis as follows:

4.3.1 Sensory Testing

TDT testing (visual and tactile) was carried out in a single session, in a soundproof dark room. Two methods exist to collect visual TDT. One implementation of the paradigm employs a table mounted system consisting of stimulating lights positioned in the left and right peripheral vision and is carried out in a dimly lit room. In order to obtain more accurate and repeatable measurements, a head mounted system was later developed which helped to ensure that the stimulus position remained consistent relative to head movements. This head mounted system (Figure 4.1) is of particular importance for cervical dystonia, where patients report difficulty in maintaining a neutral head position during the original implementation, and was therefore used in the research studies presented here.

Asynchronous stimuli were progressively presented to an individual. Participants were tested for two modalities: (i) a visual task - two flashing light-emitting diodes (LEDs) lights were used, horizontally orientated and placed on the table in front of the subject. The lights were 7° into the subject's peripheral vision on the side of the body being tested; and (ii) a tactile task - non-painful, above-threshold electrical stimulation was used on the second (index) and third (middle) fingers on the side of the body being tested using square-wave stimulators (Lafayette Instruments Europe, LE12 7XT, UK). Stimulus current was progressively increased from zero in 0.1 mA steps to the lowest point at which the subject could reliably detect the impulse (tested using a paradigm with 10 trials of randomly assigned real or sham impulses requiring a response from the subject). Equality of stimulus intensity was then established between the digits if necessary. The stimulus current required ranged between 2 and 4.5 mA. Pairs of stimuli were synchronized initially and were progressively separated in 5 ms steps. When the subject reported that the pairs of stimuli were perceived as asynchronous on three consecutive occasions, the first of these was taken as the TDT. This procedure was

repeated four times on the left and right side of the body. The median of the runs was used for each subject to allow for practice effect and these results were averaged to obtain a summary (combined) TDT score (Bradley et al., 2009).

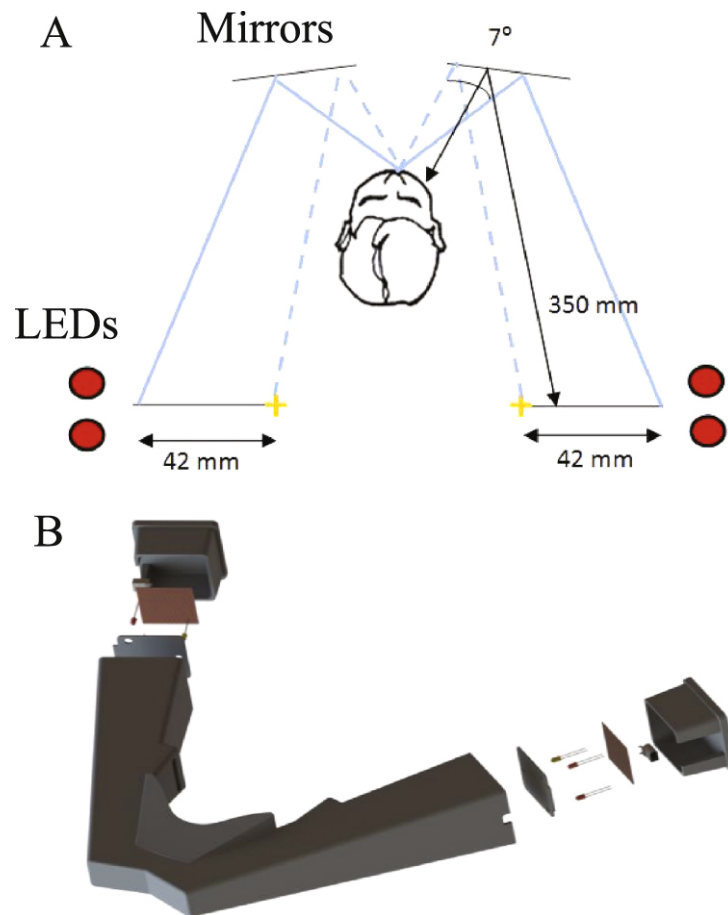


Figure 4.1: The TDT testing apparatus for the visual-visual stimuli method (A) a plan view schematic of the headset design. Light from the stimulating LEDs travels approximately 350mm to the eye of the participant via a reflecting mirror. (B) An enlarged 3D model representation of the headset. Adapted from (Molloy et al., 2014).

4.3.2 TDT Analysis

All TDT results (in milliseconds) were converted to standardized Z-scores using the formula shown in Equation 4.1. For each participant, the Z-score was calculated using the relevant age-related and gender related control data set. A TDT value resulting in a $Z\text{-score} \geq 2.5$ was considered an abnormal TDT.

$$Z\text{-score} = \frac{(\text{Actual TDT}) - (\text{Age and Gender Related Control Mean TDT})}{(\text{Age and Gender Related Control Standard Deviation})} \quad (4.1)$$

4.3.3 Subject Stratification

To aid in the comparison of relatives with normal vs. abnormal TDT and apply TDT as a regressor in further analysis, the aim was to stratify patients and unaffected relatives with abnormal TDT, and healthy controls and unaffected relatives with normal TDT. This led to the formation of four cohorts described (Figure 4.2) as follows:

a Cervical Dystonia Patients

16 cervical dystonia patients (10 women; four familial, 12 sporadic) (mean age: 53.5 years \pm 6.9 years) with abnormal TDT z-scores formed this cohort. They were patients from the Dystonia Clinic at the Department of Neurology at St. Vincent's University Hospital. Each patient's clinical diagnosis was confirmed by two neurologists with expertise in dystonia. Thirteen patients were receiving regular BoNT injections for their condition. The mean time since last injection in these patients was 41 days (\pm 24 days).

b Unaffected Relatives

32 unaffected first-degree relatives with 16 demonstrating abnormal TDT values and 16 demonstrating normal TDT values (22 women, mean age: 52.1 years \pm 8.7 years) were recruited. Seven had first-degree relatives with familial cervical dystonia; 25 had first-degree relatives with sporadic cervical dystonia. All had been clinically examined by two Neurologists with expertise in dystonia; none had any evidence of dystonia or dystonic tremor. The unaffected relatives were segregated into two cohorts for further analysis in each study – relatives with normal TDT (Relatives_{normal TDT}) and relatives with abnormal TDT (Relatives_{abnormal TDT}).

c Healthy Controls

From hospital staff as well as relatives of the research team, 16 healthy control participants with a normal TDT z-score were recruited (10 women; mean age: 51.0

years \pm 8.0 years).

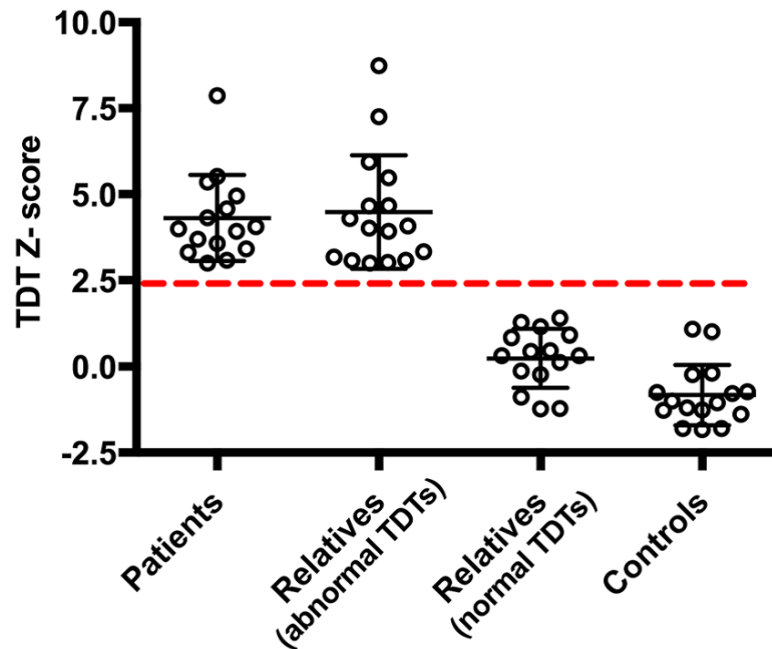


Figure 4.2: Participants' temporal discrimination threshold Z-scores: Temporal discrimination threshold (TDT) Z-scores in 16 patients, 32 relatives and 16 healthy controls. The black open circles represent individual TDT Z-scores. An abnormal TDT Z-score was defined 2.5 standard deviations above the age- and sexmatched population mean. The dashed-red line denotes a TDT Z-score of 2.5. All sixteen cervical dystonia patients had TDT Z-scores \geq 2.5, 16 unaffected relatives had a TDT Z-score \geq 2.5 (relatives with abnormal TDT), 16 unaffected relatives had a TDT Z-score $<$ 2.5 (relatives with normal TDT) and all 16 healthy controls had a TDT Z-score $<$ 2.5.

4.4 MRI Acquisition

MRI data was collected on a Philips 3T Achieva MRI Scanner at the Trinity College Institute of Neuroscience (Figure 4.3).

4.4.1 Structural MRI

A high-resolution three dimensional T1-weighted magnetisation-prepared rapid acquisition gradient echo sequence was acquired (TR = 8.4 ms; TE = 3.9 ms, TI = 1150 ms, flip angle = 8°) with a transverse orientation, a 256 by 256 matrix size and 0.9 mm isotropic voxels. A Vitamin E tablet was attached over the left eye in order to visualise orientation during scan processing.



Figure 4.3: Philips Achieva 3T MRI Scanner at Trinity College Institute of Neuroscience (TCIN), Dublin.

4.4.2 Functional MRI

Functional images were collected using 40 slices covering the whole brain (slice thickness 3 mm, inter-slice distance 0 mm, in-plane resolution 3 by 3 mm) with an echo planar imaging sequence ($TR = 2$ s, $TE = 25$ ms, flip angle = 90°). Each functional run consisted of 140 volumes. To ensure full coverage of the Superior Colliculi we orientated the slices parallel to the brainstem at the height of the Pons. The first four volumes from each run were discarded during the pre-processing stage in order to avoid T1 equilibrium effects. Restrictive padding was placed around the participant's head to minimize major head movements. The task employed during fMRI data acquisition will be discussed in the following chapter (Chapter 5).

4.4.3 Resting-fMRI

The resting state scan lasted around 5.30 min and involved an eyes open fixation on a white cross on a black screen. Resting functional images were collected using 40 slices covering the whole brain (slice thickness 3 mm, inter-slice distance 0 mm, in-plane resolution 3x3 mm) with an echo planar imaging (EPI) sequence ($TR = 2$ s, $TE = 25$ ms, flip angle = 90°).

4.4.4 Pre-processing

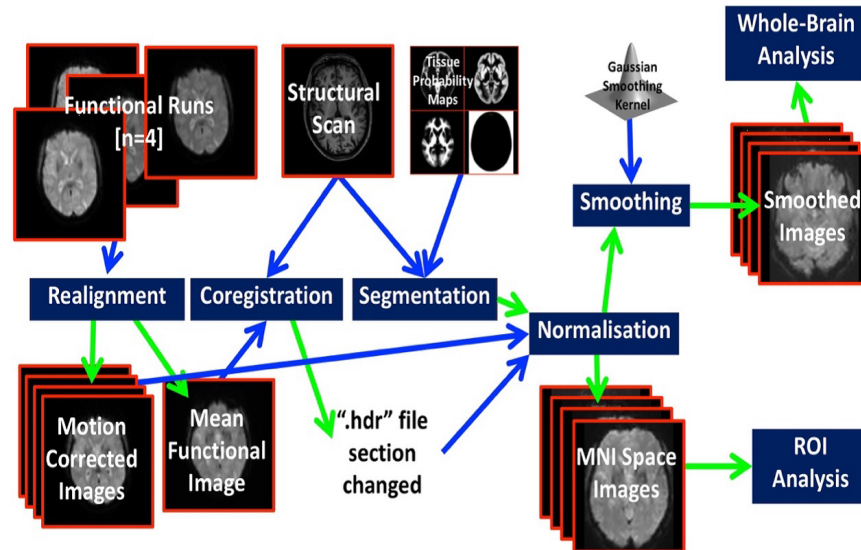


Figure 4.4: The general pipeline followed for pre-processing the functional MRI data.

Pre-processing of all subject scans was performed according to a pipeline developed as per the SPM 12 analysis suite as shown in Figure 4.4. Pre-processing consisted of resetting the origin, realignment, unwrapping, segmentation, coregistration and normalization, to allow intra- and inter-subject comparisons. Quality control was performed at all stages of pre-processing. Anatomical images were inspected for artifacts during the origin reset phase. They were again inspected and compared to the corresponding original after the completion of the pre-processing pipeline. The subjects' task performance data were examined for inattention and accuracy. Functional scans were monitored for quality by the automated quality reports generated.

- **Realignment** – consisted of linear rigid-body transformations to manipulate the scan images in order to correct for subject movement during the scan. Movement of the subject during the scan causes a decrease in Signal to Noise Ratio (SNR) and accuracy of spatial location as a given voxel can represent many different brain areas over time. Motion correction is thus necessary in order to optimise SNR. Translations along three planes and rotations over the three axes were used to minimise the sum of the squared differences between any two scans. Furthermore, scans from each functional run (during task-fMRI acquisition) were

separately realigned. A mean functional image was created which was used later in the pre-processing pipeline as well as text files containing the motion parameters estimated by the realignment function. Occurrence of motion artifacts was assessed across all acquired images. Mean \pm standard deviation of root mean square motion values were as follows: Healthy controls (0.47 ± 0.36), Relatives_{normal TDT} (0.48 ± 0.23), Relatives_{abnormal TDT} (0.39 ± 0.55) and CD patients (0.61 ± 0.28). Although participants in the CD did move slightly more than the other groups during scanning, no significant differences between groups means were found as determined by a one-way analysis of variance (ANOVA) with each subject's motion values [$F(3,60) = 1.718$, $p = .29$]. Nevertheless, motion correction measures were stringently applied during pre-processing, along with the usage of motion parameters as covariates during analyses, in order to limit its effects as a confounding variable.

- **Unwarping** – consisted of correction of warping in the magnetic field of the scanner due to motion artefact. Warping is a major component of movement-related residual variance which remains after realignment. This amounts to a correctable reduction in SNR, specificity and sensitivity. Different tissues and materials cause changing field inhomogeneities which can be observed with a deformation field. The motion artefact combined with these changes give rise to variance in the scan. Thus unwarping allowed for the non-linear correction of image distortion due to local changes in field strength. The images were then be resampled to allow artefact correction.
- **Coregistration** – consisted of the alignment of the structural (anatomical) image to the mean functional image generated as part of the realignment phase. This within subject matching allows for more accurate anatomical localisation of effects. Coregistration represents the automation of an otherwise laborious process of identifying individual landmarks on both the functional scans and the anatomical scans. This is done by registering the source image (origin reset anatomical) to the static reference image (mean functional image from the realignment phase), followed by translations and rotations for realignment, scaling and shearing. Interpolation is then performed where the intensity of the surrounding voxels in the functional image are compared with the voxels in the

structural image.

- **Segmentation** – consisted of identifying different brain tissues in the structural image. It aids in the normalisation process by overcoming noise artifacts, inhomogeneities and inter-sequence differences which render normalisation more error-prone. In SPM12, segmentation utilises 6 standard space Tissue Probability Maps (TPMs) which estimate the location of Grey Matter, White Matter and CSF.
- **Normalisation** – consisted of mapping subject scans to a standard space in order to allow for the comparison of inter-subject differences. This is achieved by mapping subjects' brains to a standard brain which aims to achieve correspondence of each voxel across all brains. This is vital for comparison of data across groups and across studies. Normalisation was carried out in the Montreal Neurological Institute (MNI) space (average of 152 healthy brains). Normalisation is vital for averaging results across subjects and through 2nd level GLM generalising study findings to a population level. Registration is based upon the inverse of the deformation fields applied to the TPMs in order to fit them to a subject's anatomical image during the Segmentation phase.
- **Smoothing** – consisted of applying a Gaussian low-pass filter to blur anatomical differences between subjects and local registration errors that were not corrected by pre-processing. While smoothing is generally used to increase SNR by reinforcing high or low signal areas and averaging out noise, the increased sensitivity is focused mostly on effects occurring on a scale similar to the smoothing kernel applied. A kernel size used is usually twice the voxel size and various FWHM kernels have been used in the past ranging from 0-20mm. Smoothing was/was not applied according to the study in question and has been specified in each chapter separately.

This pipeline was the basic framework for pre-processing followed for all research studies described in this thesis, and represents a robust and replicable method which is well-supported in the literature.

4.5 Chapter Conclusion

In order to address the research questions and central hypothesis, subject recruitment consisted of CD patients, unaffected relatives and healthy controls. This was followed by neuroimaging data acquisition (rs-fMRI, t-fMRI and s-MRI) from each of the four cohorts. The following chapter details the first study that was undertaken to study the role of the SC in the manifestation of CD and an abnormal TDT.

5 Heading for the Hills: A Study of the Response of the Superior Colliculus to a Looming Event in Patients, Unaffected Relatives and Controls

The SC (Latin for 'upper hill') is a paired structure located in the midbrain (Figure 5.1). The literature and current hypothesis in cervical dystonia implicate dysfunctional GABA activity in this layered structure, resulting in subclinical manifestation of the endophenotype (an abnormal TDT) and clinical manifestation of the disorder. While animal models suggest a role of the SC in its pathophysiology, this link has yet to be established in humans. Therefore, the following chapter seeks to address Research Questions 1-5 in Chapter 3.

The SC is a multimodal junction, which receives high-speed inputs mainly from the visual system as well as tactile and auditory modalities (May, 2006; Anderson and Rees, 2011). It is capable of determining rapid changes in visual stimuli through a network of inhibitory neurons (Kaneda et al., 2008). Defects in this inhibitory network are hypothesized to cause a loss in temporal sensitivity (Hutchinson et al., 2014) resulting in the phenomenon of an abnormal Temporal Discrimination Threshold. The SC also has a role in motor outputs to the head, neck and arms, responsible for coordinating head and eye movement (Hutchinson et al. 2014). Defective inhibition at the level of the SC and its inputs from the Substantia Nigra has been shown to give rise to abnormal motor outputs to the neck (Kaneda et al., 2008), akin to Cervical Dystonia (Holmes et al., 2012). The proposed task fMRI study will, therefore, aim to test the hypothesis that CD and an abnormal TDT are associated with dysfunction in the SC. Due to its size and location in the brain, there are a number of challenges associated with imaging of this structure, which need to be addressed for optimal activation detection. The study presented in this chapter was carried out in collaboration with Dr. Eavan McGovern and Owen Killian, and has resulted in the following peer-reviewed publication:

- Eavan M. McGovern, Owen Killian, Shruti Narasimham, Brendan Quinlivan, John B. Butler, Rebecca Beck, Ines Beiser, Laura W. Williams, Ronan P. Killeen, Michael Farrell, Sean O’Riordan, Richard B. Reilly, Michael Hutchinson. 2017.

Disrupted SC activity may reveal cervical dystonia disease pathomechanisms. *Scientific Reports*, 7(1), p.16753.

5.1 Introduction

Although basal ganglia dysfunction has been implicated in the pathogenesis of cervical dystonia, cortical, subcortical and cerebellar regions in the brain have been shown to play an equally significant role in its pathogenesis (Öztürk et al., 2018; Kaji et al., 2018). Additionally, alterations in basal ganglia-brainstem (Blood et al., 2012b) and cerebellum-brainstem connections have been implicated in the dysfunctional network (Neychev et al., 2011; Bologna and Berardelli, 2017a). The discovery of the head neural integrator and the stimulation of the interstitial nucleus of the Cajal causing postures resembling cervical dystonia helped decode one possible part of this disorder's complex circuitry (Klier et al., 2002; Shaikh et al., 2016; Sedov et al., 2017). Mounting evidence advocates an impaired SC as a causal node in the circuitry of this disorder.

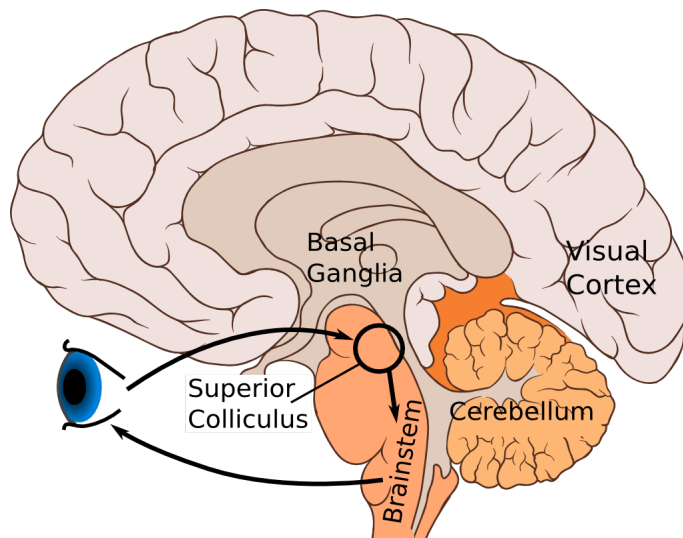


Figure 5.1: The retina projects to the SC located at the top of the midbrain. The SC in turn connects to motor neurons in the brainstem that control eye movements. This circuit generates saccades — quick eye movements from one location to the other.

The SC plays a pivotal part in the detection of looming stimuli and is a key node in the fight/flight response (Gandhi and Katnani, 2011). It transforms spatial information about a target location into orienting eye and head movements via projections to brainstem saccadic centres and the cervical spinal cord (May, 2006). These defensive

responses are modulated by GABA inputs to the SC and by intrinsic inhibitory interneurons within the SC. The midbrain covert attentional network detects sudden variation in the environment and alarms the individual to a salient stimulus, which requires appropriate assessment and subsequent action, which in many situations may be essential for survival. This confers species with a survival advantage which relies on the accurate and swift detection of approaching (looming) objects. Looming-sensitive neurons have been identified in the superficial layer of the optic tectum in early vertebrates and in the SC in mammals. In man, an fMRI study revealed that looming stimuli (but not random stimuli) activated the SC. In macaques, anatomical studies have shown that projections to downstream oculomotor and neck muscle structures originate in the deep layers of the SC. The tecto-spinal tract which innervates the neck, forearm and hand muscles, and the tecto-reticulospinal tract which partly make contact with motor neurons in the head muscles, all originate in the DLSC (Harris, 1980; Guitton and Volle, 1987; Corneil et al., 2002). A moving or sudden luminant visual stimulus was found to elicit electromyographic responses in cervical muscles involved in ipsilateral head-turning (Corneil et al., 2004; Boehnke and Munoz, 2008).

A fundamental neurophysiological feature of dystonia is reduced inhibition at all levels of the central nervous system. The SNpr has been found to play a principal role in this disorder, as it tonically inhibits the oculomotor and cephalomotor pre-motor neurons of the DLSC for saccade generation and head-turning (Dybdal et al., 2013). A study in macaques demonstrated a functional relationship between the SNpr and DLSC in regulating posture and movement illuminating the nigrotectal pathway's role in CD (Holmes et al., 2012). While a unilateral lesion of the SNpr in macaques caused movements resembling CD, further lesion in the SC abolished/attenuated these abnormal movements.

Understanding the role of the SC in the manifestation of sensory, motor and non-motor symptoms, is vital in order to develop a deeper understanding of the origin of irregular muscle contractions in the neck. With intensifying evidence of the role of abnormal temporal discrimination threshold as an endophenotype in CD, and in light of the visual sensory data concerning the SLSC and the motor evidence concerning the DLSC, it has been previously hypothesised that both the endophenotype (an abnormal TDT) and the clinical phenotype (cervical dystonia) are due to a disordered midbrain network for CAO (Hutchinson et al., 2014). A subclinical manifestation of GABA

disinhibition by abnormal temporal discrimination visual sensory neurons in the SLSC would entail the TDT presenting as an effective marker for the function of a subcortical network for novelty detection and attentional orienting.

Therefore, in order to assess the relationship between temporal discrimination, SC activity and cervical dystonia, the aim of this study was to examine, by fMRI, the activation of the superior colliculi in response to looming stimuli in healthy control participants, cervical dystonia patients and their unaffected relatives with normal and abnormal temporal discrimination.

5.2 Methods

5.2.1 Ethics, Participants and Data Acquisition

Please refer to Chapter 4.

5.2.2 Task - Visual Paradigm

The paradigm employed during the t-fMRI data acquisition was an event-related design developed in Presentation Software (Neurobehavioral Systems Inc.), according to a stimulus developed by Billington et al. (2010), which has been proven successful at activating the SC. The paradigm comprised of an Event-Related Design (ERD) which is ideal for measuring transient neural activity and allows for the inclusion of more natural stimuli with a random presentation of the stimuli and variable inter-stimulus intervals (ISIs), known as jittering (Petersen and Dubis, 2012).

The paradigm was displayed on a screen with a resolution of 1280 by 1024 pixels and a refresh rate of 60Hz. This screen was viewed by participants within the scanner bore by way of an angled mirror of 7 x 3.5cm, located 12cm away from their eyes. The paradigm was presented monocularly, to the left eye. Throughout the paradigm, a fixation cross was maintained in the centre of the screen. Additionally, two pairs of vertical lines were displayed on screen, behind the stimuli. These lines underwent a colour change for each of the three tasks displayed (green during the looming condition, yellow during receding and blue during random motion). During each condition, a sphere comprising 100 white dots was projected on the screen. The sphere faded in over 1.5s and underwent motion for 1s before disappearing. The paradigm was

designed to consist of a constant number of white lights comprising a sphere in order to avoid changes in luminance and chrominance that would occur in the setting of a fully textured sphere expanding on the screen. Such changes may activate discrete brain areas dedicated to low-level visual processing of motion, colour and brightness and confound the effects of a pure looming task (Landwehr et al., 2013). A series of screen captures from the paradigm illustrating the three events is shown (Figure 5.2).

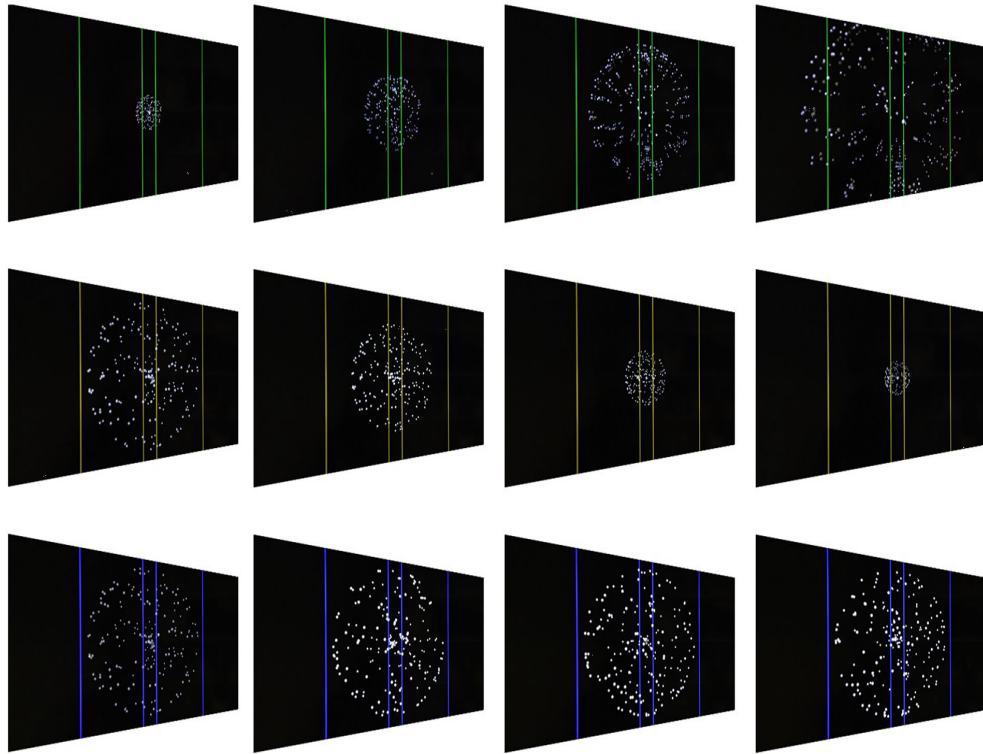


Figure 5.2: The visual stimulus paradigm employed to elicit activity in the SC. Screen capture of the sequence of events that occurs during each of the three conditions: loom, recede and random. The colour of the vertical lines indicates the trial type: loom (green), recede (yellow), random (blue). In the loom condition, the size of the sphere expands during motion towards the outer vertical lines before disappearing. The recede condition is the reverse of the loom condition; the sphere begins at its maximum diameter and contracts towards the inner vertical lines before disappearing. The random condition consists of an unchanging sphere volume with randomly moving points that maintain the same velocity of the previous conditions.

- Loom: During the looming condition a sphere faded into view with an optical diameter of 8° over the initial 1.5s. It then underwent linear and rotational movement towards the participant for 1s and disappeared approximately 0.25s before contacting the outer set of vertical lines, at this point the sphere had a visual diameter of 18° . Participants were instructed to press a button when they

judged the diameter of the sphere would match the width of the outer vertical lines.

- Recede: During receding trials the sphere started with an optical diameter of 18 degrees and moved away from the participant until it had an optical diameter of 18°. Fade-in and movement timings were matched to the loom condition. In this condition, participants were directed to press a button when they estimated that the diameter of the sphere would match the width of the inner vertical lines. This condition was included to control for visual movement in space and the requirement to make a TTC judgment.
- Random: During the random condition a sphere faded-in with an optical diameter of 18°. In this condition, the dots did not undergo any linear or rotational movement but instead underwent random motion at a speed equivalent to the mean rate of dot motion from the other two conditions. This persisted for 1s and the participant was directed to press the button when a blue square appeared approximately 0.25s after the sphere disappeared. This condition was included to act as a low-level visual control.

Velocities and starting positions were randomized with a jitter of $\pm 10\%$ across trials to minimize habituation of the TTC motor response.

5.2.3 Pre-processing

A detailed description of the pre-processing is provided in Chapter 4. Smoothed images were generated using a kernel with 8mm FWHM for whole-brain analysis. ROI analysis of the SC presents a number of additional challenges and the optimisation process necessitated the comparison of a number of different pre-processing pipelines.

5.2.4 Whole-brain Analysis

Whole-brain one-sample and two-sample t-test using condition estimates (β values) from a 1st level GLM analysis were performed to compare whole-brain activation associated with each experimental condition (loom, recede, random motion). A set of contrast images for each participant was generated for testing at group level. The contrast images were divided into two groups: basic 1-sample t-test which tested for

activation against a 0 background (condition $>/< 0$) and contrast 2-sample t-tests which looked for differences in activation between different conditions (condition A $>/<$ condition B). The contrast images were generated at the first level and then submitted to 2nd level analysis. To test for group differences in SC activation the 64 participants were divided into two groups: those with abnormal TDT (n = 32, patients and abnormal relatives) and normal TDT (n = 32, normal relatives and controls). A repeat 2nd level analysis was calculated for each group incorporating the contrasts examined in the whole group analysis.

5.2.5 Optimization of ROI Analysis of the SC for Improved Activation Detection in CD

In order to optimise the SNR of the ROI analysis pipeline, we probed a number of different pipelines, working under the assumption that for healthy controls with normal TDTs, the results should fit with that of (Billington et al. 2011) and the largest β values for the Loom versus Recede condition would represent the highest possible SNR. Ten healthy controls were randomly selected and employed in the pipeline comparison. A four-tier approach was followed for accurate ROI activation detection. This consisted of:

- (i) Neuropathological dissection of human brainstem specimens by a consultant neuropathologist who identified the size and anatomical landmarks of the left and right superior colliculi Figure 5.3.
- (ii) Cardiac gating during acquisition for physiological noise correction. A photo-plethysmographer unit (Peripheral Pulse Unit: PPU) was employed for a subset of three healthy controls during the functional runs to acquire a cardiac signal.
- (iii) Hand drawn ROIs on each subject (Figure 5.4) by a neuroradiologist and consultant neurologist.
- (iv) Different pre-processing pipelines obtained from combinations of smoothed (6mm)/unsmoothed data, 4s/6s HRF and 1s/2.5s event durations.

The following comparisons were included in the pipeline comparison:

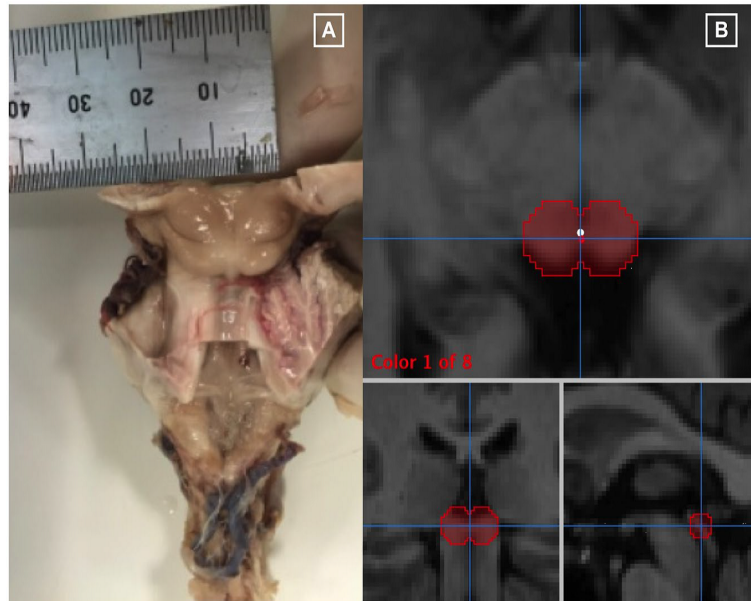


Figure 5.3: A) Neuropathological Dissection B) Anatomical Boundary Definition

- (i) Canonical versus novel HRF: The canonical HRF with a peak at 6s is employed in most fMRI analysis and dominated the literature review which explored articles analysing midbrain ROIs (Chapter 2). However, Wall et al. (2009) reported more significant SC activation in response to a 4s HRF during the use of a stimulus paradigm of subtending spheres, similar to the one currently under investigation.
- (ii) Onset at loom motion with total event duration of 1s versus onset at fade in with total event duration of 2.5s: The original Billington study (Billington et al., 2010) upon which our paradigm is based, utilized an event duration of 2.5s commencing from the fade-in time. The first 1.5s of this consisted of the object fading in but not moving with loom, recede or random motion. Thus, it made sense to compare 1s duration with onset on commencement of motion to the original 2.5s duration.
- (iii) Application of smoothing kernel during pre-processing versus no smoothing kernel: The relevance of the application of a smoothing kernel was tested. While smoothing increases SNR to neural activity at a scale similar to the size of the smoothing kernel, it also increases the risk of perturbation of the signal with noise from adjacent areas. The location of the SC with vasculature and CSF in close proximity suggests that application of a smoothing kernel may be problematic. However, a small smoothing kernel akin to that employed in most of the studies reviewed may be of value (Bellot et al., 2016).

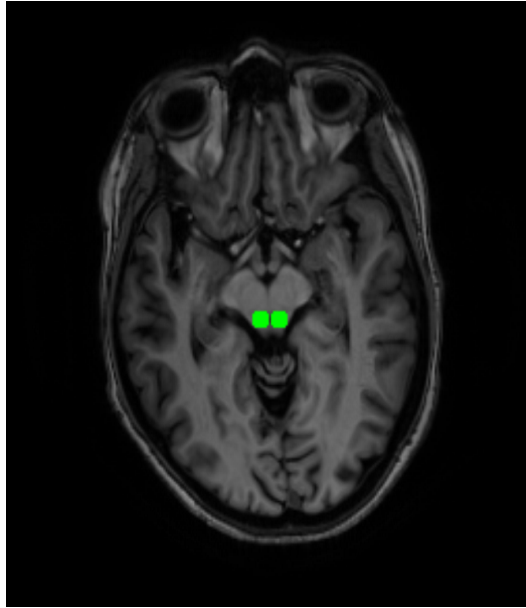


Figure 5.4: Region of Interest Definition on Structural MRI of an Exemplary Subject

- (iv) Inclusion of physiological noise correction versus no correction: Retrospective application of physiological noise correction based upon recordings made during the scan have delivered mixed results with some achieving improvements in SNR with this correction (Limbrick-Oldfield et al., 2012b; Bellot et al., 2016) and others noting no significant change (Verstynen and Deshpande, 2011). A subset of our subjects (n=3) were scanned with additional pulse-oximetry recording using a PPU, as described before.

This required the development of two pre-processing pipelines which were each subjected to four possible GLMs. The eight resulting datasets were then employed for β extraction using the SPM summarise package and hand-drawn SC ROIs. Eight possible pipelines resulted from this and were compared to determine which produced maximum Loom versus Recede β weights. β Loom versus Recede was employed a marker of SC activation for the task and allowed a clear assessment of SNR changes due to pipeline specifications. Kruskal-Wallis statistical test was employed to test the null hypothesis of no difference between the pipelines.

The most successful pipeline was then subjected to additional comparison with an alternative GLM and a retrospectively derived physiological noise regressor in order to compare physiological noise correction methods. The physiological noise regressor was derived from the RETROICOR (Glover et al., 2000b) algorithm with regressors

created using the Matlab PhysIO Toolbox (Kasper et al., 2017). Physiological data was available for three subjects.

5.2.6 Region of Interest Analysis

The final β weight and PSC data were presented using the optimum pipeline. Statistical analysis was performed using SPSS (IBM Corp. Released 2013. IBM SPSS Statistics for Macintosh, Version 22.0. Armonk, NY) and graphs were plotted in GraphPad Prism. The β Loom versus Recede contrast was compared across normal abnormal subjects in addition to a scatter plot which compared β Loom versus Recede against TDT Z-scores. A Mann-Whitney test was employed to test for a significant difference between the medians of the subjects with abnormal TDT and those with normal TDT.

a Effect of condition

The raw event-related PSC time courses were extracted from each participant's SC using the methodology from a previous study in healthy control adult participants (Billington et al., 2010). The three stimulus types (looming, receding and random motion) were modelled at the 1st level and incorporated into a 2nd level analysis. To calculate the change in BOLD signal over time within the region of interest, time courses were estimated for individual subjects. The peak was taken as a more accurate estimate of the magnitude of an individual's functional activation than the β estimate. Participants were grouped according to normal or abnormal TDT for ROI analysis. The extracted peak PSC was directly compared by means of an independent student t-test for three main contrasts - loom > random, recede > random and loom > recede. By comparing contrast of conditions (as opposed to conditions) within-subjects, we reduced the potential for noise that may arise from inter-subject variability.

b Correlation with TDT

In order to explore the relationship between temporal discrimination and BOLD activations at SC level, participant TDT Z-scores was correlated with the peak percentage signal change in the region of interest for the three main contrasts (loom > random, recede > random, loom > recede). Participants were grouped according to normal or abnormal TDT for correlation analysis.

5.3 Results

5.3.1 TDT Testing

Temporal discrimination threshold testing results from sixty-four participants were expressed as Z-scores as shown in Chapter 4. 16 CD patients with abnormal TDTs had a mean Z-score of 4.3 (± 1.2). 16 of the 32 first degree relatives had abnormal TDTs (4.5 ± 1.6) and 16 had normal TDTs (0.25 ± 0.82). All 16 healthy control subjects had normal TDTs (-0.64 ± 1.02).

5.3.2 Whole-brain Analysis

a Behavioural analysis

There was no statistical difference in responses times between the three conditions: looming stimuli, receding stimuli and random stimuli.

b 2nd level GLM analysis

This was carried out to include all 64 participants. Whole group analysis for the basic contrast 1-sample t-test (loom $> / < 0$, recede $> / < 0$ and random $> / < 0$) are presented (Figure 5.6 A). The loom condition demonstrated significant and focal activation of both superior colliculi. The recede and random conditions failed to demonstrate statistically significant activations at SC level. The activation in response to structured movement (loom and recede) was less focal than in the loom condition. The images for all visual input (loom, recede and random) showed a weaker activation significant cluster for the loom $>$ random condition at both superior colliculi. No statistically significant clusters were observed within the SC boundary for the recede $>$ random or the loom $>$ recede condition. Segmented group analysis for the 1-sample and 2-sample t-test contrast is presented (Figure 5.6 B). A statistically significant cluster at SC level was observed for both the looming condition and the loom $>$ random condition in the normal TDT group. No such activations were observed for the abnormal TDT group. The recede and random conditions failed to demonstrate statistically significant clusters in either group at SC level.

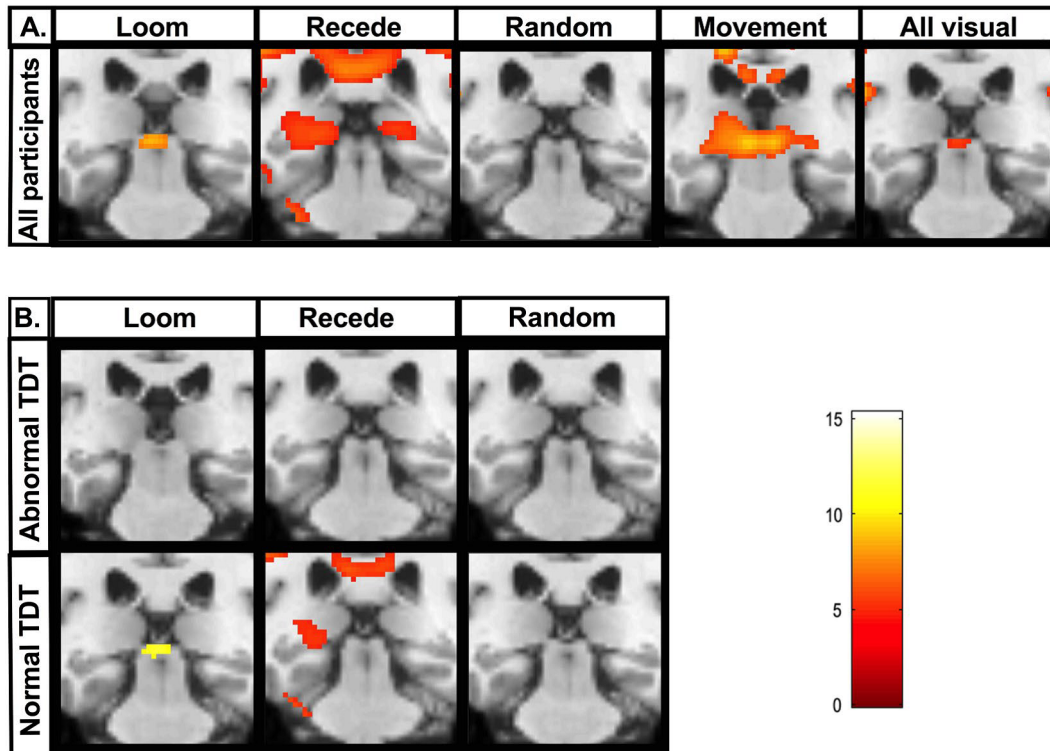


Figure 5.5: Whole-brain analysis of SC activation to visual stimuli: (A) Whole brain, whole group 2nd level general linear model (GLM) analysis in all 64 participants (16 patients, 32 unaffected relatives, 16 healthy controls) for the following basic contrasts: loom, recede, random, structured movement (loom and recede) and all visual (loom, recede and random). Coronal brain images are displayed. Slices were selected to highlight peak SC activity. A Family wise error corrected p-value < 0.05 was employed. K = cluster size. A significant and focal activation of both superior colliculi was seen for the loom condition ($K = 69$, $p < 0.002$). The recede random and structured movement conditions failed to demonstrate statistically significant clusters at SC level. (B) Segmented group 2nd level GLM analysis brain analysis in 32 participants with abnormal temporal discrimination thresholds (TDTs) (16 cervical dystonia patients and 16 relatives with abnormal TDTs) and 32 participants with normal TDTs (16 relatives and 16 control participants with normal TDTs). A statistically significant cluster at SC level was observed for the looming condition in the normal TDT group. In the abnormal TDT group, no statistically significant clusters were observed within the SC boundary for the loom, recede or random condition.

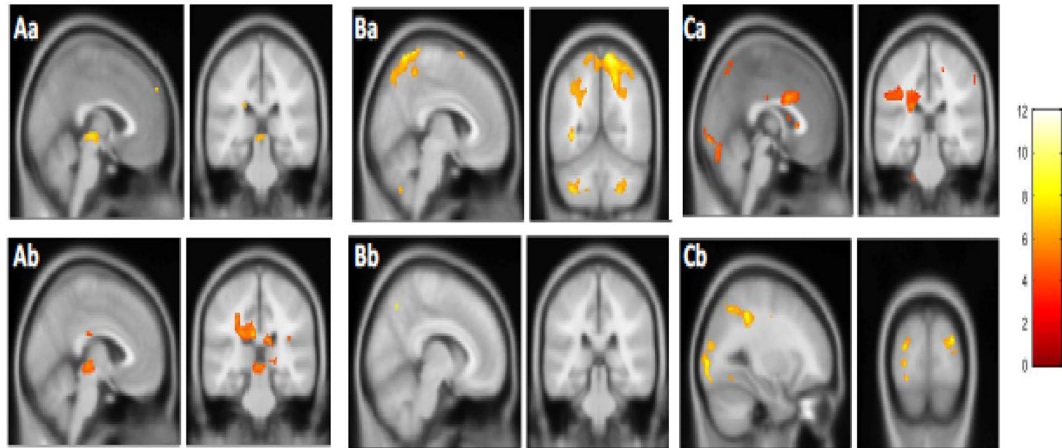


Figure 5.6: Whole brain group 2nd level general linear model (GLM): analysis in 32 participants with normal temporal discrimination threshold (TDT) and 32 participants with abnormal TDT for the following three contrasts are presented; Aa = Loom > Random (normal TDT); Ab = Loom > Random (abnormal TDT); Ba = Loom > Recede (normal TDT); Bb = Loom > Recede (abnormal TDT); Ca = Recede > Random (normal TDT); Recede > Random (abnormal TDT). A Family wise error corrected pvalue < 0.05 was employed . TDT = temporal discrimination threshold. K = cluster size. BA = Broadmann's area.

Whole group analysis for loom > random, recede > random and recede > random contrasts are presented for the 32 participants with normal TDT (unaffected relatives and healthy controls) and the abnormal TDT group (patients and unaffected relatives) (Figure 5.6). A statistically significant cluster at the SC level was observed for the loom > random contrast (K = 299, $p < 0.05$) in the normal TDT group. This activation was not observed in the abnormal TDT group.

5.3.3 Optimization of ROI Analysis for the SC

Results from the comparison of the β values for the Loom versus Recede Contrast across eight different pipelines are displayed in Figure 5.7. The Kruskal-Wallis test found that there were no significant differences between the pipelines. A physiological correction was thus applied to the four pipelines which employed the 4s HRF due to the higher values associated with this approach as seen in Figure 5-7, in addition to the evidence found by (Billington et al., 2010) for a 4s peak in response to the loom condition in the SC. Kruskal-Wallis testing found no significant difference between the pipelines with and without physiological noise correction ($p=0.1276$).

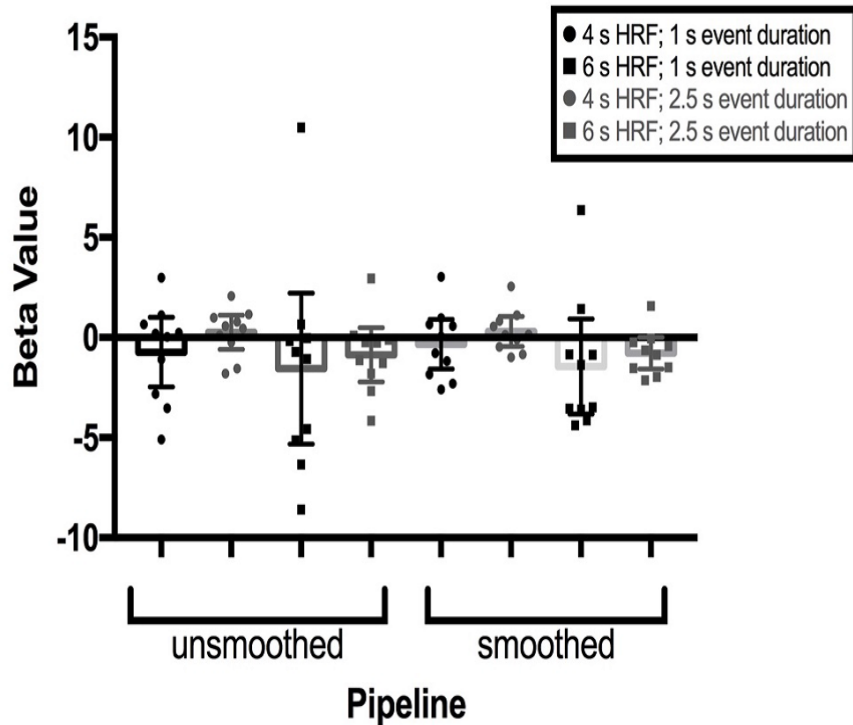


Figure 5.7: Comparison of the different pipelines for optimal region of interest analysis of the SC.

5.3.4 ROI Analysis

a Effect of condition

The raw event-related time courses were extracted for the loom, recede and random conditions from each participant's SC. The greatest signal difference was observed between the loom and random condition (Figure 5.8). The peak PSC during the loom condition was observed at 4s across participants with normal temporal discrimination. This peak PSC for the loom condition was absent in participants with abnormal TDTs. An independent-samples t-test was conducted to compare BOLD activations for the three main contrasts (loom > random, recede > random, loom > recede) for both the abnormal TDT and normal TDT group. A significant difference was observed for the loom > random contrast for the abnormal TDT group (-0.092 ± 0.266) and the normal TDT group [0.076 ± 0.17 ; $t(62) = 3.0$, $p = 0.004$]. The magnitude of the differences in the means was very large ($\eta^2 = 0.14$) (Figure 5.8).

A less significant difference was observed for the recede > random contrast for the abnormal TDT group (-0.12 ± 0.32) and the normal TDT group [0.02 ± 0.19 ; $t(62)$

= 2.05, $p = 0.05$]. The magnitude of the differences in the means was moderate (eta squared = 0.06). There was no significant difference observed for the loom > recede contrast for the abnormal TDT group (0.027 ± 0.17) and the normal TDT group [0.05 ± 0.27 ; $t(62) = 0.08$, $p = 0.768$]. Participants were then divided into four groups (Group 1: patients; Group 2: relatives with abnormal TDT; Group 3: relatives with normal TDT; Group 4: Healthy controls). A one-way between-groups ANOVA was conducted to explore the impact of group level on loom > random peak value. There was a statistically significant difference at the $p < 0.05$ in loom > random peak values for the four groups [$F(3,60) = 5.85$, $p < 0.001$]. The difference in the mean scores was large. The effect size, calculated using eta squared, was 0.23. Post-hoc comparisons using the Turkey Honest Significant Difference test indicated that the most statistically significant group difference was observed between relatives with abnormal TDTs (-0.18 ± 0.33) and relatives with normal TDTs (0.12 ± 0.20 , $p < 0.001$).

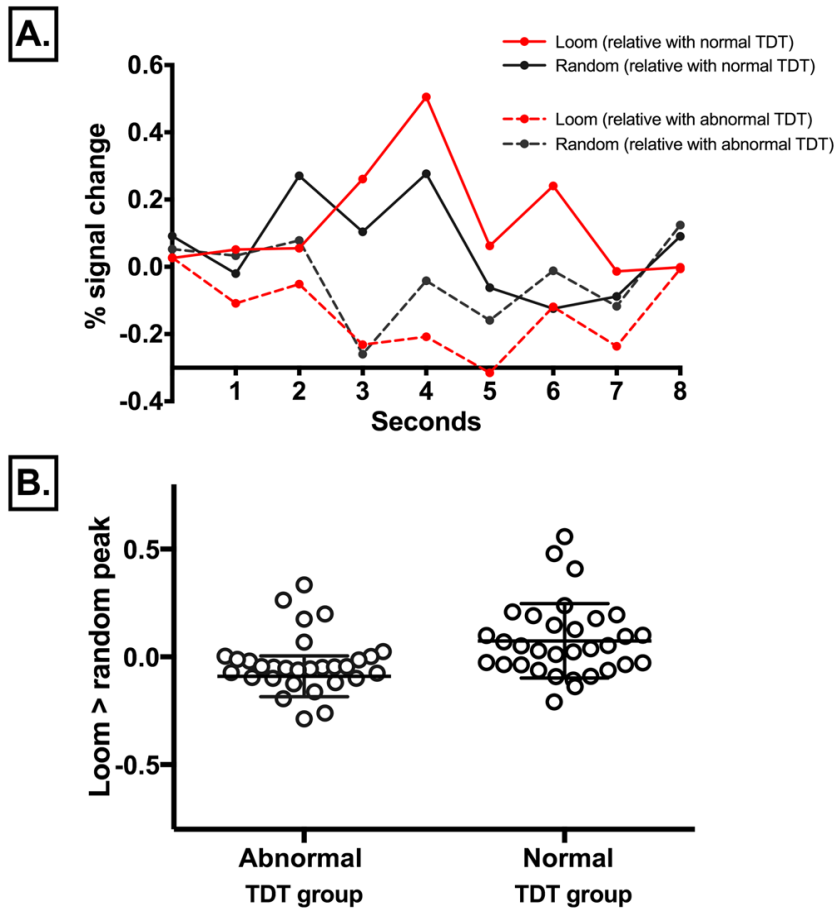


Figure 5.8: Event related time courses: (A) Event-related time course for the SC during the loom and random condition in two candidate subjects: one relative with abnormal temporal discrimination threshold (TDT) and one relative normal TDT. Red solid line = looming condition in a relative with normal TDT; black solid line = looming condition in a relative with normal TDT; red dashed line = random condition in a relative with abnormal TDT; black dashed line = random condition in a relative with abnormal TDT. (B) Loom > random peak signal in all 64 participants. Each circle represents an individual's peak signal for the loom > random contrast.

b Correlation analysis with TDT

The relationship between SC BOLD activation for each contrast (as measured by the peak percent signal) and TDT Z-score was investigated using Pearson product-moment correlation coefficient. Preliminary analysis was performed to ensure no violation of the assumption of normality, linearity and homoscedasticity. There was a statistically significant negative correlation between the loom > random contrast and TDT Z-score [$r = -0.25$, $n = 62$, $p < 0.04$], with lower levels of SC activation associated with a higher (abnormal) TDT Z-score (Figure 5.9).

There was a non-significant negative correlation between the recede > random contrast and TDT Z-score [$r = -0.22$, $n = 62$, $p < 0.08$]. There was a lack of association observed between the loom > recede contrast and TDT Z-score [$r = 0.006$, $n = 62$, $p < 0.96$].

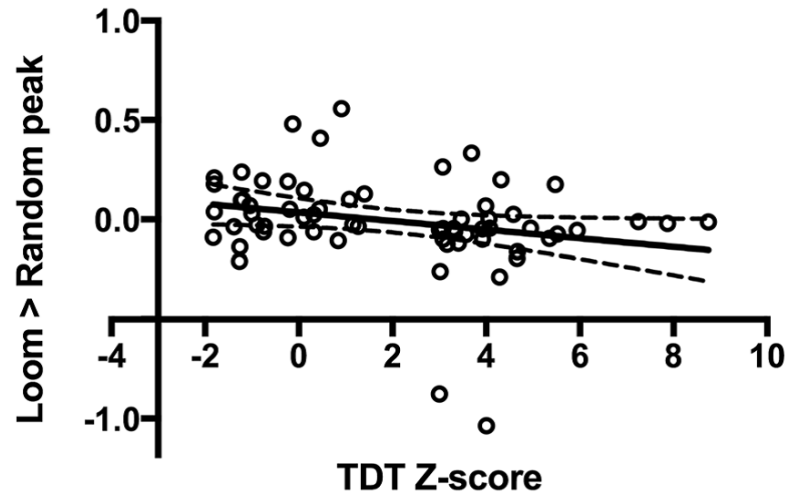


Figure 5.9: Correlation analysis: Pearson's product moment correlation-coefficient analysis examining the relationship between SC peak PSC for the loom > random contrast and temporal discrimination threshold (TDT) Z-score. Each open black circle represents one of the 64 participants; TDT Z-scores are plotted on the x-axis; the peak PSC observed for the loom > random contrast is plotted on the y-axis. The analysis showed a statistically significant negative correlation between the loom > random contrast and TDT Z-score [$r = -0.25$, $n = 62$, $p < 0.04$], with lower levels of SC activation associated with a higher (abnormal) TDT Z-score.

5.4 Discussion

Our results reveal that patients with cervical dystonia and their unaffected relatives with abnormal temporal discrimination, demonstrated (i) disrupted SC activation; (ii) significantly reduced SC activation for whole brain and region of interest analysis; and (iii) a statistically significant negative correlation between TDT Z-score and SC peak values. These findings which provide evidence of a functional abnormality within the SC in both patients and first-degree relatives carrying a disease-specific endophenotype supports the hypothesis that dysfunctional SC processing may be involved in the pathogenesis of cervical dystonia.

Our experimental paradigm was constructed principally to activate the superficial layer of the SC during the loom condition. During whole-brain, whole-group analysis,

we observed a significant and focal activation of the SC for the loom condition, whereas the recede and random conditions failed to induce significant activation within the SC boundary. The random condition produced the least SC activation and the loom > random contrast revealed the most statistically significant cluster at the SC level. This contrast maximised SC activation and controlled for inter-subject variability across participants. Our initial findings confirmed that our experimental paradigm was a robust method for producing SC activation and aligned with the existing literature regarding optimal activation. Following our initial results, we proceeded to examine for any group differences observed during whole-brain analysis.

Whole-brain analysis revealed a between-group difference in SC activation for the loom condition. Participants with abnormal temporal discrimination (cervical dystonia patients and relatives) had an absence of SC activation to looming stimuli. There was no statistically significant difference amongst the cervical dystonia patients between the loom, recede and random conditions. In contrast, participants with normal temporal discrimination (relatives and controls) showed significant activation to looming stimuli at the SC level. The absence of a normal activation pattern observed in participants with abnormal temporal discrimination (the endophenotype) suggests that they have disrupted SC processing. To explore this, further, we proceeded to region-of-interest analysis, specifically focusing on functional activations at SC level.

The ROI analysis further revealed a statistically significant between-group difference in SC activation. Patients and relatives with abnormal temporal discrimination had statistically significantly reduced SC activation for the loom condition compared to participants with normal temporal discrimination. This between-group difference was further supported by the raw event-related time series extracted from each individual participant's region-of-interest. In participants with normal temporal discrimination, a 4s peak signal was observed for the loom condition. However, in those with abnormal temporal discrimination there was a reverse of this peak signal for the loom condition at 4s (Figure 5.8).

Amongst cervical dystonia patients, there was no significant difference in either whole brain or region of interest analysis between those receiving regular botulinum toxin (BoNT) injections (n = 13) and those who did not (n = 3). Previous functional imaging studies have demonstrated a partial restoration of abnormal brain activations following BoNT injections (Delnooz et al., 2013; Nevrlly et al., 2018; Brodoehl et al.,

2019). Unlike our study, these protocols were devised to specifically examine the effect of BoNT on abnormal brain activations and imaging was frequently performed before and after injections. In our study repeat imaging was not performed and intervals following the last BoNT injection were variable. As such it was unlikely that any differences would exist between the two groups.

A correlation analysis was also undertaken in order to corroborate the findings from whole-brain and region-of-interest analysis. The correlation analysis demonstrated a statistically significant negative correlation between SC peak activation and individual TDT Z-scores, indicating that as SC activation diminished, TDT Z-score worsened. This was in harmony with the mediational endophenotype theory which emphasises the presence of the endophenotype before acquiring the disease. Under normal conditions, neurons in the superficial layer of the SC respond to looming stimuli; the time of the peak response in these neurons is linearly related to the size/speed ratio of the approaching object (Liu et al., 2011). In our study, participants with normal temporal discrimination had this predicted response - a statistically significant greater activation to looming stimuli (loom > random contrast) at the SC level. In cervical dystonia patients and relatives with abnormal temporal discrimination group, there was no significant SC activation to looming stimuli. Thus, disrupted SC processing is unique to those with an abnormal TDT (i.e. those with the endophenotype) and is independent of phenotype (cervical dystonia or unaffected relatives). This also suggests that processing intrinsic to the SC is involved in temporal discrimination.

The visuo-sensory neurons in the superficial layer of the SC exert inhibitory influences on the pre-motor neurons in the intermediate and deep layer of the SC. The deep layer in turn projects via the tecto-reticulospinal and tectospinal pathways to the upper cervical spinal cord. Prolonged duration firing of visuo-sensory neurons because of impaired GABA inhibition would cause hyperexcitability of the pre-motor neurons in the deep layer of the SC. These hyperexcitable premotor neurons could stimulate motor neurons in the upper cervical spinal cord perhaps resulting in the abnormal, jerky head spasms characteristic of cervical dystonia.

Potential Limitations: While the results of this study support a model of reduced SC GABAergic activity as contributing to sensory processing abnormalities and motor features of cervical dystonia, the study cannot specifically determine the exact location at which this deficit arises, and whether defective SC activity occurs specifically

because of GABAergic abnormalities. Further research is required to determine this. Additionally, although rigorous measures were undertaken in this study to limit the influence of head motion, this continues to be a potential confounder, considering the disorder being studied. Future studies implementing more tailored motion regression methods may largely benefit the study of the SC in cervical dystonia.

5.5 Chapter Conclusion

The findings from our study that SC processing is disrupted in both patients and relatives harbouring the endophenotype (an abnormal TDT), supports the hypothesis that disrupted SC processing is involved in temporal discrimination. As an abnormal TDT is a mediational endophenotype for cervical dystonia, we might assume that disordered sensory processing in the SC is also involved in the pathogenesis of this condition. Any reduction in GABA activity will not only have functional consequences for this dorsal midbrain structure but also its connections. Since the SC is a key node in the oculomotor and cephalomotor system, and also a central hub in the CAO network, can we track connectivity-related changes across the covert attention network as a result of disrupted SC activity? The next chapter seeks to address this question via an effective connectivity study using Dynamic Causal Modelling.

6 Atop the Hill, as Far as ‘Eye’ Can See: Examining the Midbrain Network for Covert Attentional Orienting in Cervical Dystonia using Dynamic Causal Modelling

In the previous study we demonstrated disrupted activity within the Superior Colliculus in both patients and first-degree relatives carrying a disease-specific endophenotype (abnormal TDT). Since the SC is a sentinel structure in the covert attention network; integrating complex multimodal sensory information and motor responses, how does dysfunctional SC activity perturb the CAO circuit in CD patients as a result of the SC’s upstream/downstream connections with the Thalamus and Basal Ganglia? This chapter seeks to address Research Questions 6 and 7 in Chapter 3.

Covert attention orienting involves shifts in attention to locations with or without saccade initiation. While the SC plays a crucial role in the generation of saccades, it is also a central node in the midbrain covert attentional network, capturing sudden changes in the environment and alerting an individual to a salient stimulus. The pathways from the SC to the Putamen via the Thalamus and SNpc fall under the subcortical network for covert attention. The Putamen has been observed to be physically enlarged and less active in dystonic patients and unaffected first degree relatives with temporal discrimination abnormalities. Under the current hypothesis in CD, the observed putaminal changes must also be explained by the proposed GABAergic abnormality in the superior colliculus and the covert attention network. The proposed DCM work will, therefore, aim to test if these putaminal abnormalities are an upstream/downstream effect of abnormal GABAergic activity in the superior colliculus. The study presented in this chapter has resulted in the following peer-reviewed conference publication and presentation:

- Oisin Duggan, Shruti Narasimham, Eavan Mc Govern, Owen Killian, Sean O’Riordan, Michael Hutchinson, Richard B. Reilly. 2019. A Study of the Midbrain Network for Covert Attentional Orienting in Cervical Dystonia

Patients using Dynamic Causal Modelling. *Proceedings of the 41st International Engineering in Medicine and Biology Conference*, Berlin, Germany.

6.1 Introduction

Attention refers to a set of cognitive processes that are crucial for survival and development, allowing us to direct our neurocognitive resources towards behavioural goals in an optimal manner (Ungerleider and G, 2000; Fecteau and Munoz, 2006). Typically, changes in attention can occur with the eyes moving, overtly, or with the eyes remaining fixated, covertly. via overt movements of the eyes (saccades) to the information source and covert shifts of attention (without saccades) (Miller, 2000; Kulke et al., 2015). The functional coupling between the oculomotor system and spatial attention mechanisms has been explored in numerous studies (Schiller and Tehovnik, 2005; Fecteau and Munoz, 2006; Shires et al., 2010; Krauzlis et al., 2013; Kulke et al., 2015).

Of particular relevance here is the Superior Colliculus, due to its role in eye movements and saccadic generation (Wurtz and Albano, 1980; Chelazzi et al., 1995; Ignashchenkova et al., 2004; Schiller and Tehovnik, 2005; Krauzlis et al., 2013), as well its connections with the frontal eye field, parietal areas, sensorimotor areas, Thalamus and Substantia Nigra as discussed previously in Chapter 2. Shires et al. (2010) presented a simplified model of the midbrain circuits for CAO with the inclusion of excitatory and inhibitory connections, associated with GABAergic inhibitory projections, glutamatergic and dopaminergic excitatory projections. Multiple neuron recording and analysis, as well as behavioural procedures, informed the model proposed by Shires et al., wherein the SC is modulated by an inhibitory GABAergic connections, while the SC has excitatory projections to the Thalamus and SNpc. The Thalamus and SNpc have excitatory projections to the Caudate.

The current hypothesis is that CD as well as abnormal TDT result from a midbrain network disorder of CAO arising due to abnormal GABA levels in the SC (Hutchinson et al., 2014). Besides a dysfunctional SC, the Putamen (part of the Striatum along with the caudate nucleus) has also been implicated in CD. The Putamen has been observed to be physically enlarged and less active in dystonic patients and unaffected first degree relatives with temporal discrimination abnormalities. Given the links between the

SC and Striatum (Bradley et al., 2009; Delnooz et al., 2013), it is possible that an abnormality in the superior colliculus may lead to the putaminal abnormalities that have been observed to date. The aim of this study was to test this hypothesis as well as contribute to the central hypothesis of CD being a disorder of the midbrain network for covert attention.

The majority of research studies in dystonia and CD to date have considered brain imaging from a functional segregation perspective in order to localize abnormalities in the brain. This has been based on the view that distinct brain regions are specialized for specific functions. While this may indeed be true for lower-level processing, higher-level functions (such as oculomotor and cephalomotor movement) require the coordinated action of many brain areas that cannot be sufficiently explained by BOLD signal analysis approach to neuroimaging. Furthermore, events leading to BOLD signal alterations are not precisely defined and the signal, therefore, is not a direct measure of neuronal activity (Ekstrom, 2010; Harris et al., 2011). Thus, though the results from Study 1 (Chapter 5) demonstrated a functional activation in the SC and observed abnormalities in patients and unaffected relatives, the interaction of the SC with other regions, under the influence of the visual looming event, needs to be further explored. In order to precisely decode the pathways of information flow across the CAO network. Hence, the focus of this study was to examine the effective connectivity of this network via dynamic causal modelling (DCM).

6.1.1 Dynamic Causal Modelling

Interactions between regions can be of two types: i) synchronous; general network level synchronization which leads to concurrent and coherent activity in multiple brain regions and ii) causal; information flow which leads to a causal relationship between activities in different regions. Friston termed these as functional and effective connectivity (Friston, 1994, 2011b) respectively. Functional connectivity is usually inferred on the basis of correlations among measurements of neuronal activity. However, correlations can arise in a variety of ways that are not necessarily indicative of biological interactions. Effective connectivity, therefore, refers explicitly to the influence that one neural system exerts over another, either at a synaptic or population level. Effective connectivity is i) dynamic (activity-dependent) and ii) depends on

a model of interactions or coupling. DCM is a novel approach for testing effective connectivity, first introduced for fMRI by Friston et al. (2003). The aim of a DCM is to estimate, and make inference about, the effective connectivity among brain areas and to determine how this connectivity is influenced by changes (Figure 6.1) in experimental context (Friston et al., 2003).

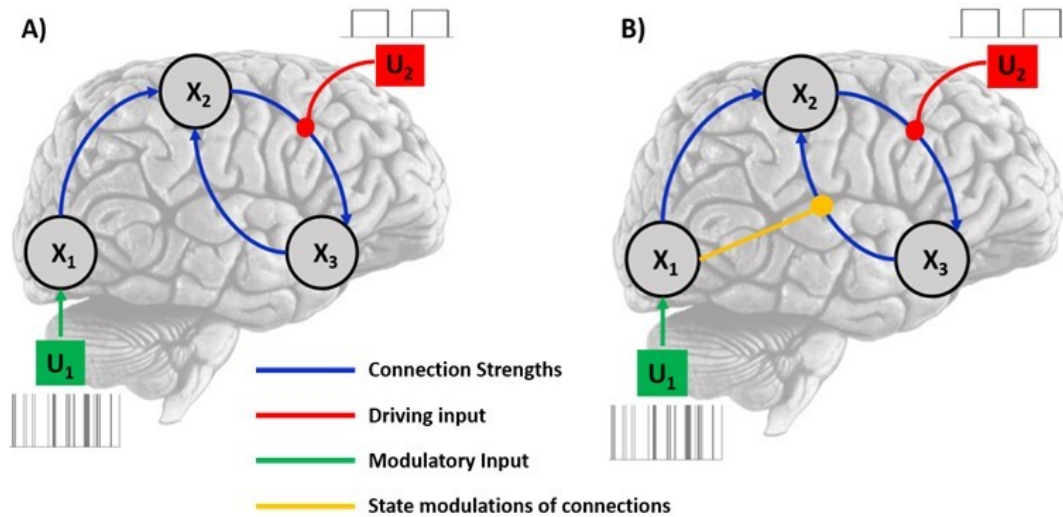


Figure 6.1: Dynamic Causal Models in fMRI fall under a A) bilinear or B) non-linear form. x is a vector of DCM hidden states that quantifies activity in each node of the relevant brain network and u are user-specified inputs that drive or modulate activity in network nodes.

The central idea behind dynamic causal modelling (DCM) is to treat the brain as a deterministic nonlinear dynamic system that is subject to inputs and produces outputs (Friston et al., 2013). The DCM is a framework built on differential equations describing neuronal population dynamics, which are combined with a hemodynamic forward model. The model has parameters, such as the strength of neural connections, which are estimated from the data using a Bayesian (probabilistic) method (Friston et al., 2016). This provides a probability density over the possible values of the parameters (e.g., connection strengths), as well as a score for the quality of the model, called the log-evidence.

Mathematically, DCM is based on bilinear equations (Equation (6.1)), where the bilinear term models the effect of experimental manipulations on neuronal interactions (Friston et al., 2013, 2003). The bilinear framework, however, precludes how the connection between two neuronal units is enabled or gated by activity in other units, which represents a key aspect of various neural mechanisms including top-down modulation, learning and adaptive plasticity. A non-linear DCM (Equation (6.2)) was

introduced for fMRI analysis by Stephan et al. (2008), by assigning explicit neuronal population to account for the modulation of network interactions.

Within the DCM approach, designed inputs may produce responses in one of two ways:

1. Inputs can elicit changes in the state variables (i.e., neuronal activity) directly. For example, sensory input is modelled as causing direct responses in primary visual or auditory areas.
2. Inputs can change the effective connectivity or interactions.

$$\frac{dx}{dt} = \left(A + \sum_{i=1}^m u(i)B(i) \right) x + Cu \quad (6.1)$$

$$\frac{dx}{dt} = \left(A + \sum_{i=1}^m u(i)B(i) + \sum_{j=1}^m x(j)D(j) \right) x + Cu \quad (6.2)$$

A represents the fixed strength of connections between the modelled regions, B(i) represents the context-dependent modulation of these connections, induced by the i^{th} input $u(i)$, and C represents the influence of perturbing inputs to the system (e.g. visual stimuli). The new component in the nonlinear equations are the D(j) matrices, which encode how the n regions gate connections in the system (Stephan et al., 2008).

Due to the manner in which these inputs can perturb a system, DCM studies in neuroscience research attempt to address questions that broadly fall under the following three categories (Stephan et al., 2010; Kahan and Foltynie, 2013):

1. What is the underlying functional architecture of a network of brain regions?
2. Which connections are modulated by experimental manipulation?
3. Are the coupling parameters of a network of brain regions different in two groups of people (e.g. patients vs. healthy controls)?

6.2 Methods

6.2.1 Participants, Data Acquisition and Pre-processing

Since this study followed the region of interest analysis of the SC task-fMRI study, the same task and data were employed. This consisted of 16 patients, 16 unaffected

relatives with normal TDT, 16 unaffected relatives with abnormal TDT and 16 healthy controls (Chapter 4).

6.2.2 Dynamic Causal Modelling (DCM)

The DCM process consisted of a number of steps. GLM whole-brain analysis for region of interest activation identification and time series extraction, followed by the application of a model space definition for testing the various plausible connectivity architectures, model estimation in order to compute the predicted model and find the best fit to the real observed data, model inference and finally parameter inference (Figure 6.2). This will be explained in detail in the following sections.

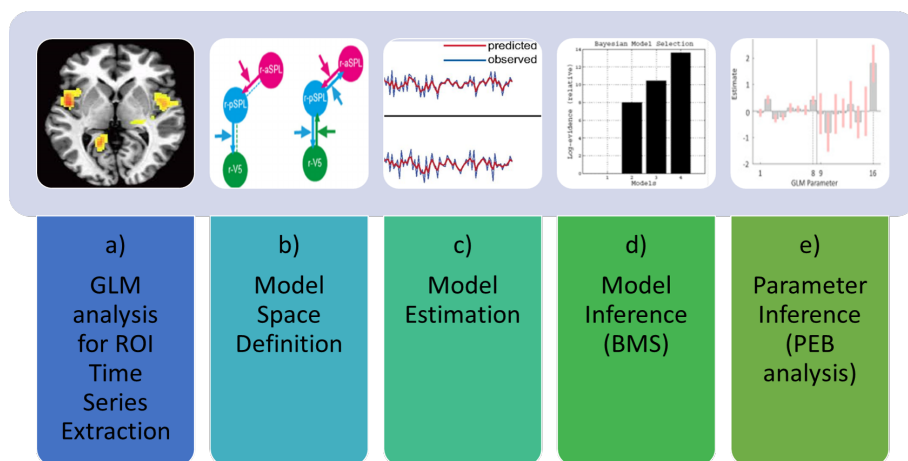


Figure 6.2: The DCM analysis in the current study consisted of time series extraction, model space definition, model estimation, model inference and parameter inference. ROI = Region of Interest, BMS = Bayesian Model Selection, PEB = Parametric Empirical Bayes.

a GLM analysis for ROI time series extraction

A circuit postulated to be involved in the detection of salient unexpected environmental change and in the temporal discrimination task (from Peter Redgrave) encompasses inputs to the subcortical Basal Ganglia via the Thalamus and Substantia Nigra (Figure 6.3). This is based on the review by Redgrave et al. (2010).

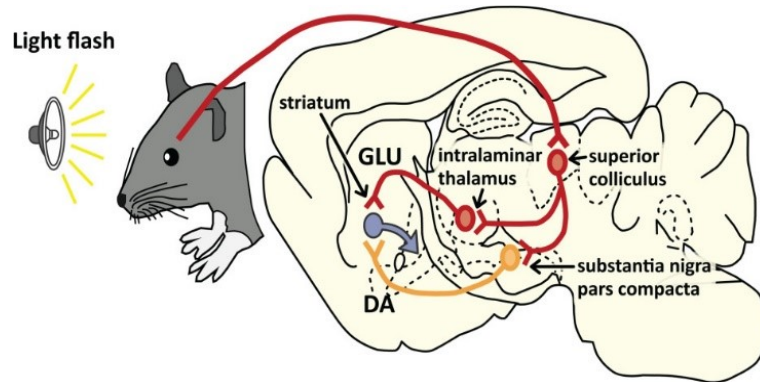


Figure 6.3: The postulated anatomical connections involved in the detection of salient stimuli as shown in the mouse brain model. Adapted from Redgrave et al. (2010). GLU=Glutaminergic pathways DA=Dopaminergic pathways.

Retinal input to the SC affects branched projections to the intralaminar Thalamic nuclei and to the SNpc. Converging phasic inputs to the Striatum from the Thalamic intralaminar nuclei and Substantia Nigra signal sudden salient environmental change and affect striatal output. Therefore, in order to i) probe the effective connectivity of this circuit in cervical dystonia, and ii) examine if changes observed in the Putamen in patients and unaffected relatives were triggered by dysfunction in the SC, the following nodes were considered for analysis:

- Thalamus (left and right)
- Striatum (Putamen and Caudate, left and right)
- Superior Colliculus (left and right)
- Global Pallidus interna (left and right)
- Global Pallidum externa (left and right)
- Substantia Nigra (SNpc and SNpr) (left and right)
- Frontal Eye Fields (left and right)

A 1st level and 2nd level GLM whole-brain analysis was undertaken (as described in Chapter 5). The 2nd level GLMs informed the selection of nodes for inclusion in the DCM. The structures of the midbrain network for CAO were scrutinized, and the structures that showed activity ($p < 0.001$ uncorrected) were identified. Then,

the relevant region of interest masks (masks obtained using WFU_PickAtlas 3.0.5, an SPM12 toolbox) were applied. This enabled time-series extraction for each participant, for each session, and for each masked region of interest, from the pre-processed data, contrasted with respect to the same F-contrast used to generate the 2nd level GLMs. Thus, to summarize, each time-series was generated from the voxels within the anatomical mask that showed statistical activity, as determined by the GLMs.

b Model Space Definition

As described above, multiple regions of interest were identified from the GLM analysis as well as the literature. However, due to computational limitations, it is not possible to model the entirety of the anatomical looming circuit and the CAO network. This model would be too complex, contain too many nodes and be likely to run into problems during model estimation. Furthermore, each of these nodes would need to be active for all participants and so it is likely that many would have to be rejected from the analysis. To avoid these issues when using DCM, it is advisable to select a subsection of a given circuit that will have the most relevance to a given hypothesis. Therefore, this led to the design of two studies; Study 1 and Study 2 as described in this chapter. The selected ROIs with the model space definition have been discussed in further detail in the following sections.

c Model Estimation (DCM computation)

In order to ensure computational efficiency, several steps were taken. For each study and each participant, one single template model with all connections turned ON was computed. Each of the sub-model was extrapolated from the respective template model with some connections, inputs and modulatory effects turned OFF. For between-region connections, prior knowledge was an excitatory connection. For self-connections, prior knowledge was an inhibitory connection. The DCM analysis was computed as linear, deterministic and single-state. The DCMs took approximately 12 hours to implement for a single cohort of participants. Enabling nonlinear, two-state and/or stochastic DCM would dramatically increase this time. This was unfeasible with the available computing resources, therefore all DCM models were executed as bilinear, single-state and with stochastic effects turned off (deterministic).

d Model Inference via Bayesian Model Selection (BMS)

Bayesian model selection (BMS) (Stephan et al., 2007, 2009; Wasserman, 2000) was carried out after DCM analysis as a means of comparing models and ascertaining the winning model. For any Bayesian statistical analysis, the distribution chosen will have associated parameters, such as an expected value and variance in a Gaussian distribution (as is employed in DCM), as well as an associated normalising constant that can be employed as a metric for the comparison of the strength in one's belief in a given model. BMS may be implemented in two ways; fixed (FFX) or random effects (RFX) at the group level (Stephan et al., 2010). Fixed effect BMS assumes one model wins for all participants in a given group, and thus one model wins overall. Whereas random effect BMS assumes a unique model wins for each participant, and that for a group, the results of the individual BMSs are combined to give a distribution of probabilities among all competing models. As the conformity of each participant to one specific model could not be guaranteed, the current BMS consisted of an RFX analysis.

e Parameter Inference via Parametric Empirical Bayes (PEB) Analysis

Parametric Empirical Bayes analysis is a method of testing connectivity hypotheses by comparing group effective connectivity (Zeidman et al., 2019a). The alternative to a PEB is a classical two-sample t-test on connection strengths which could be carried out between groups. However, the classical approach only uses the parameter estimations for each participant and not the associated uncertainties (Zeidman et al., 2019a,b). Therefore, a PEB analysis was carried out as it also utilizes the uncertainties generated in the DCM.

6.2.3 Study 1 – Striatum, Thalamus, SC Circuit in Patients vs. Controls

Study 1 consisted of analysing effective connectivity in CD patients and controls. In the case of the current study with the proposed looming circuit, CAO network and the regions that showed activity in the wholebrain analysis, the most relevant subset of nodes and connections that were analysed were the SC, the Striatum (Caudate and Putamen) and the Thalamus. The evolution of the model which was used in the final analysis is depicted in Figure 6.4). These ROIs were considered the best balance

between DCM model space definition complexity and accuracy.

Two levels of models were assessed and are depicted in Figure 6.5. Given the nature of the SC as a sensorimotor structure with visual inputs and its purpose to respond to changes in the visual field, the visual stimulus (loom, recede, random) was maintained as a driving input on the SC for all models. The Thalamus and Striatum were split into left and right structures, while the SC, due to its small size, was maintained as one node. In Model A, the loom stimulus was assigned as a modulatory input on the inhibitory connections of the SC. Further, the architecture of the connection between the left and right Thalamus and striatum in patients and controls were explored in detail via Models A.1, A.2, A.3 and A.4. Model B was designed to explore the effect of loom as a modulatory input on the connections from the SC to the Thalamus, Thalamus to the Striatum and Striatum to the SC. Therefore, Model B combined all the fixed connections in Model A, while studying the effect of the position of the modulatory input.

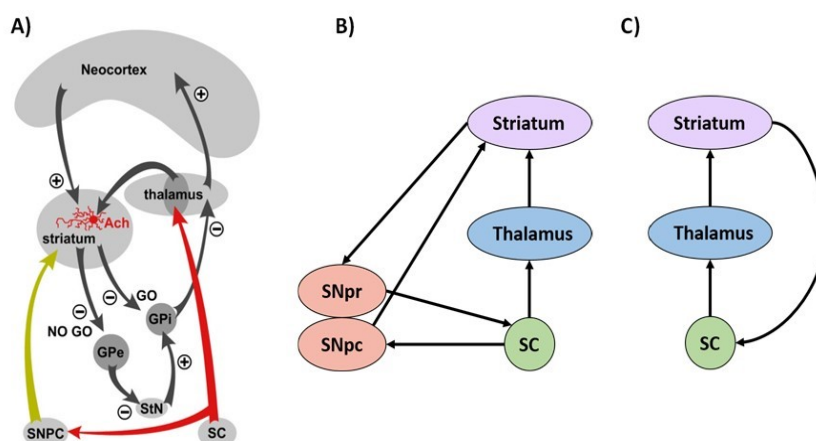


Figure 6.4: The GO and NO-GO pathways involving the Basal Ganglia, Thalamus Cortex, Superior Colliculus, and Substantia Nigra besides other structures. B) A reduced anatomical version of the postulated looming and temporal discrimination circuits C) Nodes and connectivity that will be analysed in the present study.

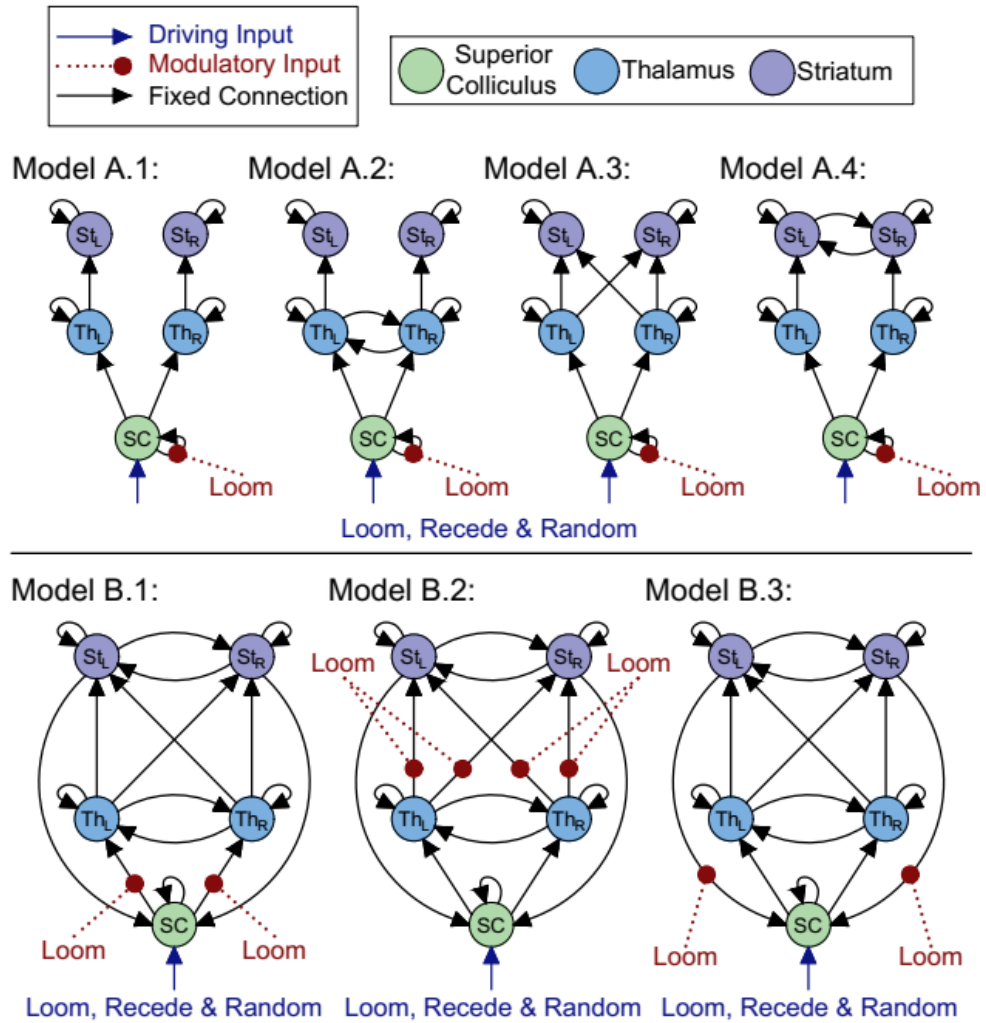


Figure 6.5: Two levels of models and hypothesis tested in Study 1. The black arrows represent the fixed connections, the blue represent the driving input (loom and recede visual stimuli) and the red denotes the modulatory input (loom stimulus).

6.2.4 Study 2 – Striatum, Thalamus, SC, Substantia Nigra Circuit in Patients, Relatives and Controls

Informed by the outcomes of Study 1 (discussed in the Results section of this chapter), Study 2 incorporated the Substantia Nigra as a node (Figure 6.6) in the new model space definition (Figure 6.7), to probe the hypothesis that there exist changes in effective connectivity between the Substantia Nigra and the SC in CD patients vs. controls. The model space consisted of Models 1-10 which differed in the connection the modulatory input had an effect upon. Furthermore, this study also sought to implement the same DCM analysis in the unaffected relative cohort, to compare effective connectivity in relatives with normal vs. abnormal TDT. In order to prevent subject elimination based on ROI activation detection in the Substantia Nigra and enable time-series extraction from this node, the significance threshold in the GLM analysis in this study was changed to a less stringent $p < 0.05$ uncorrected. The Substantia Nigra was modelled as including both the SNpr and the SNpc due to the small size and location of these structures in the brain.

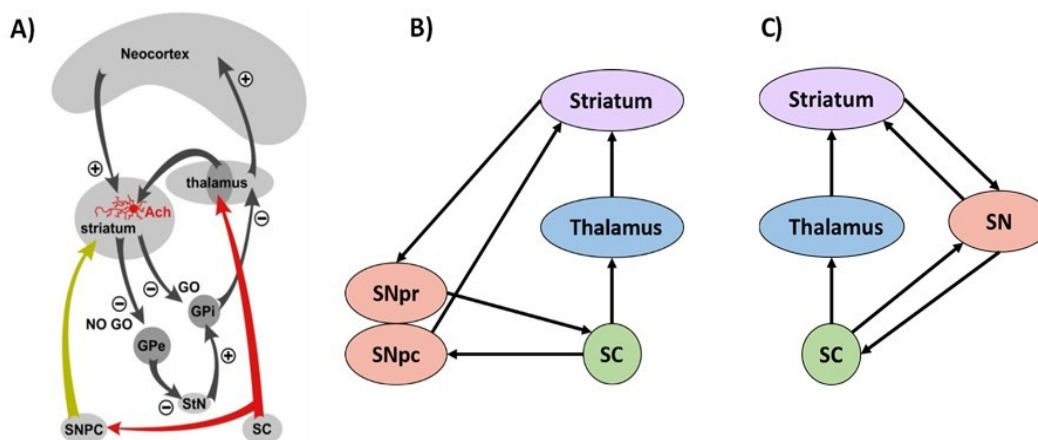


Figure 6.6: The GO and NO-GO pathways involving the Basal Ganglia, Thalamus Cortex, Superior Colliculus, and Substantia Nigra besides other structures. B) A smaller anatomical version of the postulated looming and temporal discrimination circuits C) Nodes and connectivity that will be analysed in the present study.

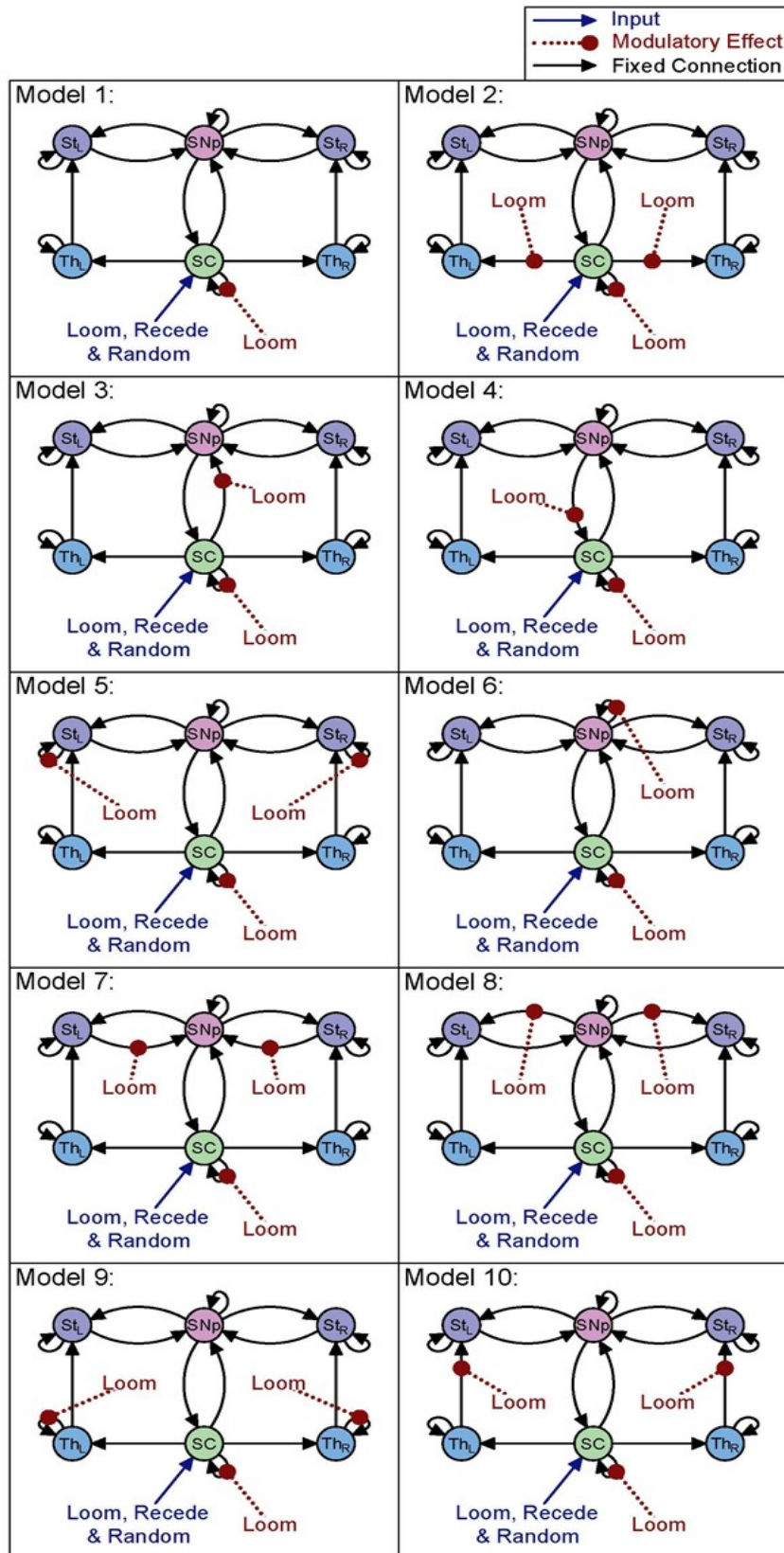


Figure 6.7: Ten different models were tested in Study 2. The black arrows represent the fixed connections, the blue represent the driving input (loom and recede visual stimuli) and the red denotes the modulatory input (loom stimulus).

6.3 Results

6.3.1 GLM analysis

The GLM analysis enabled time series extraction from the Striatum, SC and the Thalamus for Study 1 (Figure 6.8) and for the Striatum, SC, Thalamus and the Substantia Nigra for Study 2.

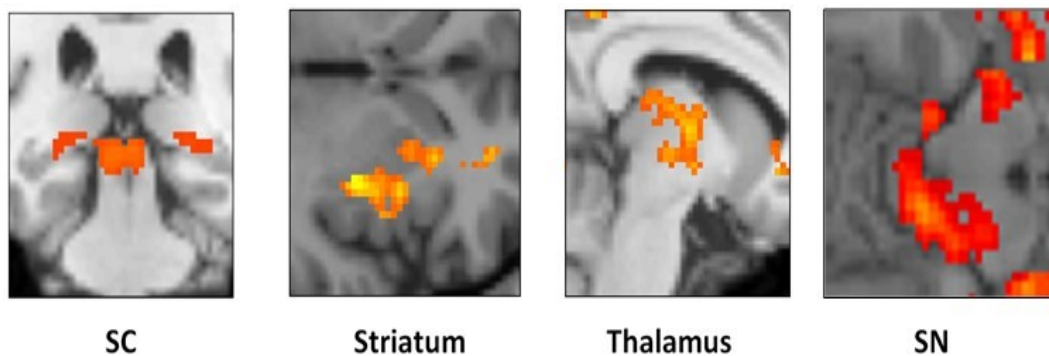


Figure 6.8: The regions that showed differential activation in the GLM analysis (Superior Colliculus, Striatum, Thalamus and Substantia Nigra) were used for time series extraction required for the subsequent DCM analysis.

6.3.2 Study 1 analysis

a BMS

On comparing the connectivity architecture (Figure 6.5 - Models A.1, A.2, A.3) in patients and controls, the BMS analysis resulted in no significant difference when different combinations of Model A were compared. Model A.2 which represented the inter-hemispheric thalamic fixed connections, remained unchanged in patients, and was the winning model in both patients and controls (Figure 6.9 - Model A). On the other hand, on comparing the influence of the loom modulatory input on the connections between the nodes (Figure 6.5 - Models B.1, B.2, B.3), a major contrast was observed in the winning model of patients and controls (Figure 6.9 - Model B). Model B.1 (the loom modulatory input had an effect of the SC - Thalamus connection) was the winning model in controls, whereas Model B.3 (the loom modulatory input had an effect of the Striatum - SC connection) was the winning model in CD patients.

b PEB analysis

Parametric empirical Bayes (PEB) analysis was undertaken to give a posterior expected value for the connection strengths in the winning models, namely the connection strengths that differ across patients vs. controls, under the influence of the loom modulatory input. Participant gender and age was included in the PEB as covariates. Therefore the effects of age and gender were regressed from the models. Results of the PEB were considered to be statistically significant at a p -value < 0.05 . Patients demonstrated a change in effective connectivity from the SC to the Thalamus and from the Striatum to the SC ($p < 0.05$) under the influence of the loom stimulus, as shown in Figure 6.10.

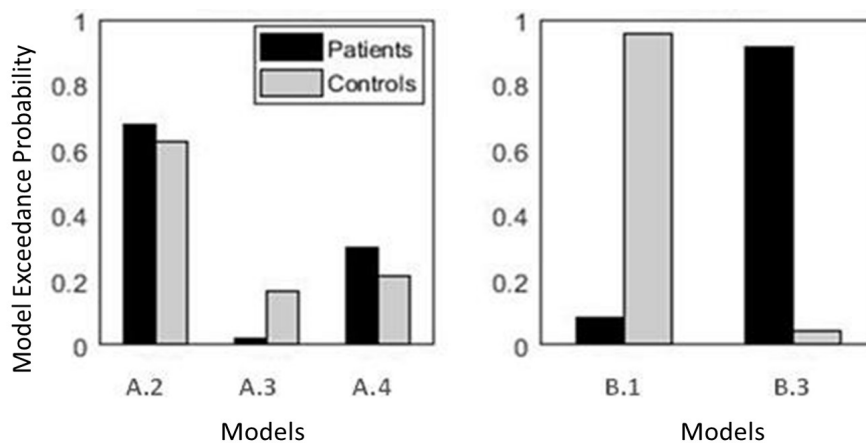


Figure 6.9: Results of the Bayesian Model Selection analysis when Models A.1, A.2 and A.3 were compared in patients and controls, and Models B.1 and B.3 were compared in patients and controls. The x-axis represents the model exceedance probability, while the y-axis represents the models being compared.

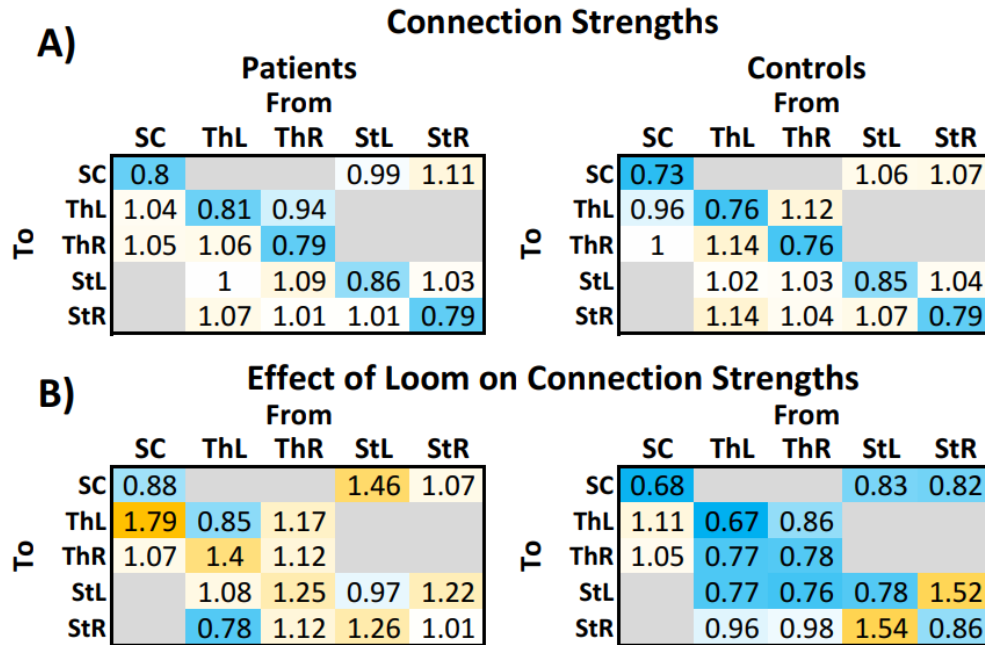


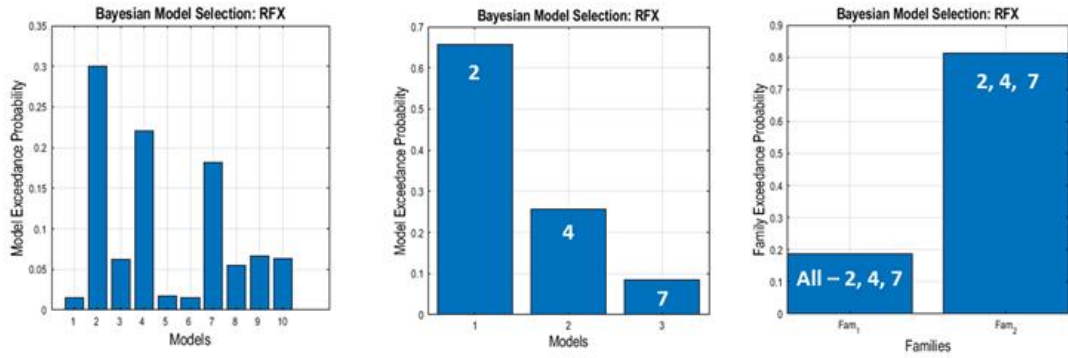
Figure 6.10: A) Matrix of the PEB results for Model C, patients and controls, showing the self-connection strengths and the between-region connection strengths. Numbers > 1 (yellow) represent either a greater excitatory connection (between-region connections), or a stronger self-inhibitory connection (self-connections), relative to the prior. Numbers < 1 (blue) represent a smaller excitatory influence (between-region connections) or weaker self-inhibitory connection (self-connections), relative to the prior. B) Modulatory effect of Loom on the connection strengths. Numbers > 1 represent an increase in connection strength (or an increase in self-inhibition) and numbers < 1 represent a decrease in connection strength (or a decrease in self-inhibition) caused by the Loom event relative to the prior.

6.3.3 Study 2 analysis

a BMS

Models 2, 4 and 7 emerged as the winning models in patients (Figure 6.11). In controls, Models 2, 7 and 8 emerged as the winning models. Model 7 (Figure 6.7) was observed to be consistent in $Relative_{S_{abnormal} TDT}$ and $Relative_{S_{normal} TDT}$. However, while the next winning model in $Relative_{S_{normal} TDT}$ was Model 4 (loom had an effect on the inhibitory connections of the SC and the excitatory connections between the Striatum and SC), the winning models in $Relative_{S_{abnormal} TDT}$ were Models 2 (loom had an effect on the inhibitory connections of the SC and the excitatory connections between the Thalamus and SC) and 10 (loom had an effect on the inhibitory connections of the SC and the excitatory connections between the Thalamus and Striatum) (Figure 6.12).

Patients



Controls

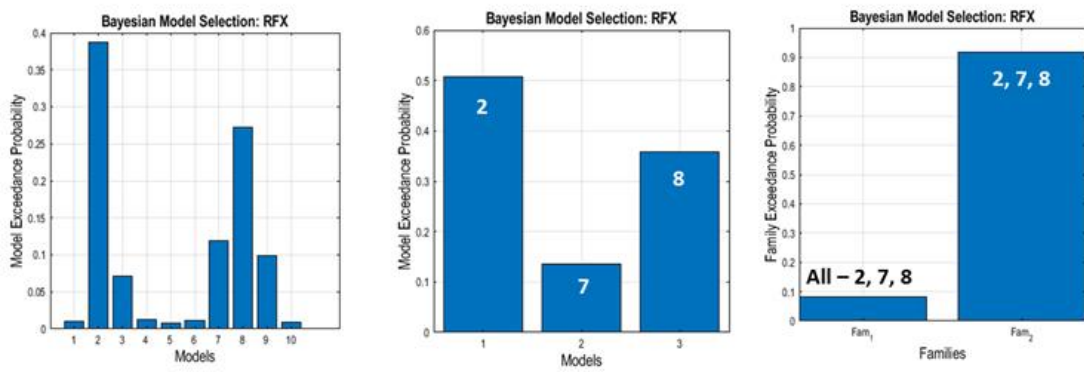
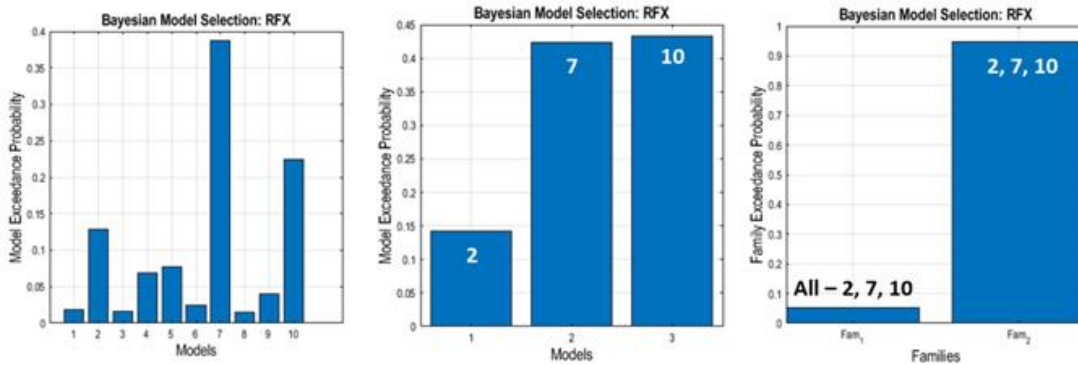


Figure 6.11: Results of the Bayesian Model Selection analysis when Models 1 through 10 were compared in patients and controls. The x-axis represents the model exceedance probability, while the y-axis and numbers written in white represent the models/families of models being compared.

Relatives with Abnormal TDT



Relatives with Normal TDT

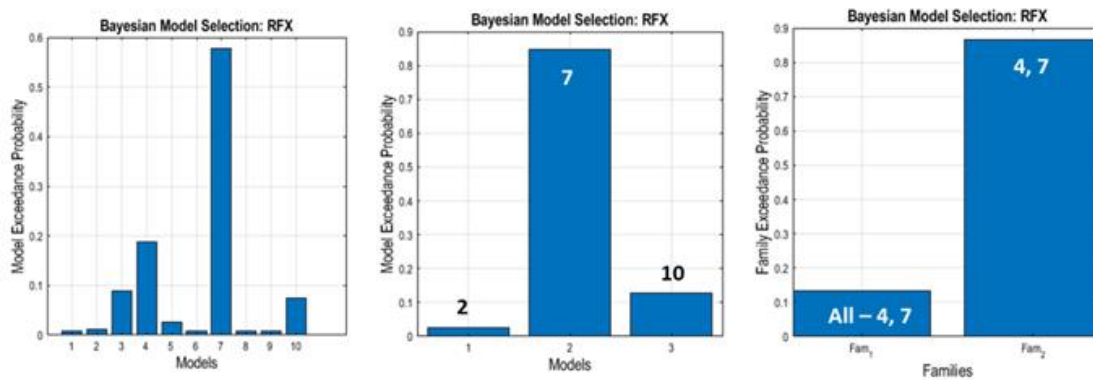


Figure 6.12: Results of the Bayesian Model Selection analysis when Models 1 through 10 were compared in relatives with abnormal and those with normal TDT. The x-axis represents the model exceedance probability, while the y-axis and numbers written in white represents the models/families of models being compared.

b PEB analysis

The PEB analysis took into consideration Models 2, 4, 7, 8 and 10 (as per the winning models obtained from the BMS analysis). The results demonstrated significant differences ($p < 0.05$) in effective connectivity due to the loom stimulus on the SC inhibitory connection between patients vs. controls (Figure 6.13), and on the excitatory connection from the Substantia Nigra to the SC in Relatives_{abnormal TDT} vs. Relatives_{normal TDT}. In both cases, the loom stimulus resulted in a decrease in effective connectivity (compared to the prior). Upon using a less stringent significance threshold for patients vs. controls ($p < 0.09$), the effective connectivity due to the loom stimulus on the excitatory connection from the Substantia Nigra to the SC was also observed to be different, similar to Relatives_{abnormal TDT} vs. Relatives_{normal TDT}.

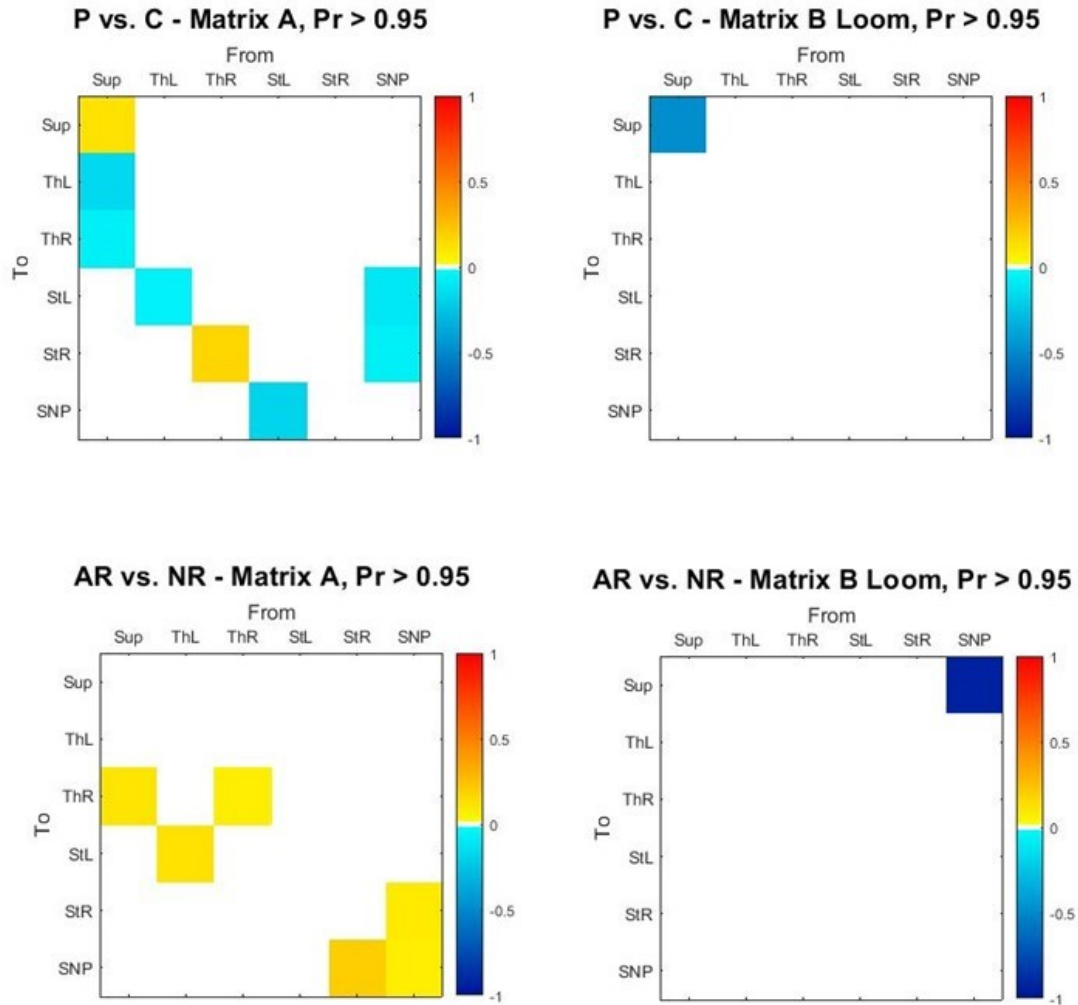


Figure 6.13: Results of the Parametric Empirical Bayes analysis when Models 2, 4, 7, 8 and 10 (obtained as the winning models from the BMS analysis) were compared in patients, unaffected relatives and controls. The results quantify the effective connectivity that exists between two regions and the change in effective connectivity under the influence of the loom modulatory input on the circuitry. A >0 factor denotes an increase in effective connectivity relative to the prior, while a <0 factor denotes a decrease in effective connectivity relative to the prior. P=Patients, C=Controls, AR=Relatives_{abnormal TDT}, NR=Relatives_{normal TDT}.

6.4 Discussion

Cervical Dystonia has been proposed as a midbrain disorder involving the bottom-up CAO network with the Superior Colliculus as the principal nodes (Hutchinson et al., 2014). The current study probed this hypothesis via Dynamic Causal Modelling. Examination of effective connectivity among key regions in the CAO network elucidated the mechanistic patterns underlying regional abnormalities in CD patients as well as unaffected relatives with an abnormal TDT. The findings i) demonstrated

that disrupted SC activity may be due to its abnormal self-inhibitory function and ii) provided evidence for altered bottom-up connectivity across the colliculo-nigro-striatal pathways in the CAO network.

In Study 1, upon comparison of the connectivity architecture among the SC, Thalamus and Striatum, the winning model in both patients and controls was A.2. This suggests that the inter-hemispheric connections between the right and left Thalamus remain unchanged in patients. This was similarly reflected when Model B.2 was compared with B.1 and B.3; there were no significant differences in bilateral thalamic connectivity for both patients and controls. However, a significant difference was observed in patients vs. controls upon comparison of Models B.1 and B.3. The PEB analysis further confirmed these BMS findings, the loom event had a significant differential effect on the striatal-SC connection in patients vs. controls (Figure 6.14). These results revealed the influence of a looming event on the effective connectivity between the Striatum and SC in patients, and are consistent with the CAO network dysfunction hypothesis in CD.

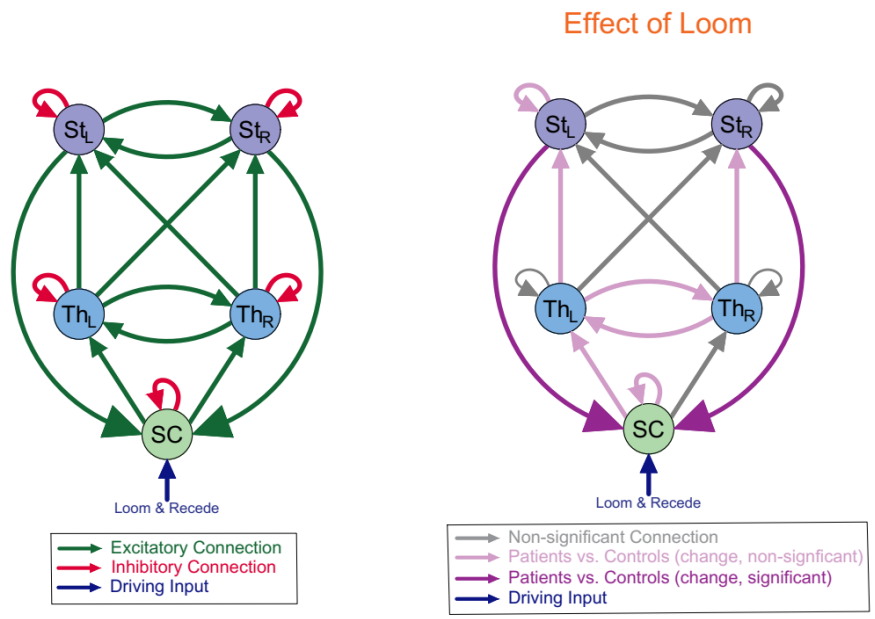


Figure 6.14: On evaluating the change in effective connectivity due to the influence of the loom stimulus, the loom modulatory input had a significant impact (dark pink) on the Striatum-SC connection in patients when compared to controls.

Study 2 incorporated the Substantia Nigra in addition to the previous nodes; the SC, Thalamus and Striatum. Upon probing this network of nodes via the BMS, it was observed that while the Striatum-Substantia Nigra connections as well as the

effective connectivity from the Substantia Nigra to the SC, under the influence of the loom modulatory input, differed for patients vs. controls. Furthermore, the most significant difference in effective connectivity between patients vs. controls ($p < 0.05$) was observed in the SC-SC inhibitory self-connection under the influence of the loom modulatory input. This difference was also observed in the $\text{Relatives}_{\text{abnormal TDT}}$ vs. $\text{Relatives}_{\text{normal TDT}}$ cohorts but was less significant ($p < 0.09$). In the case of the $\text{Relatives}_{\text{abnormal TDT}}$ cohort, the loom modulatory input was observed to have a significant effect on the Substantia Nigra-SC connection (Figure 6.15). Self-connections are always inhibitory in DCM and for a structure like the SC which relies on GABAergic inhibition, this connection in the model may be therefore viewed as a representation for GABA. Via the PEB analysis in Study 2, the loom modulatory input was observed to cause a change in effective connectivity in the inhibitory connection of the SC in patients vs. controls. While this difference was not significant in the $\text{Relatives}_{\text{abnormal TDT}}$ vs. $\text{Relatives}_{\text{normal TDT}}$ cohort, a difference was nevertheless observed at a less stringent probability threshold ($p < 0.09$). Thus, the results of the current study provided further information on the directionality and precise site of effective connectivity changes in the Striato-Nigro-Collicular pathway in CD patients as well as their unaffected relatives with abnormal TDT.

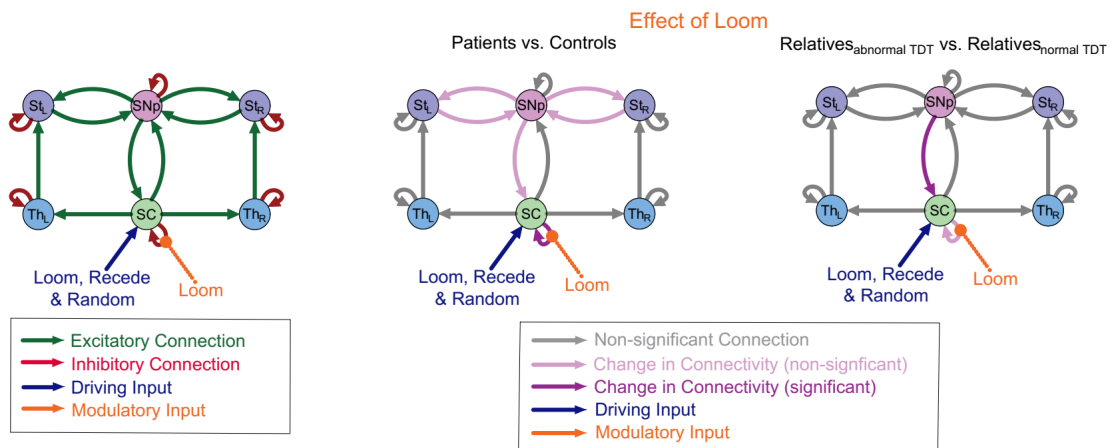


Figure 6.15: On evaluating the change in effective connectivity due to the influence of the loom stimulus, the loom modulatory input (orange) had a significant impact on the SC-SC intrinsic connection, Substantia Nigra-SC and Substantia Nigra-Striatal connection in patients when compared to controls. When relatives were compared, the SC-SC intrinsic connection and the Substantia Nigra-SC connection demonstrated a change in connectivity (light and dark pink) under the loom modulatory input. The driving input (in this case, the loom, recede, random visual stimuli, is shown in blue.

Visual-spatial attention is indispensable for survival as it facilitates motor decisions

based on relevant environmental stimuli and suppresses irrelevant signals (Fecteau and Munoz, 2006; Ungerleider and G, 2000). Shifts of spatial attention are closely associated with orienting movements of the eyes and head (Chelazzi et al., 1995; Karnath et al., 1996; Neggers et al., 2005; Schiller and Tehovnik, 2005; Khan et al., 2009). Due to the fact that the visual cortex projects directly to the SC, this pathway is regarded as the predominant way by which the cortex exerts higher-level control over SC-mediated behaviours (Wurtz and Albano, 1980; Fecteau and Munoz, 2006). The SC and the Basal Ganglia's role in oculomotor and cephalomotor control has been well documented (as discussed in Chapter 2) (Harris, 1980; Guitton and Volle, 1987; Corneil et al., 2004; Pong et al., 2008; Redgrave et al., 2010). It has been demonstrated that defective inhibition at the level of the SC and its inputs from the Substantia Nigra (a key node of the Basal Ganglia) gave rise to anomalous motor outputs to the neck (Kaneda et al., 2008). In animal models, this has been replicated with the resulting head movements analogous to Cervical Dystonia (Holmes et al., 2012), giving rise to the theory that the SC-Basal Ganglia circuit is defunct in CD. Furthermore, inhibitory neurons in the superficial layers of the SC are capable of determining with high temporal accuracy the appearance or disappearance of a stimulus (Kaneda et al., 2008). Defects in this inhibitory network are suggested to result in a decreased ability to perceive short duration temporal differences with sensitivity; giving rise to the phenomenon of an abnormal TDT. Mechanistically, abnormal TDT seems to also stem from a deficit in a neural network incorporating the Basal Ganglia and the SC, which responds to novel environmental stimuli (Jiang et al., 2011; Mayo and Sommer, 2013; Fontes et al., 2016; Basso and May, 2017; Magalhães et al., 2018). The current findings corroborate the above postulations by revealing defective inhibitory connections in the SC in patients vs. controls, and a defective excitatory connection from the Substantia Nigra to the SC in relatives with abnormal TDT vs. relatives with normal TDT. Previous work has also shown putaminal abnormalities in abnormal relatives in the form of increased size by VBM and reduced activation during a temporal discrimination task (Bradley et al., 2009). The results provide evidence that the observed putaminal abnormalities may be due to altered inhibitory connectivity within the SC as well as altered bottom-up striato-nigro-collicular connectivity in the CAO network.

Potential Limitations: The DCM in this study was implemented as a single-state, deterministic and linear model. While this has proved to be effective in the current

study, turning on a stochastic and two-state DCM may help resolve further nuances in the modelling of the pathways and the network and lead to more robust analysis. Also, in order to prevent elimination of subjects from the analysis due to the GLM p-thresholds, less stringent were used to extract activity from the Substantia Nigra. Future studies could incorporate an increase in sample size for high SNR and improved Substantia Nigra activation.

6.5 Chapter Conclusion

Altogether, our findings exhibit changes in effective connectivity in a simplified circuit of the proposed overlapping covert attentional orienting dystonia network. The results corroborate the theory of disrupted SC functioning possibly due to defective GABAergic activity and indicate that the observed putaminal abnormalities may be a characteristic of an alteration in the excitatory and inhibitory connections within the bottom-up striato-nigro-collicular circuitry. Since deficits have also been observed in unaffected relatives with abnormal TDT, is it possible to identify other neural correlates of this endophenotype in these relatives? If the genetic and endophenotype theory indeed holds true, will there be resting-state connectivity differences that exist between the two cohorts? The next chapter seeks to address this question via a functional connectivity study with rs-fMRI data.

7 It's a Small World: Probing Resting State Connectivity and Brain Network Topology in Unaffected Relatives of Cervical Dystonia Patients

In the previous study, a functional abnormality was demonstrated within the SC in both patients and first-degree relatives carrying a disease-specific endophenotype (abnormal TDT); supporting the hypothesis that dysfunctional superior collicular processing may be involved in the pathogenesis of cervical dystonia. However, what is known about the neural circuitry involved in abnormal temporal discrimination? The following chapter seeks to address Research Questions 8-12 in Chapter 3. Genetic and environmental factors have a major influence on individual differences in brain connectivity; understanding their contributions to brain architecture and functioning is of fundamental importance in neuroscience and neurological disorders. As discussed previously, unaffected Relatives_{abnormal TDT} have been hypothesized to be non-manifesting gene carriers of adult-onset idiopathic focal dystonia. However, abnormal temporal discrimination also exists in a variety of basal ganglia disorders. The precise neural circuitry of temporal discrimination remains unknown, resulting in a cloud of uncertainty regarding its endophenotypic role in CD specifically. Furthermore, the heterogeneity of phenotypes makes it imperative to study each phenotype and its associated endophenotype in patients as well as unaffected relatives (Battistella et al., 2015). Therefore, the following research study seeks to explore the neural correlates of abnormal temporal discrimination in unaffected relatives of CD patients. The studies presented in this chapter have resulted in the following peer-reviewed publications:

- Shruti Narasimham, Eavan McGovern, Brendan Quinlivan, Owen Killian, Rebecca Beck, Sean O’Riordan, Michael Hutchinson and Richard B. Reilly. 2019. Neural Correlates of Abnormal Temporal Discrimination in Unaffected Relatives of Cervical Dystonia Patients. *Frontiers in Integrative Neuroscience*, 13, p.8.

- Shruti Narasimham, Vikram Sundarajan, Eavan McGovern, Brendan Quinlivan, Owen Killian, Sean O’Riordan, Michael Hutchinson, Richard B. Reilly. 2019. Characterizing Brain Network Topology in Cervical Dystonia Patients and Unaffected Relatives using Graph Theory. *Proceedings of the 41st International Engineering in Medicine and Biology Conference*, Berlin, Germany.

7.1 Introduction

The sensory TDT is defined as the shortest interval at which two sequential sensory stimuli are perceived as asynchronous (Lacruz et al., 1991); stimuli may be visual, tactile, or auditory. The neural basis of time processing has been examined using tasks such as frequency discrimination, time estimation, and temporal order judgment (Lacruz et al., 1991; Pastor et al., 2004). Evidence from lesion and neurophysiological studies suggests that temporal discrimination involves the time-locked activation of both subcortical and cortical neural networks (Handy et al., 2003). However, the precise neural circuitry involved in temporal discrimination remains unknown. Furthermore, the TDT has been shown to vary physiologically by age (Ramos et al., 2016) and sex (Butler et al., 2015). Temporal discrimination is disordered in a number of basal ganglia diseases including adult-onset dystonia.

Recent studies suggest that an abnormal TDT is an endophenotype of adult-onset focal dystonia. Abnormal TDTs have been found in CD, with high sensitivity and specificity, and in up to 52% of unaffected relatives of patients with CD (Bradley et al., 2009; Kimmich et al., 2014). It is hypothesized that an abnormal TDT is a mediational endophenotype in CD and, as such, is considered a subclinical marker of gene carriage, not altered by disease penetrance or expression. A mediational endophenotype shares common pathogenetic mechanisms with the phenotype; study of the endophenotype may illuminate mechanisms which are not obvious from the phenotype (Hutchinson et al., 2013). Despite the potential importance of temporal discrimination as a marker of disordered sensory processing in the pathophysiology of CD, the neural network function underlying abnormal temporal discrimination in CD patients and their unaffected relatives is poorly understood.

The heterogeneity of phenotypes along with the existence of abnormal TDT in other neurological movement disorders (such as Parkinson’s) makes it imperative to study the

neural correlates of each phenotype and its associated endophenotype in patients as well as unaffected relatives (Battistella et al., 2015) together. Some studies in the past have explored functional changes in unaffected relatives of dystonia patients. For example, regional metabolic changes (Carbon et al., 2004b) were observed in non-manifesting DYT1 (an autosomal dominant, early-onset, generalized dystonia) mutation carriers. Abnormal putaminal structure (hypertrophy by voxel-based morphometry) and function (reduced activation by fMRI during a temporal discrimination task) have been reported in unaffected relatives with abnormal TDTs (Bradley et al., 2009; Termsarasab et al., 2016). Because mutated genes (even without disease penetrance) have an impact on brain function and organization (Meyer-Lindenberg, 2009), it was hypothesized that unaffected relatives with abnormal TDTs would exhibit disordered resting-state connectivity in areas involved in the pathophysiology of CD. Thus, the assessment of possible neural connectivity abnormalities in unaffected first-degree relatives of CD patients harbouring the endophenotype was considered an important next step in elucidating the shared pathomechanisms of abnormal temporal discrimination and CD.

While task-specific neuroimaging studies have great potential to explore the neural basis underlying temporal discrimination and CD, differences found with task-fMRI could reflect compensatory effects of a specific task, thus confounding the primary pathophysiological mechanisms involved. Rs-fMRI studies in CD in the past have primarily demonstrated brain function abnormalities between CD patients and controls (Delnooz et al., 2013; Li et al., 2017). Rs-fMRI data was thus acquired from unaffected first-degree relatives and analyzed in the current study as it offers a means of observing how functional connectivity relates to human behaviour, and how this organization may be altered in neurological diseases (Lee et al., 2013b). To provide evidence for the hypothesis that large-scale topology of functional brain networks and functional connectivity is altered in unaffected relatives with an abnormal TDT vs. a normal TDT, a two-tiered approach of analysis was undertaken which included implementing i) Independent Component Analysis (ICA), regional homogeneity (ReHo) and amplitude of low-frequency fluctuations (ALFF) assessment and ii) graph theoretical analysis (Bullmore and Sporns 2009) of fMRI data. As diverse facets of brain network architecture may be assessed using complementary analytical approaches, ICA was employed in order to investigate functional connectivity among specific resting-state networks across the two groups of unaffected relatives, and graph theoretical analysis

was employed in order to scrutinize the global and local features of functional network architecture in patients, their unaffected relatives and healthy controls.

7.1.1 ICA, ReHo and ALFF

ICA was implemented in order to explore within network functional connectivity (i.e., functional integration) in the standard resting networks across the two cohorts. In addition to this analysis, ReHo and ALFF analyses was also implemented in order to study whole-brain local neural activity (i.e., functional segregation) differences between the two cohorts. ALFF measures rs-fMRI signal variability of each voxel in the frequency domain and is considered one of the most reliable and reproducible rs-fMRI parameters reflecting the level of regional neural activity (Yu-Feng et al., 2007). The ReHo measures the similarity of a given voxel to its neighbourhood voxels in the time domain (Zang et al., 2004). ALFF and ReHo have been applied together to reveal different aspects of brain regional function and abnormalities arising in clinical populations (Lei et al., 2012; Cui et al., 2014; Premi et al., 2014). Therefore, multiple measures were used in the present study to examine different aspects of the resting-state brain in unaffected $\text{Relatives}_{\text{normal TDT}}$ vs. $\text{Relatives}_{\text{abnormal TDT}}$, in order to yield a more complete data-driven characterization of resting-state whole-brain connectivity (Lv et al., 2018). Based on prior rs-fMRI studies in CD and the hypothesis that unaffected relatives are non-manifesting gene carriers, it was postulated that there would be: i) Significant differences in functional connectivity in the resting state networks previously reported in CD, i.e., the sensory-motor network, the executive control network and the primary visual network; ii) Significant differences in connectivity in other networks relevant to dystonia pathophysiology, i.e., the basal ganglia, midbrain and cerebellar networks; iii) ReHo and power differences across the normal and abnormal TDT cohorts in these regions.

7.1.2 Graph Theory

In order to investigate network-wide aberrations in CD patients and unaffected $\text{Relatives}_{\text{abnormal TDT}}$, the aim was to probe large-scale network architecture and topology using a graph theoretical approach. Graph theory-based approaches model the brain as a complex network represented graphically by a collection of nodes and

edges (Bullmore and Sporns, 2009; Wang et al., 2010; Sporns, 2018). In the virtual graph, nodes represent anatomical brain regions, and edges signify the relationships between nodes (e.g., connectivity). Following the network modelling procedure, graph theoretical metrics may be used to examine the structural and functional organization underlying the relevant networks.

7.2 Methods

7.2.1 Ethics, Participants and Pre-processing

Please refer to Chapter 4.

7.2.2 Data Analysis

a Study A - ICA, ReHo and ALFF

Analysis 1: Independent Component Analysis and Dual Regression

In order to examine large-scale functional connectivity patterns within the standard resting-state networks across the two cohorts, ICA and dual regression were employed on the pre-processed data. The pre-processed time series were decomposed into independent components using a multi-session temporal concatenation approach with the MELODIC¹ tool within FSL (Jenkinson et al., 2012). This group-ICA resulted in 41 independent components that were visually examined along with their frequency and time courses. They were also spatially correlated with standard resting-state networks selected from (Smith et al., 2009) using the `Fslcc` utility in FSL to extract the networks relevant to dystonia pathophysiology for further analysis. The components corresponding to the networks relevant to dystonia pathophysiology, i.e., the sensory-motor, executive control and primary visual networks were extracted into one group for a hypothesis based analysis, and those corresponding to the midbrain, basal ganglia and cerebellar networks were extracted into another group for an exploratory analysis.

To assess between-group differences, dual regression was implemented on the set of spatial maps generated from the group-ICA (Figure 7.1). Dual regression is a reliable and robust mathematical back reconstruction method that utilizes the

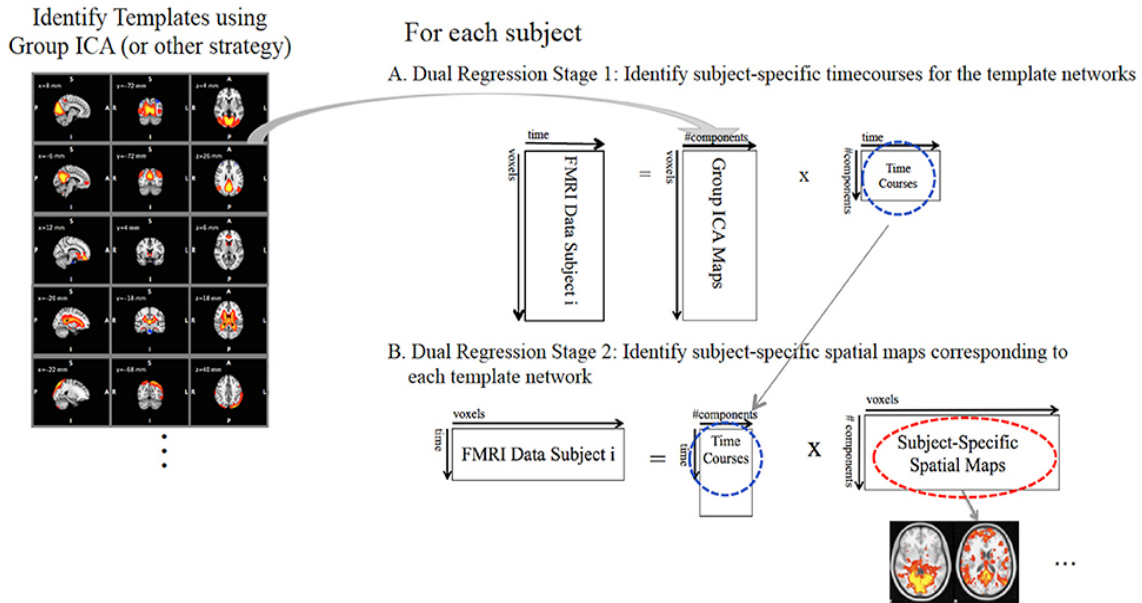


Figure 7.1: Independent Component Analysis and Dual Regression stages A and B for inferring subject-specific spatial maps of components identified. Adapted from Nickerson et al. (2017).

independent component maps as network templates to identify the corresponding functional connectivity maps in each subject (Beckmann et al., 2009). It was implemented using FSLv.5.0.4. A standard general linear model was designed with additional covariates for the six motion regressors, age and gender. This general linear model was input to a non-parametric permutation method for inference thresholding using the randomize function in FSL. The different component maps of each subject were assembled into a 4-D file per subject and tested voxel-wise for significant differences ($Relative_{S_{abnormalTDT}} > Relative_{S_{normalTDT}}$ and $Relative_{S_{abnormalTDT}} < Relative_{S_{normalTDT}}$) by performing 5000 random permutations using a threshold-free cluster enhanced (TFCE) method to control for multiple comparisons (Smith and Nichols, 2009) This was carried out separately for the hypothesis based analysis and for the exploratory analyses. The statistical significance was set at $p \leq 0.05$ after family-wise error (FWE) correction for multiple comparisons over the component of interest. In addition, Bonferroni correction for the number of resting-state networks tested (three networks each in the hypothesis based analyses and exploratory analysis), resulted in a statistical threshold of $p < 0.017$.

Analysis 2: Regional Homogeneity

¹Multivariate Exploratory Linear Optimized Decomposition into Independent Components

The pre-processed (normalized but unsmoothed) images were subjected to a detrending (linear trend subtraction) and temporal filtering (0.01–0.08Hz) procedure on the time series of each voxel to reduce the effect of low-frequency drifts and high-frequency noise. This was carried out with the REST suite (Song et al., 2011). Following this, ReHo analysis was executed for each participant by computing the Kendall Coefficient of Concordance (KCC) of the time series of a given voxel with those of its nearest neighbours (18 voxels) at a voxel-wise level. For normalization, each ReHo map was divided by its Kendall global mean value. The data was smoothed with a Gaussian filter of 6mm full width at half-maximum, to reduce noise and residual differences in gyral anatomy. Age and gender were added as covariates. In order to observe the spatial patterns of each group's brain ReHo distribution, a one-sample t-test ($p < 0.001$) was performed to identify brain regions where the $KCC > 1$. Voxel-wise two-sample t-tests were employed to evaluate between-group differences. The between-group difference was reported at a corrected $p < 0.05$ (voxel $p < 0.005$ and cluster size $> 534\text{mm}^3$), using the AlphaSim method as part of the REST suite (Song et al., 2011).

Analysis 3: Amplitude of Low-Frequency Fluctuations

The previously obtained detrended and filtered signals (from Analysis 2) were used to calculate the amplitude of the low-frequency fluctuations (a measure of each voxel's signal intensity) with the REST suite (Yu-Feng et al., 2007; Song et al., 2011). Briefly, this involved converting the time courses to the frequency domain and computing the square root of the power spectrum, followed by averaging across 0.01–0.08 Hz at each voxel. The averaged square root was taken as the ALFF and a normalized map for each voxel was obtained for each subject. Following smoothing with a 6mm Gaussian filter, a two-sample t-test was implemented to determine the ALFF differences between the normal vs. abnormal TDT cohorts with age and gender as covariates. The between-group difference was reported at a corrected $p < 0.05$ (voxel $p < 0.005$ and cluster size $> 534\text{mm}^3$), using the AlphaSim method as part of the REST suite (Song et al., 2011).

b Study B - Graph Theory Analysis

The pre-processed data was analyzed via the Graph Analysis Toolbox (Hosseini et al., 2012) for investigating between-group differences in a large-scale functional

brain network topology. To examine and quantify features of brain architecture, after time-series extraction and correlation matrix acquisition (Figure 7.2), network parameters were extracted and analyzed, such as the global and local efficiency, characteristic path length and clustering coefficient (Appendix B). These graph metrics were calculated at each cost value ($0.1 < c < 0.7$). A 2-sample t-test was employed in order to evaluate the small-world topological differences between groups (patients vs. controls and $\text{Relatives}_{\text{normal TDT}}$ vs. $\text{Relatives}_{\text{abnormal TDT}}$). P-values ≤ 0.05 were considered significant.

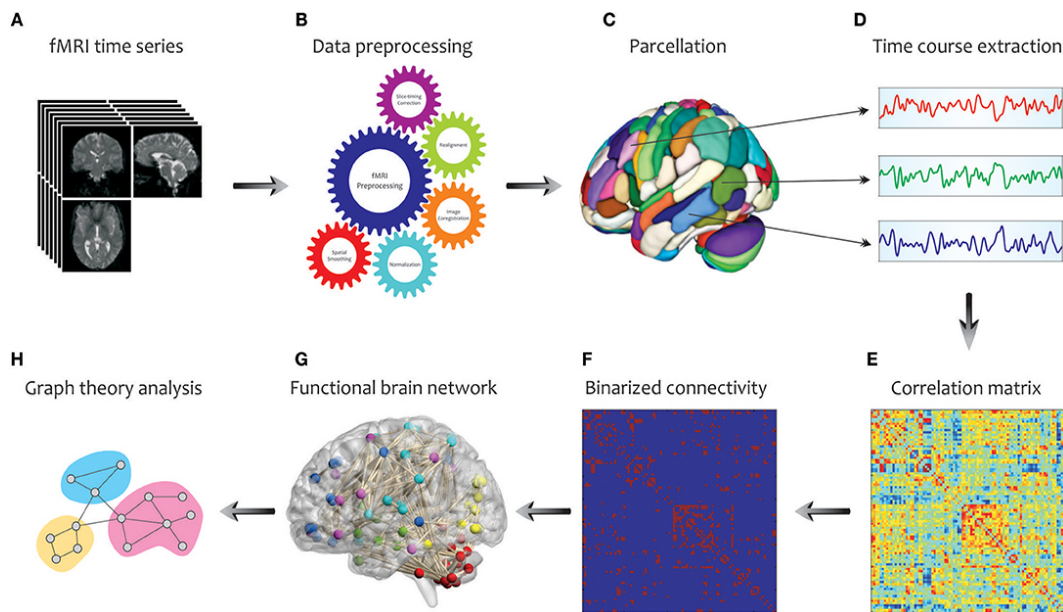


Figure 7.2: Steps employed in the graph theory analysis of the pre-processed rs-fMRI data acquired from CD patients, unaffected relatives and healthy controls. Time series were extracted after region of interest parcellation. A correlation matrix was then calculated and thresholded followed by derivation of graph metrics and network topology construction. Adapted from Karwowski et al. (2019).

7.3 Results

7.3.1 Study A - ICA, ReHo and ALFF

a ICA and Dual Regression

- Hypothesis-based Analysis

Differences in the spatial distribution of the functional connectivity maps in the sensorimotor, executive controls and visual resting-state networks were previously found in CD patients when compared to controls (Delnooz et al.,

2013; Li et al., 2017). Therefore, these networks formed our hypothesis-based analysis in the two cohorts of unaffected relatives. Significant between-group differences (FWE corrected $p < 0.017$) in the spatial distribution of the functional connectivity maps were found in the sensory-motor and the executive control networks (Figure 7.3). $Relatives_{\text{abnormal TDT}}$ demonstrated an increase in connectivity in the left and right Brodmann Area (BA) 32 and right BA 8. While BA 32 is the dorsal region of the cingulate gyrus and is associated with rational thought processes and reaction times, BA 8 is involved in planning complex movements. $Relatives_{\text{abnormal TDT}}$ demonstrated a decrease in connectivity in the right and left primary motor areas, left primary sensory area and left sensory associative regions. Contrary to our hypothesis, no significant difference in the spatial distribution of the functional connectivity maps in the visual network was observed.

- Exploratory Analysis

Due to the cerebellum's role in temporal perception, balance and its implication in the dystonia network, further exploration of functional connectivity differences in the cerebellum, derived from, applying a less stringent inference of $p < 0.05$. The midbrain and basal ganglia networks was also investigated in a similar way. The exploratory analysis revealed functional connectivity differences between the abnormal and normal TDT groups for the cerebellar network corresponding to a less stringent threshold of $p < 0.05$ FWE-corrected without Bonferroni correction, as it did not survive the Bonferroni corrected $p < 0.017$ (Figure 7.3). However, no significant differences were found between these cohorts for the midbrain and basal ganglia networks.

b ReHo

The between cohorts ReHo analysis revealed significant differences (corrected $p < 0.05$) in ReHo values for the cerebellum, Thalamus, primary auditory, primary sensory and Brodmann areas as described in Table 7.1 and shown in Figure 7.4. $Relatives_{\text{abnormal TDT}}$ demonstrated a decrease in ReHo compared to $Relatives_{\text{normal TDT}}$ in the left and right BA 8 (corroborating the findings of the ICA results), in the parahippocampal gyrus and in the left BA 10. $Relatives_{\text{abnormal TDT}}$ demonstrated an

increase in ReHo compared to $Relative_{normal\ TDT}$ in the Thalamus, cerebellum and BA 45 responsible for motor inhibition.

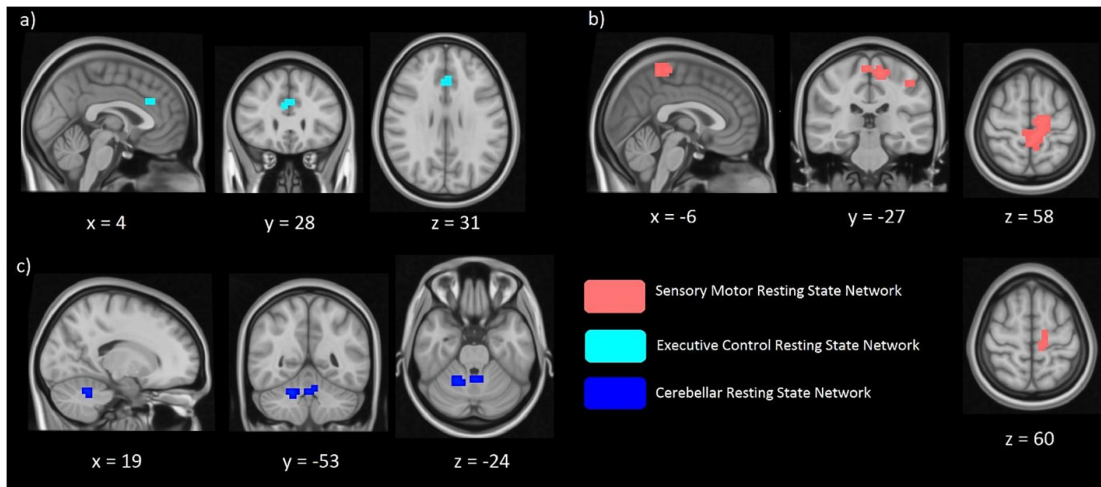


Figure 7.3: Significant differences of functional connectivity (FC) within the executive control network (a) sensorimotor network (b), and cerebellar network (c) between $Relative_{normal\ TDT}$ vs. $Relative_{abnormal\ TDT}$ values. $Relative_{abnormal\ TDT}$ demonstrated increased FC within the executive control ($p < 0.017$) and cerebellar networks ($p < 0.05$) but decreased FC within the sensorimotor network ($p < 0.017$).

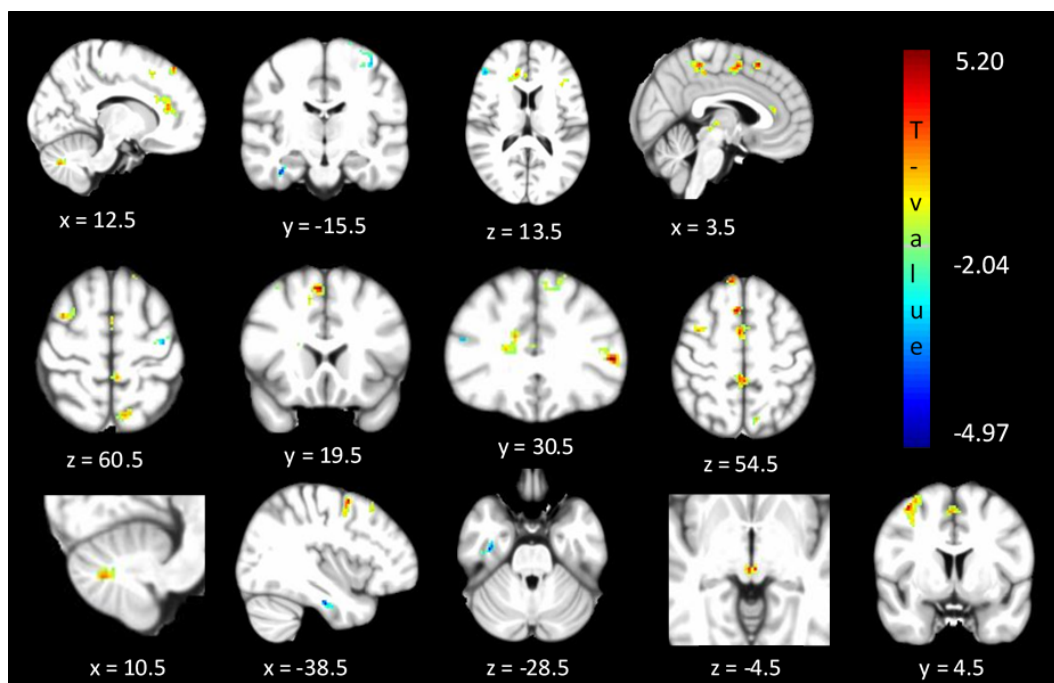


Figure 7.4: Significant differences (corrected $p < 0.05$) in ReHo values between $Relative_{normal\ TDT}$ vs. $Relative_{abnormal\ TDT}$ values. The blue/green colors represent regions where $Relative_{abnormal\ TDT}$ have decreased local coherence than $Relative_{normal\ TDT}$. The red/yellow colors represent regions where $Relative_{abnormal\ TDT}$ have increased local coherence than $Relative_{normal\ TDT}$.

Table 7.1: Significant differences in ReHo differences (corrected $p < 0.05$) between relatives with normal and abnormal TDT. BA=Brodmann Area, FEF=Frontal Eye Field, R=Right, L=Left.

Relatives_{abnormal TDT} < Relatives_{normal TDT}					
x (mm)	y (mm)	z (mm)	Region	Side	Function
-7	20	55	BA 8	L	FEF-Control of eye movements
-30	56	-6	BA 10	L	Motor Planning
-39	-16	61	BA 6	L	Motor Sequencing and Planning Movements, Saccades
36	-15	-21	ParaHippocampal Gyrus	R	Scene recognition
48	38	14	BA 46	R	Motor planning, organization and regulation, Saccades
12	41	52	BA 8	R	FEF-Control of eye movements
Relatives_{abnormal TDT} > Relatives_{normal TDT}					
x (mm)	y (mm)	z (mm)	Region	Side	Function
13	-70	38	Cerebellum	R	Movement, Coordination, Precision, Timing, Balance
12	44	8	BA 10	R	Motor Planning
4	-36	53	Sensory Associative	R	Visuospatial, visuo-motor processing, saccades
-7	20	55	BA 8	R	FEF-Control of eye movements
-3	-23	-1	Thalamus	L/R	Sensory perception, motor Regulation
5	-1	53	BA 6	R	Motor Sequencing and Planning Movements, Saccades
-2	-26	-5	Brainstem Midbrain	and L/R	Control, Conduction, Multisensory Integration
-49	31	7	BA 45	L	Motor inhibition
-12	-63	61	BA 7	L	Visual-Motor coordination, Motor execution, Saccades

c ALFF

The between cohort analysis revealed significant differences (corrected $p < 0.05$) in the ALFF between the two cohorts of unaffected relatives in the cerebellum, hypothalamus, primary visual, primary sensory and Brodmann areas as described in Table 7.2 and shown in Figure 7.5. $Relatives_{\text{abnormal TDT}}$ demonstrated a decrease in ALFF in the primary visual area, hypothalamus, BA 46 related to saccadic activity and left primary auditory area. However, there was a decrease in BA 7, BA 45 and the sensory associative regions.

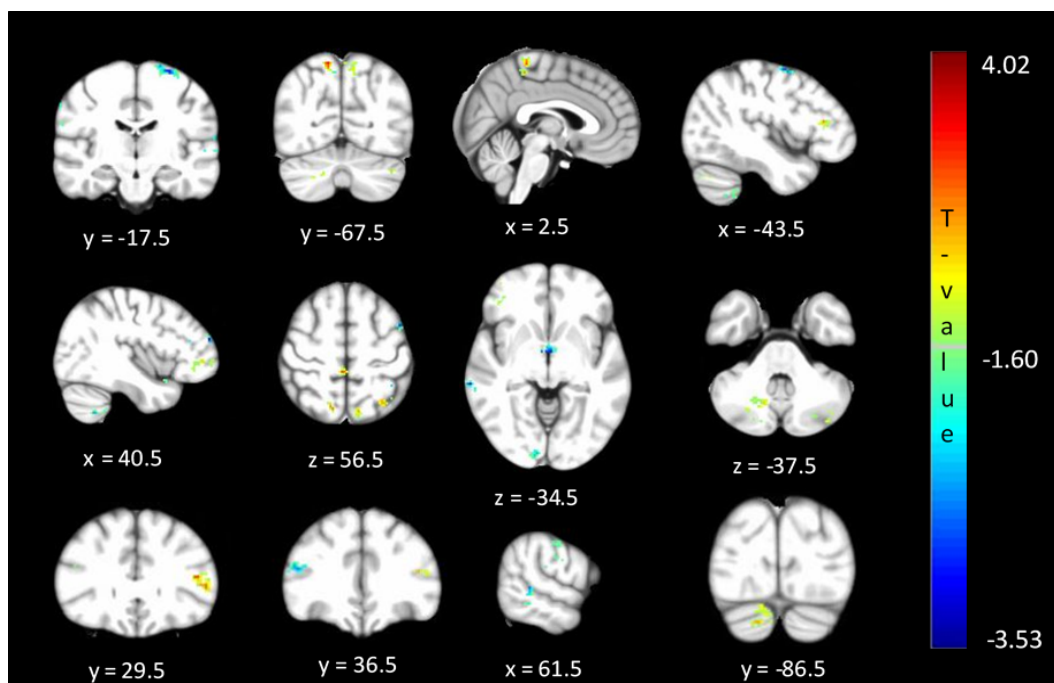


Figure 7.5: Significant differences (corrected $p < 0.05$) in ALFF values between $Relatives_{\text{normal TDT}}$ vs. $Relatives_{\text{abnormal TDT}}$ values. The blue/green colors represent regions where $Relatives_{\text{abnormal TDT}}$ have decreased signal power than $Relatives_{\text{normal TDT}}$. The red/yellow colors represent regions where $Relatives_{\text{abnormal TDT}}$ have increased signal power than $Relatives_{\text{normal TDT}}$.

Table 7.2: Significant differences in ALFF differences (corrected $p < 0.05$) between relatives with normal and abnormal TDT. BA=Brodmann Area, FEF=Frontal Eye Field, R=Right, L=Left.

Relatives_{abnormal TDT} < Relatives_{normal TDT}					
x (mm)	y (mm)	z (mm)	Region	Side	Function
42	36	16	BA 46	R	Motor planning, organization and regulation, Saccades
42	53	20	BA 10	R	Motor Planning
-29	-18	67	BA 6	L	Motor Sequencing and Planning Movements, Saccades
11	-95	-6	Primary Visual	R	Visual processing
-3	-3	-5	Hypothalamus	L/R	Emotions, temperature
62	-35	2	BA 21	R	Visual, auditory, deductive reasoning, language
34	-71	-38	Cerebellum	R	Movement, Coordination, Precision, Timing, Balance
-67	-22	7	Primary Auditory	L	Auditory information processing
Relatives_{abnormal TDT} > Relatives_{normal TDT}					
x (mm)	y (mm)	z (mm)	Region	Side	Function
-33	-61	57	BA 7	L/R	Object spatial location
3	-35	62	Primary Motor	R	Movement execution
3	-34	53	Sensory Associative	R	Integration of sensory information, memory, learning
-51	30	7	BA 45	L	Movement, response inhibition, memory
15	-87	-34	Cerebellum	R/L	Movement, Coordination, Precision, Timing, Balance

7.3.2 Study B - Graph Theory Analysis

As described previously, in order to study global network topology and probe differences in $\text{Relatives}_{\text{normal TDT}}$ vs. $\text{Relatives}_{\text{abnormal TDT}}$, graph metrics and network topology were studied across patients, relatives and controls. To explore and visualize region to region connectivity and study how this differs across the four cohorts, the pairwise association between each region was computed, forming a connectivity matrix. The brain network was then constructed from the nodes (180 regions from the Automated Anatomic Labeling atlas (Tzourio-Mazoyer et al., 2002)) and the edges (pairwise associations), as shown in Figures 7.6 and 7.11. The results demonstrated a similarity in connectivity patterns between controls and $\text{Relatives}_{\text{normal TDT}}$ and between patients and $\text{Relatives}_{\text{abnormal TDT}}$. These two sets however differed from each other with decreased connectivity between the sensory-motor region and precuneus in patients and $\text{Relatives}_{\text{abnormal TDT}}$ vs. controls and $\text{Relatives}_{\text{normal TDT}}$. Figures 7.6 and 7.11 show the overall network organization and connectivity architecture in each of the four groups. The dots representing nodes in the brain depict the weights of the nodes, i.e. hub formation. Hubs have been found to have a significant impact on the network topology. The results indicate a change in hub formation in unaffected relatives of CD patients. Relatives with normal and abnormal TDT demonstrate a change in network topology compared to controls. Changes in hub formation may be observed in the cerebellum, supra-marginal gyrus, occipital visual region, Thalamus and amygdala.

In order to further quantify the changes in network architecture, graph metrics measuring global topology characteristics were extracted for relatives, patients and controls. These metrics were plotted as a function of network density ($0.1 < \text{cost} < 0.7$). There was a significant difference ($p \leq 0.05$) in clustering coefficient (Figure 7.7) between $\text{Relatives}_{\text{normal TDT}}$ vs. $\text{Relatives}_{\text{abnormal TDT}}$ at cost values 0.1 to 0.4. Local efficiency was significantly different ($p \leq 0.05$) across the two groups at density values between 0.1 and 0.35. Characteristic path lengths and global efficiency were also compared across the cohorts. When comparing path length (Figure 7.9), patients $>$ controls at density 0.1 and 0.12, but patients $<$ controls at density > 0.12 . On the other hand, the path length of $\text{Relatives}_{\text{abnormal TDT}}$ was greater than that of $\text{Relatives}_{\text{normal TDT}}$ at density > 0.1 . Upon analyzing global efficiency values (Figure 7.8), there was a significant difference between patients and controls but not between relatives with

normal and abnormal TDT. Patients had a higher value than controls at density 0.1 to 0.17.

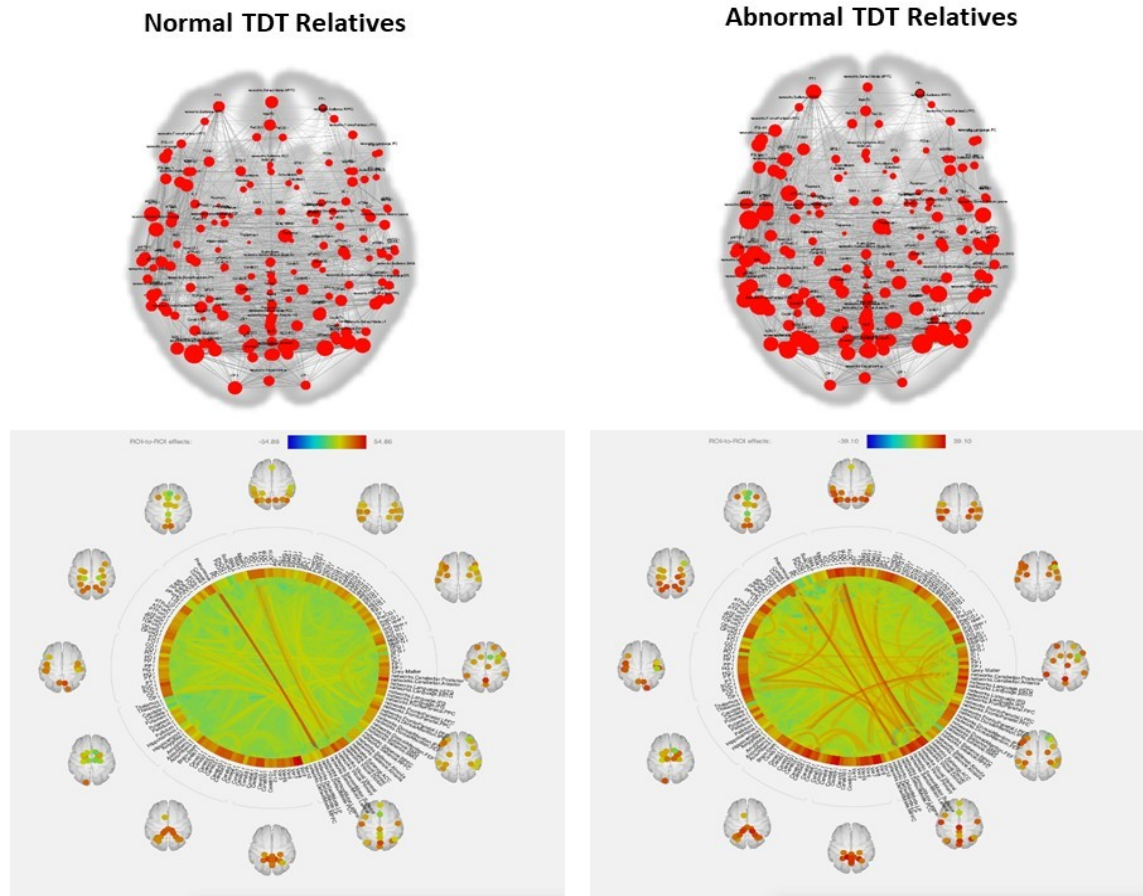


Figure 7.6: Top: Overall connectivity architecture and organization obtained for 180 ROIs (at density = 0.15) for $\text{Relatives}_{\text{normal TDT}}$ (left) and $\text{Relatives}_{\text{abnormal TDT}}$ (right). The sizes of the dots depict regional weight / hub formation. Bottom: Network graphs of $\text{Relatives}_{\text{normal TDT}}$ (left) and $\text{Relatives}_{\text{abnormal TDT}}$ (right). Color of edges indicates connectivity strength between two regions of interest (ROIs).

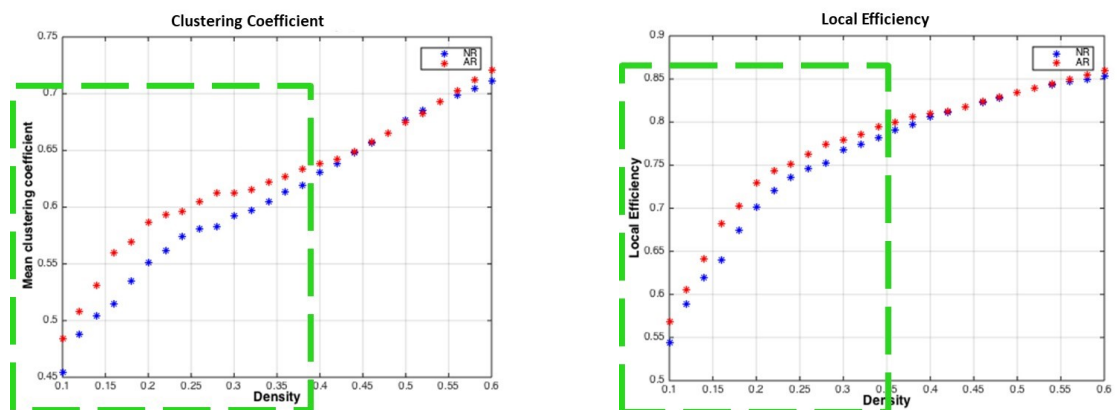


Figure 7.7: Clustering Coefficient and Local Efficiency metrics compared for $\text{Relatives}_{\text{normal TDT}}$ vs. $\text{Relatives}_{\text{abnormal TDT}}$ across a range of cost values.

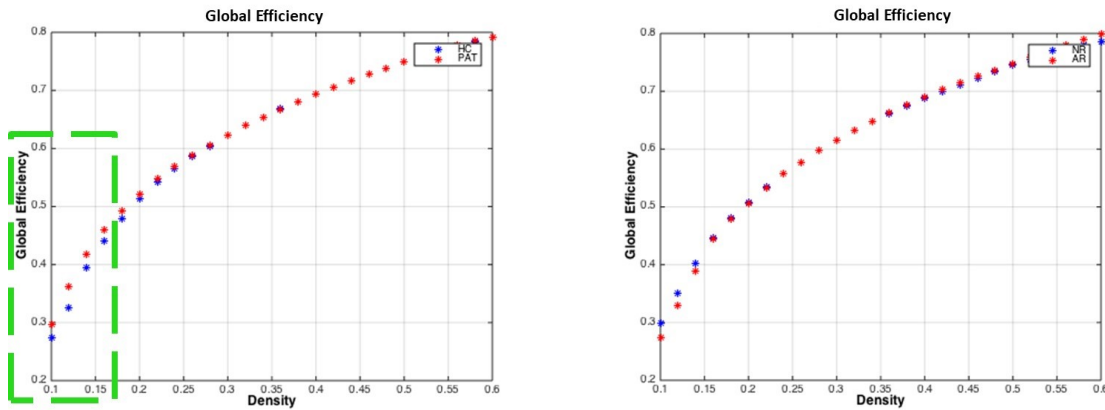


Figure 7.8: Global Efficiency metric compared for patients vs. controls and for $Relative_{normal\ TDT}$ vs. $Relative_{abnormal\ TDT}$ across a range of cost values.

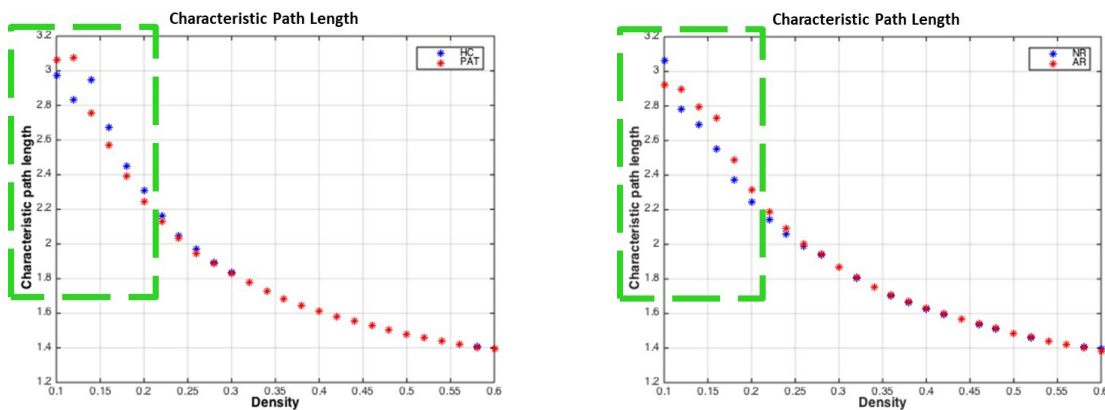


Figure 7.9: Characteristic Path Length metric compared for patients vs. controls and for $Relative_{normal\ TDT}$ vs. $Relative_{abnormal\ TDT}$ across a range of cost values.

7.4 Discussion

7.4.1 Study A - ICA, ReHo and ALFF

This study explored the neural connectivity basis of abnormal temporal discrimination as an endophenotype for CD. The findings revealed altered intrinsic regional activity in unaffected relatives of CD patients, who have abnormal temporal discrimination. These connectivity differences were measured by studying within network metrics via ICA and Dual Regression analyses, as well as ReHo and signal fluctuation amplitude analyses. As part of the hypothesis based analysis, our results demonstrated altered resting-state functional connectivity in the sensory-motor (decreased connectivity) and executive control (increased connectivity). As part of the exploratory-based analysis, our results demonstrated altered resting-state connectivity in the cerebellar (increased

connectivity) network in $Relatives_{\text{abnormal TDT}}$ when compared to $Relatives_{\text{normal TDT}}$ values. Areas related to motor planning, motor learning, visual motion processing, saccades, emotion and visual-motor coordination were observed to have local functional incongruities between the two groups. An abnormal TDT in unaffected first-degree relatives was found to be linked with local brain function abnormalities in regions associated with CD pathophysiology. This would be consistent with the hypothesis that these relatives are non-manifesting dystonia gene carriers. Event-related fMRI studies have examined the time course of activation associated with different components of time perception (Rao et al., 2001; Nenadic et al., 2003; Pastor et al., 2004). The results of these studies demonstrated a dynamic and complex network of cortical and subcortical activation associated with different components of temporal processing, implicating the basal ganglia, cerebellum and sensory-motor regions in the tasks involved. Similar patterns of differential brain function were observed in these areas when comparing relatives with abnormal and normal TDTs.

A rs-fMRI study, carried out with CD patients and controls (Delnooz et al., 2013; Li et al., 2017), established within-network functional connectivity differences in the sensory-motor, executive control and primary visual networks. CD patients showed a decrease in connectivity within the sensory-motor network and an increase in connectivity within the executive control network compared to controls. Since these areas could also be expected to be involved in the visual temporal discrimination task, and in keeping with the hypothesis that both CD and abnormal TDT arise from common defective cortical and sub-cortical mechanisms, it was hypothesized that there would also be within-network functional connectivity differences in these networks (sensory-motor, executive control and primary visual) across abnormal vs. normal TDT subjects. Consistent with our hypothesis and previous literature, connectivity differences were found in the sensory-motor and executive control networks. Relatives with abnormal TDTs demonstrated decreased connectivity in the sensory-motor network compared to relatives with normal TDTs. For the executive control network, relatives with abnormal TDTs demonstrated an increase in connectivity compared to relatives with normal TDTs. This was complemented by results from the ReHo and ALFF analyses. Together the results from the present and previously reported studies (Figure 7.10), suggest that the CD and temporal discrimination circuit share common dysfunctional nodes. This cautiously suggests that TDT may indeed be a true

endophenotype of dystonia (given the finding of similar abnormalities), while, on the other hand, the data does not indicate the actual origin of the abnormal TDT itself. Although a causal/consequential role cannot be determined at this stage, the presence of neural connectivity related changes in unaffected relatives with abnormal TDTs supports the concept of the TDT as an endophenotype in this disorder. Network-related changes have been observed in non-manifesting carriers of DYT1 mutations in the posterior Putamen / Globus Pallidus, Cerebellum and Sensorimotor Area and thus were unrelated to the presence of symptoms (Trost et al., 2002; Carbon et al., 2004b). Our results also suggest that the observed network-related changes are not due to dystonia manifestation, but relate instead to the altered neural mechanisms caused by poorly penetrant genetic mutations.


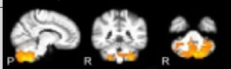
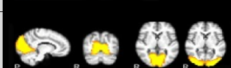


Resting State Networks		FINDINGS FROM THE PRESENT STUDY	FINDINGS FROM PREVIOUS STUDIES IN THE LITERATURE
		Relatives with Abnormal TDTs compared to Relatives with Normal TDTs	Patients with Cervical Dystonia compared to Healthy Controls
Sensory Motor Network		↓ (FWE Bonferroni corrected $p < 0.017$)	↓ (Delnooz, 2013; Li et al., 2017)
Cerebellar Network		↑ (FWE corrected $p < 0.05$)	↑ (Li et al., 2017)
Visual Network		↓ (FWE corrected $p < 0.05$)	↓ (Delnooz, 2013; Li et al., 2017)
Basal Ganglia Network		↑ and ↓ in different regions of the basal ganglia (FWE corrected $p < 0.05$)	↑ with the sensorymotor regions ↓ with the frontopareital regions (Delnooz, 2015; Li et al., 2017)
Executive Control Network		↑ (FWE Bonferroni corrected $p < 0.017$)	↑ (Delnooz, 2013)

Figure 7.10: Changes in within network functional connectivity in Relatives_{abnormal TDT} when compared to Relatives_{normal TDT}. Comparative analyses with previous rs-fMRI connectivity studies carried out with patients with CD and healthy controls. ↑ Increased connectivity; ↓ Decreased connectivity; Dark Red, Significant changes in functional connectivity, ReHo and ALFF; Light Red, No significant changes in functional connectivity detected via the ICA method but significant changes in regional coherence (ReHo) and power (ALFF) detected.

A fundamental element of sensorimotor function is the accurate discernment and organization of the temporal characteristics of sensory stimuli and motor output. Optimal movement execution entails precise processing of sensory information from the environment, as is evidenced from visuo-motor, touch, and proprioception experiments (Tinazzi et al., 2013, 2014). In the present study, the presence of local sensory-motor connectivity discrepancies in unaffected relatives with abnormal TDTs points to the existence of abnormal connectivity patterns in the sensorimotor and executive control

areas, prior to disease manifestation. Future studies involving varied sensory-motor tasks in unaffected relatives need to be carried out, in order to probe the extent of involvement and manifestation of the sub-clinical sensory-motor and executive control abnormalities.

The cerebellum is also involved in a complex network for sensory-motor integration (Brunamonti et al., 2014). Due to the role of the cerebellum in timing-related events (Manganelli et al., 2013) and the increasing evidence of the cerebellum's role in dystonia (Prudente et al., 2014), exploratory analysis was carried out to study resting-state connectivity in this region. The results revealed significant differences in connectivity within the cerebellum between subjects with abnormal and normal TDTs; those with abnormal TDTs showed an increase in functional connectivity compared to those with normal TDTs. This was corroborated by higher signal power (ALFF) and local coherence (ReHo) in the area. Studies have reported diminished time perception in patients with cerebellar deficits (Di Biasio et al., 2015; Raghavan et al., 2016). The bulk of cortical input to the cerebellum (via the pons) comes from the sensory and parietal areas (Pastor et al., 2004). Time perception deficits have been correlated with abnormalities in the vermis, as well as the lateral cerebellar hemispheres (Rao et al., 2001). The activation of the cerebellum in both spatial and temporal discrimination tasks using tactile stimuli in an fMRI study, suggested its role in optimizing the perception of sensory inputs (Pastor et al., 2004). Our results corroborate past neuroimaging research with these temporal discrimination tasks and cerebellar atrophy studies (Manganelli et al., 2013). Furthermore, our results point to the presence of cerebellar deficits in unaffected first-degree Relatives_{abnormal} TDT, which could be a substrate for eventual CD manifestation (which may depend on environmental insults). The presence of increased as well as decreased ALFF values in different regions of the cerebellum may indicate the development of compensatory mechanisms in unaffected relatives.

In an fMRI study exploring temporal information processing and the basal ganglia (Nenadic et al., 2003), time estimation (vs. rest condition) elicited a distinct pattern of activity in the right medial and both left and right dorsolateral prefrontal cortices, Thalamus, basal ganglia (caudate nucleus and Putamen), left anterior cingulate cortex, and superior temporal auditory areas. The Thalamus and Putamen have been considered as important nodes in the temporal discrimination circuit (Lacruz et al., 1991). Some

neural models of temporal information processing consider that fronto-subcortical circuits linking the prefrontal cortical areas with the striatum and Thalamus have a specific role in temporal processing (Gibbon et al., 1997). Our results likewise demonstrated increased ReHo in the Thalamus in relatives with abnormal TDTs. The absence of connectivity-related differences in the visual, basal ganglia and midbrain networks, as measured by the independent component analyses, indicates the non-existence of the manifestation of abnormalities in these regions in relatives. Further, it could also be due to visual related connectivity differences manifesting only during task activation or the need for specific region of interest masks for more precise identification (Delnooz et al., 2015). Regional connectivity changes in these areas were however detected via ReHo and ALFF metric abnormalities between the two groups. The involvement of areas related to motor planning, learning, movement coordination, saccades, executive function, cross-modal association and emotion, suggests a multi-network dysfunction manifestation due to (as yet unidentified) gene carriage in unaffected relatives of CD patients. Dysfunction in these regions is consistent with CD pathophysiology (Müller et al., 2005; Chillemi et al., 2017) and our results thus support the plausible concept of susceptibility gene carriage in these unaffected relatives.

Smoothing is an essential step during data analysis / preprocessing as it increases the signal-to-noise ratio, compensates for imperfect registration, compensates for intersubject variability in neural organization and also reduces the number of independent comparisons during multiple comparison correction. Spatial smoothing using a 6mm Gaussian kernel at full-width half maximum is the most preferred kernel used in ReHo analysis as evidenced by a variety of studies conducted previously (Li et al., 2012; Zuo et al., 2013; An et al., 2013; Zhao et al., 2018; Brodoehl et al., 2019; Shao et al., 2019). While small smoothing kernels can make data non-normal and therefore impact statistical assumptions, it has been suggested that if only small regions of activity are expected, or in only a very limited anatomical region, it is more beneficial to smooth with a small filter (Mikl et al., 2008). Furthermore, KCC-ReHo is a rank-based non-parametric data-driven approach, that allows for examining the temporally auto-correlated samples with non-normal distributions, and is more robust against noise in the data, which is useful for real R-fMRI time series (Zuo et al., 2013). In addition, as smoothing before ReHo calculation will largely increase the

regional similarity, smoothing after calculating ReHo is the preferred option (Song et al., 2011). Studies in the past have demonstrated that spatial smoothing (with a 6mm Gaussian kernel) robustly strengthened the global ReHo while also reducing the ratio of voxels exhibiting substantial intra-session reliability (Li et al., 2012; Zuo et al., 2013; Zhao et al., 2018). Nevertheless, there have been a few studies using 4mm (Ni et al., 2017; Jiang et al., 2019), 5mm (Cao et al., 2020) and 8mm smoothing kernels for ReHo analysis (Wang et al., 2017). Therefore, future rs-fMRI studies implementing ReHo measures in Dystonia need to probe the influence of smoothing kernels on the non-normality of the data.

7.4.2 Study B - Graph Theory

In the present study, alterations in global network properties in CD patients along with their first degree unaffected relatives (stratified according to their TDT values) were examined, by using graph theoretical analysis on resting-state fMRI data. The results demonstrate patterns of dysfunction similar to patients (to a certain extent) in unaffected relatives and suggest the manifestation of possible compensatory mechanisms in play in unaffected Relatives_{abnormal TDT} compared to those with normal TDT.

Differences in hub formation (Figure 7.11) and network topology depicted via inter-nodal correlations suggest that micro alterations in brain structure and function are also present in unaffected Relatives_{abnormal TDT} (as well as in CD patients). These findings support the concept that relatives may be unidentified gene carriers, and external influences (such as environment, accident, etc.) might further contribute to the ultimate manifestation of CD. Involvement of altered hub formation at the amygdala and subcallosal gyrus provides evidence for neural substrates of the social and emotional aspects associated with this disorder (Camfield et al., 2002; Pekmezovic et al., 2009; Tomic et al., 2016; Czekoova et al., 2017).

Global efficiency reflects the speed of information transfer across nodes. There were no significant differences in global efficiency between Relatives_{abnormal TDT} and Relatives_{normal TDT} but patients demonstrated increased values compared to controls. Local efficiency and clustering coefficient were used to evaluate network ability for processing specialized information and functional segregation. The higher the clustering coefficient and local efficiency, the more segregated the network. An increase

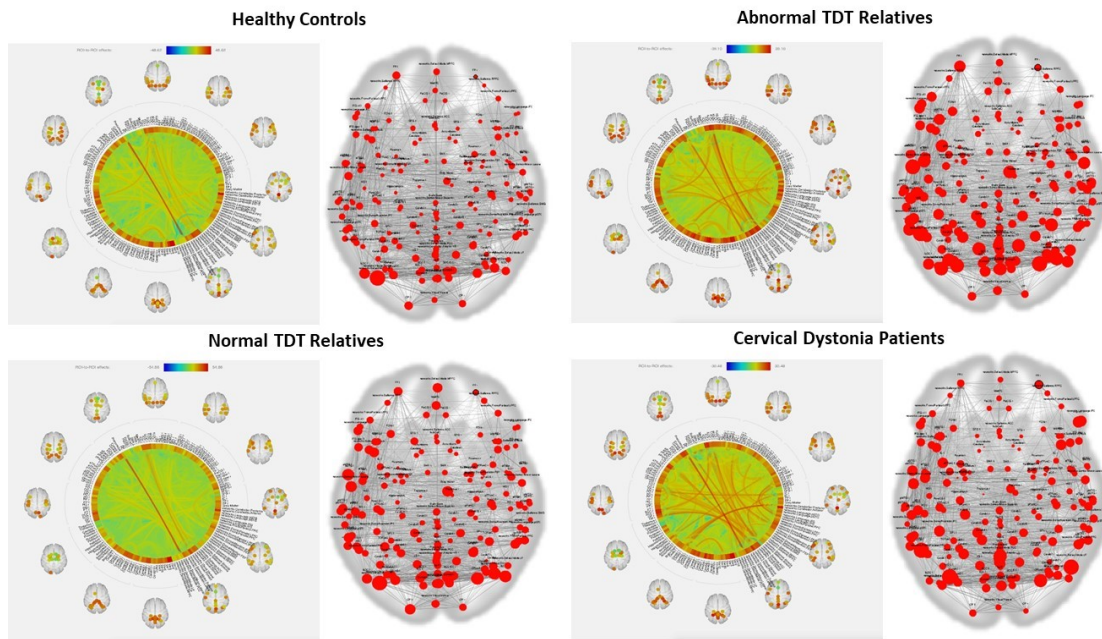


Figure 7.11: Network graphs of controls and Relatives_{normal TDT}, as well as of Relatives_{abnormal TDT} and patients. Color of edges indicates connectivity strength between two regions of interest (ROIs). Overall connectivity architecture and organization obtained for 180 ROIs (at density=0.15). The sizes of the dots depict regional weight.

in local efficiency, mean clustering coefficient as well as characteristic path length, was observed in Relatives_{abnormal TDT} compared to Relatives_{normal TDT}, but a decrease was observed in patients compared to controls (Figures 7.7 and 7.9). This could imply compensatory mechanisms under play that sustain an abnormal TDT but do not lead to the manifestation of CD. The cause for such a compensation and anomaly needs to be further explored.

Thus, the existence of differences detected between unaffected relatives with normal and abnormal TDT could represent the effects of a subclinical pre-symptomatic phase due to the expression of an abnormal gene or a protective neuroplastic response to that gene. This needs to be probed in a longitudinal study with relatives and patients.

Limitations: The primary limitation of the current study is that it cannot be ascertained whether the abnormalities detected represent the effects of a pre-symptomatic phase due to the expression of an abnormal gene or a protective neuroplastic response to that gene. The number of subjects in each group is quite low. Future studies may look into hub metrics and nodal/local metrics in each of the abnormal regions identified, for a more detailed graph theory analysis in unaffected relatives.

7.5 Chapter Conclusion

In the present study, the neural circuitry of disordered temporal discrimination was studied in the context of its role as an endophenotype in CD. Our results demonstrated significant differences in resting functional connectivity in the sensorimotor, executive control and cerebellar networks, in relatives with abnormal TDTs when compared to relatives with normal TDTs. The aberrations detected in the present study occurred in regions previously associated with the pathophysiology of CD. They suggest possible resting brain function alterations that may be an indicator of neural plasticity or impending disorder manifestation, caused by the carriage of, as yet unidentified, genes in unaffected first degree Relatives_{abnormal TDT}. It was also possible to delineate changes in network topology in first-degree unaffected relatives (with abnormal TDT) of cervical dystonia patients. The results collectively: i) Indicate a multi-network system-level dysfunction in relatives with abnormal TDTs involving hubs associated with CD. ii) Demonstrate that this occurs by virtue of regional changes (markers of dysfunction – connectivity, homogeneity and frequency power) in these networks. iii) Support the hypothesis that the manifestation of this network dysfunction in unaffected relatives is due to the carriage of as yet unidentified and poorly penetrant genes. iv) Provide evidence that unaffected relatives with abnormal TDTs have certain network aberrations, which, following appropriate environmental exposures may result in disease penetrance. A longitudinal analysis carried out by studying relatives with abnormal TDTs who later go on to manifest dystonia and probing the extent of manifestation via changes in hub formation and network architecture, would strengthen the clinical value of abnormal TDT as an indicator of as yet unidentified genes, as well as its utility as a predictive marker of the eventual disease manifestation and further enhance our understanding of the pathophysiology of this disorder.

8 A Bird's Eye View: Investigating Multimodal Multivoxel Pattern Analysis and Ensemble Learning in Dystonia

Via the previous studies, abnormal regional activity and connectivity related changes were detected across patients and unaffected relatives with abnormal TDT. While this has proven to be valuable in developing a better understanding of the disorder, these abnormalities have been detected via a univariate analyses of unimodal data. There has been little progress to link the abnormalities observed in structure and function in dystonia to date. Can multimodal integration help solve this conundrum and is it feasible to be carried out in cervical dystonia? The current study seeks to address research questions 13 - 19 in Chapter 3. The relationship among the differences across the multiple modalities is usually complex, making traditional linear models ineffective. Univariate analysis can lead to missing important information that is jointly encoded by voxels. A multivoxel pattern analyses approach along with multimodal data fusion can help resolve this issue due to its greater sensitivity, and ability to decode the association between structural and functional alterations. Furthermore, the advantages of ensemble learning as a robust algorithm has been used in various other studies but not in dystonia to date. Therefore, the aim of the following research study was to utilize multivariate pattern analysis and ensemble learning in order to integrate the identified abnormalities in structure and function and classify patients and controls. The studies presented in this chapter have resulted in the following peer-reviewed publications under-review and in-preparation:

- Shruti Narasimham, Alexander Meulemans, Rebecca Beck, Sean O'Riordan, Michael Hutchinson, Richard B Reilly. Investigating Ensemble Learning and Multivoxel Pattern Analysis for Multimodal Neuroimaging Insights into Cervical Dystonia. *Journal of Neuroscience Methods*, Under Review - JNEUMETH-D-19-00467.

8.1 Introduction

Probing neuroimaging data using multivariate pattern recognition algorithms has been garnering attention in the recent decade due to their ability to encode joint information from voxels across the brain rather than the traditional univariate approach (Mahmoudi et al., 2012; Stephan et al., 2017). This compliments the brain's method of functioning and models its complexity (Norman et al., 2006). However, while multivariate approaches have been shown to result in greater statistical power and provide more information about brain function, the topographic information offered is usually more complex to decode due to the mathematical convolutions of the neural substrates underlying brain processes (Snoek et al., 2019). Nevertheless, they are increasingly being used to not only make crucial inferences in clinical neurological disorders but also assist in prediction analysis in a new patient cohort (Rivolta et al., 2014; Whitfield-Gabrieli et al., 2016; Gilron et al., 2017; Nguyen et al., 2019). The exploitation of multivariate pattern recognition in dystonia, a neurological movement disorder, remains uncharted.

Several neuroimaging studies have been carried out to investigate neural correlates of AOIFD in an effort to probe the neural mechanisms and pathophysiology of this disorder (Zoons et al., 2011). Regional metabolic changes (Eidelberg et al., 1995; Carbon et al., 2004b), resting state functional network changes (Delnooz et al., 2013; Li et al., 2017), task based fMRI activity discrepancies (Neychev et al., 2011; Dresel et al., 2014; Battistella et al., 2015; Prudente et al., 2016) and structural alterations in the form of volume and tract integrity have been identified in patients when compared to controls (Ramdhani and Simonyan, 2013). These studies to date have predominantly followed a univariate approach of analysis. Structural imaging studies using the voxel-based morphometry (VBM) approach have implicated the Putamen, caudate, Thalamus, globus pallidus and cerebellar Vermis [21, 24-28] but the results reported have been vastly variable (Jinnah et al., 2017a). Traditionally, functional neuroimaging studies have also relied on univariate analysis via t-test of results from the general linear model (GLM) approach, which examines each voxel in isolation and is primarily designed to identify regions showing differential activity between conditions and groups (Monti, 2011). This approach has been invaluable in identifying and focusing attention on specific brain regions in the pathophysiology of dystonia (Filip et al., 2017; Mc Govern

et al., 2017c). However, univariate methods provide limited information regarding the distributed nature of neural processing (Formisano et al., 2008; Davis et al., 2014) as they deal with each voxel's time course separately and do not take into account inter-regional correlations which may be of importance in studies that are directed at exploring various neural systems associated with a particular aspect of brain function. In AOIFD, it is become increasingly evident this disorder involves a multi-network system-level dysfunction in the brain, involving multiple regions such as the basal ganglia, midbrain, sensory-motor network and the Cerebellum (Hendrix and Vitek, 2012; Battistella et al., 2015). A multivoxel pattern analysis (MVPA) approach can exploit the entire topography of responses and is more sensitive to fine grained spatial pattern differences in the absence of regional-average differences (Habeck, 2010; Gilron et al., 2017). MVPA incorporates statistical pattern recognition methods which exploit and integrate the information available at many spatial locations, thus allowing the detection of differences that may produce only weak single-voxel effects (Habeck, 2010; Mahmoudi et al., 2012; Davis et al., 2014) (Figure 8.1). Most importantly, unlike univariate approaches that do not offer the possibility of employing a predictive learning approach, MVPA offers the prospect of pattern recognition via machine learning, which may be of significant diagnostic relevance. There is an increasing number of machine learning studies for detecting new clinically meaningful biomarkers from large neuroimaging datasets, but little to none undertaken in dystonia.

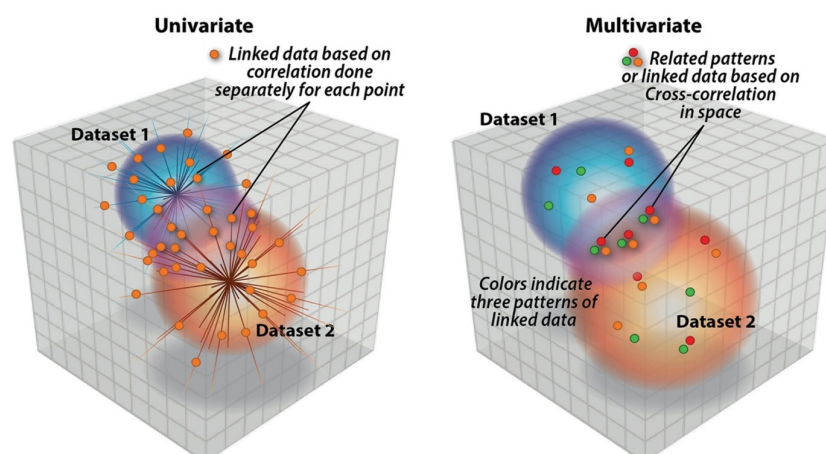


Figure 8.1: Univariate approaches consists of finding relations between single points (e.g., voxels in a neuroimaging dataset) whereas multivariate approaches focus on associations between patterns (e.g., weighted combinations of voxels in different brain regions and/or weighed combinations of data from multiple modalities). Aadapted from (Pearlson et al., 2015).

Moreover, there has been no study which combines the differences observed in structure and function observed in cervical dystonia to date. In the pursuit of clinical utility, a reliable classification accuracy using data from one modality only would be ideal. However, owing to the varied functional and structural aberrations observed to date in dystonia patients compared to controls, we sought to harness the strength of these findings in multiple modalities and explore the best method to combine information from multiple modalities to study the complementarity of information they may offer in dystonia. Via ensemble learning, we sought to probe the efficacy of multimodal feature combination in understanding the pathophysiology of dystonia. Ensemble learning is a machine learning paradigm where multiple estimators are trained to solve the same problem (Dietteric, 2000). In contrast to ordinary machine learning approaches which learn one hypothesis from training data, ensemble methods construct a set of hypotheses and combine them together for maximum inclusivity (Figure 8.2).

Few neuroimaging studies have explored ensemble classification as a means for integrating and classifying features from multimodal datasets (Fratello et al., 2017; Yang et al., 2010; Qureshi et al., 2017). Of these, while some have constructed an ensemble of one type of classifier, others have explored new implementations such as adaptive ensemble manifold learning (Zhuo et al., 2016). Li et al. (Li et al., 2017) achieved a group classification accuracy of 90.6% by implementing a Support Vector Machine classifier with resting state fMRI data (unimodal). They achieved this by extracting features that showed significant differences via voxel-wise comparisons (univariate methods), followed by recursive feature elimination (RFE) procedure to further identify the most important features (possibly leading to overfitting as a result). Harnessing information from multiple modalities has been explored in other disorders such as Alzheimer's disease (Zhang et al., 2011; Hao and Zhang, 2013; Challis et al., 2015; Zhanga et al., 2018), Parkinson's disease (Fratello et al., 2017), Autism Spectrum Disorder (Liberio et al., 2015) and psychiatric disorders such as schizophrenia (Yoon et al., 2008; Yang et al., 2010). There have been no reported multimodal MVPA studies in dystonia to date.

Therefore, the aim of this study was to 1) probe structural and functional neuroimaging data in CD via MVPA in order examine the dysfunctional nodes with greater sensitivity 2) empirically compare feature vs. decision integration for

merging information from multiple neuroimaging modalities 3) investigate the utility of ensemble learning for consolidating complementary information in a MVPA study in CD.

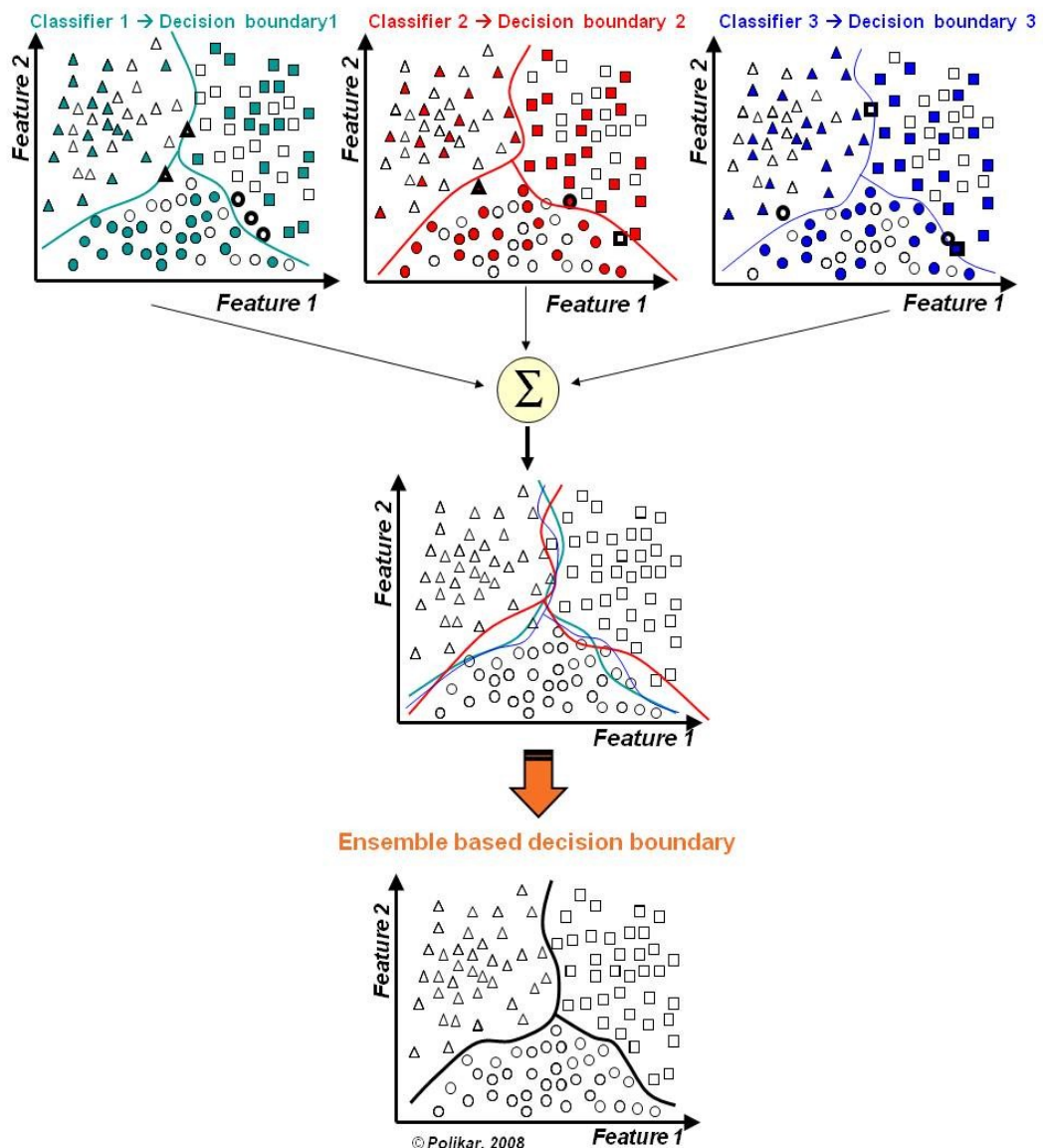


Figure 8.2: Ensemble learning involves combining decision boundaries from individual estimators, to result in a new improved decision boundary that better classifies the features according to the group they belong to. Therefore, a number of weak estimators are combined to give one strong estimator for pattern classification. Aadapted from (Polikar, 2012).

8.2 Methods

8.2.1 Participants, Ethics, Data Acquisition and Pre-processing

Please refer to Chapter 4 - General Methodology. For the multimodal MVPA, imaging data of CD patients and healthy controls were analyzed.

8.2.2 Feature Extraction

a VBM gray matter images from structural MRI

There has been extensive research showing significant volumetric differences across CD patients and controls based on VBM analysis (Obermann et al., 2007; Bradley et al., 2009; Pantano et al., 2011; Prell et al., 2013; Ramdhani et al., 2014). Therefore a standard VBM protocol (Kurth et al., 2015) was followed using SPM8 for extracting the gray matter images which were used as input feature vectors for the feature selection stage.

b ReHo maps from resting-state fMRI

A previous study reported significant differences in across CD patients and controls. These features provided high classification accuracy in differentiating patients from controls (Li et al., 2017). Therefore in order to obtain ReHo maps, the pre-processed (normalized but unsmoothed) images were subjected to a detrending (linear trend subtraction) and temporal filtering (0.01-0.08 Hz) procedure on the time series of each voxel to reduce the effect of low frequency drifts and high-frequency noise. The procedure was implemented with the REST suite (Song et al., 2011). Following this, ReHo analysis was executed for each participant by computing the Kendall Coefficient of Concordance of the time series of a given voxel with those of its nearest neighbours (27 voxels) at a voxel-wise level. For normalization, each ReHo map was divided by its Kendall global mean value. The data was smoothed with a Gaussian filter of 6mm full width at half-maximum, to reduce noise and residual differences in gyral anatomy.

c β -maps task fMRI

After the standard pre-processing steps, a GLM was created for each subject which incorporated the regressors of interest (loom, recede and random) and nuisance regressors. The six movement parameters estimated during the re-alignment procedure were included as nuisance regressors to account for unwanted movement. The 1st level GLM resulted in β -maps for the various conditions, e.g.: loom only, loom-random and loom-recede conditions as described in Chapter 5. The loom-random β -maps were employed as input features for the present analyses (as they had shown the greatest difference between patients and controls).

8.2.3 Masks

In order to carry out a-priori knowledge based MVPA as well as wholebrain MVPA, three masks were generated based on previous univariate research done in CD (Chapter 2). The masks were created with the help of Wake Forest University PickAtlas (Maldjian et al., 2003) and SPM8 software.

a A-priori Vermis Putamen_SC (VPSC) mask

Three regional masks were generated, one for each of the three modalities; the Vermis mask (rs-fMRI), the Putamen mask (s-MRI) and the SC mask (t-fMRI). These were combined to form one mask that was used in the analyses.

b A-priori Combination mask

A mask was generated consisting of the Claustrum, Caudate, Thalamus, Putamen, Substantia Nigra, SubThalamic Nucleus, Red Nucleus, Putamen, Pallidum, midbrain, Pons, occipital lobe, Vermis, sensory motor area, motor areas, supplementary motor area and the Amygdala.

c Wholebrain mask

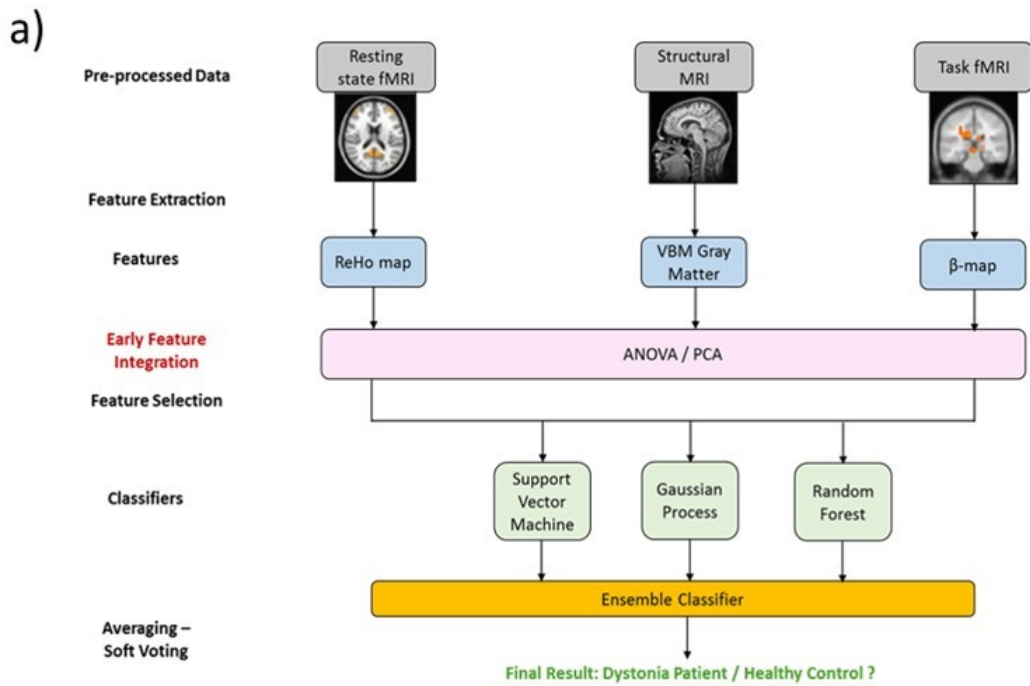
The mean binary image generated from all patients and controls was used to include all brain voxels and exclude non-brain voxels.

8.2.4 Feature Extraction and Selection

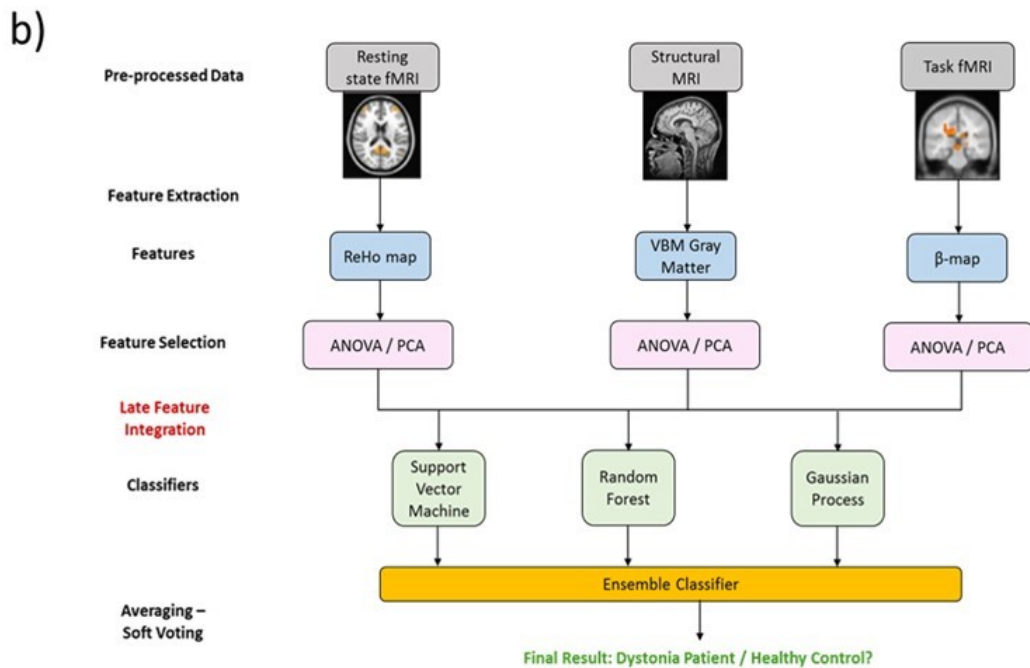
Neuroimaging data tends to have very high dimensionality (pre-processed brain scans may contain >100,000 non-zero voxels) compared to the generally small number of available subject samples (usually <100). This is the case in the present study. This ‘curse of dimensionality’ is a common problem in many machine learning applications. Therefore, feature extraction and feature selection are fundamental steps before applying a machine learning model to neuroimaging data. Variance thresholding, Analysis of Variance (ANOVA), and Principal Component Analysis (PCA) were therefore implemented; due to their adeptness with high dimensional feature sets. All feature extraction, feature selection and classification algorithms were written and implemented in Python (PyCharm[©] 2017.2.1) with the Scikit-learn (Pedregosa et al., 2011) and Ni-learn (Abraham et al., 2014) packages. This stage resulted in an optimal subset of features (\leq number of samples) to reach the most robust classification performance. Figure 8.5 shows the features selected and used as input feature vectors in the subsequent classification stage.

a Multimodal Analyses: Feature vs. Decision Integration

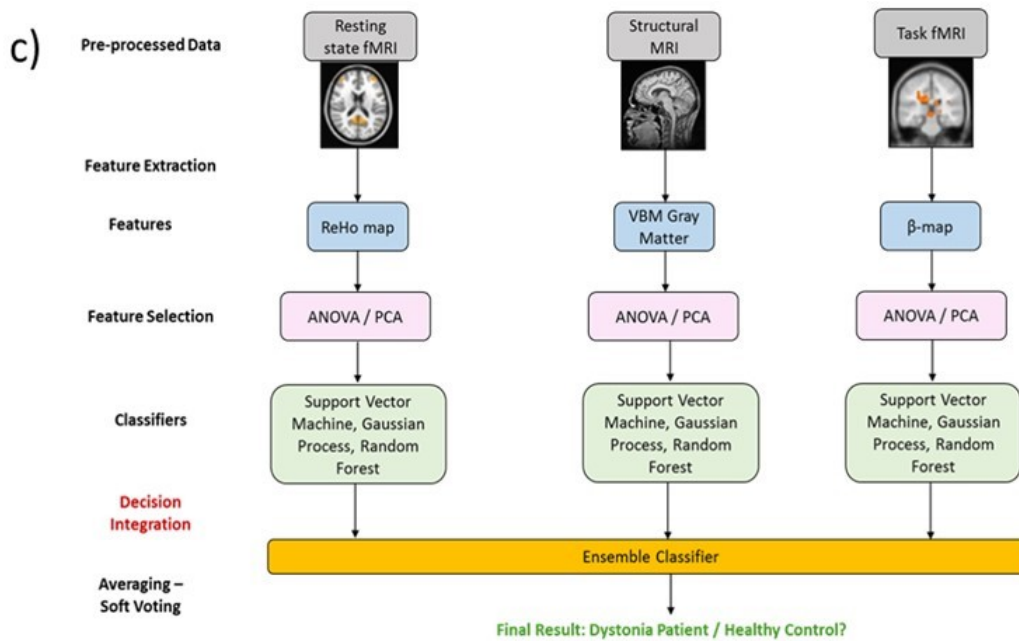
Three methods of multimodal feature combination were tested, as shown in Figure 8.3. The early feature integration approach (Figure 8.3.a) refers to the concatenation of features before the feature selection stage. This is then followed by classification and ensemble voting. The late feature integration approach (Figure 8.3.b) refers to the concatenation of features after the feature selection stage. This is then followed by classification and ensemble voting. Feature extraction and feature selection is carried out on each modality separately and the resulting feature sets obtained from each modality are concatenated to form one final feature set that is used as an input to train different classifiers. The decision integration approach (Figure 8.3.c) refers to the steps of feature extraction, selection and classification carried out on the dataset for each modality separately, and the final results from each classifier integrated in the ensemble voting classifier.



(a) Early Feature Integration Ensemble



(b) Late Feature Integration Ensemble



(c) Decision Integration Ensemble

Figure 8.3: Early feature integration (a), late feature integration (b) and decision integration (c) approaches of abnormalities detected from cervical dystonia neuroimaging data. The multiple modalities included resting state, functional and structural MRI. Feature extraction consisted of extracting the relevant features from each modality whereas feature selection involved dimensionality reduction. The classifiers tested and used were support vector machine, gaussian process and random forest. An ensemble classifier was then employed which consisted of averaging via hard or soft voting.

8.2.5 Classifiers and Ensemble Classification

Three different classifiers were implemented in order to differentiate CD patients from controls. Default hyperparameters were used with the feature sets.

- The Support Vector Machine (SVM)
- Gaussian Process Classifier (GPC)
- Random Forest (RF)

These classifiers were selected as they are beneficial for neuroimaging data analyses and have previously shown to yield robust results (Mourao-Miranda et al., 2005; Magnin et al., 2009; Ball et al., 2014; Lebedev et al., 2014; Challis et al., 2015; Serra et al., 2018). Finally, a voting ensemble classifier was used to aggregate results from each of the individual classifiers and deliver a final output, as shown in Figure 8.3. Both hard and soft voting methods (with and without weighting) were examined. Due to

the small sample size, the leave one out cross validation (LOOCV) strategy was used to evaluate classification accuracy across the groups. The classifier performance was evaluated based on the accuracy (acc.), sensitivity (recall), specificity and precision (prec.), which were calculated via the metrics described in Figure 8.4.

		Prediction	
		Healthy Control	Patient
Actual	Healthy Control	True Negative (TN)	False Positive (FP)
	Patient	False Negative (FN)	True Positive (TP)

$$Precision = \frac{TP}{TP+FP}$$

$$Recall = \frac{TP}{TP+FN}$$

$$Sensitivity = \frac{TP}{TP+FN}$$

$$Specificity = \frac{TN}{TN+FP}$$

$$Accuracy = \frac{TP+TN}{TP+TN+FP+FN}$$

$$F - 1 \text{ score} = 2 \frac{(Precision \cdot Recall)}{(Precision + Recall)}$$

Figure 8.4: Classifier performance tested via metrics such as accuracy, precision and recall as per the number of true predictions and false predictions.

8.3 Results

8.3.1 Feature Extraction and Selection

Features which enabled a significant ($p < 0.05$) classification accuracy via the ANOVA feature selection method have been depicted in the Figure 8.5. The features selected by the dimensionality reduction algorithms (ANOVA and PCA) were used as input feature vectors for the classifier. For the PCA feature selection, the top 10 principal components that explained $>85\%$ variance in the data were employed as inputs in the classifiers.



Figure 8.5: Features extracted and selected via the ANOVA feature selection method in the late feature integration and the decision integration methods. The blue represents features selected from the structural MRI modality, red depicts features selected from the resting state MRI modality and green represents the features selected from the task fMRI modality.

Tables 8.1, 8.2 and 8.3 show the results obtained from the unimodal data (univariate and multivariate feature selection) classifier with the VPSC mask, Combination mask and Wholebrain mask respectively. The highest accuracy with the unimodal classifier was 67.85% for the VPSC mask, 85.71% for the combination mask and 75% for the wholebrain mask. The Receiver Operating Characteristic (ROC) curves have been depicted in Figures 8.6, 8.7 and 8.8.

Tables 8.4, 8.5 and 8.6 show the results obtained from the multimodal data classifier with the VPSC mask, Combination mask and Wholebrain mask respectively. The highest accuracy with the multimodal approach was 75% for the VPSC mask, 85.71%

for the combination mask and 82.14% for the wholebrain mask. The ROC curves have been depicted in Figure 8.9.

Table 8.1: Unimodal data with the VPSC mask as input features to univariate (ANOVA) and multivariate (PCA) feature selection methods, along with MVPA via a Support Vector Machine (SVM), Gaussian Process Classifier (GPC) and Random Forest (RF) classifier. * denotes significant findings ($p < 0.05$).

Unimodal Analysis – Vermis, Putamen and SC Mask			
Modality	Feature Selector	Classifier	Accuracy (%)
rs-MRI	PCA	SVM	57.14*
	Variance and ANOVA	SVM	50
	PCA	GPC	50*
	Variance and ANOVA	GPC	50
	PCA	RF	67.85*
	Variance and ANOVA	RF	57.14*
s-MRI	PCA	SVM	67.85*
	Variance and ANOVA	SVM	50
	PCA	GPC	57.14*
	Variance and ANOVA	GPC	46.42
	PCA	RF	67.85*
	Variance and ANOVA	RF	64.28*
t-MRI	PCA	SVM	57.14*
	Variance and ANOVA	SVM	50
	PCA	GPC	50
	Variance and ANOVA	GPC	50
	PCA	RF	46.42
	Variance and ANOVA	RF	39.28

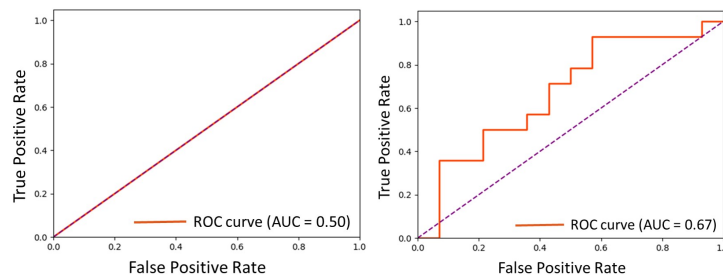


Figure 8.6: Receiver Operating Characteristic (ROC) curves for the lowest (left: $AUC=0.50$) and highest (right: $AUC=0.67$) performance with the unimodal data using the Vermis, Putamen and Superior Colliculus mask for analysis in CD patients vs. healthy controls. AUC = Area Under the Curve.

Table 8.2: Unimodal data with the Combination mask as input features to univariate (ANOVA) and multivariate (PCA) feature selection methods, along with MVPA via a Support Vector Machine (SVM), Gaussian Process Classifier (GPC) and Random Forest (RF) classifier. * denotes significant findings ($p < 0.05$) in CD patients vs. healthy controls.

Unimodal Analysis – Combination Mask			
Modality	Feature Selector	Classifier	Accuracy (%)
rs-MRI	PCA	SVM	85.71*
	Variance and ANOVA	SVM	82.14*
	PCA	GPC	85.71*
	Variance and ANOVA	GPC	53.57
	PCA	RF	78.57*
	Variance and ANOVA	RF	50
s-MRI	PCA	SVM	67.86*
	Variance and ANOVA	SVM	42.85
	PCA	GPC	67.86*
	Variance and ANOVA	GPC	50
	PCA	RF	60.71*
	Variance and ANOVA	RF	46.42
t-MRI	PCA	SVM	50
	Variance and ANOVA	SVM	50
	PCA	GPC	50*
	Variance and ANOVA	GPC	50
	PCA	RF	53.57*
	Variance and ANOVA	RF	42.85

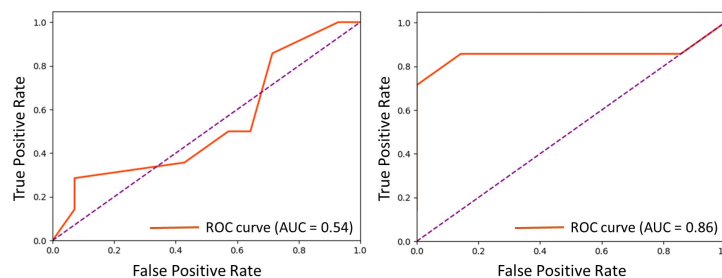


Figure 8.7: Receiver Operating Characteristic (ROC) curves for the second lowest (left: AUC=0.54) and highest (right: AUC=0.86) performance with the unimodal data using the a-priori Combination mask for analysis in CD patients vs. healthy controls. AUC = Area Under the Curve.

Table 8.3: Unimodal data with the Wholebrain mask as input features to univariate (ANOVA) and multivariate (PCA) feature selection methods, along with MVPA via a Support Vector Machine (SVM), Gaussian Process Classifier (GPC) and Random Forest (RF) classifier in CD patients vs. healthy controls. * denotes significant findings ($p < 0.05$).

Unimodal Analysis – Wholebrain Mask			
Modality	Feature Selector	Classifier	Accuracy (%)
rs-MRI	PCA	SVM	75*
	Variance and ANOVA	SVM	50
	PCA	GPC	75*
	Variance and ANOVA	GPC	53.57
	PCA	RF	64.28*
	Variance and ANOVA	RF	67.85*
s-MRI	PCA	SVM	57.14*
	Variance and ANOVA	SVM	50
	PCA	GPC	50*
	Variance and ANOVA	GPC	50
	PCA	RF	53.57
	Variance and ANOVA	RF	50
t-MRI	PCA	SVM	50*
	Variance and ANOVA	SVM	50
	PCA	GPC	50*
	Variance and ANOVA	GPC	50
	PCA	RF	42.85
	Variance and ANOVA	RF	46.43

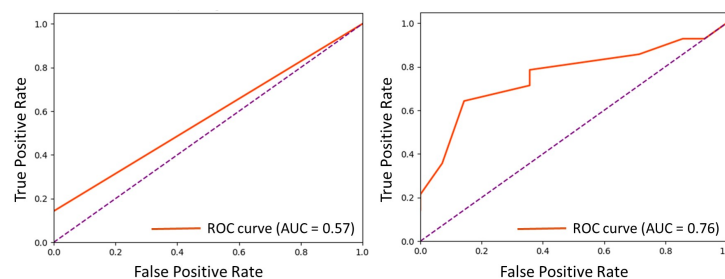


Figure 8.8: Receiver Operating Characteristic (ROC) curves for the second lowest (left: AUC=0.57) and highest (right: AUC=0.76) performance with the unimodal data using the Wholebrain mask for analysis in CD patients vs. healthy controls. AUC = Area Under the Curve.

Table 8.4: Multimodal data with the VPSC mask as input features to an MVPA ensemble classifier in CD patients vs. healthy controls. The yellow represents the highest accuracy achieved. *denotes significant findings ($p < 0.05$).

Multimodal Analysis – VPSC Mask				
Integration and Ensemble	Accuracy (%)	Precision	Recall	Conf. Matrix
Early Feature Integration – No Ensemble	57.14*	0.57	0.57	[8 6 6 8]
Early Feature Integration – Ensemble (Hard)	57.14*	0.57	0.57	[8 6 6 8]
Early Feature Integration – Ensemble (Soft)	60.71*	0.59	0.71	[7 7 4 10]
Late Feature Integration – No Ensemble	60.71*	0.6	0.64	[8 6 5 9]
Late Feature Integration – Ensemble (Hard)	50	0.5	0.5	[7 7 7 7]
Late Feature Integration – Ensemble (Soft)	60.71	0.6	0.64	[8 6 5 9]
Decision Integration (Hard)	75*	0.71	0.86	[9 5 2 12]
Decision Integration (Soft)	64.28*	0.64	0.64	[9 5 5 9]

Table 8.5: Multimodal data with the Combination mask as input features to an MVPA ensemble classifier in CD patients vs. healthy controls. The yellow represents the highest accuracy achieved. *denotes significant findings ($p < 0.05$).

Multimodal Analysis – Combination Mask				
Integration and Ensemble	Accuracy (%)	Precision	Recall	Conf. Matrix
Early Feature Integration – No Ensemble	82.14*	0.91	0.71	[13 1 4 10]
Early Feature Integration – Ensemble (Hard)	82.14*	0.8	0.87	[11 3 2 12]
Early Feature Integration – Ensemble (Soft)	85.71*	0.86	0.86	[12 2 2 12]
Late Feature Integration – No Ensemble	71.42	0.75	0.64	[11 3 5 9]
Late Feature Integration – Ensemble (Hard)	75	0.77	0.71	[11 3 4 10]
Late Feature Integration – Ensemble (Soft)	78.57*	0.83	0.71	[12 2 4 10]
Decision Integration (Hard)	82.14	0.76	0.93	[10 4 1 13]
Decision Integration (Soft)	85.71*	0.86	0.86	[12 2 2 12]

Table 8.6: Multimodal data with the Wholebrain mask as input features to an MVPA ensemble classifier in CD patients vs. healthy controls. The yellow represents the highest accuracy achieved. *denotes significant findings ($p < 0.05$).

Multimodal Analysis – Wholebrain Mask				
Integration and Ensemble	Accuracy (%)	Precision	Recall	Conf. Matrix
Early Feature Integration – No Ensemble	82.14*	0.85	0.79	[12 2 3 11]
Early Feature Integration – Ensemble (Hard)	78.57*	0.83	0.71	[12 2 4 10]
Early Feature Integration – Ensemble (Soft)	78.57*	0.79	0.79	[11 3 3 11]
Late Feature Integration – No Ensemble	60.71	0.61	0.57	[9 5 6 8]
Late Feature Integration – Ensemble (Hard)	50	50	0.49	[8 6 8 6]
Late Feature Integration – Ensemble (Soft)	60.71	0.63	0.5	[10 4 7 7]
Decision Integration (Hard)	64.29*	0.75	0.43	[12 2 8 6]
Decision Integration (Soft)	75*	0.77	0.71	[11 3 4 10]

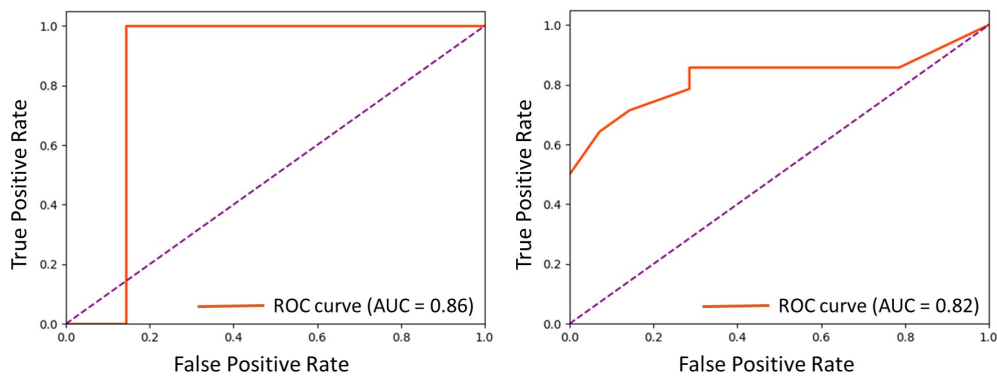


Figure 8.9: Receiver Operating Characteristic curves with the rs-fMRI, s-MRI and t-fMRI data fused together via different approaches in an MVPA ensemble in CD patients vs. healthy controls. The ROC curves for the best performances (accuracy and precision) with two masks have been shown (Combination mask - AUC 0.86, Wholebrain mask - AUC 0.82). AUC = Area Under the Curve.

8.4 Discussion

The present study investigated different methods of combining features from multiple neuroimaging modalities with a multivoxel pattern analysis and ensemble learning approach in the neurological movement disorder - cervical dystonia.

Most existing models of brain abnormalities underlying AOIFD and CD emphasize widespread connectivity-related disturbances, ranging from microstructural white matter changes and volumetric changes, to metabolic neurochemical transmitter incongruities and functional connectivity pattern abnormalities (Asanuma et al., 2005; Simonyan, 2018). This study sought to comprehend the strengths of each neuroimaging measure while probing the possible pathways to fuse multimodal neuroimaging data for a potentially enhanced understanding and classification of brain structural and functional differences between CD patients and controls.

The highest classification accuracy achieved with both the unimodal and multimodal methods was comparable (85.71%), however, this is highly dependent on the mask used for feature extraction. While it was hypothesized that a multimodal approach would lead to improved classification with an ensemble classifier, the results are particularly favourable in a clinical setting where data acquisition from multiple modalities is neither cost nor time efficient. However, in favour of the hypothesis, there was an improvement from 67.85% in the unimodal approach to 75% via the multimodal approach for the VPSC mask, and from 75% in the unimodal approach to 82.14% via the multimodal approach for the wholebrain mask. The results cautiously suggest the necessity of both structural and functional abnormalities for dystonia manifestation and provide evidence that the study of multimodal measures cumulatively could enhance abnormality detection and classification of patients and controls.

The highest unimodal accuracy was achieved with rs-fMRI data (ReHo maps extracted from patients and controls used as input features). This was also given the highest weight by the classifier in the multimodal ensemble approach (with the lowest weight assigned to the t-fMRI data), which could explain the similarity in the results between the unimodal and decision integration ensemble approach. The unimodal results also suggested the superiority of the rs-fMRI data over the VBM structural and t-fMRI data in the present CD cohort. The structural and t-fMRI beta maps fared poorly in this study and indicate their unsuitability for diagnostic purposes. Furthermore, the utility of the a-priori based mask encompassing hypothesized brain regions succeeded over an (a-priori) univariate analysis based mask (VPSC mask). It led to a more robust and enhanced feature learning classification. This could be due to the fact that with the VPSC case, important multivoxel features could have been discarded while with the wholebrain mask, too many features could have led to a potential obfuscation during

feature selection and classifier training. This also supports the concept that structural and functional deviations in CD patients may not be confined to a few regions in the brain (Delnooz et al., 2013; Battistella et al., 2015; Pinheiro et al., 2015; Filip et al., 2017).

With the growing indication that the neural dysfunction underlying dystonia involves multiple brain regions comes the need for increasingly sophisticated and sensitive methods for detecting complex alterations. Furthermore, the relationship between the mined multimodal imaging features and class labels is usually complex, making traditional linear models ineffective (Habeck, 2010). The interpretation of a result of MVPA is that the brain regions delineated as having valuable information are those that can be used to assign a particular individual dataset to a group; in this study, a CD patient or control. Using an MVPA approach, we identified regions in the brain that in aggregation may be implicated in the manifestation of dystonia. Figure 8.5 shows the features that were selected by the feature selection and dimensionality reduction method and where pattern abnormalities yielded significant classification accuracies ($p < 0.05$). Regional homogeneity, grey matter and functional differences were detected in the Putamen, cerebellar Vermis, Thalamus, visual, and primary motor regions, indicating a dysfunction in the coupling of these regions (effective connectivity) rather than in their local activity in isolation. These results support the concept that the abnormal postures and movements in cervical dystonia are a result of a malfunctioning neural integrator circuit (Shaikh et al., 2016). With the whole brain mask, additional areas that had distinguishable patterns between CD patients and controls included the sensorimotor area, sensory associative area, Putamen, Thalamus, Brodmann Area (BA) 6 (supplementary motor area), BA7 (responsible for visuomotor coordination), BA8 (frontal eye fields), BA9 (responsible for overriding automatic responses, inferring deduction from spatial imagery and inductive reasoning), BA 19 (visual area) BA21 and BA22 (auditory processing). The results uncovered regions that have not previously been shown to be significantly different in the univariate analysis, which is based on a voxel-by-voxel wise comparison. Additionally, while some of the identified regions have been previously reported to be abnormal in dystonia in a unimodal univariate setting, this study took into consideration the network concept of AOIFD to link widespread pattern abnormalities into a cohesive model that enabled robust classification of patients and controls.

The results also corroborated previous studies that show ensemble learning as a beneficial method for linking differences in brain structure and function (Hao and Zhang, 2013; Pettersson-Yeo et al., 2014; Zhuo et al., 2016; Fratello et al., 2017). The results validated an ensemble classifier's potential for multimodal neuroimaging data fusion in dystonia. Despite dystonia being the third most common movement disorder, subject recruitment can be challenging due to its clinical and etiological heterogeneity (Albanese et al., 2013). Other confounding variables such as age and gender further impact the results (Butler et al., 2015). Therefore, most dystonia neuroimaging datasets have fewer than 25 subjects which are less than optimal for a machine learning study. Combining data from multiple modalities across multiple locations can address this problem. The present study was an effort in this direction for rare idiopathic movement disorders.

Due to the fact that only a few studies have applied integrative practices to neuroimaging data and varied approaches towards combining data from multiple modalities have been implemented, the purpose of the current study was to take an exploratory approach regarding the most appropriate method of feature fusion for the datasets in question. Feature extraction and selection play an important role and the method of combination of features from different modalities (Pavlidis, 2001) can have a significant impact on classifier performance. Our results revealed that late feature integration of features from multiple modalities degrades classification accuracy compared to the unimodal classification, while early feature integration and decision integration ensembles can achieve better results. These results suggest that information from each neuroimaging modality could be lost via late feature fusion in dystonia.

Despite the insights discussed above, the present study had one key limitation. Our study had a small sample size. It was therefore only possible to use the LOOCV method to report classification accuracies. Future studies replicating the winning procedure on an independent cohort of CD patients and controls as well as on a larger cohort of AOIFD patients could prove to be beneficial in confirming the current study's results.

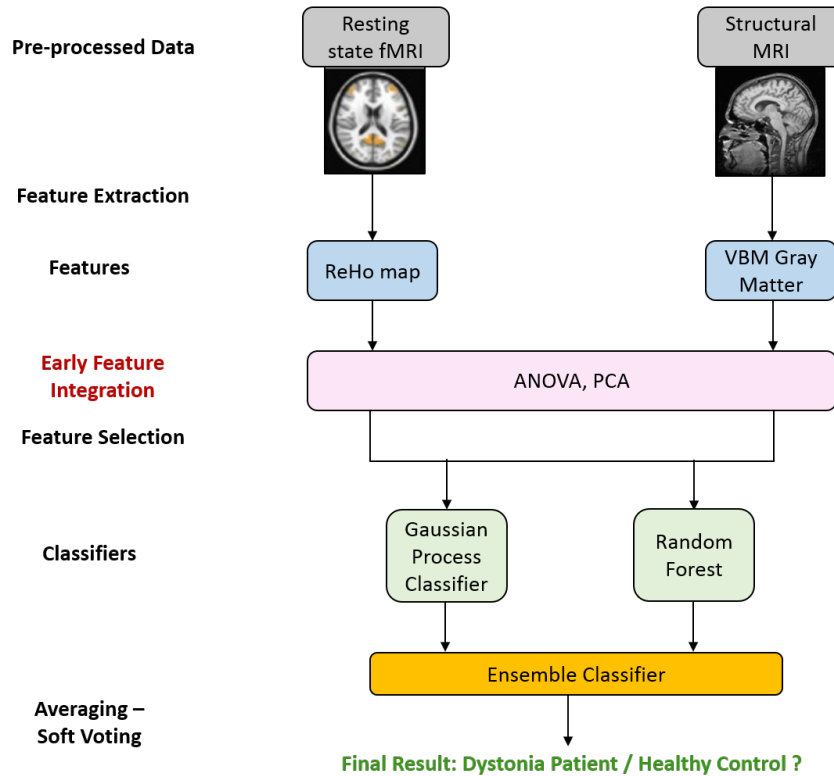
8.5 Validation Study

8.5.1 Methods

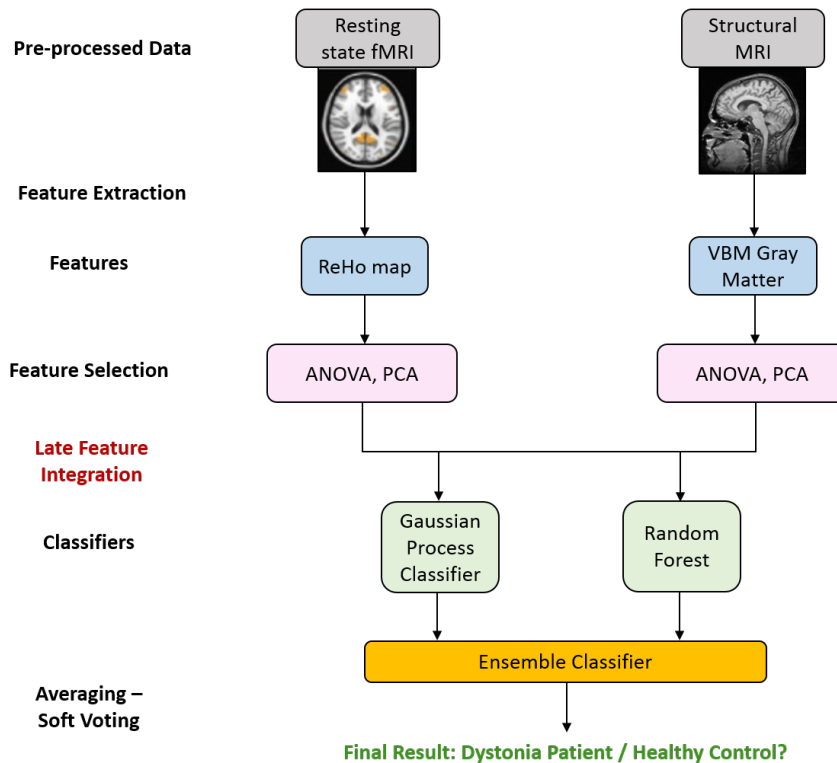
In order to overcome the limitations with respect to the sample size in the previous study and in order to validate the algorithm and its results on an independent cohort of dystonia patients and healthy controls, a validation study was undertaken. This study was carried out at the Department of Speech and Motor Control, Massachusetts General Hospital, Harvard Medical School in Boston, USA, where all the neuroimaging data was (previously) acquired. The neuroimaging data consisted of s-fMRI and rs-fMRI scans from >100 patients and controls, of which 70 patients (10 CD, 10 BSP, 18 MD, 18 WC, 14 SD) and 70 age-matched controls were employed in the present analysis to ensure age and sex-matched cohorts in the patient and control population. Because access to subjects with cervical dystonia was limited, a mixed phenotype cohort of adult-onset idiopathic focal dystonia patients (was analyzed with the previously described multimodal MVPA and ensemble learning algorithm. The demographics of the cohort population has been described in Table 8.7. Since the current scenario consisted of AOIFD patients in comparison to the previous which had only CD patients, the a-priori combination mask and the wholebrain mask were employed in this analysis (and not the VPSC mask).

Table 8.7: Demographics of the AOIFD patients and healthy controls neuroimaging dataset analyzed.

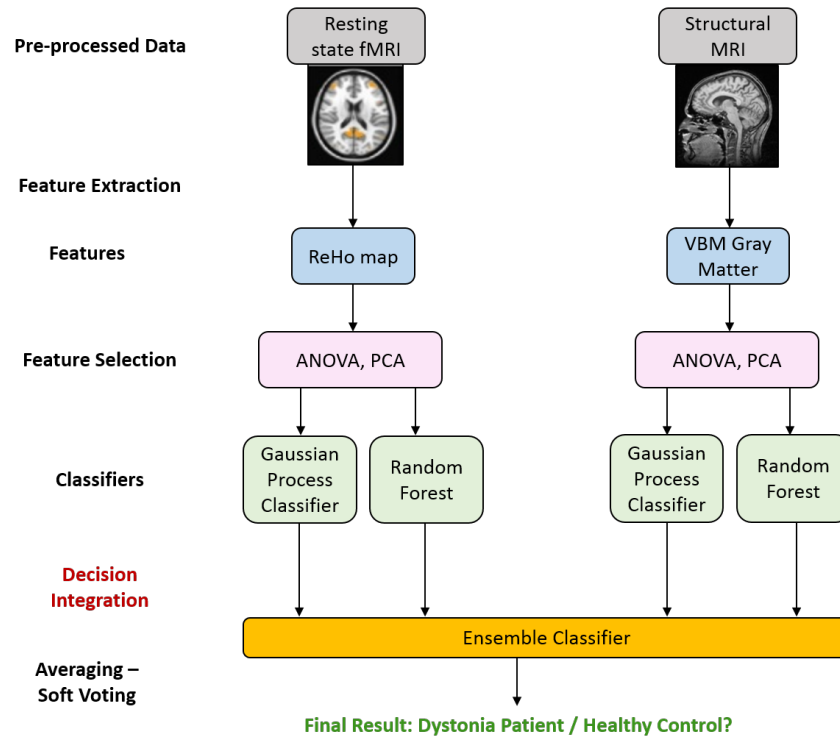
	AOIFD patients	Healthy controls
Age (years)	53.64 ± 12.83	53.32 ± 11.71
Gender	38 Female, 32 Male	37 Female, 33 Male
Number of participants	70	70



(a) Early Feature Integration Ensemble



(b) Late Feature Integration Ensemble



(c) Decision Integration Ensemble

Figure 8.10: Early feature integration (a), late feature integration (b) and decision integration (c) approaches of abnormalities detected from AOIFD neuroimaging data. The multiple modalities included resting state and structural MRI. Feature extraction consisted of extracting the relevant features from each modality whereas feature selection involves dimensionality reduction. The classifiers employed were the gaussian process classifier and random forest. An ensemble classifier was then employed which consists of averaging via hard and soft voting.

The methods employed were similar to the previous study, and have been described in Figure 8.10. Since the sample size was high, algorithm included a cross-validation as well as test-accuracy methodology as shown in Figure 8.11.

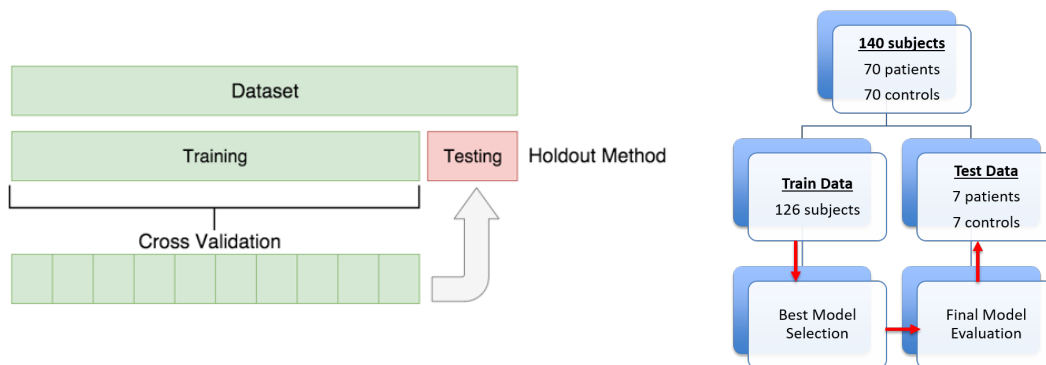


Figure 8.11: The dataset was randomly partitioned into train and test (hold-out) sets. The test set was kept completely hidden from the algorithm which was trained on 126 subjects. The best model from this procedure was then tested on the held-out dataset (14 subjects) in order to report the final test accuracy.

8.5.2 Results

The MVPA feature selection approach resulted in a combination of structural and functional activity differences detected with greater sensitivity across all voxels in the visual/occipital region, Thalamus, cerebellar and sensorimotor area as shown in Figure 8.12, which helped improve the identification of AOIFD patients from the combined patient and control population. MVPA multimodal analysis led to an increase in classification performance in comparison to the unimodal approach, from 71.42% to 85.71% for the A-priori mask, and from 85.71% to 92.85% for the Wholebrain mask, as depicted in Table 8.8 and Figures 8.13 and 8.14.

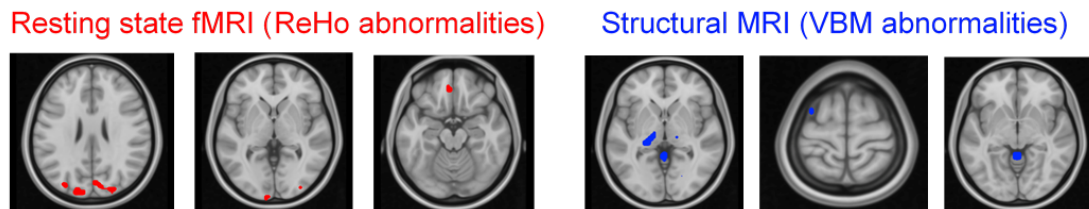


Figure 8.12: The multimodal MVPA feature selection approach resulted in a combination of structural and functional activity differences detected with greater sensitivity across all voxels, which helped improve the identification of AOIFD patients from the combined patient and control population.

Table 8.8: Results of the unimodal and multimodal classification performance with the neuroimaging data using an a-priori combination mask and wholebrain mask as input features to multivariate (PCA) feature selection methods. The yellow represents the highest significant ($p < 0.05$) accuracy achieved. *denotes significant findings ($p < 0.05$).

Mask/Mode		rs-fMRI		sfMRI		Early Feature Integration		Late Feature Integration		Decision Integration	
		Acc.(%)	Prec.	Acc.(%)	Prec.	Acc.(%)	Prec.	Acc.(%)	Prec.	Acc.(%)	Prec.
A-priori Mask	RF	64.28	0.6	71.42	0.7	71.42	0.8	78.57	0.8	85.71	0.9
	GPC	57.14	0.5	64.28	0.6	71.42	0.6	71.42	0.7	78.57	0.7
Wholebrain Mask	RF	71.42	0.8	85.71	1	92.85	0.9	85.71	1	92.85	1
	GPC	85.71	0.7	85.71	0.8	85.71	0.7	85.71	0.7	92.85	0.8

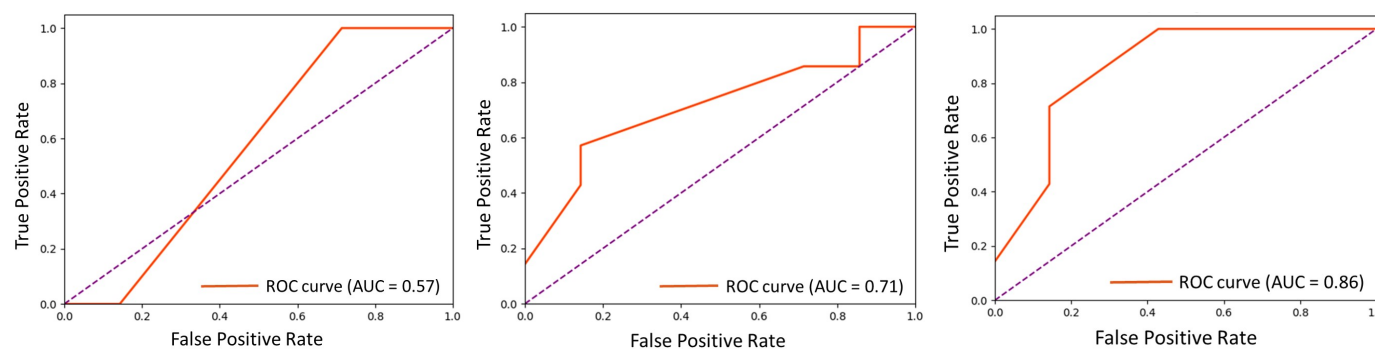


Figure 8.13: Receiver Operating Characteristic (ROC) curves for the lowest unimodal (left: AUC=0.57), highest unimodal (center: AUC=0.71), and highest multimodal classification performance (right: AUC=0.86) with the a-priori Combination mask employed. AUC = Area Under the Curve.

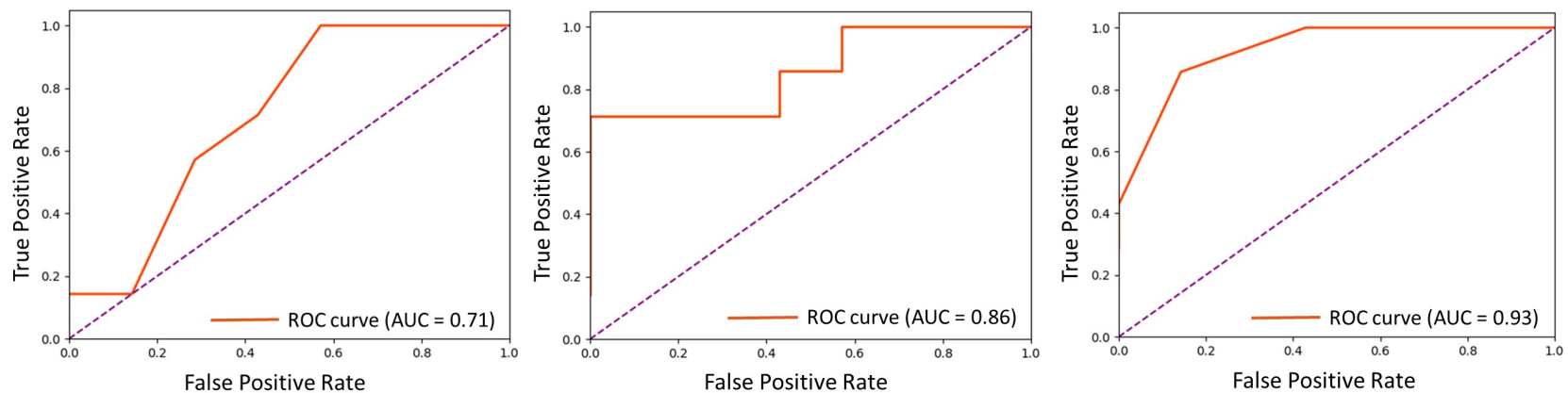


Figure 8.14: Receiver Operating Characteristic (ROC) curves for the lowest unimodal (left: AUC=0.71), highest unimodal (center: AUC=0.86), and highest multimodal classification performance (right: AUC=0.93) with the Wholebrain mask employed. AUC = Area Under the Curve.

8.5.3 Discussion

The results from this validation study undertaken with AOIFD patients in the US, reinforced the previously obtained results from the analysis on the CD cohort in Dublin. Decision integration proved to be the most effective way of combining information from different modalities in AOIFD. When the analysis was limited to the a-priori mask, it led to lower classification performance than the whole-brain mask. Data from regions across the brain were essential when classifying patients and controls, thus supporting the multi-network concept of the disorder. This was further supported by the PCA feature selection method which outperformed the univariate ANOVA feature selection method. The multimodal analysis led to a moderate increase in classification performance (71.42% to 85.71% for the a-priori mask, 85.71% to 92.85% for the whole-brain mask) when compared to the unimodal setting. Although a unimodal setting is more practical and beneficial for a clinician (time and cost constraints), the results suggest that structural and functional abnormalities when studied together, may aid in classification of patients and controls. Furthermore, both may need to exist for disorder manifestation.

8.6 Conclusion

In conclusion, we combined data from multiple neuroimaging modalities (structural, functional and resting state) via multivoxel pattern analysis and ensemble learning to enable robust detection of network abnormalities and subsequent classification of healthy controls and patients with cervical dystonia. The multimodal MVPA and ensemble learning approach facilitated abnormality detection and enhanced classification accuracy between patients and controls. The features delineated from the MVPA algorithm identified key areas associated with CD and uncovered a network of multiple dysfunctional areas that when analyzed cumulatively, supported the multi-regional system-level dysfunction concept in AOIFD. Early feature integration and decision integration ensemble approaches enabled a robust way to analyze the complexity and complementarity of information from multiple modalities in CD. Fusing genetic data with these neuroimaging measures in future studies may offer more profound insights into the pathomechanisms of this disorder.

9 Discussion

9.1 Main Findings

The research studies reinforced two main hypothesis pillars in Cervical Dystonia, i) CD is a disorder of the midbrain network for covert attention and ii) an abnormal TDT is an endophenotype in CD and a subclinical manifestation of a defective SC. This was established by findings from a number of studies that queried diverse aspects of brain function in CD patients, their unaffected first-degree relatives and healthy controls, by employing novel neuroimaging and neural engineering methods. The main findings from these studies along with their interpretation will now be critically discussed with respect to the research questions previously deliberated in Chapter 3, and in light of the literature detailed in Chapter 2. Key limitations as well as future directions, arising from the studies undertaken, will also be discussed.

9.1.1 Midbrain structures and the network for covert attentional orienting may be implicated in Cervical Dystonia and abnormal temporal discrimination (addressing Research Questions 1, 2 and 6)

As discussed in Chapter 2, current evidence suggests that a defective SC is responsible for both the phenotype (CD) and the endophenotype (abnormal TDT). The results demonstrated in the studies described in Chapters 5 and 6, provided strong indication in favour of the SC's role in the development of both the motor pathomechanisms (via cephalomotor outputs) and the sensory processing pathomechanisms (via its sensory inputs and oculomotor outputs).

In Chapter 5, a looming visual stimulus was used to activate the SC as this paradigm was previously proven to be effective in a study on healthy controls. Via a 2nd level GLM whole-brain analysis, participants with abnormal temporal discrimination (CD patients and relatives) had an absence of superior collicular activation to looming stimuli. However, those with normal temporal discrimination (relatives and controls) showed significant activation to looming stimuli at the superior collicular level. To explore this with greater sensitivity, a region-of-interest analysis was carried out,

focussing on functional activations strictly within the boundaries of the SC. ROI analysis exposed a statistically significant between-group difference in SC activity. Patients and relatives with abnormal temporal discrimination had statistically lower SC activation for the loom condition when compared to participants with normal temporal discrimination (healthy controls and unaffected relatives). Additionally, the results from peak percent signal change between-group analysis for relatives corroborated these results. This provides evidence for a relationship between SC activation and normal TDT Scores. These results strongly support a model of CD and TDT where the SC has a fundamental role in facilitating covert attentional orienting, which involves the rapid redirection of attention to novel environmental stimuli.

The Putamen has been observed to be physically enlarged and less active in dystonic patients and unaffected first-degree relatives with temporal discrimination abnormalities. Under the current hypothesis, these changes must also be explained by the proposed GABAergic abnormality in the SC. The findings from the ROI analysis study in Chapter 5 and the DCM analysis study in Chapter 6 suggest that the Putaminal abnormalities in unaffected relatives with abnormal TDT, may be the consequence of an upstream effect of abnormal GABAergic activity in the SC. The inhibitory connections of the SC, and the effective connectivity between the Substantia Nigra and SC demonstrated significant differences in CD patients when compared to healthy controls, and in relatives with abnormal TDT when compared to those with normal TDT. This alteration in the bottom-up connectivity supports the midbrain covert attention hypothesis in CD.

9.1.2 Functional activation of the SC may be reliably captured in CD patients, their unaffected relatives and controls via the loom-recede visual paradigm (addressing Research Questions 3, 4 and 5)

The loom-recede-random visual paradigm was previously shown to be effective in a study with healthy controls. Billington et al. (2010) demonstrated this with whole-brain 1st level and 2nd level GLM results along with an event-related ROI analysis. However, these results only reflected findings on a cohort of ten participants. Therefore, while it was anticipated that this paradigm would elicit a response in the SC, a replicability analysis with an increased subject number was necessary to validate the stimuli's effect

on the SC. This prompted an investigation of the paradigm's results in all participants first, followed by a between-group analysis. An 8mm smoothing kernel was applied to the pre-processed data for the whole-brain analysis unlike the 5mm smoothing kernel applied earlier. This was carried out in conformity with previous literature as well as to increase the signal-to-noise ratio. Significant and focal activation of the SC for the loom condition was successfully demonstrated using the whole-brain, whole-group analysis, whereas the recede and random conditions failed to induce significant activation within the SC boundary. Regular quality checks of the scans during every stage of pre-processing, stringent motion correction and reset of the origin to the anterior commissure to align functional and anatomical images in the same plane were undertaken to ensure reliable detection of SC activation.

9.1.3 ROI analysis of the SC and other midbrain structures requires optimization for improved activation detection in Cervical Dystonia patients (addressing Research Question 4)

In Billington et al. (2010), boundary definition for the ROI analysis consisted of using landmarks derived from a standard brain atlas to draw a 27 mm³ cube over each the SC. While this seemed to work in their study, a more robust ROI analysis was crucial while studying SC activation in CD patients (due to the motion-related artifacts and therefore increased risk of unreliable activation detection). What ensued was a four-tier approach for accurate region of interest analysis activation detection, in order to optimise the SNR of the ROI results, as described in Chapter 5. While the comparison of pre-processing pipelines and incorporation of pulse-oximetry data did not yield significant results, this was probably due to the number of subjects compared (n=10). However, robust boundary definition involving i) neuropathological dissection of human brainstem specimens by a consultant neuropathologist which resulted in identification of anatomical landmarks of the left and right superior colliculi, as well as the diameter of each SC measured to be 7mm, and ii) hand-drawn ROIs on each subject iii) drawing spheres of diameter 10 mm (7mm measured diameter + 3mm compensation for the difference between slice-thickness). This enabled a vigorous and reliable approach for SC delineation as may be seen from the results mentioned in Chapters 5 and 6.

9.1.4 Dynamic causal modelling may be used to probe effective connectivity in the covert attention network with the loom-recede visual stimulus driving SC activity (Research Questions 6 and 7)

The high reliability and reproducibility of the DCM methodology applied to fMRI data have been demonstrated in previous studies (Schuyler et al., 2010). However, given the size and location of the SC, coupled with the paucity of DCM studies in deep brain subcortical structures relevant to movement disorders such as dystonia, it was unclear whether a DCM approach could be successfully employed with the fMRI data generated from the loom-recede-random visual task, to probe the functional architecture of the covert attentional orienting network in CD patients. Guided by the covert attentional orienting hypothesis, an amalgamation of anatomical and physiological principles, and by striking a balance between accuracy and complexity in designing the relevant circuits for modelling, the study described in Chapter 6 was successful at identifying key effective connectivity differences between CD patients and controls, and between relatives with abnormal and normal TDT, that originated from the SC and propagated throughout the modelled networks. Furthermore, the influence of the looming stimulus as a modulatory input was studied and the results demonstrated the differential effect of this stimulus in patients vs. controls as well as in unaffected relatives with normal vs. abnormal TDT.

9.1.5 Unaffected relatives (of CD patients) with an abnormal TDT harbour resting-state abnormalities consistent with CD pathophysiology (Research Questions 8-10 and 12)

To date, many functional connectivity studies have explored brain abnormalities in AOIFD and CD patients compared to controls. While an abnormal TDT has been hypothesized as an endophenotype in CD, and both CD and an abnormal TDT are believed to originate from the same pathomechanisms (dysfunctional SC activity due to abnormal GABA levels), very little is known about the neural circuitry of temporal discrimination. The study described in Chapter 7, demonstrated a manifestation of abnormalities in the sensory-motor network, cerebellar network and the executive control network, consistent with CD pathophysiology. While this study did not observe any differences between relatives with normal and abnormal TDT in the Basal Ganglia

network and visual network via the ICA approach, local changes were detected via the ReHo and ALFF approach. These results provide evidence that the CD and temporal discrimination circuit share common dysfunctional nodes and cautiously suggest that TDT may indeed be a true endophenotype of dystonia. Since mutated genes (even without disease penetrance) have an impact on brain function and organization, the results are consistent with the theory that these relatives are non-manifesting dystonia gene carriers. At the same time, the data does not indicate the actual origin of the abnormal TDT itself. This warrants a future investigation into the precise neural dysfunction associated with abnormal TDT. An examination of the global network properties and topological architecture of unaffected relatives with normal vs. abnormal TDT led to the unmasking of similar as well as dissimilar patterns of information transfer in unaffected relatives with abnormal TDT and CD patients when compared to relatives with normal TDT and healthy controls. Differences in hub formation identified by a graph theoretical analysis of the rs-fMRI data suggest micro-alterations in brain structure and function of unaffected relatives. The study exhibited these alterations at the amygdala and subcallosal gyrus, providing evidence that the neural substrates of social and emotional cognitive deficits may be implicated with this disorder as well as an abnormal TDT, via the collicular-pulvinar-amygdala pathway (Almeida et al., 2015; Wang et al., 2018; Koller et al., 2019). Future studies probing this pathway in unaffected relatives with normal TDT and those with abnormal TDT may help ascertain the implication of these structures in the saliency and temporal discrimination network. The topological organization depicted with the circular graphs, demonstrated a similarity in brain architecture between relatives with abnormal TDT and CD patients. Therefore, a combination of similarities and differences in information processing and connectivity architecture between CD patients and unaffected relatives with abnormal TDT, supports the hypothesis that unaffected relatives (with abnormal TDT) of CD patients are non-manifesting carriers of as yet unidentified genes.

9.1.6 Resting-state fMRI may be used to uncover local, regional and network-related connectivity patterns in unaffected relatives (addressing Research Questions 11 and 12)

A variety of statistical and mathematical approaches have been previously applied to analyse rs-fMRI data. Employing different methods may offer a complementarity in information, which may be neglected by the application of only one approach. The analysis of rs-fMRI involves the extraction of information on the function of specific brain regions and also the functional connectivity within and between different correlated brain regions. Therefore, functional segregation and integration analytical methods were explored in the current study. ICA, ReHo and ALFF were successfully implemented to demonstrate subtle differences existing in connectivity among unaffected relatives of CD patients. ReHo and ALFF explored functional segregation differences in unaffected relatives with normal vs. abnormal TDT, while ICA demonstrated function integration. The utility of these approaches had been earlier demonstrated only in patients vs. controls. The hypothesis-driven and exploratory analysis that was undertaken based upon findings from previous rs-fMRI studies carried out in CD patients vs. controls, as well as the current analysis involving the midbrain, cerebellar and Basal Ganglia networks, yielded a holistic and complementary characterization of the rs-fMRI data. Additionally, graph theory proved to be a suitable and sensitive method for examining network topology and information processing architecture in unaffected relatives of CD patients and successfully revealed that unaffected relatives (of CD patients) with an abnormal TDT harbour regional functional connectivity changes consistent with CD network abnormalities.

9.1.7 Abnormalities detected across rs-fMRI, s-MRI and t-fMRI may be combined to improve automatic classification of CD Patients and healthy controls (addressing Research Questions 13-15)

An increasing number of studies are collecting brain data from multiple modalities. The chief motivation for collectively analyzing multimodal data is to leverage their mutual information, thereby uncovering crucial relationships that cannot be accessed by using a single modality. However, given the known benefits, the number of studies that combine information across the modalities and capitalize on data fusion methods

is still small. This may be partly due to the complexity in implementation of these methods, as well as in interpretation of the results. Although this was also one of the key hurdles faced in the current study, the findings helped lay the foundations of analyzing multimodal data and executing multivoxel pattern analysis in rare disorders like dystonia, where low penetrance may affect recruitment and thus subject numbers. Furthermore, assessing information jointly across different modalities is particularly beneficial in complex multi-regional and network disorders such as dystonia, where previous unimodal research has led to the detection of significant differences in structure and function individually, however few studies have reported the interplay between them. The study described in Chapter 8 was an effort in this direction. On one hand, the results favour the hypothesis that a multimodal (rs-fMRI, s-MRI and t-fMRI) approach would lead to improved classification with an ensemble classifier, for the regional mask (VPSC) and the wholebrain masks. An increase in classification accuracy was detected from the unimodal to multimodal setting. The modest increase favours the opinion that one modality is sufficient to detect CD with realistic accuracy. Due to cost and time constraints in a clinical setting a unimodal approach may be more feasible. Rs-fMRI proved to be the most robust dataset in the current study and the results indicated that this modality alone may be used to classify CD patients and controls. Nevertheless, the current study successfully examined diverse ways of combining multimodal data and demonstrated the approach that is most applicable to neuroimaging data in CD. These findings strongly suggest that future studies in CD with improved subject numbers may harness multi-modal classification facilitated by advanced modelling methodologies to yield a more accurate and early detection of brain abnormalities in the disorder, surpassing methods that use only a single modality.

9.1.8 PCA and ensemble learning are powerful tools for multivoxel pattern analysis and multimodal data integration in AOIFD (addressing Research Questions 16-19)

Most neuroimaging studies face the curse-of-dimensionality, as the number of features (voxels in case of neuroimaging data) always outnumbers the number of observations (sample size). This, in turn, leads to the problem of overfitting, which is the poor generalizability of a machine learning model resulting in its inability to make accurate

predictions on novel data. Therefore, the common practice is to apply feature and dimensionality reduction approaches before applying a classifier/regression model to the data. A multitude of feature reduction methods exists and vary depending on the data being analysed. Chapter 8 explored ANOVA and PCA for dimensionality reduction. While both performed similarly, PCA, when combined with an ensemble learning approach for multimodal data fusion, proved to be the most effective for obtaining improved classification accuracies in CD. PCA is a mathematical approach that formulates pertinent features by linearly transforming correlated variables (e.g. raw voxels in a brain scan) into a smaller number of uncorrelated variables (Jolliffe, 2011) and has been proven to be highly effective in various neuroimaging studies (Wang et al., 2012; McIntosh and Misisic, 2013; Mwangi et al., 2014). Additionally, the potency of ensemble learning in combining multimodal data was validated. Subject recruitment may be challenging in studies involving dystonia patients due to clinical and etiological heterogeneity. Fusing data from multiple locations/countries may prove to be extremely beneficial in such a scenario, and therefore, the strengths of ensemble learning may be further exploited in future studies involving multimodal and multi-geographical data.

9.2 Limitations and Challenges

The results presented as part of this research need to take into consideration the limitations and challenges associated with the implementation of the discussed methodologies. What follows is a description of the common limitations as well as study-specific challenges faced:

9.2.1 Common Challenges

a Subject Number

Although our studies were satisfactorily powered, an increase in this number could significantly aid in data interpretation. Due to the size and location of the SC, increasing the power of the study could enable a more robust GLM and ROI analysis, better inform the DCM analysis and lead to more significant findings in the ICA and Dual Regression as well as Graph Theory analysis. However, cost and time constraints in neuroimaging research often define feasibility. Being a rare disorder (592 individuals in Ireland with

adult-onset idiopathic isolated focal dystonia)(Williams et al., 2017), recruitment of age and gender-specific participants (patients and their unaffected relatives) is challenging. Therefore, to address this challenge, cooperation between research groups is needed with MRI scans aggregated.

b Movement in Scanner

The time taken for a scanner to acquire one full scan coupled with the slow response of the BOLD signal translates to subject movement which results in a “blurring” of data. By estimating movement and including this in our models we may explain the variance related to this unwanted movement. However, the effectiveness of this method is reduced with an increase in movement size and frequency. This limitation may make the inclusion of some AOIFD patients infeasible in future work due to the presence of tremor.

c MRI Scanner

The superior colliculi are very small and located on the anterior section of the brain stem, adjacent to the internal carotid artery. This depth rules out a direct investigation using EEG¹. Even MEG², which is generally capable of targeting deeper brain areas than EEG, would struggle given the small size and therefore small neuronal population of the SC. fMRI is not limited to cortical regions and with a voxel size of 2-3mm for a 3T scanner, it is generally considered to have excellent spatial resolution. However, a voxel size of 3mm is still comparatively large given the superior colliculus is only about 6-7mm in diameter. This relatively low spatial resolution certainly limits the ability of any current 3T fMRI work from distinguishing between the superficial and deeper layers of the SC which would be required to fully address the current hypothesis. Recent studies using 7T and 9.4T scanners have shown promising results in delineating activity from individual SC layers (Loureiro et al., 2017, 2018; Garcia-Gomar et al., 2019).

¹EEG: ElectroEncephaloGraphy, an electrophysiological monitoring method to record electrical activity of the brain.

²MEG: MagnetoEncephaloGraphy, a functional neuroimaging method to record magnetic fields produced by electrical currents in the brain.

9.2.2 Study 1 – Looming Responses in the SC

a SC Location and Size

Cardiovascular noise which is introduced by the internal carotid artery (located very close to the SC) also represents a significant problem when investigating the BOLD signal arising from this region, and adds a significant limitation to any fMRI work in this area. Pulse oximetry data was collected only for eight subjects in this study. It is highly probable that data collected in the current study is effected by cardiovascular noise. Future imaging work would benefit from the inclusion of pulse oximetry during all scans. This would allow researchers to include heart rate as a nuisance regressors and explain irrelevant variance in the BOLD signal.

b Task-fMRI replicability and reproducibility

The interpretations of fMRI data is regularly questioned in the literature. A key concern is the replicability of such studies. fMRI is by nature challenging to report upon as the raw measured signal is not readily amenable to interpretation. Methodological attempts to correct for such measurable sources of noise and artifact as movement within the scanner, physiological activity such as breathing and circulation, scanner drift and both low and high-frequency noise sources mean that the results finally reported upon are already substantially abstracted from the raw data.

9.2.3 Study 2 – Dynamic Causal Modelling in the Covert Attention Network

a Model Complexity

In the DCM study undertaken, the models were designed to be linear, single-state and deterministic (it was assumed that the SC, Thalamus, Substantia Nigra and Striatum did not have any gating influence on the inter-connections) in order to reduce computation time as well as complexity. However, this may not be an accurate representation of the network. Information exchange may be affected in a non-linear, two-state, stochastic setting which could then more precisely encode the circuitry being studied.

b Visual Stimulus

Due to the magnetic nature of fMRI, the visual stimulus was presented via a mirror to a projected image outside the scanner, while in TDT setup (Chapter 4), VR headsets are used to present stimuli. It may be difficult to ensure that all subjects experience a similar stimulus as misalignment of the mirror or headset, or differences in face size/shape may affect the image arriving at the retina. It is likely that a more immersive presentation method, such as the head-mounted-display device discussed in Chapter 5, would improve BOLD responses, although this was not possible with the available 3T Philips Achieva scanner at Trinity College.

c Task-based Focus

The analysis presented in the current study has been hypothesis-driven and has focused on activation of the SC by the visual stimulus and the effect of looming signals on the covert attention network. The current dataset contains key findings as outlined earlier, but further exploratory analysis of this dataset should be carried out to investigate other cortical, sub-cortical and connectivity abnormalities related to AOIFD and abnormal temporal discrimination; possibly a DCM analysis with fMRI data acquired during a temporal discrimination task.

9.2.4 Study 3 – Neural Correlates of Abnormal Temporal Discrimination

a Resting-state fMRI Data

It has been established that the resting state networks involved depend on the nature of neural processes being evoked by the paradigm in question, or the surrounding context of the resting-state scan. Additionally, altering the model order dimensionality estimation in ICA (Smith et al., 2009; Abou Elseoud et al., 2011), may have a significant impact on the spatial characteristics of the resting state networks identified. While the optimal number of independent components was identified for the study, this number may have an impact on the results. The replicability and reproducibility of these results need to be validated on additional datasets.

b Independent Component Analysis

An ICA decomposition is achieved via iterative optimization. This stochastic characteristic results in a degree of run-to-run instability, and therefore the results obtained from such analysis usually varies between analysis runs on even the same data (Ylipaavalniemi and Vigario, 2008). In a future study, ICA repeatability testing may be performed to assess this variability, impact on the results and interpretation of the data.

c Dual Regression Results

No significant differences were observed in the midbrain, Basal Ganglia and visual networks via the ICA and Dual Regression analysis of the data from unaffected relatives. Although the opposite was hypothesized, the findings may stem from the ICA and Dual Regression results not being specifically sensitive to detect these changes, the varied flaws identified with resting-state fMRI data or even due to the limitations as discussed above. Contrarily, it may also simply signify that both cohorts of relatives do not show differences in these networks. The reasons for this need to be further investigated.

9.2.5 Study 4 – Multimodal MVPA in Cervical Dystonia and AOIFD

a Feature Back-Propagation and PCA

While principal component analysis was successful for finding hidden associations in the features, localizing the new subset of features in the brain was not possible, resulting in limiting our understanding regarding the origin of the abnormal patterns. This was exacerbated by the high dimensionality of the original data and considerably condensed version of new feature subset via PCA.

b Initial Univariate Feature Extraction

While the aim of this study was to implement MVPA and investigate the most appropriate method to combine multimodal neuroimaging datasets to aid in the classification of CD patients and controls, the high dimensionality and nature of

neuroimaging data posed a problem. It gave rise to the pre-requisite of using univariate methods (GLM) at the subject-level in order to obtain feature sets from each participant, which then underwent a multivariate analysis and multimodal integration at the group-level analysis. Further research needs to be carried out in order to eliminate the need to use univariate methods in the future.

c ROC curves for a Hard Voting Ensemble

The receiver operator characteristic (ROC) curves were generated by plotting the true positive rate (TPR) against the false positive rate (FPR) at various threshold settings and illustrated the diagnostic ability of a binary classifier. In soft voting, classifiers calculate probabilities for the outcomes by averaging out the probabilities calculated by individual algorithms. However, hard voting doesn't involve probabilities and uses a majority vote to calculate accuracy. Thus, ROC curves couldn't be plotted for the hard voting ensemble classifications.

d AOIFD study

While the surge in subject number and exceptional data resulted in high classification accuracies, the major limitation of this study was the mixed cohort of AOIFD patients. There were 10 CD, 10 BSP, 18 MD, 18 WC and 14 SD patients which made identification of region involvement according to the disorder unfeasible. This, coupled with the PCA limitation (described above) for feature back-propagation, rendered the current algorithm incapable of discerning regions in the brain that enabled these high classification accuracies.

9.3 Future Research Directions

9.3.1 Magnetic Resonance Imaging of GABA in Patients and Unaffected Relatives

Evidence suggests that sensorimotor integration discrepancies in AOIFD are linked to deficits in GABAergic activity, contributing to a dysfunction in a subcortical network operating between the SC and the Basal Ganglia which has a role in attentional orienting and novelty detection. Accumulating evidence advocates disordered GABAergic

inhibitory mechanisms in the pathogenesis of both an abnormal TDT and CD (Butler et al., 2015; Hutchinson et al., 2014). The studies undertaken as part of this research were able to demonstrate disrupted SC activity as well as an alteration of connectivity in the covert attentional orienting network in patients and controls, as well as in relatives with normal and abnormal TDT, which provided evidence for the GABAergic hypothesis. The methodologies employed were intended to test for defective GABA levels implicitly, by examining functional activity within the SC and connectivity within the covert attention network. Thus, while the results implied defective GABAergic mechanisms at play, a study explicitly investigating GABA levels is required. Examining GABA levels in the SC and Putamen via an MRS study is warranted in order to endorse TDT as a reliable indicator and its neural correlates as an endophenotype. This would help identify GABA thresholds and TDT values as objective biomarkers for the detection of individuals at risk of developing CD. Due to the fact that age and gender have been shown to influence the penetrance of CD as well as the expression of abnormal TDT, the study may include factors such as age and gender, in order to regress out the variation of GABA levels with these factors.

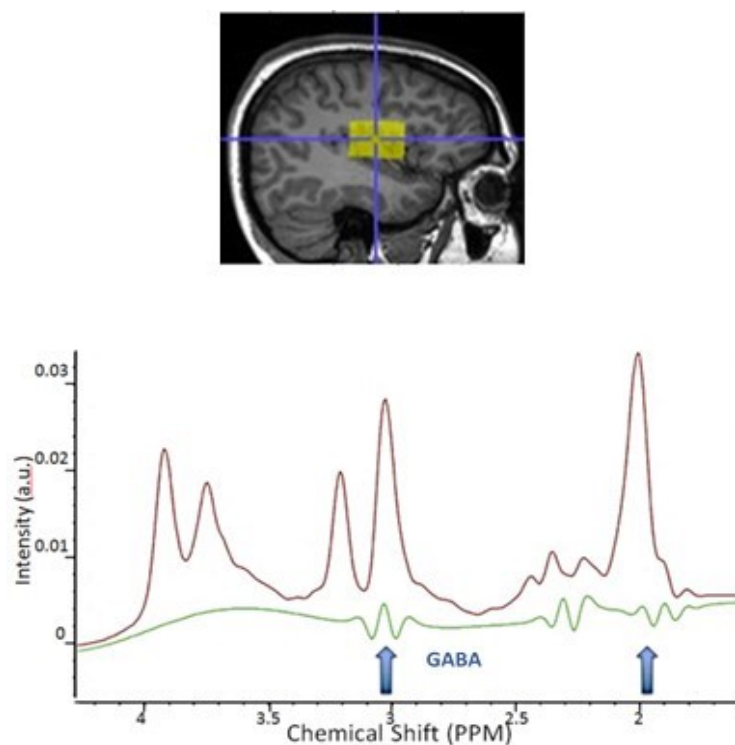


Figure 9.1: MRS-GABA levels detected in the Putamen of an exemplary healthy control scanned at Trinity College Dublin.

A pilot MRS-GABA spectroscopy study (Figure 9.1) was thus conducted on a healthy control at the Trinity College Institute of Neuroscience with a 3T Philips Achieva scanner. GABA-edited MEGA-PRESS spectra was acquired using TE/TR = 1800/68ms, 4096 data points with 2kHz spectral width, 14ms Gaussian editing pulses and a voxel size of 3x3x3mm. Due to the size and location of the SC, single-voxel spectra was acquired in the putaminal regions. The participant's data acquisition and analysis pipeline were then undertaken with the help of colleagues at the Johns Hopkins University School of Medicine, thus demonstrating the feasibility of the MRS study in the Putamen, and possibly later in the SC.

9.3.2 Dynamic Causal Modelling in Cervical Dystonia and AOIFD

The studies undertaken focussed on the SC as a central node in the hypothesized loom and temporal discrimination circuit and studied the modulatory effect of a visual stimulus (particularly looming) on the effective connectivity associated with the SC, striatum, Thalamus and Substantia Nigra. While this study was successful at detecting changes in the circuitry, a more detailed and in-depth analysis of all possible models needs to be investigated in order to develop a more comprehensive understanding of both the temporal discrimination circuitry as well as that of CD.

Implementation of a DCM analysis with nonlinear, two-state and stochastic effects would be the next step in this study. A non-linear DCM (as depicted in Figure 6.1 and Equation 6-2) is reflected by the gating of connections between regions (Friston, 2008). While in the study undertaken, it was assumed that the regions did not have a gating influence on the connections, this needs to be explored due to the complex cortical and subcortical sensorimotor loops through the Basal Ganglia, as well as the as yet incompletely understood oculomotor and cephalomotor pathways. Another alteration in the approach used would be to model the DCM as a two-state instead of as a one-state DCM. A two-state DCM has richer dynamics than a one-state DCM, as it separately models the excitation and the inhibition (Marreiros, 2008). Excitatory and inhibitory connections play a crucial part in the sensorimotor loops. With the current hypothesis pointing towards defective GABA inhibition, a two-state DCM could help provide a better model fit for studying effective connectivity in these circuits. Likewise, implementing a stochastic DCM instead of a deterministic model might

benefit the study further. Stochastic DCM allows for unknown (random) fluctuations or innovations to drive the neural system, in addition to the known (deterministic) experimental stimulation or control (Friston, 2012). This is of particular significance in the present scenario due to the incompletely understood CD, temporal discrimination and sensorimotor circuitry; as accounting for random effects on the system's dynamics allows us to cope with imperfect model assumptions and non-specific physiological perturbations (Valdés-Sosa et al., 2011).

More models evaluating the modulatory effects of the visual stimuli on other fixed connections may be tested in the future. Furthermore, the SN could be split into the SNpc and SNpr in order to test the upstream and downstream connectivity with the SC and the Striatum. Additionally, the subthalamic nucleus (STN) and globus pallidus interna (GPi) could be incorporated into the current models, to test for effective connectivity changes across this more complex network. Additionally, understanding the influence of contralateral and ipsilateral connections between these structures would also be beneficial in developing a more robust model. Testing all the above connections in the future would ensure accurate anatomical modelling of the pathways and information flow during temporal discrimination and salient visual stimuli processing in patients, relatives and controls.

9.3.3 Longitudinal Neuroimaging Studies with Unaffected Relatives and other Movement Disorder Cohorts

Very few neuroimaging studies have been carried out on unaffected relatives of dystonia patients. Most of these have been with DYT1 and DYT6 carriers, and very few with AOIFD patients. While an abnormal temporal discrimination threshold is hypothesized to be a strong endophenotype candidate in AOIFD, it is also present in a other neurological movement disorders such as Parkinson's disease (Lee, 2017; Rammsayer, 1997; Artieda, 1992), isolated tremor (Conte, 2015), and functional tremor (Tinazzi, 2014). Neuroimaging studies exploring the neural basis of an abnormal temporal discrimination threshold in these other movement disorder patients remains to be fully explored. Simultaneously, the role that TDT has in common with these movement disorders need to be further investigated. Therefore, neuroimaging studies probing the neural correlates of abnormal temporal discrimination across the

various movement disorders will help understand the association, if any. Additionally, longitudinal neuroimaging studies with unaffected relatives of AOIFD patients will aid in tracking neural substrate changes (if any) and how these influence the expression of the endophenotype (abnormal temporal discrimination) and the phenotype (CD). The studies that were undertaken in the present scenario (as discussed in the previous chapters) were capable of detecting neural correlates of temporal discrimination in unaffected relatives of CD patients. However, it was not possible to establish whether the observed differences in network dynamics, connectivity and function are due to a pre-symptomatic phase of disorder manifestation or a neuroplastic protective response to the poorly penetrant as yet unidentified gene. Therefore, a longitudinal study would help establish the implication of the presence of poor temporal discrimination and other sensory abnormalities, in the eventual manifestation of the disorder.

9.3.4 Tractography of the Cerebello-Thalamo-Cortical (CbTC) and SC-Fastigial Nucleus Pathways in Unaffected Relatives

Apart from the Cerebellum's direct involvement in sensory, motor and timing related mechanisms, the integrity of the CbTC tract has been extensively explored with diffusion tensor imaging studies in dystonia. Carriers of the DYT1 dystonia mutation, even if clinically non-penetrant, exhibit abnormalities in CbTC motor pathways. Reduced integrity of CbTC fibre tracts (Figure 9.2) was reported in both manifesting and clinically non-manifesting dystonia mutation carriers (Argyelan et al., 2009). In a DYT1 mice study, besides CbTC tract changes in mutant mice with no abnormal movements, metabolic activity in the sensorimotor cortex was found to be correlated with measures of CbTC tract integrity. In another study carried out, tractography revealed significant phenotype-related differences in the thalamocortical tracts while cortico-striatal and corticospinal pathways did not differ between groups (Vo et al., 2014). Cerebello-thalamic microstructural abnormalities were also seen in the dystonia subjects with changes associated with genotype, rather than with the phenotype. Several other whole-brain diffusion imaging studies (Colosimo et al., 2005; Simonyan et al., 2007; Fabbrini et al., 2008; Shalash et al., 2012) have pointed to not only cerebellar involvement in dystonia but also to microstructural tract changes across the brain; that could contribute to this disorder's pathophysiology.

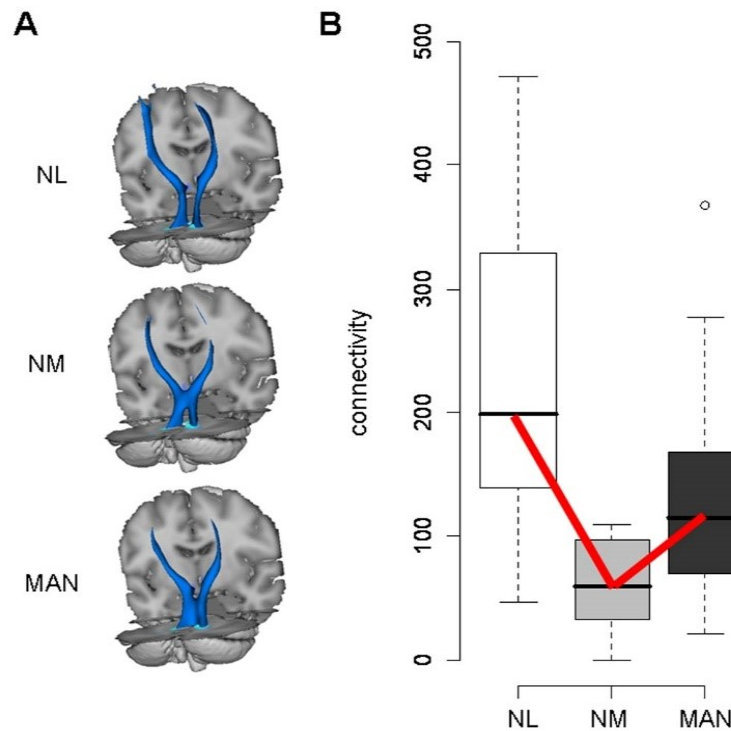


Figure 9.2: Reduced thalamo-cortical connectivity detected in non-manifesting dystonia gene carriers. A) Three-dimensional displays of the group mean probabilistic connectivity tracts generated B) Box-and-whisker plots showing connectivity values in the distal portion of the CbTC pathway. NL = Normal (Healthy Controls), MAN = Manifesting dystonia DYT1 and DYT6 gene carriers, NM = Non-manifesting dystonia DYT1 and DYT6 gene carriers. A significant trend (NL > MAN > NM, bold lines) was detected across the three groups. Adapted from (Argyelan, 2009).

The fastigial nucleus (FN) is one of the deep cerebellar nuclei, responsible for motor coordination (Zhang et al., 2016). It is located nearest to the middle line at the anterior end of the superior vermis and situated immediately over the roof of the fourth ventricle. Cerebellar afferents to the SC have been confirmed via multiple animal studies (Roldan and Reinoso-Suarez, 1981; Takahashi et al., 2013). It has been reported that the projections from the fastigial nucleus reach into the caudal and deeper layers of the SC (Roldan and Reinoso-Suarez, 1981). Their results suggested that, besides the plausible existence of direct cerebellar connections to the oculomotor nuclei, the visual Cerebellum modulates the activity of the deep layers of the SC which is related directly to the regulation of the eye- and head-orienting movements. Efferent connections to the midbrain and Thalamus from parts of the cerebellar fastigial nucleus were also reported in another study (Person et al., 1986). Besides its known relation to the control of eye

movements, it has also been suggested to control head movements via reticulospinal neurons targeted by the SC (Takahashi et al., 2013; Zhang et al., 2016).

Despite accumulating evidence of cerebellar involvement in Dystonia and its role in temporal discrimination, there has been evidence of cerebellar functions staying intact in Dystonia patients (Sadnicka et al., 2012; Prudente et al., 2014; Bologna and Berardelli, 2017a; Kaji et al., 2018). In light of the contrary views regarding the extent of cerebellar involvement, it will be beneficial to study specific pathways and tracts. Also, given the extensive role of the SC and the Cerebellum in the control of various complex processes shown to be faulty in CD (such as saccades, motor coordination, voluntary movement, eye-gaze and visual processes), and their suggested role in AOPTD, studying tracts projecting via the SC and Cerebellum (Vermis and Fastigial Nucleus) may help in delineating more specifically the structural patterns possibly causing defective connectivity. Furthermore, studying these tracts in unaffected relatives with and without abnormal TDT would help to investigate tract integrity correlations with the endophenotype. A pilot study was undertaken to delineate this tract in healthy controls (Appendix D). 3T diffusion imaging data from the Human Connectome Project (HCP) was obtained and efforts were undertaken to delineate the SC-FN pathway. Further investigation is needed in the future about the feasibility of delineating this pathway with 3T data and 7T in healthy controls, followed by a study in CD patients, if successful in the control population.

Diffusion Tensor Imaging is a robust method used to analyse structural and functional connectivity changes and characterize microstructural white matter changes in multiple regions of the brain in dystonia patients (Chapter 2). Unfortunately, no study has examined structural connectivity in relation to temporal discrimination in AOPTD. DTI research in patients and unaffected relatives with and without abnormal temporal discrimination is warranted. In light of the literature discussed, it may be hypothesized that CbTC tract integrity correlates with the mediational endophenotype TDT.

9.3.5 Multi-centre Data Integration along with Genetic Data via MVPA

The study undertaken as part of the current research work focussed on multimodal neuroimaging data integration in CD and faced a major challenge: subject number. Neuroimaging analysis and insights are greatly affected by the power of the study

(Button et al., 2013; Poldrack et al., 2017). When planning neuroimaging studies, it is important to have a sufficiently large number of subjects to detect the signal or effect of interest. Simultaneously, it is also important to include as few subjects as possible in order to avoid unnecessarily exposing subjects to unforeseen risks (e.g.: unknown environmental factors which may have an effect on disease penetrance) and to reduce the costs associated with the study (Hayasaka et al., 2007). Therefore, determining the appropriate number of subjects is an important step in study planning. Subject recruitment in dystonia (considered a rare disorder) and more specifically AOPTD is usually difficult particularly when further scientific study restrictions such as age- and gender- match, previous family history, etc. also come into play. All these factors reduce the number of subjects (patients) available to recruit per location. This may be solved by data sharing across multiple centres and geographical locations to help increase the power of a study and enable drawing powerful insights (Van Horn and Toga, 2009b, 2014). Ethical data sharing issues come into play here as a major obstacle to this solution (Van Horn and Toga, 2009a). Fortunately, the only input needed for machine-learning studies is a feature-set. These may be extracted per location and then combined at one centre. However, multiple steps have to be taken in order to ensure adequate consistency in acquisition, analysis and feature extraction. Further, multiple feature selection and extraction methods, permutations and combinations of the pipeline of a machine learning algorithm may significantly affect classification and prediction sensitivity and specificity. A carefully planned multi-centre and multi-modal AOPTD machine learning study may help aid in further probing the pathomechanisms of this disorder. The study undertaken as part of this research was a step in this direction.

Another important avenue is the incorporation of genetic datasets into the current MVPA pipeline as an additional feature set. While the results from the study undertaken successfully demonstrated MVPA as a powerful tool in finding hidden neural patterns intra- as well as inter-modality, the core postulation remains that these disorders arise due to the carriage of poorly penetrant and as yet unidentified genes. A number of studies have been undertaken to encompass genetic data in the MVPA study along with neuroimaging data (Yang et al., 2010; Zhang et al., 2011; Yerys and Herrington, 2014; Jie et al., 2015; Liu et al., 2015; Zhou et al., 2017). This has proven to enhance not only the classification accuracy but also draw key observations in the neural substrates and brain dynamics underlying gene carriage. Thus, genetic data as an additional feature

set could help the pattern recognition algorithms as well as link the disorder to specific causative genes engendering neural network changes.

9.4 Conclusion

The research studies undertaken were instrumental in addressing key research questions posed in Chapter 2. State-of-the-art computational approaches and pattern recognition methodologies were employed in the analyses and have assisted in furthering our understanding of adult onset focal dystonia. Neuroimaging based quantitative measures of brain abnormalities in patients and unaffected relatives have offered insights into the neural pathomechanisms of this disorder. While replicability and reproducibility of studies remains a priority in the neuroimaging community, the results are crucial indicators of disruptions in regional activity as well as global connectivity patterns across the brain in patients and their unaffected relatives, harbouring the endophenotype. The studies are some of the first to provide evidence for the recent midbrain and neural integrator hypothesis in Cervical Dystonia. The main findings from the experiments undertaken as part of this research, indicate altered neural mechanisms in first degree unaffected relatives of patients (with sensory abnormalities) and strongly advocate the need for longitudinal studies that track changes in these neural mechanisms with/without the manifestation of dystonia at a later stage.

Bibliography

- Abou Elseoud, A., Littow, H., Remes, J., Starck, T., Nikkinen, J., Nissila, J., Tervonen, O., Timonen, M., and Kiviniemi, V. J. (2011). Group-ica model order highlights patterns of functional brain connectivity. *Frontiers in systems neuroscience*, 5:37.
- Abraham, A., Pedregosa, F., Eickenberg, M., Gervais, P., Mueller, A., Kossaifi, J., Gramfort, A., Thirion, B., and Varoquaux, G. (2014). Machine learning for neuroimaging with scikit-learn. *Front Neuroinform*, 8:14.
- Accorsi, R. (2008). Brain single-photon emission ct physics principles. *AJNR Am J Neuroradiol*, 29(7):1247–1256.
- Aglioti, S. M., Fiorio, M., Forster, B., and Tinazzi, M. (2003). Temporal discrimination of cross-modal and unimodal stimuli in generalized dystonia. *Neurology*, 60(5):782–785.
- Akkal, D., Dum, R. P., and Strick, P. L. (2007). Supplementary motor area and presupplementary motor area: targets of basal ganglia and cerebellar output. *J Neurosci*, 27(40):10659–10673.
- Alarcon, F., Tolosa, E., and Munoz, E. (2001). Focal limb dystonia in a patient with a cerebellar mass. *Arch Neurol*, 58(7):1125–1127.
- Albanese, A., Abbruzzese, G., Dressler, D., Duzynski, W., Khatkova, S., Marti, M. J., Mir, P., Montecucco, C., Moro, E., Pinter, M., et al. (2015). Practical guidance for cd management involving treatment of botulinum toxin: a consensus statement. *Journal of neurology*, 262(10):2201–2213.
- Albanese, A., Bhatia, K., Bressman, S. B., DeLong, M. R., Fahn, S., Fung, V. S., Hallett, M., Jankovic, J., Jinnah, H. A., Klein, C., et al. (2013). Phenomenology and classification of dystonia: a consensus update. *Movement disorders*, 28(7):863–873.
- Albin, R. L., Cross, D., Cornblath, W. T., Wald, J. A., Wernette, K., Frey, K. A., and Minoshima, S. (2003). Diminished striatal [123i]iodobenzovesamicol binding in idiopathic cervical dystonia. *Ann Neurol*, 53(4):528–532.
- Albin, R. L., Young, A. B., and Penney, J. B. (1989). The functional anatomy of basal ganglia disorders. *Trends Neurosci*, 12(10):366–375.
- Alexander, A. L., Lee, J. E., Lazar, M., and Field, A. S. (2007). Diffusion tensor imaging of the brain. *Neurotherapeutics*, 4(3):316–329.
- Alexander, G. E., Crutcher, M. D., and DeLong, M. R. (1990). Basal ganglia-thalamocortical circuits: parallel substrates for motor, oculomotor, "prefrontal" and "limbic" functions. *Prog Brain Res*, 85:119–146.
- Almeida, I., Soares, S. C., and Castelo-Branco, M. (2015). The distinct role of the amygdala, superior colliculus and pulvinar in processing of central and peripheral snakes. *PLoS One*, 10(6):e0129949.
- Alongi, P., Iaccarino, L., and Perani, D. (2014). Pet neuroimaging: Insights on dystonia and tourette syndrome and potential applications. *Front Neurol*, 5:183.
- Alvarez-Fischer, D., Grundmann, M., Lu, L., Samans, B., Fritsch, B., Moller, J. C., and Bandmann, O. (2012). Prolonged generalized dystonia after chronic cerebellar application of kainic acid. *Brain Research*, 1464:82–88.
- An, L., Cao, Q.-J., Sui, M.-Q., Sun, L., Zou, Q.-H., Zang, Y.-F., and Wang, Y.-F. (2013). Local synchronization and amplitude of the fluctuation of spontaneous brain activity in attention-deficit/hyperactivity disorder: a resting-state fmri study. *Neuroscience bulletin*, 29(5):603–613.
- Anderson, E. J. and Rees, G. (2011). Neural correlates of spatial orienting in the human superior colliculus. *Journal of Neurophysiology*, 106(5):2273–2284.
- Appell, P. P. and Behan, M. (1990). Sources of subcortical gabaergic projections to the superior colliculus in the cat. *Journal of Comparative Neurology*, 302(1):143–158.
- Arcizet, F. and Krauzlis, R. J. (2018). Covert spatial selection in primate basal ganglia. *PLoS biology*, 16(10):e2005930.
- Argyelan, M., Carbon, M., Niethammer, M., Ulug, A. M., Voss, H. U., Bressman, S. B., Dhawan, V., and Eidelberg, D. (2009a). Cerebellothalamocortical connectivity regulates penetrance in dystonia. *J Neurosci*, 29(31):9740–7.
- Argyelan, M., Carbon, M., Niethammer, M., Ulug, A. M., Voss, H. U., Bressman, S. B., and Eidelberg,

- D. (2009b). Cerebellothalamocortical connectivity regulates penetrance in dystonia. *J Neurosci*, 29(31):9740–9747.
- Asanuma, K., Carbon-Correll, M., and Eidelberg, D. (2005). Neuroimaging in human dystonia. *The Journal of Medical Investigation*, 52(Supplement):272–279.
- Avanzino, L., Bove, M., Pelosin, E., Ogliastro, C., Lagravinese, G., and Martino, D. (2015a). The cerebellum predicts the temporal consequences of observed motor acts. *PLoS One*, 10:2.
- Avanzino, L. and Fiorio, M. (2014). Proprioceptive dysfunction in focal dystonia: from experimental evidence to rehabilitation strategies. *Front Hum Neurosci*, 8:1000.
- Avanzino, L., Tinazzi, M., Ionta, S., and Fiorio, M. (2015b). Sensory-motor integration in focal dystonia. *Neuropsychologia*, 79:288–300.
- Avanzino, L., Tinazzi, M., Ionta, S., and Fiorio, M. (2015c). Sensory-motor integration in focal dystonia. *Neuropsychologia*, 79(Pt B):288–300.
- Baker, R. S., Andersen, A. H., Morecraft, R. J., and Smith, C. D. (2003). A functional magnetic resonance imaging study in patients with benign essential blepharospasm. *J Neuroophthalmol*, 23(1):11–15.
- Balint, B. and Bhatia, K. P. (2014). Dystonia: an update on phenomenology, classification, pathogenesis and treatment. *Current opinion in neurology*, 27(4):468–476.
- Balint, B., Mencacci, N. E., Valente, E. M., Pisani, A., Rothwell, J., Jankovic, J., Vidailhet, M., and Bhatia, K. P. (2018). Dystonia. *Nature Reviews Disease Primers*, 4(1):25.
- Ball, T. M., Stein, M. B., Ramsawh, H. J., Campbell-Sills, L., and Paulus, M. P. (2014). Single-subject anxiety treatment outcome prediction using functional neuroimaging. *Neuropsychopharmacology*, 39(5):1254–61.
- Bara-Jimenez, W., Shelton, P., and Hallett, M. (2000). Spatial discrimination is abnormal in focal hand dystonia. *Neurology*, 55(12):1869–1873.
- Basso, M. A. and May, P. J. (2017). Circuits for action and cognition: a view from the superior colliculus. *Annual review of vision science*, 3:197–226.
- Battistella, G., Termsarasab, P., Ramdhani, R. A., Fuertinger, S., and Simonyan, K. (2015). Isolated focal dystonia as a disorder of large-scale functional networks. *Cerebral Cortex*, page bhv313.
- Beauchaine, T. P. (2009). The role of biomarkers and endophenotypes in prevention and treatment of psychopathological disorders. biomarkers in medicine 3, 1–3. *Biomarkers in Medicine*, 3(1):1–3.
- Beck, R. B., Kneafsey, S. L., Narasimham, S., O’Riordan, S., Isa, T., Hutchinson, M., and Reilly, R. B. (2018a). Reduced frequency of ipsilateral express saccades in cervical dystonia: Probing the nigro-tectal pathway. *Tremor and Other Hyperkinetic Movements*, 8.
- Beck, R. B., McGovern, E. M., Butler, J. S., Birsanu, D., Quinlivan, B., Beiser, I., Narasimham, S., O’Riordan, S., Hutchinson, M., and Reilly, R. B. (2018b). Measurement & analysis of the temporal discrimination threshold applied to cervical dystonia. *JOVE (Journal of Visualized Experiments)*, (131):e56310.
- Beckmann, C. F., Mackay, C. E., Filippini, N., and Smith, S. M. (2009). Group comparison of resting-state fmri data using multi-subject ica and dual regression. *Neuroimage*, 47(Suppl 1):S148.
- Bell, A. H., Meredith, M. A., Van Opstal, A. J., and Munoz, D. P. (2005). Crossmodal integration in the primate superior colliculus underlying the preparation and initiation of saccadic eye movements. *Journal of Neurophysiology*, 93(6):3659–3673.
- Bellman, R. E. (1957). Dynamic programming. *Princeton, NJ: Princeton University Press*.
- Bellot, E., Coizet, V., Warnking, J., Knoblauch, K., Moro, E., and Dojat, M. (2016). Effects of aging on low luminance contrast processing in humans. *NeuroImage*, 139:415–426.
- Berardelli, A., Rothwell, J. C., Day, B. L., and Marsden, C. D. (1985). Pathophysiology of blepharospasm and oromandibular dystonia. *Brain*, 108:593–608.
- Bhatia, K. P. and Marsden, C. D. (1994). The behavioural and motor consequences of focal lesions of the basal ganglia in man. *Brain*, 117(4):859–876.
- Bhidayasiri, R. and Tarsy, D. (2006). Treatment of dystonia. *Expert review of neurotherapeutics*, 6(6):863–886.
- Bianchi, S., Battistella, G., Huddleston, H., Scharf, R., Fleysher, L., and Rumbach, A. F. (2017). . . . Simonyan, K. Phenotype- and genotype-specific structural alterations in spasmodic dysphonia. *Mov Disord*, 32(4):560–568.
- Billington, J., Wilkie, R. M., Field, D. T., and Wann, J. P. (2010). Neural processing of imminent collision in humans. *Proceedings of the Royal Society of London B: Biological Sciences*, page rspb20101895.
- Billington, J., Wilkie, R. M., Field, D. T., and Wann, J. P. (2011). Neural processing of imminent collision

- in humans. *Proc Biol Sci*, 278(1711):1476–1481.
- Blake, D. T., Byl, N. N., Cheung, S., Bedenbaugh, P., Nagarajan, S., Lamb, M., and Merzenich, M. (2002). Sensory representation abnormalities that parallel focal hand dystonia in a primate model. *Somatosensory & motor research*, 19(4):347–357.
- Blood, A. J., Kuster, J. K., Woodman, S. C., Kirlic, N., Makhlof, M. L., Multhaupt-Buell, T. J., Makris, N., Parent, M., Sudarsky, L. R., Sjalander, G., Breiter, H., Breiter, H. C., and Sharma, N. (2012a). Evidence for altered basal ganglia-brainstem connections in cervical dystonia. *PLoS One*, 7(2):e31654.
- Blood, A. J., Kuster, J. K., Woodman, S. C., Kirlic, N., Makhlof, M. L., Multhaupt-Buell, T. J., Makris, N., Parent, M., Sudarsky, L. R., Sjalander, G., et al. (2012b). Evidence for altered basal ganglia-brainstem connections in cervical dystonia. *PloS one*, 7(2):e31654.
- Blood, A. J., Tuch, D. S., Makris, N., Makhlof, M. L., Sudarsky, L. R., and Sharma, N. (2006). White matter abnormalities in dystonia normalize after botulinum toxin treatment. *Neuroreport*, 17(12):1251–1255.
- Boehnke, S. E. and Munoz, D. P. (2008). On the importance of the transient visual response in the superior colliculus. *Current opinion in neurobiology*, 18(6):544–551.
- Bologna, M. and Berardelli, A. (2017a). Cerebellum: An explanation for dystonia? *Cerebellum and ataxias*, 4(1):6.
- Bologna, M. and Berardelli, A. (2017b). Cerebellum: An explanation for dystonia? *Cerebellum Ataxias*, 4:6.
- Bonilha, L., de Vries, P. M., Hurd, M. W., Rorden, C., Morgan, P. S., Besenski, N., Bergmann, K. J., and Hinson, V. K. (2009). Disrupted thalamic prefrontal pathways in patients with idiopathic dystonia. *Parkinsonism & related disorders*, 15(1):64–67.
- Bonilha, L., de Vries, P. M., Vincent, D. J., Rorden, C., Morgan, P. S., Hurd, M. W., Besenski, N., Bergmann, K. J., and Hinson, V. K. (2007). Structural white matter abnormalities in patients with idiopathic dystonia. *Mov Disord*, 22(8):1110–6.
- Born, G. and Schmidt, M. (2004). Inhibition of superior colliculus neurons by a gabaergic input from the pretectal nuclear complex in the rat. *European Journal of Neuroscience*, 20(12):3404–3412.
- Bostan, A. C., Dum, R. P., and Strick, P. L. (2010). The basal ganglia communicate with the cerebellum. *Proc Natl Acad Sci U S A*, 107(18):8452–8456.
- Bostan, A. C. and Strick, P. L. (2010). The cerebellum and basal ganglia are interconnected. *Neuropsychol Rev*, 20(3):261–270.
- Bradley, D., Whelan, R., Kimmich, O., O’Riordan, S., Mulrooney, N., Brady, P., Walsh, R., Reilly, R., Hutchinson, S., Molloy, F., et al. (2012). Temporal discrimination thresholds in adult-onset primary torsion dystonia: an analysis by task type and by dystonia phenotype. *Journal of neurology*, 259(1):77–82.
- Bradley, D., Whelan, R., Walsh, R., Reilly, R., Hutchinson, S., Molloy, F., and Hutchinson, M. (2009). Temporal discrimination threshold: Vbm evidence for an endophenotype in adult onset primary torsion dystonia. *Brain*, 132(9):2327–2335.
- Breakefield, X. O., Blood, A. J., Li, Y., Hallett, M., Hanson, P. I., and Standaert, D. G. (2008). The pathophysiological basis of dystonias. *Nature Reviews Neuroscience*, 9(3):222.
- Bressman, S. B. (2004). Dystonia genotypes, phenotypes, and classification. *Advances in neurology*, 94:101.
- Bressman, S. B., De Leon, D., Brin, M. F., Risch, N., Burke, R. E., Greene, P. E., Shale, H., and Fahn, S. (1989). Idiopathic dystonia among ashkenazi jews: evidence for autosomal dominant inheritance. *Annals of Neurology: Official Journal of the American Neurological Association and the Child Neurology Society*, 26(5):612–620.
- Brin, M. F., Fahn, S., Moskowitz, C., Friedman, A., Shale, H. M., Greene, P. E., Blitzler, A., List, T., Lange, D., Lovelace, R. E., et al. (1987). Localized injections of botulinum toxin for the treatment of focal dystonia and hemifacial spasm. *Movement disorders: official journal of the Movement Disorder Society*, 2(4):237–254.
- Brodoehl, S., Wagner, F., Prell, T., Klingner, C., Witte, O., and Günther, A. (2019). Cause or effect: Altered brain and network activity in cervical dystonia is partially normalized by botulinum toxin treatment. *NeuroImage: Clinical*, 22:101792.
- Brunamonti, E., Chiricozzi, F. R., Clausi, S., Olivito, G., Giusti, M. A., Molinari, M., Ferraina, S., and Leggio, M. (2014). Cerebellar damage impairs executive control and monitoring of movement

- generation. *PLoS one*, 9(1):e85997.
- Buchel, C., Josephs, O., Rees, G., Turner, R., Frith, C. D., and Friston, K. J. (1998). The functional anatomy of attention to visual motion. *A functional MRI study*, 121:1281–1294.
- Bullmore, E. and Sporns, O. (2009). Complex brain networks: graph theoretical analysis of structural and functional systems. *Nature reviews neuroscience*, 10(3):186.
- Butler, J. S., Beiser, I. M., Williams, L., McGovern, E., Molloy, F., Lynch, T., Healy, D. G., Moore, H., Walsh, R., Reilly, R. B., et al. (2015). age-related sexual dimorphism in temporal discrimination and in adult-onset dystonia suggests gabaergic mechanisms. *Frontiers in neurology*, 6.
- Butterworth, S., Francis, S., Kelly, E., McGlone, F., Bowtell, R., and Sawle, G. V. (2003). Abnormal cortical sensory activation in dystonia: an fmri study. *Mov Disord*, 18(6):673–682.
- Button, K. S., Ioannidis, J. P., Mokrysz, C., Nosek, B. A., Flint, J., Robinson, E. S., and Munafò, M. R. (2013). Power failure: why small sample size undermines the reliability of neuroscience. *Nature Reviews Neuroscience*, 14(5):365.
- Byl, N. (2003). What can we learn from animal models of focal hand dystonia? *Revue neurologique*, 159(10 Pt 1):857–873.
- Byl, N. N. (2004). Focal hand dystonia may result from aberrant neuroplasticity. *Adv Neurol*, 94:19–28.
- Camfield, L., Ben-Shlomo, Y., Warner, T. T., and of Dystonia in Europe (ESDE) Collaborative Group, E. S. (2002). Impact of cervical dystonia on quality of life. *Movement disorders*, 17(4):838–841.
- Cao, J., Tu, Y., Wilson, G., Orr, S. P., and Kong, J. (2020). Characterizing the analgesic effects of real and imagined acupuncture using functional and structure mri. *NeuroImage*, page 117176.
- Carbon, M., Argyelan, M., and Eidelberg, D. (2010). Functional imaging in hereditary dystonia. *Eur J Neurol*, 17 Suppl 1:58–64.
- Carbon, M., Kingsley, P. B., Su, S., Smith, G. S., Spetsieris, P., Bressman, S., and Eidelberg, D. (2004a). Microstructural white matter changes in carriers of the *dyt1* gene mutation. *Ann Neurol*, 56(2):283–286.
- Carbon, M., Kingsley, P. B., Tang, C., Bressman, S., and Eidelberg, D. (2008a). Microstructural white matter changes in primary torsion dystonia. *Mov Disord*, 23(2):234–9.
- Carbon, M., Kingsley, P. B., Tang, C., Bressman, S., and Eidelberg, D. (2008b). Microstructural white matter changes in primary torsion dystonia. *Mov Disord*, 23(2):234–239.
- Carbon, M., Su, S., Dhawan, V., Raymond, D., Bressman, S., and Eidelberg, D. (2004b). Regional metabolism in primary torsion dystonia: effects of penetrance and genotype. *Neurology*, 62(8):1384–1390.
- Carbonell, J. G., Michalski, R. S., and Mitchell, T. M. (1983). An overview of machine learning. In *Machine learning*, pages 3–23. Elsevier.
- Carpaneto, J., Micera, S., Galardi, G., Micheli, A., Carboncini, M. C., Rossi, B., and Dario, P. (2004). A protocol for the assessment of 3d movements of the head in persons with cervical dystonia. *Clin Biomech (Bristol, Avon)*, 19(7):659–663.
- Ce, P. (2000). Central effects of botulinum toxin: study of brainstem auditory evoked potentials. *Eur J Neurol*, 7(6):747.
- Cecala, A. L. (2016). Introducing students to subcortical sensory, motor, and cognitive processes associated with saccades using a series of papers by goldberg and wurtz. *J Undergrad Neurosci Educ*, 15(1):R4–R11.
- Challis, E., Hurley, P., Serra, L., Bozzali, M., Oliver, S., and Cercignani, M. (2015). Gaussian process classification of alzheimer’s disease and mild cognitive impairment from resting-state fmri. *Neuroimage*, 112:232–243.
- Chelazzi, L., Biscaldi, M., Corbetta, M., Peru, A., Tassinari, G., and Berlucchi, G. (1995). Oculomotor activity and visual spatial attention. *Behavioural brain research*, 71(1-2):81–88.
- Chillemi, G., Calamuneri, A., Morgante, F., Terranova, C., Rizzo, V., Girlanda, P., Ghilardi, M. F., and Quartarone, A. (2017). Spatial and temporal high processing of visual and auditory stimuli in cervical dystonia. *Frontiers in Neurology*, 8:66.
- Coffman, K. A., Dum, R. P., and Strick, P. L. (2011). Cerebellar vermis is a target of projections from the motor areas in the cerebral cortex. *Proc Natl Acad Sci U S A*, 108(38):16068–16073.
- Colosimo, C., Pantano, P., Calistri, V., Totaro, P., Fabbrini, G., and Berardelli, A. (2005). Diffusion tensor imaging in primary cervical dystonia. *J Neurol Neurosurg Psychiatry*, 76(11):1591–1593.
- Conte, A., McGovern, E. M., Narasimham, S., Beck, R., Killian, O., O’Riordan, S., Reilly, R. B., and Hutchinson, M. (2017). Temporal discrimination: mechanisms and relevance to adult-onset dystonia.

- Frontiers in neurology*, 8:625.
- Corbetta, M. (1998). Frontoparietal cortical networks for directing attention and the eye to visual locations: identical, independent, or overlapping neural systems? *Proc Natl Acad Sci U S A*, 95(3):831–838.
- Corbetta, M., Akbudak, E., Conturo, T. E., Snyder, A. Z., Ollinger, J. M., Drury, H. A., and Shulman, G. L. (1998). *Neuron. A common network of functional areas for attention and eye movements*, 21(4):761–773.
- Corneil, B. D., Olivier, E., and Munoz, D. P. (2002). Neck muscle responses to stimulation of monkey superior colliculus. ii. gaze shift initiation and volitional head movements. *J Neurophysiol*, 88(4):2000–2018.
- Corneil, B. D., Olivier, E., and Munoz, D. P. (2004). Visual responses on neck muscles reveal selective gating that prevents express saccades. *Neuron*, 42(5):831–841.
- Crapse, T. B., Lau, H., and Basso, M. A. (2018). A role for the superior colliculus in decision criteria. *Neuron*, 97(1):181–194.
- Crowner, B. E. (2007). Cervical dystonia: disease profile and clinical management. *Physical therapy*, 87(11):1511–1526.
- Cui, G., Jun, S. B., Jin, X., Pham, M. D., Vogel, S. S., Lovinger, D. M., and Costa, R. M. (2013). Concurrent activation of striatal direct and indirect pathways during action initiation. *Nature*, 494(7436):238–242.
- Cui, Y., Jiao, Y., Chen, Y.-C., Wang, K., Gao, B., Wen, S., Ju, S., and Teng, G.-J. (2014). Altered spontaneous brain activity in type 2 diabetes: a resting-state functional mri study. *Diabetes*, 63(2):749–760.
- Curra, A., Berardelli, A., Rona, S., Fabri, S., and Manfredi, M. (1998). Excitability of motor cortex in patients with dystonia. *Adv Neurol*, 78:33–40.
- Cynader, M. and Berman, N. (1972). Receptive-field organization of monkey superior colliculus. *J Neurophysiol*, 35(2):187–201.
- Czekoova, K., Zemankova, P., Shaw, D. J., and Bares, M. (2017). Social cognition and idiopathic isolated cervical dystonia. *Journal of Neural Transmission*, 124(9):1097–1104.
- Dauer, W. T., Burke, R. E., Greene, P., and Fahn, S. (1998). Current concepts on the clinical features, aetiology and management of idiopathic cervical dystonia. *Brain: a journal of neurology*, 121(4):547–560.
- Davis, T., LaRocque, K. F., Mumford, J. A., Norman, K. A., Wagner, A. D., and Poldrack, R. A. (2014). What do differences between multi-voxel and univariate analysis mean? how subject-, voxel-, and trial-level variance impact fmri analysis. *Neuroimage*, 97:271–83.
- Davison, C. and Goodhart, S. P. (1938). Dystonia musculorum deformans: A clinicopathologic study. *Archives of Neurology and Psychiatry*, 39(5):939–972.
- De Beyl, D. Z. and Salvia, P. (2009a). Neck movement speed in cervical dystonia. *Movement disorders: official journal of the Movement Disorder Society*, 24(15):2267–2271.
- De Beyl, D. Z. and Salvia, P. (2009b). Neck movement speed in cervical dystonia. *Mov Disord*, 24(15):2267–2271.
- de Vries, P. M., Johnson, K. A., de Jong, B. M., Gieteling, E. W., Bohning, D. E., George, M. S., and Leenders, K. L. (2008). Changed patterns of cerebral activation related to clinically normal hand movement in cervical dystonia. *Clin Neurol Neurosurg*, 110(2):120–128.
- Dean, P., Redgrave, P., and Westby, G. (1989). Event or emergency? two response systems in the mammalian superior colliculus. *Trends in neurosciences*, 12(4):137–147.
- Delnooz, C. C., Helmich, R. C., Toni, I., and van de Warrenburg, B. P. (2012). Reduced parietal connectivity with a premotor writing area in writer’s cramp. *Mov Disord*, 27(11):1425–1431.
- Delnooz, C. C., Pasman, J. W., Beckmann, C. F., and van de Warrenburg, B. P. (2013). Task-free functional mri in cervical dystonia reveals multi-network changes that partially normalize with botulinum toxin. *PloS one*, 8(5):e62877.
- Delnooz, C. C., Pasman, J. W., Beckmann, C. F., and van de Warrenburg, B. P. (2015). Altered striatal and pallidal connectivity in cervical dystonia. *Brain Structure and Function*, 220(1):513–523.
- DeSimone, J. C., Archer, D. B., Vaillancourt, D. E., and Wagle Shukla, A. (2019). Network-level connectivity is a critical feature distinguishing dystonic tremor and essential tremor. *Brain*, 142(6):1644–1659.
- Di Biasio, F., Conte, A., Bologna, M., Iezzi, E., Rocchi, L., Modugno, N., and Berardelli, A. (2015).

- Does the cerebellum intervene in the abnormal somatosensory temporal discrimination in parkinson's disease? *Parkinsonism and related disorders*, 21(7):789–792.
- Di Chiara, G., Porceddu, M., Morelli, M., Mulas, M., and Gessa, G. (1979). Evidence for a gabaergic projection from the substantia nigra to the ventromedial thalamus and to the superior colliculus of the rat. *Brain research*, 176(2):273–284.
- Dietteric, T. G. (2000). Ensemble methods in machine learning. *International Workshop on Multiple Classifier Systems*, LNCS 1857:1–15.
- Dinov, I., Van Horn, J., Lozev, K., Magsipoc, R., Petrosyan, P., Liu, Z., MacKenzie-Graha, A., Eggert, P., Parker, D. S., and Toga, A. W. (2009). Efficient, distributed and interactive neuroimaging data analysis using the Ioni pipeline. *Frontiers in neuroinformatics*, 3:22.
- Draganski, B., Schneider, S. A., Fiorio, M., Kloppel, S., Gambarin, M., Tinazzi, M., Ashburner, J., Bhatia, K. P., and Frackowiak, R. S. (2009). Genotype-phenotype interactions in primary dystonias revealed by differential changes in brain structure. *Neuroimage*, 47(4):1141–7.
- Draganski, B., Thun-Hohenstein, C., Bogdahn, U., Winkler, J., and May, A. (2003). Motor circuit gray matter changes in idiopathic cervical dystonia. *Neurology*, 61(9):1228–1231.
- Dresel, C., Haslinger, B., Castrop, F., Wohlschlaeger, A. M., and Ceballos-Baumann, A. O. (2006). Silent event-related fmri reveals deficient motor and enhanced somatosensory activation in orofacial dystonia. *Brain*, 129:36–46.
- Dresel, C., Li, Y., Wilzeck, V., Castrop, F., Zimmer, C., and Haslinger, B. (2014). Multiple changes of functional connectivity between sensorimotor areas in focal hand dystonia. *J Neurol Neurosurg Psychiatry*, 85(11):1245–1252.
- DuBois, R. M. and Cohen, M. S. (2000). Spatiotopic organization in human superior colliculus observed with fmri. *Neuroimage*, 12(1):63–70.
- Dybdal, D., Forcelli, P. A., Dubach, M., Oppedisano, M., Holmes, A., Malkova, L., and Gale, K. (2013). Topography of dyskinesias and torticollis evoked by inhibition of substantia nigra pars reticulata. *Movement Disorders*, 28(4):460–468.
- Egger, K., Mueller, J., Schocke, M., Brenneis, C., Rinnerthaler, M., Seppi, K., and Poewe, W. (2007). Voxel based morphometry reveals specific gray matter changes in primary dystonia. *Mov Disord*, 22(11):1538–1542.
- Eidelberg, D., Moeller, J., Ishikawa, T., Dhawan, V., Spetsieris, P., Przedborski, S., and Fahn, S. (1995). The metabolic topography of idiopathic torsion dystonia. *Brain*, 118(6):1473–1484.
- Ekstrom, A. (2010). How and when the fmri bold signal relates to underlying neural activity: the danger in dissociation. *Brain research reviews*, 62(2):233–244.
- Eldridge, R. and Gottlieb, R. (1976). The primary hereditary dystonias: genetic classification of 768 families and revised estimate of gene frequency, autosomal recessive form, and selected bibliography.
- Ellenbroek, B., Schwarz, M., Sontag, K.-H., and Cools, A. (1985). The importance of the striato-nigro-collicular pathway in the expression of haloperidol-induced tonic electromyographic activity. *Neuroscience letters*, 54(2-3):189–194.
- Engel, S. A., Glover, G. H., and Wandell, B. A. (1997). Retinotopic organization in human visual cortex and the spatial precision of functional mri. *Cereb Cortex*, 7(2):181–192.
- ESDE (2000). A prevalence study of primary dystonia in eight european countries. *Journal of neurology*, 247(10):787–792.
- Esmaeli-Gutstein, B., Nahmias, C., Thompson, M., Kazdan, M., and Harvey, J. (1999). Positron emission tomography in patients with benign essential blepharospasm. *Ophthalmic Plast Reconstr Surg*, 15(1):23–27.
- Fabbrini, G., Pantano, P., Totaro, P., Calistri, V., Colosimo, C., Carmellini, M., and Berardelli, A. (2008). Diffusion tensor imaging in patients with primary cervical dystonia and in patients with blepharospasm. *Eur J Neurol*, 15(2):185–189.
- Fahn, S. (1984). The varied clinical expressions of dystonia. *Neurologic clinics*, 2(3):541–554.
- Fahn, S. (2011). Classification of movement disorders. *Movement Disorders*, 26(6):947–957.
- Fahn, S. and Eldridge, R. (1976). Definition of dystonia and classification of the dystonic states. *Advances in neurology*, 14:1–5.
- Fecteau, J. H. and Munoz, D. P. (2005). Correlates of capture of attention and inhibition of return across stages of visual processing. *J Cogn Neurosci*, 17(11):1714–1727.
- Fecteau, J. H. and Munoz, D. P. (2006). Saliency, relevance, and firing: a priority map for target selection. *Trends in cognitive sciences*, 10(8):382–390.

- Fecteau, S., Pascual-Leone, A., and Theoret, H. (2006). Paradoxical facilitation of attention in healthy humans. *Behav Neurol*, 17(3-4):159–162.
- Feiwel, R. J., Black, K. J., McGee-Minnich, L. A., Snyder, A. Z., MacLeod, A. M., and Perlmutter, J. S. (1999). Diminished regional cerebral blood flow response to vibration in patients with blepharospasm. *Neurology*, 52(2):291–297.
- Feldon, P. and Kruger, L. (1970). Topography of the retinal projection upon the superior colliculus of the cat. *Vision Res*, 10(2):135–143.
- Figliozzi, F., Guariglia, P., Silvetti, M., Siegler, I., and Doricchi, F. (2005). Effects of vestibular rotatory accelerations on covert attentional orienting in vision and touch. *J Cogn Neurosci*, 17(10):1638–1651.
- Filip, P., Gallea, C., Lehericy, S., Bertasi, E., Popa, T., Marecek, R., Lungu, O. V., Kasperek, T., Vanicek, J., and Bares, M. (2017). Disruption in cerebellar and basal ganglia networks during a visuospatial task in cervical dystonia. *Mov Disord*, 32(5):757–768.
- Filip, P., Lungu, O. V., and Bares, M. (2013a). Dystonia and the cerebellum: a new field of interest in movement disorders? *Clin Neurophysiol*, 124(7):1269–1276.
- Filip, P., Lungu, O. V., Shaw, D. J., Kasperek, T., and Bares, M. (2013b). The mechanisms of movement control and time estimation in cervical dystonia patients. *Neural Plast*, 2013(90874):1.
- Fimm, B., Zahn, R., Mull, M., Kemeny, S., Buchwald, F., Block, F., and Schwarz, M. (2001). Asymmetries of visual attention after circumscribed subcortical vascular lesions. *Journal of Neurology, Neurosurgery and Psychiatry*, 71(5):652–657.
- Fiorio, M., Gambarin, M., Valente, E. M., Liberini, P., Loi, M., Cossu, G., Moretto, G., Bhatia, K. P., Defazio, G., Aglioti, S. M., et al. (2006a). Defective temporal processing of sensory stimuli in dyt1 mutation carriers: a new endophenotype of dystonia? *Brain*, 130(1):134–142.
- Fiorio, M., Tinazzi, M., and Aglioti, S. M. (2006b). Selective impairment of hand mental rotation in patients with focal hand dystonia. *Brain*, 129:47–54.
- Fiorio, M., Tinazzi, M., Bertolasi, L., and Aglioti, S. M. (2003). Temporal processing of visuotactile and tactile stimuli in writer's cramp. *Ann Neurol*, 53(5):630–635.
- Fontes, R., Ribeiro, J., Gupta, D. S., Machado, D., Lopes-Junior, F., Magalhaes, F., Bastos, V. H., Rocha, K., Marinho, V., Lima, G., et al. (2016). Time perception mechanisms at central nervous system. *Neurology international*, 8(1).
- Formisano, E., De Martino, F., and Valente, G. (2008). Multivariate analysis of fmri time series: classification and regression of brain responses using machine learning. *Magn Reson Imaging*, 26(7):921–34.
- Fox, P. T., Miezin, F. M., Allman, J. M., Van Essen, D. C., and Raichle, M. E. (1987). Retinotopic organization of human visual cortex mapped with positron-emission tomography. *J Neurosci*, 7(3):913–922.
- Fratello, M., Caiazzo, G., Trojsi, F., Russo, A., Tedeschi, G., Tagliaferri, R., and Esposito, F. (2017). Multi-view ensemble classification of brain connectivity images for neurodegeneration type discrimination. *Neuroinformatics*, 15(2):199–213.
- Freedman, E. G. and Sparks, D. L. (1997). Eye-head coordination during head-unrestrained gaze shifts in rhesus monkeys. *J Neurophysiol*, 77(5):2328–2348.
- Freeze, B. S., Kravitz, A. V., Hammack, N., Berke, J. D., and Kreitzer, A. C. (2013). Control of basal ganglia output by direct and indirect pathway projection neurons. *Journal of Neuroscience*, 33(47):18531–18539.
- Frima, N., Nasir, J., and Grunewald, R. A. (2008). Abnormal vibration-induced illusion of movement in idiopathic focal dystonia: an endophenotypic marker? *Mov Disord*, 23(3):373–377.
- Frima, N., Rome, S. M., and Grunewald, R. A. (2003). The effect of fatigue on abnormal vibration induced illusion of movement in idiopathic focal dystonia. *J Neurol Neurosurg Psychiatry*, 74(8):1154–1156.
- Friston, K. (2011a). Dynamic causal modeling and granger causality comments on: The identification of interacting networks in the brain using fmri: Model selection, causality and deconvolution. *Neuroimage*, 58(2-2):303.
- Friston, K., Moran, R., and Seth, A. K. (2013). Analysing connectivity with granger causality and dynamic causal modelling. *Current opinion in neurobiology*, 23(2):172–178.
- Friston, K., Preller, K. H., Mathys, C., Cagnan, H., Heinzle, J., Razi, A., and Zeidman, P. (2017). Dynamic causal modelling revisited. *Neuroimage*.
- Friston, K. J. (1994). Functional and effective connectivity in neuroimaging: a synthesis. *Human brain*

- mapping, 2(1-2):56–78.
- Friston, K. J. (2011b). Functional and effective connectivity: a review. *Brain connectivity*, 1(1):13–36.
- Friston, K. J., Harrison, L., and Penny, W. (2003). Dynamic causal modelling. *Neuroimage*, 19(4):1273–1302.
- Friston, K. J., Litvak, V., Oswal, A., Razi, A., Stephan, K. E., Van Wijk, B. C., Ziegler, G., and Zeidman, P. (2016). Bayesian model reduction and empirical bayes for group (dcm) studies. *Neuroimage*, 128:413–431.
- Fuertinger, S. and Simonyan, K. (2017). Connectome-wide phenotypical and genotypical associations in focal dystonia. *J Neurosci*, 37(31):7438–7449.
- Fujita, K. and Eidelberg, D. (2017). Imbalance of the direct and indirect pathways in focal dystonia: a balanced view. *Brain*, 140(12):3075–3077.
- Fukuda, H., Kusumi, M., and Nakashima, K. (2006). Epidemiology of primary focal dystonias in the western area of tottori prefecture in japan: comparison with prevalence evaluated in 1993. *Movement Disorders*, 21(9):1503–1506.
- Fukushima, K., Kaneko, C. R., and Fuchs, A. F. (1992). The neuronal substrate of integration in the oculomotor system. *Progress in neurobiology*, 39(6):609–639.
- Furigo, I. C., de Oliveira, W. F., de Oliveira, A. R., Comoli, E., Baldo, M. V., Mota-Ortiz, S. R., and Canteras, N. S. (2010). The role of the superior colliculus in predatory hunting. *Neuroscience*, 165(1):1–15.
- Galardi, G., Perani, D., Grassi, F., Bressi, S., Amadio, S., Antoni, M., and Fazio, F. (1996). Basal ganglia and thalamo-cortical hypermetabolism in patients with spasmodic torticollis. *Acta Neurologica Scandinavica*, 94(3):172–176.
- Gallea, C., Herath, P., Voon, V., Lerner, A., Ostuni, J., Saad, Z., and Hallett, M. (2018). Loss of inhibition in sensorimotor networks in focal hand dystonia. *Neuroimage Clinical*, 17:90–97.
- Galpern, W. R., Coffey, C. S., Albanese, A., Cheung, K., Comella, C. L., Ecklund, D. J., Fahn, S., Jankovic, J., Kiebertz, K., Lang, A. E., McDermott, M. P., Shefner, J. M., Teller, J. K., Thompson, J. L., Yeatts, S. D., and Jinnah, H. A. (2014). Designing clinical trials for dystonia. *Neurotherapeutics*, 11(1):117–27.
- Gandhi, N. J., Barton, E. J., and Sparks, D. L. (2008). Coordination of eye and head components of movements evoked by stimulation of the paramedian pontine reticular formation. *Experimental Brain Research*, 189(1):35–47.
- Gandhi, N. J. and Katnani, H. A. (2011). Motor functions of the superior colliculus. *Annual Review of Neuroscience*, 34:205–231.
- Gandhi, N. J. and Sparks, D. L. (2007). Dissociation of eye and head components of gaze shifts by stimulation of the omnipause neuron region. *Journal of neurophysiology*, 98(1):360–373.
- Garcia-Gomar, M. G., Strong, C., Toschi, N., Singh, K., Rosen, B. R., Wald, L. L., and Bianciardi, M. (2019). In vivo probabilistic structural atlas of the inferior and superior colliculi, medial and lateral geniculate nuclei and superior olivary complex based on 7 tesla mri. *Frontiers in Neuroscience*, 13:764.
- Garibotto, V., Romito, L. M., Elia, A. E., Soliveri, P., Panzacchi, A., Carpinelli, A., and Perani, D. (2011). In vivo evidence for gaba(a) receptor changes in the sensorimotor system in primary dystonia. *Movement Disorders*, 26(5):852–857.
- Garraux, G., Bauer, A., Hanakawa, T., Wu, T., Kansaku, K., and Hallett, M. (2004). Changes in brain anatomy in focal hand dystonia. *Annals of Neurology: Official Journal of the American Neurological Association and the Child Neurology Society*, 55(5):736–739.
- Geremia, E., Clatz, O., Menze, B. H., Konukoglu, E., Criminisi, A., and Ayache, N. (2011). Spatial decision forests for ms lesion segmentation in multi-channel magnetic resonance images. *Neuroimage*, 57(2):378–90.
- Gibbon, J., Malapani, C., Dale, C. L., and Gallistel, C. R. (1997). Toward a neurobiology of temporal cognition: advances and challenges. *Current opinion in neurobiology*, 7(2):170–184.
- Gilron, R., Rosenblatt, J., Koyejo, O., Poldrack, R. A., and Mukamel, R. (2017). What’s in a pattern? examining the type of signal multivariate analysis uncovers at the group level. *Neuroimage*, 146:113–120.
- Girault, J.-A. (2012a). Integrating neurotransmission in striatal medium spiny neurons. In *Synaptic Plasticity*, pages 407–429. Springer.
- Girault, J. A. (2012b). Signaling in striatal neurons: the phosphoproteins of reward, addiction, and

- dyskinesia. *Progress in molecular biology and translational science*, 106:33–62.
- Gitelman, D. R., Parrish, T. B., Friston, K. J., and Mesulam, M. M. (2002). Functional anatomy of visual search: regional segregations within the frontal eye fields and effective connectivity of the superior colliculus. *Neuroimage*, 15(4):970–982.
- Glover, G. H., Li, T. Q., and Ress, D. (2000a). Image-based method for retrospective correction of physiological motion effects in fmri: Retroicor. *Magnetic Resonance in Medicine*, 44(1):162–167.
- Glover, G. H., Li, T.-Q., and Ress, D. (2000b). Image-based method for retrospective correction of physiological motion effects in fmri: Retroicor. *Magnetic Resonance in Medicine: An Official Journal of the International Society for Magnetic Resonance in Medicine*, 44(1):162–167.
- Goldberg, M. E. and Wurtz, R. H. (1972). Activity of superior colliculus in behaving monkey. ii. effect of attention on neuronal responses. *Journal of Neurophysiology*, 35(4):560–574.
- Goldenberg, D. and Galvan, A. (2015). The use of functional and effective connectivity techniques to understand the developing brain. *Developmental cognitive neuroscience*, 12:155–164.
- Gottesman, I. I. and Gould, T. D. (2003). The endophenotype concept in psychiatry: etymology and strategic intentions. *American Journal of Psychiatry*, 160(4):636–645.
- Gregori, B., Agostino, R., Bologna, M., Dinapoli, L., Colosimo, C., Accornero, N., and Berardelli, A. (2008). Fast voluntary neck movements in patients with cervical dystonia: a kinematic study before and after therapy with botulinum toxin type a. *Clinical Neurophysiology*, 119(2):273–280.
- Guimaraes, H. N. and Santos, R. A. (1998). A comparative analysis of preprocessing techniques of cardiac event series for the study of heart rhythm variability using simulated signals. *Brazilian Journal of Medical and Biological Research*, 31(3):421–430.
- Guitton, D. and Volle, M. (1987). Gaze control in humans: eye-head coordination during orienting movements to targets within and beyond the oculomotor range. *Journal of neurophysiology*, 58(3):427–459.
- Habeck, C., Foster, N. L., Perneczky, R., Kurz, A., Alexopoulos, P., Koeppe, R. A., Drzezga, A., and Stern, Y. (2008). Multivariate and univariate neuroimaging biomarkers of alzheimer’s disease. *Neuroimage*, 40(4):1503–15.
- Habeck, C. G. (2010). Basics of multivariate analysis in neuroimaging data. *J Vis Exp*, (41).
- Hallett, M. (1995). Is dystonia a sensory disorder? *Annals of neurology*, 38(2):139–140.
- Hallett, M. (2006). Pathophysiology of dystonia. *Movement Disorders*, 70:485–488.
- Hallquist, M. N. and Hillary, F. G. (2018). Graph theory approaches to functional network organization in brain disorders: A critique for a brave new small-world. *Network Neuroscience*, 3(1):1–26.
- Handy, T. C., Gazzaniga, M. S., and Ivry, R. B. (2003). Cortical and subcortical contributions to the representation of temporal information. *Neuropsychologia*, 41(11):1461–1473.
- Hao, X. and Zhang, D. (2013). Ensemble universum svm learning for multimodal classification of alzheimer’s disease. *Machine Learning in Medical Imaging*, page 227–234.
- Hardwick, R. M., Rottschy, C., Miall, R. C., and Eickhoff, S. B. (2013). A quantitative meta-analysis and review of motor learning in the human brain. *Neuroimage*, 67:283–297.
- Harris, J. J., Reynell, C., and Attwell, D. (2011). The physiology of developmental changes in bold functional imaging signals. *Developmental cognitive neuroscience*, 1(3):199–216.
- Harris, L. R. (1980). The superior colliculus and movements of the head and eyes in cats. *The Journal of physiology*, 300(1):367–391.
- Haslinger, B., Altenmuller, E., Castrop, F., Zimmer, C., and Dresel, C. (2010). Sensorimotor overactivity as a pathophysiologic trait of embouchure dystonia. *Neurology*, 74(22):1790–1797.
- Hassler, R., Vasilescu, C., and Dieckmann, G. (1981). Electromyographic activity of neck muscles in patients affected by retrocollis under the influence of stimulation and coagulation of the prethalamic nucleus of the midbrain. *Stereotactic and Functional Neurosurgery*, 44(5-6):291–301.
- Hayasaka, S., Peiffer, A. M., Huggenschmidt, C. E., and Laurienti, P. J. (2007). Power and sample size calculation for neuroimaging studies by non-central random field theory. *NeuroImage*, 37(3):721–730.
- Hendrix, C. M. and Vitek, J. L. (2012). Toward a network model of dystonia. *Ann N Y Acad Sci*, 1265:46–55.
- Hendrix, C. M. and Vitek, J. L. (2015). Pathophysiology of dystonia: Models and mechanisms. *Dystonia and Dystonic Syndromes*, pages 187–207.
- Herath, P., Gallea, C., van der Veen, J. W., Horovitz, S. G., and Hallett, M. (2010). In vivo neurochemistry of primary focal hand dystonia: a magnetic resonance spectroscopic neurometabolite profiling study at 3t. *Movement Disorders*, 25(16):2800–2808.

- Hierholzer, J., Cordes, M., Schelosky, L., Richter, W., Keske, U., Venz, S., and Felix, R. (1994). Dopamine d2 receptor imaging with iodine-123-iodobenzamide spect in idiopathic rotational torticollis. *Journal of Nuclear Medicine*, 35(12):1921–1927.
- Hikosaka, O., Takikawa, Y., and Kawagoe, R. (2000). Role of the basal ganglia in the control of purposive saccadic eye movements. *Physiological reviews*, 80(3):953–978.
- Himmelbach, M., Linzenbold, W., and Ilg, U. J. (2013). Dissociation of reach-related and visual signals in the human superior colliculus. *Neuroimage*, 82:61–67.
- Hinkley, L. B., Webster, R. L., Byl, N. N., and Nagarajan, S. S. (2009). Neuroimaging characteristics of patients with focal hand dystonia. *Journal of Hand Therapy*, 22(2):125–134.
- Holmes, A. L., Forcelli, P. A., DesJardin, J. T., Decker, A. L., Teferra, M., West, E. A., Malkova, L., and Gale, K. (2012). Superior colliculus mediates cervical dystonia evoked by inhibition of the substantia nigra pars reticulata. *Journal of Neuroscience*, 32(38):13326–13332.
- Horstink, C. A., Praamstra, P., Horstink, M. W., Berger, H. J., Booij, J., and Van Royen, E. A. (1997). Low striatal d2 receptor binding as assessed by [123i]ibzsm spect in patients with writer’s cramp. *Journal of neurology, neurosurgery, and psychiatry*, 62(6):672–673.
- Hosseini, S. H., Hoefft, F., and Kesler, S. R. (2012). Gat: a graph-theoretical analysis toolbox for analyzing between-group differences in large-scale structural and functional brain networks. *PLoS one*, 7(7):e40709.
- Hotson, J. R. and Boman, D. R. (1991). Memory-contingent saccades and the substantia nigra postulate for essential blepharospasm. *Brain*, 114(1):295–307.
- Hubsch, C., Vidailhet, M., Rivaud-Pechoux, S., Pouget, P., Brochard, V., Degos, B., and Roze, E. (2011). Impaired saccadic adaptation in dyt1 dystonia. *Journal of Neurology, Neurosurgery and Psychiatry*, 82(10):1103–1106.
- Hutchinson, M., Isa, T., Molloy, A., Kimmich, O., Williams, L., Molloy, F., Moore, H., Healy, D. G., Lynch, T., Walsh, C., et al. (2014). Cervical dystonia: a disorder of the midbrain network for covert attentional orienting. *Frontiers in neurology*, 5:54.
- Hutchinson, M., Kimmich, O., Molloy, A., Whelan, R., Molloy, F., Lynch, T., Healy, D. G., Walsh, C., Edwards, M. J., Ozelius, L., et al. (2013). The endophenotype and the phenotype: Temporal discrimination and adult-onset dystonia. *Movement Disorders*, 28(13):1766–1774.
- Hutchinson, M., McGovern, E. M., Narasimham, S., Beck, R., Reilly, R. B., Walsh, C. D., Malone, K. M., Tijssen, M. A., and O’Riordan, S. (2018). The premotor syndrome of cervical dystonia: Disordered processing of salient environmental stimuli. *Movement disorders: official journal of the Movement Disorder Society*, 33(2):232.
- Hutchinson, M., Nakamura, T., Moeller, J. R., Antonini, A., Belakhlef, A., Dhawan, V., and Eidelberg, D. (2000). The metabolic topography of essential blepharospasm: a focal dystonia with general implications. *Neurology*, 55(5):673–677.
- Ignashchenkova, A., Dicke, P. W., Haarmeier, T., and Thier, P. (2004). Neuron-specific contribution of the superior colliculus to overt and covert shifts of attention. *Nature neuroscience*, 7(1):56.
- Isa, T. (2002). Intrinsic processing in the mammalian superior colliculus. *Current opinion in neurobiology*, 12(6):668–677.
- Islam, T., Kupsch, A., Bruhn, H., Scheurig, C., Schmidt, S., and Hoffmann, K. T. (2009). Decreased bilateral cortical representation patterns in writer’s cramp: a functional magnetic resonance imaging study at 3.0 t. *Neurological sciences*, 30(3):219–226.
- Jankovic, J. and Nutt, J. (1988). Blepharospasm and cranial-cervical dystonia (meige’s syndrome): familial occurrence. *Advances in neurology*, 49:117–123.
- Jenkinson, M., Beckmann, C. F., Behrens, T. E., Woolrich, M. W., and Smith, S. M. (2012). Fsl. *Neuroimage*, 62(2):782–790.
- Jhunjhunwala, K., Kotikalapudi, R., Lenka, A., Thennarassu, K., Yadav, R., Saini, J., and Pal, P. K. (2017). Abnormalities of eye-hand coordination in patients with writer’s cramp: Possible role of the cerebellum. *Tremor and Other Hyperkinetic Movements*, 7:499.
- Jiang, H., Stein, B. E., and McHaffie, J. G. (2011). Physiological evidence for a trans-basal ganglia pathway linking extrastriate visual cortex and the superior colliculus. *The Journal of physiology*, 589(23):5785–5799.
- Jiang, W., Lan, Y., Cen, C., Liu, Y., Feng, C., Lei, Y., Guo, W., and Luo, S. (2019). Abnormal spontaneous neural activity of brain regions in patients with primary blepharospasm at rest. *Journal of the Neurological Sciences*, 403:44–49.

- Jie, B., Zhang, D., Cheng, B., Shen, D., and Initiative, A. D. N. (2015). Manifold regularized multitask feature learning for multimodality disease classification. *Human brain mapping*, 36(2):489–507.
- Jinnah, H. and Factor, S. A. (2015). Diagnosis and treatment of dystonia. *Neurologic clinics*, 33(1):77–100.
- Jinnah, H. A., Neychev, V., and Hess, E. J. (2017a). The anatomical basis for dystonia: The motor network model. *Tremor Other Hyperkinet Mov (N Y)*, 7:506.
- Jinnah, H. A., Neychev, V., and Hess, E. J. (2017b). The anatomical basis for dystonia: The motor network model. *Tremor and Other Hyperkinetic Movements*, 7:506.
- Jochim, A., Li, Y., Gora-Stahlberg, G., Mantel, T., Berndt, M., Castrop, F., and Haslinger, B. (2018). Altered functional connectivity in blepharospasm/orofacial dystonia. *Brain and Behavior*, 8:1.
- Jolliffe, I. (2011). *Principal component analysis*. Springer.
- Jorge, J., Figueiredo, P., Gruetter, R., and van der Zwaag, W. (2018). Mapping and characterization of positive and negative bold responses to visual stimulation in multiple brain regions at 7t. *Human brain mapping*, 39(6):2426–2441.
- Jost, W. H. and Tatu, L. (2015). Selection of muscles for botulinum toxin injections in cervical dystonia. *Movement disorders clinical practice*, 2(3):224.
- Kahan, J. and Foltynie, T. (2013). Understanding dcm: ten simple rules for the clinician. *Neuroimage*, 83:542–549.
- Kaji, R., Bhatia, K., and Graybiel, A. M. (2018). Pathogenesis of dystonia: is it of cerebellar or basal ganglia origin? *J Neurol Neurosurg Psychiatry*, 89(5):488–492.
- Kaneda, K., Isa, K., Yanagawa, Y., and Isa, T. (2008). Nigral inhibition of gabaergic neurons in mouse superior colliculus. *Journal of Neuroscience*, 28(43):11071–11078.
- Kanovsky, P., Bares, M., Streitova, H., Klajblova, H., Daniel, P., and Rektor, I. (2003). Abnormalities of cortical excitability and cortical inhibition in cervical dystonia. *Journal of neurology*, 250(1):42–50.
- Kardamakis, A. A., Saitoh, K., and Grillner, S. (2015). Tectal microcircuit generating visual selection commands on gaze-controlling neurons. *Proceedings of the National Academy of Sciences*, 112(15):E1956–E1965.
- Karimi, M., Moerlein, S. M., Videen, T. O., Luedtke, R. R., Taylor, M., Mach, R. H., and Perlmutter, J. S. (2011). Decreased striatal dopamine receptor binding in primary focal dystonia: a d2 or d3 defect? *Movement Disorders*, 26(1):100–106.
- Karimi, M. and Perlmutter, J. S. (2015). The role of dopamine and dopaminergic pathways in dystonia: insights from neuroimaging. *Tremor and Other Hyperkinetic Movements*, 5:280.
- Karnath, H.-O., Fetter, M., and Dichgans, J. (1996). Ocular exploration of space as a function of neck proprioceptive and vestibular input—observations in normal subjects and patients with spatial neglect after parietal lesions. *Experimental brain research*, 109(2):333–342.
- Karwowski, W., Vasheghani Farahani, F., and Lighthall, N. (2019). Application of graph theory for identifying connectivity patterns in human brain networks: A systematic review. *Frontiers in Neuroscience*, 13:585.
- Kasper, L., Bollmann, S., Diaconescu, A. O., Hutton, C., Heinzle, J., Iglesias, S., Hauser, T. U., Sebold, M., Manjaly, Z.-M., Pruessmann, K. P., et al. (2017). The physio toolbox for modeling physiological noise in fmri data. *Journal of neuroscience methods*, 276:56–72.
- Keitel, C., Andersen, S. K., Quigley, C., and Müller, M. M. (2012). Independent effects of attentional gain control and competitive interactions on visual stimulus processing. *Cerebral Cortex*, 23(4):940–946.
- Kendall, M. G. and Gibbons, J. (1990). Rank correlation methods. *London : E. Arnold ; New York, NY : Oxford University Press*, vii:260.
- Kerrison, J. B., Lancaster, J. L., Zamarripa, F. E., Richardson, L. A., Morrison, J. C., Holck, D. E., and Fox, P. T. (2003). Positron emission tomography scanning in essential blepharospasm. *American journal of ophthalmology*, 136(5):846–852.
- Khan, A. Z., Blohm, G., McPeck, R. M., and Lefevre, P. (2009). Differential influence of attention on gaze and head movements. *Journal of neurophysiology*, 101(1):198–206.
- Killian, O., McGovern, E. M., Beck, R., Beiser, I., Narasimham, S., Quinlivan, B., O’Riordan, S., Simonyan, K., Hutchinson, M., and Reilly, R. B. (2017). Practice does not make perfect: Temporal discrimination in musicians with and without dystonia. *Movement disorders: official journal of the Movement Disorder Society*, 32(12):1791.
- Kimmich, O., Molloy, A., Whelan, R., Williams, L., Bradley, D., Balsters, J., Molloy, F., Lynch, T., Healy, D. G., Walsh, C., et al. (2014). Temporal discrimination, a cervical dystonia endophenotype:

- penetrance and functional correlates. *Movement Disorders*, 29(6):804–811.
- King, A. J. (2004). The superior colliculus. *Current Biology*, 14(9):R335–338.
- Kirke, D. N., Battistella, G., Kumar, V., Rubien-Thomas, E., Choy, M., Rumbach, A., and Simonyan, K. (2017). Neural correlates of dystonic tremor: a multimodal study of voice tremor in spasmodic dysphonia. *Brain imaging and behavior*, 11(1):166–175.
- Kita, H. (1993). Gabaergic circuits of the striatum. In *Progress in brain research*, volume 99, pages 51–72. Elsevier.
- Klein, C. (2014). Genetics in dystonia. *Parkinsonism and related disorders*, 20:S137–S142.
- Klein, C. and Fahn, S. (2013). Translation of oppenheim’s 1911 paper on dystonia. *Movement Disorders*, 28(7):851–862.
- Klier, E. M., Wang, H., Constantin, A. G., and Crawford, J. D. (2002). Midbrain control of three-dimensional head orientation. *Science*, 295(5558):1314–1316.
- Knudsen, E. I. (2011). Control from below: the role of a midbrain network in spatial attention. *European Journal of Neuroscience*, 33(11):1961–1972.
- Kojima, Y. and Soetedjo, R. (2018). Elimination of the error signal in the superior colliculus impairs saccade motor learning. *Proceedings of the National Academy of Sciences*, 115(38):E8987–E8995.
- Koller, K., Rafal, R. D., Platt, A., and Mitchell, N. D. (2019). Orienting toward threat: Contributions of a subcortical pathway transmitting retinal afferents to the amygdala via the superior colliculus and pulvinar. *Neuropsychologia*, 128:78–86.
- Konczak, J. and Abbruzzese, G. (2013). Focal dystonia in musicians: linking motor symptoms to somatosensory dysfunction. *Frontiers in human neuroscience*, 7:297.
- Korczyński, A. D., Kahana, E., Zilber, N., Streifler, M., Carasso, R., and Alter, M. (1980). Torsion dystonia in israel. *Annals of Neurology*, 8(4):387–391.
- Kramer, P., Heiman, G., Gasser, T., Ozelius, L., De Leon, D., Brin, M., Burke, R., Hewett, J., Hunt, A., Moskowitz, C., et al. (1994). The *dyt1* gene on 9q34 is responsible for most cases of early limb-onset idiopathic torsion dystonia in non-jews. *American journal of human genetics*, 55(3):468.
- Kramer, P. L., De Leon, D., Ozelius, L., Risch, N., Bressman, S. B., Brin, M. F., Schuback, D. E., Burke, R. E., Kwiatkowski, D. J., Shale, H., et al. (1990). Dystonia gene in ashkenazi jewish population is located on chromosome 9q32–34. *Annals of Neurology*, 27(2):114–120.
- Krauzlis, R. J., Liston, D., and Carello, C. D. (2004). Target selection and the superior colliculus: goals, choices and hypotheses. *Vision research*, 44(12):1445–1451.
- Krauzlis, R. J., Lovejoy, L. P., and Zenon, A. (2013). Superior colliculus and visual spatial attention. *Annual review of neuroscience*, 36:165–182.
- Kulke, L., Atkinson, J., and Braddick, O. (2015). Letting go: How the disappearance of a fixation target prompts the brain to shift attention. *Journal of vision*, 15(12):737–737.
- Kurth, F., Gaser, C., and Luders, E. (2015). A 12-step user guide for analyzing voxel-wise gray matter asymmetries in statistical parametric mapping (spm). *Nat Protoc*, 10(2):293–304.
- Lacruz, F., Artieda, J., Pastor, M., and Obeso, J. (1991). The anatomical basis of somaesthetic temporal discrimination in humans. *Journal of Neurology, Neurosurgery and Psychiatry*, 54(12):1077–1081.
- Lanciego, J. L., Luquin, N., and Obeso, J. A. (2012). Functional neuroanatomy of the basal ganglia. *Cold Spring Harbor perspectives in medicine*, 2:12.
- Landwehr, K., Brendel, E., and Hecht, H. (2013). Luminance and contrast in visual perception of time to collision. *Vision research*, 89:18–23.
- Lebedev, A. V., Westman, E., Van Westen, G. J., Kramberger, M. G., Lundervold, A., Aarsland, D., Soininen, H., Kloszewska, I., Mecocci, P., Tsolaki, M., Vellas, B., Lovestone, S., and Simmons, A. (2014). Random forest ensembles for detection and prediction of alzheimer’s disease with a good between-cohort robustness. *Neuroimage Clin*, 6:115–25.
- LeDoux, M., Hurst, D., and Lorden, J. (1998). Single-unit activity of cerebellar nuclear cells in the awake genetically dystonic rat. *Neuroscience*, 86(2):533–545.
- Lee, M. H., Smyser, C. D., and Shimony, J. S. (2013a). Resting-state fmri: a review of methods and clinical applications. *American Journal of neuroradiology*, 34(10):1866–1872.
- Lee, M. H., Smyser, C. D., and Shimony, J. S. (2013b). Resting-state fmri: a review of methods and clinical applications. *American Journal of neuroradiology*, 34(10):1866–1872.
- Leenders, K., Hartvig, P., Forsgren, L., Holmgren, G., Almay, B., Eckernas, S. A., and Langstrom, B. (1993). Striatal [¹¹c]-n-methyl-spiperone binding in patients with focal dystonia (torticollis) using positron emission tomography. *Journal of Neural Transmission-Parkinson’s Disease and Dementia*,

- 5(2):79–87.
- Lehericy, S., Tijssen, M. A., Vidailhet, M., Kaji, R., and Meunier, S. (2013). The anatomical basis of dystonia: current view using neuroimaging. *Mov Disord*, 28(7):944–57.
- Lei, D., Ma, J., Du, X., Shen, G., Tian, M., and Li, G. (2012). Spontaneous brain activity changes in children with primary monosymptomatic nocturnal enuresis: a resting-state fmri study. *Neurourology and urodynamics*, 31(1):99–104.
- Lettieri, C., Rinaldo, S., Devigili, G., Pisa, F., Mucchiut, M., Belgrado, E., Mondani, M., D’Auria, S., Ius, T., Skrap, M., et al. (2015). Clinical outcome of deep brain stimulation for dystonia: constant-current or constant-voltage stimulation? a non-randomized study. *European journal of neurology*, 22(6):919–926.
- Leube, B., Hendgen, T., Kessler, K., Knapp, M., Benecke, R., and Auburger, G. (1997). Sporadic focal dystonia in northwest germany: molecular basis on chromosome 18p. *Annals of Neurology*, 42(1):111–114.
- Levy, L. M. and Hallett, M. (2002). Impaired brain gaba in focal dystonia. *Annals of Neurology*, 51(1):93–101.
- Li, Z., Kadivar, A., Pluta, J., Dunlop, J., and Wang, Z. (2012). Test–retest stability analysis of resting brain activity revealed by blood oxygen level-dependent functional mri. *Journal of magnetic resonance imaging*, 36(2):344–354.
- Li, Z., Prudente, C. N., Stilla, R., Sathian, K., Jinnah, H., and Hu, X. (2017). Alterations of resting-state fmri measurements in individuals with cervical dystonia. *Human brain mapping*, 38(8):4098–4108.
- Liao, K., Kumar, A. N., Han, Y. H., Grammer, V. A., Gedeon, B. T., and Leigh, R. J. (2005). Comparison of velocity waveforms of eye and head saccades. *Annals of the New York Academy of Sciences*, 1039:477–479.
- Libero, L. E., DeRamus, T. P., Lahti, A. C., Deshpande, G., and Kana, R. K. (2015). Multimodal neuroimaging based classification of autism spectrum disorder using anatomical, neurochemical, and white matter correlates. *Cortex*, 66:46–59.
- Limbrick-Oldfield, E. H., Brooks, J. C., Wise, R. J., Padormo, F., Hajnal, J. V., Beckmann, C. F., and Ungless, M. A. (2012a). Identification and characterisation of midbrain nuclei using optimised functional magnetic resonance imaging. *Neuroimage*, 59(2):1230–1238.
- Limbrick-Oldfield, E. H., Brooks, J. C., Wise, R. J., Padormo, F., Hajnal, J. V., Beckmann, C. F., and Ungless, M. A. (2012b). Identification and characterisation of midbrain nuclei using optimised functional magnetic resonance imaging. *NeuroImage*, 59(2):1230–1238.
- Linzenbold, W. and Himmelbach, M. (2012). Signals from the deep: reach-related activity in the human superior colliculus. *Journal of Neuroscience*, 32(40):13881–13888.
- Liu, S., Cai, W., Liu, S., Zhang, F., Fulham, M., Feng, D., Pujol, S., and Kikinis, R. (2015). Multimodal neuroimaging computing: a review of the applications in neuropsychiatric disorders. *Brain informatics*, 2(3):167.
- Liu, Y.-J., Wang, Q., and Li, B. (2011). Neuronal responses to looming objects in the superior colliculus of the cat. *Brain, behavior and evolution*, 77(3):193–205.
- Lokkegaard, A., Herz, D. M., Haagensen, B. N., Lorentzen, A. K., Eickhoff, S. B., and Siebner, H. R. (2016). Altered sensorimotor activation patterns in idiopathic dystonia—an activation likelihood estimation meta-analysis of functional brain imaging studies. *Human brain mapping*, 37(2):547–557.
- Loureiro, J. R., Hagberg, G. E., Ethofer, T., Erb, M., Bause, J., Ehses, P., Scheffler, K., and Himmelbach, M. (2017). Depth-dependence of visual signals in the human superior colliculus at 9.4 t. *Human brain mapping*, 38(1):574–587.
- Loureiro, J. R., Himmelbach, M., Ethofer, T., Pohmann, R., Martin, P., Bause, J., Grodd, W., Scheffler, K., and Hagberg, G. E. (2018). In-vivo quantitative structural imaging of the human midbrain and the superior colliculus at 9.4 t. *NeuroImage*, 177:117–128.
- Loyola, D., Camargos, S., Maia, D., and Cardoso, F. (2013). Sensory tricks in focal dystonia and hemifacial spasm. *European journal of neurology*, 20(4):704–707.
- Lozano, A. (2001). Deep brain stimulation for parkinson’s disease. *Parkinsonism and related disorders*, 7(3):199–203.
- Lozeron, P., Poujois, A., Richard, A., Masmoudi, S., Meppiel, E., Woimant, F., and Kubis, N. (2016). Contribution of tms and rtms in the understanding of the pathophysiology and in the treatment of dystonia. *Frontiers in neural circuits*, 10:90.
- Lv, H., Wang, Z., Tong, E., Williams, L., Zaharchuk, G., Zeineh, M., Goldstein-Piekarski, A., Ball, T.,

- Liao, C., and Wintermark, M. (2018). Resting-state functional mri: everything that nonexperts have always wanted to know. *American Journal of Neuroradiology*, 39(8):1390–1399.
- Magalhães, F., Rocha, K., Marinho, V., Ribeiro, J., Oliveira, T., Ayres, C., Bento, T., Leite, F., Gupta, D., Bastos, V. H., et al. (2018). Neurochemical changes in basal ganglia affect time perception in parkinsonians. *Journal of biomedical science*, 25(1):26.
- Magnin, B., Mesrob, L., Kinkingnehun, S., Pelegrini-Issac, M., Colliot, O., Sarazin, M., Dubois, B., Lehericy, S., and Benali, H. (2009). Support vector machine-based classification of alzheimer's disease from whole-brain anatomical mri. *Neuroradiology*, 51(2):73–83.
- Magyar-Lehmann, S., Antonini, A., Roelcke, U., Maguire, R. P., Missimer, J., Meyer, M., and Leenders, K. L. (1997). Cerebral glucose metabolism in patients with spasmodic torticollis. *Movement Disorders*, 12(5):704–708.
- Mahmoudi, A., Takerkart, S., Regragui, F., Boussaoud, D., and Brovelli, A. (2012). Multivoxel pattern analysis for fmri data: a review. *Comput Math Methods Med*, 2012:961257.
- Maldjian, J. A., Laurienti, P. J., Kraft, R. A., and Burdette, J. H. (2003). An automated method for neuroanatomic and cytoarchitectonic atlas-based interrogation of fmri data sets. *Neuroimage*, 19(3):1233–9.
- Malouin, F. and Bédard, P. J. (1983). Evaluation of head motility and posture in cats with horizontal torticollis. *Experimental neurology*, 81(3):559–570.
- Manganelli, F., Dubbioso, R., Pisciotta, C., Antenora, A., Nolano, M., De Michele, G., Filla, A., Berardelli, A., and Santoro, L. (2013). Somatosensory temporal discrimination threshold is increased in patients with cerebellar atrophy. *The Cerebellum*, 12(4):456–459.
- Marinelli, L., Pelosin, E., Trompetto, C., Avanzino, L., Ghilardi, M. F., Abbruzzese, G., and Bove, M. (2011). In idiopathic cervical dystonia movement direction is inaccurate when reaching in unusual workspaces. *Parkinsonism and related disorders*, 17(6):470–472.
- Marsden, C. D., Obeso, J. A., Zarranz, J. J., and Lang, A. E. (1985). The anatomical basis of symptomatic hemidystonia. *Brain*, 108:463–483.
- Matsumoto, R. R. and Pouw, B. (2000). Correlation between neuroleptic binding to $\sigma 1$ and $\sigma 2$ receptors and acute dystonic reactions. *European journal of pharmacology*, 401(2):155–160.
- Matthews, P. M. and Jezzard, P. (2004). Functional magnetic resonance imaging. *Journal of Neurology, Neurosurgery and Psychiatry*, 75(1):6–12.
- May, P. J. (2006). The mammalian superior colliculus: laminar structure and connections. *Progress in brain research*, 151:321–378.
- Mayo, J. P. and Sommer, M. A. (2013). Neuronal correlates of visual time perception at brief timescales. *Proceedings of the National Academy of Sciences*, 110(4):1506–1511.
- Mazzini, L., Zaccala, M., and Balzarini, C. (1994). Abnormalities of somatosensory evoked potentials in spasmodic torticollis. *Movement Disorders*, 9(4):426–430.
- Mc Govern, E. M., Butler, J. S., Beiser, I., Williams, L., Quinlivan, B., Narasimham, S., Beck, R., O'Riordan, S., Reilly, R. B., and Hutchinson, M. (2017a). A comparison of stimulus presentation methods in temporal discrimination testing. *Physiological measurement*, 38(2):N57.
- Mc Govern, E. M., Killian, O., Narasimham, S., Quinlivan, B., Butler, J. B., Beck, R., Beiser, I., Williams, L. W., Killeen, R. P., Farrell, M., et al. (2017b). Disrupted superior collicular activity may reveal cervical dystonia disease pathomechanisms. *Scientific reports*, 7(1):16753.
- Mc Govern, E. M., Killian, O., Narasimham, S., Quinlivan, B., Butler, J. B., Beck, R., Beiser, I., Williams, L. W., Killeen, R. P., Farrell, M., O'Riordan, S., Reilly, R. B., and Hutchinson, M. (2017c). Disrupted superior collicular activity may reveal cervical dystonia disease pathomechanisms. *Sci Rep*, 7(1):16753.
- Mc Govern, E. M., O'Connor, E., Beiser, I., Williams, L., Butler, J. S., Quinlivan, B., Narasimham, S., Beck, R., Reilly, R. B., O'Riordan, S., et al. (2017d). Menstrual cycle and the temporal discrimination threshold. *Physiological measurement*, 38(2):N65.
- McIntosh, A. R. and Misisic, B. (2013). Multivariate statistical analyses for neuroimaging data. *Annual review of psychology*, 64:499–525.
- Melhem, E. R., Mori, S., Mukundan, G., Kraut, M. A., Pomper, M. G., and van Zijl, P. C. (2002). Diffusion tensor mr imaging of the brain and white matter tractography. *American Journal of Roentgenology*, 178(1):3–16.
- Meredith, M. A. and Stein, B. E. (1986). Visual, auditory, and somatosensory convergence on cells in superior colliculus results in multisensory integration. *Journal of neurophysiology*, 56(3):640–662.

- Meredith, M. A. and Stein, B. E. (1990). The visuotopic component of the multisensory map in the deep laminae of the cat superior colliculus. *Journal of Neuroscience*, 10(11):3727–3742.
- Mesulam, M. M. (1981). A cortical network for directed attention and unilateral neglect. *Annals of Neurology*, 10(4):309–325.
- Meyer-Lindenberg, A. (2009). Neural connectivity as an intermediate phenotype: brain networks under genetic control. *Human brain mapping*, 30(7):1938–1946.
- Mikl, M., Mareček, R., Hlušík, P., Pavlicová, M., Drastich, A., Chlebus, P., Brázdil, M., and Krupa, P. (2008). Effects of spatial smoothing on fmri group inferences. *Magnetic resonance imaging*, 26(4):490–503.
- Miller, E. K. (2000). The neural basis of top-down control of visual attention in the prefrontal cortex. *Control of Cognitive Processes*, page 511.
- Mink, J. W. (2003). The basal ganglia and involuntary movements: impaired inhibition of competing motor patterns. *Archives of neurology*, 60(10):1365–1368.
- Mize, R. R. (1992). The organization of gabaergic neurons in the mammalian superior colliculus. *Progress in brain research*, 90:219–248.
- Mohammadi, B., Kollewe, K., Samii, A., Beckmann, C. F., Dengler, R., and Munte, T. F. (2012). Changes in resting-state brain networks in writer’s cramp. *Human brain mapping*, 33(4):840–848.
- Molloy, A., Kimmich, O., Williams, L., Quinlivan, B., Dabacan, A., Fanning, A., Butler, J. S., O’Riordan, S., Reilly, R. B., and Hutchinson, M. (2014). A headset method for measuring the visual temporal discrimination threshold in cervical dystonia. *Tremor and Other Hyperkinetic Movements*, 4.
- Molloy, F. M., Carr, T. D., Zeuner, K. E., Dambrosia, J. M., and Hallett, M. (2003). Abnormalities of spatial discrimination in focal and generalized dystonia. *Brain*, 126:2175–2182.
- Monteon, J. A., Martinez-Trujillo, J. C., Wang, H., and Crawford, J. D. (2005). Cross-coupled adaptation of eye and head position commands in the primate gaze control system. *Neuroreport*, 16(11):1189–1192.
- Monti, M. M. (2011). Statistical analysis of fmri time-series: A critical review of the glm approach. *Front Hum Neurosci*, 5:28.
- Morecraft, R. J., Geula, C., and Mesulam, M. M. (1993). Architecture of connectivity within a cingulo-fronto-parietal neurocognitive network for directed attention. *Archives of neurology*, 50(3):279–284.
- Moro, E., LeReun, C., Krauss, J., Albanese, A., Lin, J.-P., Walleser Autiero, S., Brionne, T., and Vidailhet, M. (2017). Efficacy of pallidal stimulation in isolated dystonia: a systematic review and meta-analysis. *European journal of neurology*, 24(4):552–560.
- Mourao-Miranda, J., Bokde, A. L., Born, C., Hampel, H., and Stetter, M. (2005). Classifying brain states and determining the discriminating activation patterns: Support vector machine on functional mri data. *Neuroimage*, 28(4):980–95.
- Müller, S. V., Gläser, P., Tröger, M., Dengler, R., Johannes, S., and Münte, T. F. (2005). Disturbed egocentric space representation in cervical dystonia. *Movement disorders: official journal of the Movement Disorder Society*, 20(1):58–63.
- Mwangi, B., Tian, T. S., and Soares, J. C. (2014). A review of feature reduction techniques in neuroimaging. *Neuroinformatics*, 12(2):229–244.
- Nagata, E., Kosakai, A., Tanaka, K., Segawa, M., Fujioka, H., Shintaku, H., and Suzuki, N. (2007). Dopa-responsive dystonia (segawa disease)-like disease accompanied by mental retardation: A case report. *Movement disorders*, 22(8):1202–1203.
- Nakazawa, M., Kobayashi, T., Matsuno, K., and Mita, S. (1999). Possible involvement of a σ receptor subtype in the neck dystonia in rats. *Pharmacology Biochemistry and Behavior*, 62(1):123–126.
- Nambu, A., Tokuno, H., and Takada, M. (2002). Functional significance of the cortico-subthalamo-pallidal ‘hyperdirect’ pathway. *Neuroscience research*, 43(2):111–117.
- Narasimham, S., Mc Govern, E. M., Quinlivan, B., Killian, O. P., Beck, R., O’Riordan, S., Hutchinson, M., and Reilly, R. B. (2019). Neural correlates of abnormal temporal discrimination in unaffected relatives of cervical dystonia patients. *Frontiers in integrative neuroscience*, 13:8.
- Naumann, M., Magyar-Lehmann, S., Reiners, K., Erbguth, F., and Leenders, K. L. (2000). Sensory tricks in cervical dystonia: perceptual dysbalance of parietal cortex modulates frontal motor programming. *Annals of Neurology: Official Journal of the American Neurological Association and the Child Neurology Society*, 47(3):322–328.
- Neggers, S., Raemaekers, M., Lampmann, E., Postma, A., and Ramsey, N. (2005). Cortical and

- subcortical contributions to saccade latency in the human brain. *European Journal of Neuroscience*, 21(10):2853–2863.
- Neadic, I., Gaser, C., Volz, H.-P., Rammsayer, T., Häger, F., and Sauer, H. (2003). Processing of temporal information and the basal ganglia: new evidence from fmri. *Experimental Brain Research*, 148(2):238–246.
- Nevrly, M., Hlustik, P., Hok, P., Otruba, P., Tudos, Z., and Kanovsky, P. (2018). Changes in sensorimotor network activation after botulinum toxin type a injections in patients with cervical dystonia: A functional mri study. *Experimental brain research*, 236(10):2627–2637.
- Neychev, V. K., Fan, X., Mitev, V. I., Hess, E. J., and Jinnah, H. A. (2008). The basal ganglia and cerebellum interact in the expression of dystonic movement. *Brain*, 131(Pt 9):2499–509.
- Neychev, V. K., Gross, R. E., Lehericy, S., Hess, E. J., and Jinnah, H. (2011). The functional neuroanatomy of dystonia. *Neurobiology of disease*, 42(2):185–201.
- Nguyen, D. T., Ryu, S., Qureshi, M. N. I., Choi, M., Lee, K. H., and Lee, B. (2019). Hybrid multivariate pattern analysis combined with extreme learning machine for alzheimer’s dementia diagnosis using multi-measure rs-fmri spatial patterns. *PLoS One*, 14(2):e0212582.
- Ni, M.-F., Huang, X.-F., Miao, Y.-W., and Liang, Z.-H. (2017). Resting state fmri observations of baseline brain functional activities and connectivities in primary blepharospasm. *Neuroscience Letters*, 660:22–28.
- Nickerson, L. D., Smith, S. M., Öngür, D., and Beckmann, C. F. (2017). Using dual regression to investigate network shape and amplitude in functional connectivity analyses. *Frontiers in neuroscience*, 11:115.
- Norman, K. A., Polyn, S. M., Detre, G. J., and Haxby, J. V. (2006). Beyond mind-reading: multi-voxel pattern analysis of fmri data. *Trends Cogn Sci*, 10(9):424–30.
- Nutt, J. G., Muentzer, M. D., Aronson, A., Kurland, L. T., and Melton III, L. J. (1988). Epidemiology of focal and generalized dystonia in rochester, minnesota. *Movement Disorders*, 3(3):188–194.
- Obermann, M., Yaldizli, O., De Greiff, A., Lachenmayer, M. L., Buhl, A. R., Tumczak, F., Gizewski, E. R., Diener, H. C., and Maschke, M. (2007). Morphometric changes of sensorimotor structures in focal dystonia. *Mov Disord*, 22(8):1117–23.
- O’Dwyer, J., O’Riordan, S., Saunders-Pullman, R., Bressman, S., Molloy, F., Lynch, T., and Hutchinson, M. (2005). Sensory abnormalities in unaffected relatives in familial adult-onset dystonia. *Neurology*, 65(6):938–940.
- Oga, T., Honda, M., Toma, K., Murase, N., Okada, T., Hanakawa, T., Sawamoto, N., Nagamine, T., Konishi, J., Fukuyama, H., et al. (2002). Abnormal cortical mechanisms of voluntary muscle relaxation in patients with writer’s cramp: an fmri study. *Brain*, 125(4):895–903.
- Okada, Y. (1992). The distribution and function of gaba in the superior colliculus. In Mize, R., Marc, R., and Sillito, A., editors, *GABA in the Retina and Central Visual System*, chapter 12, pages 249–262. Elsevier.
- Okumura, K., Ujike, H., Akiyama, K., and Kuroda, S. (1996). Bmy-14802 reversed the σ receptor agonist-induced neck dystonia in rats. *Journal of neural transmission*, 103(10):1153–1161.
- Opavsky, R., Hlustik, P., Otruba, P., and Kanovsky, P. (2012). Somatosensory cortical activation in cervical dystonia and its modulation with botulinum toxin: an fmri study. *International Journal of Neuroscience*, 122(1):45–52.
- Otsuka, M., Ichiya, Y., Shima, F., Kuwabara, Y., Sasaki, M., Fukumura, T., Kato, M., Masuda, K., and Goto, I. (1992). Increased striatal 18f-dopa uptake and normal glucose metabolism in idiopathic dystonia syndrome. *Journal of the neurological sciences*, 111(2):195–199.
- Ozelius, L. J., Hewett, J. W., Page, C. E., Bressman, S. B., Kramer, P. L., Shalish, C., De Leon, D., Brin, M. F., Raymond, D., Corey, D. P., et al. (1997). The early-onset torsion dystonia gene (dvt1) encodes an atp-binding protein. *Nature genetics*, 17(1):40.
- Öztürk, O., Gündüz, A., and Kızıltan, M. E. (2018). Cortical modulation of brainstem circuits is abnormal in cervical dystonia. *Neuroscience letters*, 677:84–87.
- Pantano, P., Totaro, P., Fabbrini, G., Raz, E., Contessa, G. M., Tona, F., Colosimo, C., and Berardelli, A. (2011). A transverse and longitudinal mr imaging voxel-based morphometry study in patients with primary cervical dystonia. *AJNR Am J Neuroradiol*, 32(1):81–4.
- Pastor, M. A., Day, B. L., Macaluso, E., Friston, K. J., and Frackowiak, R. S. (2004). The functional neuroanatomy of temporal discrimination. *Journal of Neuroscience*, 24(10):2585–2591.
- Patel, N., Hanfelt, J., Marsh, L., Jankovic, J., et al. (2014). Alleviating manoeuvres (sensory tricks) in

- cervical dystonia. *J Neurol Neurosurg Psychiatry*, 85(8):882–884.
- Pavlidis, P.; Weston, J. (2001). Gene functional classification from heterogeneous data. *Proceedings of the Fifth International Conference on Computational Molecular Biology*, page 7.
- Pearlson, G. D., Calhoun, V. D., and Liu, J. (2015). An introductory review of parallel independent component analysis (p-ica) and a guide to applying p-ica to genetic data and imaging phenotypes to identify disease-associated biological pathways and systems in common complex disorders. *Frontiers in genetics*, 6:276.
- Pedregosa, F., Varoquaux, G., Gramfort, A., Michel, V., Thirion, B., Grisel, O., Blondel, M., Prettenhofer, P., Weiss, R., Dubourg, V., Vanderplas, J., Passos, A., Cournapeau, D., Brucher, M., Perrot, M., and Duchesnay, E. (2011). Scikit-learn: Machine learning in python. *Journal of Machine Learning Research*, 12:2825–2830.
- Pekmezovic, T., Ivanovic, N., Svetel, M., Nalic, D., Smiljkovic, T., Raicevic, R., and Kostic, V. (2003). Prevalence of primary late-onset focal dystonia in the belgrade population. *Movement Disorders*, 18(11):1389–1392.
- Pekmezovic, T., Svetel, M., Ivanovic, N., Dragasevic, N., Petrovic, I., Tepavcevic, D. K., and Kostic, V. S. (2009). Quality of life in patients with focal dystonia. *Clinical neurology and neurosurgery*, 111(2):161–164.
- Peller, M., Zeuner, K., Munchau, A., Quartarone, A., Weiss, M., Knutzen, A., Hallett, M., Deuschl, G., and Siebner, H. (2006). The basal ganglia are hyperactive during the discrimination of tactile stimuli in writer’s cramp. *Brain*, 129(10):2697–2708.
- Penny, W. D., Stephan, K. E., Daunizeau, J., Rosa, M. J., Friston, K. J., Schofield, T. M., and Leff, A. P. (2010). Comparing families of dynamic causal models. *PLoS computational biology*, 6(3):e1000709.
- Person, R., Andrezik, J., Dormer, K., and Foreman, R. (1986). Fastigial nucleus projections in the midbrain and thalamus in dogs. *Neuroscience*, 18(1):105–120.
- Petersen, S. E. and Dubis, J. W. (2012). The mixed block/event-related design. *Neuroimage*, 62(2):1177–1184.
- Peterson, M. S., Kramer, A. F., and Irwin, D. E. (2004). Covert shifts of attention precede involuntary eye movements. *Perception & psychophysics*, 66(3):398–405.
- Petit, L. and Beauchamp, M. S. (2003). Neural basis of visually guided head movements studied with fmri. *Journal of neurophysiology*, 89(5):2516–2527.
- Pettersson-Yeo, W., Benetti, S., Marquand, A. F., Jules, R., Catani, M., Williams, S. C., Allen, P., McGuire, P., and Mechelli, A. (2014). An empirical comparison of different approaches for combining multimodal neuroimaging data with support vector machine. *Frontiers in neuroscience*, 8:189.
- Pettigrew, L. C. and Jankovic, J. (1985). Hemidystonia: a report of 22 patients and a review of the literature. *Journal of Neurology, Neurosurgery & Psychiatry*, 48(7):650–657.
- Pinheiro, G. L., Guimaraes, R. P., Piovesana, L. G., Campos, B. M., Campos, L. S., Azevedo, P. C., Torres, F. R., Amato-Filho, A. C., Franca, M. C., J., Lopes-Cendes, I., Cendes, F., and D’Abreu, A. (2015). White matter microstructure in idiopathic craniocervical dystonia. *Tremor Other Hyperkinet Mov (N Y)*, 5.
- Pizoli, C. E., Jinnah, H., Billingsley, M. L., and Hess, E. J. (2002). Abnormal cerebellar signaling induces dystonia in mice. *Journal of Neuroscience*, 22(17):7825–7833.
- Poldrack, R. A., Baker, C. I., Durnez, J., Gorgolewski, K. J., Matthews, P. M., Munafò, M. R., Nichols, T. E., Poline, J.-B., Vul, E., and Yarkoni, T. (2017). Scanning the horizon: towards transparent and reproducible neuroimaging research. *Nature Reviews Neuroscience*, 18(2):115.
- Polikar, R. (2012). Ensemble learning. In *Ensemble machine learning*, pages 1–34. Springer.
- Poncelet, B., Wedeen, V., Weisskoff, R., and Cohen, M. (1992). Brain parenchyma motion: measurement with cine echo-planar mr imaging. *Radiology*, 185(3):645–651.
- Pong, M., Horn, K. M., and Gibson, A. R. (2008). Pathways for control of face and neck musculature by the basal ganglia and cerebellum. *Brain research reviews*, 58(2):249–264.
- Posner, M. I., Cohen, Y., and Rafal, R. D. (1982). Neural systems control of spatial orienting. *Philosophical Transactions of the Royal Society of London. B, Biological Sciences*, 298(1089):187–198.
- Prell, T., Peschel, T., Kohler, B., Bokemeyer, M. H., Dengler, R., Gunther, A., and Grosskreutz, J. (2013). Structural brain abnormalities in cervical dystonia. *BMC Neuroscience*, 14:123.
- Premi, E., Cauda, F., Gasparotti, R., Diano, M., Archetti, S., Padovani, A., and Borroni, B. (2014). Multimodal fmri resting-state functional connectivity in granulin mutations: the case of fronto-parietal

- dementia. *PLoS One*, 9(9):e106500.
- Prudente, C., Pardo, C., Xiao, J., Hanfelt, J., Hess, E., Ledoux, M., and Jinnah, H. (2013). Neuropathology of cervical dystonia. *Experimental neurology*, 241:95–104.
- Prudente, C. N., Hess, E. J., and Jinnah, H. (2014). Dystonia as a network disorder: what is the role of the cerebellum? *Neuroscience*, 260:23–35.
- Prudente, C. N., Stilla, R., Singh, S., Buetefisch, C., Evatt, M., Factor, S. A., Freeman, A., Hu, X. P., Hess, E. J., Sathian, K., et al. (2016). A functional magnetic resonance imaging study of head movements in cervical dystonia. *Frontiers in neurology*, 7:201.
- Pujol, J., Roset-Llobet, J., Rosines-Cubells, D., Deus, J., Narberhaus, B., Valls-Sole, J., Capdevila, A., and Pascual-Leone, A. (2000). Brain cortical activation during guitar-induced hand dystonia studied by functional mri. *Neuroimage*, 12(3):257–267.
- Putzki, N., Stude, P., Konczak, J., Graf, K., Diener, H.-C., and Maschke, M. (2006). Kinesthesia is impaired in focal dystonia. *Movement disorders*, 21(6):754–760.
- Qureshi, M. N. I., Oh, J., Cho, D., Jo, H. J., and Lee, B. (2017). Multimodal discrimination of schizophrenia using hybrid weighted feature concatenation of brain functional connectivity and anatomical features with an extreme learning machine. *Front Neuroinform*, 11:59.
- Raghavan, R. T., Prevosto, V., and Sommer, M. A. (2016). Contribution of cerebellar loops to action timing. *Current opinion in behavioral sciences*, 8:28–34.
- Raike, R. S., Jinnah, H., and Hess, E. J. (2005). Animal models of generalized dystonia. *NeuroRx*, 2(3):504–512.
- Ramdhani, R. A., Kumar, V., Velickovic, M., Frucht, S. J., Tagliati, M., and Simonyan, K. (2014). What’s special about task in dystonia? a voxel-based morphometry and diffusion weighted imaging study. *Movement Disorders*, 29(9):1141–1150.
- Ramdhani, R. A. and Simonyan, K. (2013). Primary dystonia: conceptualizing the disorder through a structural brain imaging lens. *Tremor and other hyperkinetic movements*, 3.
- Ramirez, J., Gorriz, J. M., Ortiz, A., Martinez-Murcia, F. J., Segovia, F., Salas-Gonzalez, D., Castillo-Barnes, D., Illan, I. A., and Puntonet, C. G. (2018). Ensemble of random forests one vs. rest classifiers for mci and ad prediction using anova cortical and subcortical feature selection and partial least squares. *J Neurosci Methods*, 302:47–57.
- Ramos, V. F. M. L., Esquenazi, A., Villegas, M. A. F., Wu, T., and Hallett, M. (2016). Temporal discrimination threshold with healthy aging. *Neurobiology of aging*, 43:174–179.
- Rao, S. M., Mayer, A. R., and Harrington, D. L. (2001). The evolution of brain activation during temporal processing. *Nature neuroscience*, 4(3):317.
- Redgrave, P., Coizet, V., Comoli, E., McHaffie, J. G., Leriche Vazquez, M., Vautrelle, N., Hayes, L. M., and Overton, P. G. (2010). Interactions between the midbrain superior colliculus and the basal ganglia. *Frontiers in neuroanatomy*, 4:132.
- Reilly, J. A., Hallett, M., Cohen, L. G., Tarkka, I. M., and Dang, N. (1992). The n30 component of somatosensory evoked potentials in patients with dystonia. *Electroencephalography and Clinical Neurophysiology/Evoked Potentials Section*, 84(3):243–247.
- Reimold, M., Slifstein, M., Heinz, A., Mueller-Schauenburg, W., and Bares, R. (2006). Effect of spatial smoothing on t-maps: arguments for going back from t-maps to masked contrast images. *Journal of Cerebral Blood Flow & Metabolism*, 26(6):751–759.
- Rigoux, L., Stephan, K. E., Friston, K. J., and Daunizeau, J. (2014). Bayesian model selection for group studies—revisited. *Neuroimage*, 84:971–985.
- Risch, N., de Leon, D., Ozelius, L., Kramer, P., Almasy, L., Singer, B., Fahn, S., Breakefield, X., and Bressman, S. (1995). Genetic analysis of idiopathic torsion dystonia in ashkenazi jews and their recent descent from a small founder population. *Nature genetics*, 9(2):152.
- Rivolta, D., Woolgar, A., Palermo, R., Butko, M., Schmalzl, L., and Williams, M. A. (2014). Multi-voxel pattern analysis (mvpa) reveals abnormal fmri activity in both the ”core” and ”extended” face network in congenital prosopagnosia. *Front Hum Neurosci*, 8:925.
- Robinson, D. (1986). The systems approach to the oculomotor system. *Vision research*, 26(1):91–99.
- Robinson, D. and Keller, E. (1972). The behavior of eye movement motoneurons in the alert monkey. *Bibliotheca ophthalmologica: supplementa ad ophthalmologica*, 82:7–16.
- Roldan, M. and Reinoso-Suarez, F. (1981). Cerebellar projections to the superior colliculus in the cat. *Journal of Neuroscience*, 1(8):827–834.
- Sadnicka, A., Hoffland, B., Bhatia, K., Van De Warrenburg, B., and Edwards, M. (2012). The cerebellum

- in dystonia—help or hindrance? *Clinical Neurophysiology*, 123(1):65–70.
- Sako, W., Fujita, K., Vo, A., Rucker, J. C., Rizzo, J. R., Niethammer, M., Carbon, M., Bressman, S. B., Ulug, A. M., and Eidelberg, D. (2015). The visual perception of natural motion: abnormal task-related neural activity in *dyt1* dystonia. *Brain*, 138(Pt 12):3598–609.
- Sanger, T. D. and Merzenich, M. M. (2000). Computational model of the role of sensory disorganization in focal task-specific dystonia. *Journal of neurophysiology*, 84(5):2458–2464.
- Sano, H., Chiken, S., Hikida, T., Kobayashi, K., and Nambu, A. (2013). Signals through the striatopallidal indirect pathway stop movements by phasic excitation in the substantia nigra. *Journal of Neuroscience*, 33(17):7583–7594.
- Schicatanò, E. J., Basso, M. A., and Evinger, C. (1997). Animal model explains the origins of the cranial dystonia benign essential blepharospasm. *Journal of Neurophysiology*, 77(5):2842–2846.
- Schiller, P. H. and Stryker, M. (1972). Single-unit recording and stimulation in superior colliculus of the alert rhesus monkey. *Journal of neurophysiology*, 35(6):915–924.
- Schiller, P. H. and Tehovnik, E. J. (2005). Neural mechanisms underlying target selection with saccadic eye movements. *Progress in brain research*, 149:157–171.
- Schramm, A., Reiners, K., and Naumann, M. (2004). Complex mechanisms of sensory tricks in cervical dystonia. *Movement disorders: official journal of the Movement Disorder Society*, 19(4):452–458.
- Schuyler, B., Ollinger, J. M., Oakes, T. R., Johnstone, T., and Davidson, R. J. (2010). Dynamic causal modeling applied to fmri data shows high reliability. *Neuroimage*, 49(1):603–611.
- Sedov, A., Popov, V., Shabalov, V., Raeva, S., Jinnah, H., and Shaikh, A. G. (2017). Physiology of midbrain head movement neurons in cervical dystonia. *Movement Disorders*, 32(6):904–912.
- Sereno, M. I., Dale, A., Reppas, J., Kwong, K., Belliveau, J., Brady, T., Rosen, B., and Tootell, R. (1995). Borders of multiple visual areas in humans revealed by functional magnetic resonance imaging. *Science*, 268(5212):889–893.
- Serra, A., Galdi, P., and Tagliaferri, R. (2018). Machine learning for bioinformatics and neuroimaging. *Wiley Interdisciplinary Reviews: Data Mining and Knowledge Discovery*, page e1248.
- Shaikh, A. G., Wong, A. L., Zee, D. S., and Jinnah, H. (2013). Keeping your head on target. *Journal of neuroscience*, 33(27):11281–11295.
- Shaikh, A. G., Zee, D. S., Crawford, J. D., and Jinnah, H. A. (2016). Cervical dystonia: a neural integrator disorder. *Brain*, 139(10):2590–2599.
- Shao, Y., Li, Q.-H., Li, B., Lin, Q., Su, T., Shi, W.-Q., Zhu, P.-W., Yuan, Q., Shu, Y.-Q., He, Y., et al. (2019). Altered brain activity in patients with strabismus and amblyopia detected by analysis of regional homogeneity: A resting-state functional magnetic resonance imaging study. *Molecular Medicine Reports*, 19(6):4832–4840.
- Shires, J., Joshi, S., and Basso, M. A. (2010). Shedding new light on the role of the basal ganglia-superior colliculus pathway in eye movements. *Current Opinion in Neurobiology*, 20(6):717–725.
- Simonyan, K. (2018). Neuroimaging applications in dystonia. *Int. Rev. Neurobiol.*, 143:1–30.
- Simonyan, K. and Ludlow, C. L. (2010). Abnormal activation of the primary somatosensory cortex in spasmodic dysphonia: an fmri study. *Cerebral Cortex*, 20(11):2749–2759.
- Simonyan, R. A. R. and Kristina (2013). Primary dystonia conceptualizing the disorder through a structural brain lens. *Tremor and Other Hyperkinetic Movements*, 3.
- Skogseid, I. (2014). Dystonia—new advances in classification, genetics, pathophysiology and treatment. *Acta Neurologica Scandinavica*, 129:13–19.
- Smith, S. M., Fox, P. T., Miller, K. L., Glahn, D. C., Fox, P. M., Mackay, C. E., Filippini, N., Watkins, K. E., Toro, R., Laird, A. R., et al. (2009). Correspondence of the brain’s functional architecture during activation and rest. *Proceedings of the National Academy of Sciences*, 106(31):13040–13045.
- Smith, S. M. and Nichols, T. E. (2009). Threshold-free cluster enhancement: addressing problems of smoothing, threshold dependence and localisation in cluster inference. *Neuroimage*, 44(1):83–98.
- Smith, Y., Raju, D. V., Pare, J.-F., and Sidibe, M. (2004). The thalamostriatal system: a highly specific network of the basal ganglia circuitry. *Trends in neurosciences*, 27(9):520–527.
- Snoek, L., Miletic, S., and Scholte, H. S. (2019). How to control for confounds in decoding analyses of neuroimaging data. *Neuroimage*, 184:741–760.
- Song, X.-W., Dong, Z.-Y., Long, X.-Y., Li, S.-F., Zuo, X.-N., Zhu, C.-Z., He, Y., Yan, C.-G., and Zang, Y.-F. (2011). Rest: a toolkit for resting-state functional magnetic resonance imaging data processing. *PloS one*, 6(9):e25031.
- Sporns, O. (2018). Graph theory methods: applications in brain networks. *Dialogues in clinical*

- neuroscience*, 20(2):111.
- Sprague, J. M. and Meikle, T. H. (1965). The role of the superior colliculus in visually guided behavior. *Experimental neurology*, 11(1):115–146.
- Standaert, D. G. (2011). Update on the pathology of dystonia. *Neurobiology of disease*, 42(2):148–151.
- Steeves, T. D., Day, L., Dykeman, J., Jette, N., and Pringsheim, T. (2012). The prevalence of primary dystonia: a systematic review and meta-analysis. *Movement Disorders*, 27(14):1789–1796.
- Steigerwald, F. and Volkmann, J. (2012). Deep brain stimulation for movement disorders. *Der Nervenarzt*, 83(8):988–993.
- Stephan, K. E., Kasper, L., Harrison, L. M., Daunizeau, J., den Ouden, H. E., Breakspear, M., and Friston, K. J. (2008). Nonlinear dynamic causal models for fmri. *Neuroimage*, 42(2):649–662.
- Stephan, K. E., Penny, W. D., Daunizeau, J., Moran, R. J., and Friston, K. J. (2009). Bayesian model selection for group studies. *Neuroimage*, 46(4):1004–1017.
- Stephan, K. E., Penny, W. D., Moran, R. J., den Ouden, H. E., Daunizeau, J., and Friston, K. J. (2010). Ten simple rules for dynamic causal modeling. *Neuroimage*, 49(4):3099–3109.
- Stephan, K. E., Schlagenhauf, F., Huys, Q. J., Raman, S., Aponte, E. A., Brodersen, K. H., Rigoux, L., Moran, R. J., Daunizeau, J., Dolan, R. J., et al. (2017). Computational neuroimaging strategies for single patient predictions. *Neuroimage*, 145:180–199.
- Stephan, K. E., Weiskopf, N., Drysdale, P. M., Robinson, P. A., and Friston, K. J. (2007). Comparing hemodynamic models with dcm. *Neuroimage*, 38(3):387–401.
- Stojanovic, M., Cvetkovic, D., and Kostic, V. S. (1995). A genetic study of idiopathic focal dystonias. *Journal of neurology*, 242(8):508–511.
- Takahashi, M., Sugiuchi, Y., and Shinoda, Y. (2013). Convergent synaptic inputs from the caudal fastigial nucleus and the superior colliculus onto pontine and pontomedullary reticulospinal neurons. *Journal of neurophysiology*, 111(4):849–867.
- Takakusaki, K., Saitoh, K., Harada, H., and Kashiwayanagi, M. (2004). Role of basal ganglia–brainstem pathways in the control of motor behaviors. *Neuroscience research*, 50(2):137–151.
- Tanabe, L. M., Kim, C. E., Alagem, N., and Dauer, W. T. (2009). Primary dystonia: molecules and mechanisms. *Nature Reviews Neurology*, 5(11):598.
- Tarsy, D. and Simon, D. K. (2006). Dystonia. *New England Journal of Medicine*, 355(8):818–829.
- Tatu, L. and Jost, W. (2017). Anatomy and cervical dystonia. *Journal of Neural Transmission*, 124(2):237–243.
- Tempel, L. W. and Perlmutter, J. S. (1990). Abnormal vibration-induced cerebral blood flow responses in idiopathic dystonia. *Brain*, 113(3):691–707.
- Tepper, J. M., Tecuapetla, F., Koós, T., and Ibáñez-Sandoval, O. (2010). Heterogeneity and diversity of striatal gabaergic interneurons. *Frontiers in neuroanatomy*, 4:150.
- Termsarasab, P., Ramdhani, R. A., Battistella, G., Rubien-Thomas, E., Choy, M., Farwell, I. M., Velickovic, M., Blitzer, A., Frucht, S. J., Reilly, R. B., et al. (2016). Neural correlates of abnormal sensory discrimination in laryngeal dystonia. *NeuroImage: Clinical*, 10:18–26.
- Terry, H. R., Charlton, S. G., and Perrone, J. A. (2008). The role of looming and attention capture in drivers' braking responses. *Accident Analysis & Prevention*, 40(4):1375–1382.
- Tinazzi, M., Fasano, A., Peretti, A., Bove, F., Conte, A., Dall'occhio, C., Arbasino, C., Defazio, G., Fiorio, M., and Berardelli, A. (2014). Tactile and proprioceptive temporal discrimination are impaired in functional tremor. *PLoS One*, 9(7):e102328.
- Tinazzi, M., Morgante, F., Peretti, A., Mariotti, C., Panzeri, M., Fiorio, M., and Fasano, A. (2013). Impaired temporal processing of tactile and proprioceptive stimuli in cerebellar degeneration. *PLoS One*, 8(11):e78628.
- Tinazzi, M., Priori, A., Bertolasi, L., Frasson, E., Mauguier, F., and Fiaschi, A. (2000). Abnormal central integration of a dual somatosensory input in dystonia: evidence for sensory overflow. *Brain*, 123(1):42–50.
- Tomic, S., Petkovic, I., Pucic, T., Resan, B., Juric, S., and Rotim, T. (2016). Cervical dystonia and quality of life. *Acta Neurologica Belgica*, 116(4):589–592.
- Trost, M., Carbon, M., Edwards, C., Ma, Y., Raymond, D., Mentis, M. J., Moeller, J. R., Bressman, S. B., and Eidelberg, D. (2002). Primary dystonia: is abnormal functional brain architecture linked to genotype? *Annals of Neurology: Official Journal of the American Neurological Association and the Child Neurology Society*, 52(6):853–856.
- Tzourio-Mazoyer, N., Landeau, B., Papathanassiou, D., Crivello, F., Etard, O., Delcroix, N., Mazoyer,

- B., and Joliot, M. (2002). Automated anatomical labeling of activations in spm using a macroscopic anatomical parcellation of the mni mri single-subject brain. *Neuroimage*, 15(1):273–289.
- Uehara, K., Furuya, S., Numazawa, H., Kita, K., Sakamoto, T., and Hanakawa, T. (2019). Distinct roles of brain activity and somatotopic representation in pathophysiology of focal dystonia. *Human brain mapping*, 40(6):1738–1749.
- Ungerleider, S. K. and G, L. (2000). Mechanisms of visual attention in the human cortex. *Annual review of neuroscience*, 23(1):315–341.
- Usmani, N., Bedi, G., Sengun, C., Pandey, A., and Singer, C. (2011). Late onset of cervical dystonia in a 39-year-old patient following cerebellar hemorrhage. *Journal of neurology*, 258(1):149–151.
- Vagnoni, E., Lourenco, S. F., and Longo, M. R. (2015). Threat modulates neural responses to looming visual stimuli. *European Journal of Neuroscience*, 42(5):2190–2202.
- Valls-Sole, J., Tolosa, E., and Ribera, G. (1991). Neurophysiological observations on the effects of botulinum toxin treatment in patients with dystonic blepharospasm. *Journal of Neurology, Neurosurgery and Psychiatry*, 54(4):310–313.
- Van Der Steen, M., van Vugt, F. T., Keller, P. E., and Altenmüller, E. (2014). Basic timing abilities stay intact in patients with musician’s dystonia. *PloS one*, 9(3):e92906.
- Van Horn, J. D. and Toga, A. W. (2009a). Is it time to re-prioritize neuroimaging databases and digital repositories? *Neuroimage*, 47(4):1720–1734.
- Van Horn, J. D. and Toga, A. W. (2009b). Multi-site neuroimaging trials. *Current opinion in neurology*, 22(4):370.
- Van Horn, J. D. and Toga, A. W. (2014). Human neuroimaging as a “big data” science. *Brain imaging and behavior*, 8(2):323–331.
- Verstynen, T. D. and Deshpande, V. (2011). Using pulse oximetry to account for high and low frequency physiological artifacts in the bold signal. *Neuroimage*, 55(4):1633–1644.
- Vitek, J. L. (2002). Pathophysiology of dystonia: a neuronal model. *Movement disorders: official journal of the Movement Disorder Society*, 17(S3):S49–S62.
- Vogt, N. (2018). Machine learning in neuroscience. *Nature Methods*, 15(1):33.
- Volkman, J. (2012). Deep brain stimulation in parkinson’s disease: opening up the race towards better technology. *The Lancet Neurology*, 11(2):121–123.
- Volkman, J., Wolters, A., Kupsch, A., Müller, J., Kühn, A. A., Schneider, G.-H., Poewe, W., Hering, S., Eisner, W., Müller, J.-U., et al. (2012). Pallidal deep brain stimulation in patients with primary generalised or segmental dystonia: 5-year follow-up of a randomised trial. *The Lancet Neurology*, 11(12):1029–1038.
- Von Helmholtz, H. (1867). *Handbuch der physiologischen Optik: mit 213 in den Text eingedruckten Holzschnitten und 11 Tafeln*, volume 9. Voss.
- Vu, M.-A. T., Adali, T., Ba, D., Buzsaki, G., Carlson, D., Heller, K., Liston, C., Rudin, C., Sohal, V. S., Widge, A. S., et al. (2018). A shared vision for machine learning in neuroscience. *Journal of Neuroscience*, 38(7):1601–1607.
- Waddy, H., Fletcher, N., Harding, A., and Marsden, C. (1991). A genetic study of idiopathic focal dystonias. *Annals of Neurology*, 29(3):320–324.
- Wall, M. B., Walker, R., and Smith, A. T. (2009). Functional imaging of the human superior colliculus: an optimised approach. *Neuroimage*, 47(4):1620–1627.
- Walsh, R., O’Dwyer, J. P., Sheikh, I. H., O’Riordan, S., Lynch, T., and Hutchinson, M. (2007). Sporadic adult onset dystonia: sensory abnormalities as an endophenotype in unaffected relatives. *Journal of Neurology, Neurosurgery & Psychiatry*, 78(9):980–983.
- Walsh, R. A., Whelan, R., O’Dwyer, J., O’Riordan, S., Hutchinson, S., O’Laoide, R., Malone, K., Reilly, R., and Hutchinson, M. (2009). Striatal morphology correlates with sensory abnormalities in unaffected relatives of cervical dystonia patients. *Journal of neurology*, 256(8):1307–1313.
- Wang, B., Niu, Y., Miao, L., Cao, R., Yan, P., Guo, H., Li, D., Guo, Y., Yan, T., Wu, J., et al. (2017). Decreased complexity in alzheimer’s disease: resting-state fmri evidence of brain entropy mapping. *Frontiers in aging neuroscience*, 9:378.
- Wang, J., Zuo, X., and He, Y. (2010). Graph-based network analysis of resting-state functional mri. *Frontiers in systems neuroscience*, 4:16.
- Wang, L., Shen, H., Tang, F., Zang, Y., and Hu, D. (2012). Combined structural and resting-state functional mri analysis of sexual dimorphism in the young adult human brain: an mvpa approach. *Neuroimage*, 61(4):931–940.

- Wang, L., Yang, L., Meng, Q., and Ma, Y. (2018). Superior colliculus-pulvinar-amygdala subcortical visual pathway and its biological significance. *Sheng li xue bao:[Acta physiologica Sinica]*, 70(1):79–84.
- Wasserman, L. (2000). Bayesian model selection and model averaging. *Journal of mathematical psychology*, 44(1):92–107.
- Waugh, J. L., Kuster, J. K., Levenstein, J. M., Makris, N., Multhaupt-Buell, T. J., Sudarsky, L. R., Breiter, H. C., Sharma, N., and Blood, A. J. (2016). Thalamic volume is reduced in cervical and laryngeal dystonias. *PLoS One*, 11(5):e0155302.
- Whitfield-Gabrieli, S., Ghosh, S. S., Nieto-Castanon, A., Saygin, Z., Doehrmann, O., Chai, X. J., Reynolds, G. O., Hofmann, S. G., Pollack, M. H., and Gabrieli, J. D. (2016). Brain connectomics predict response to treatment in social anxiety disorder. *Mol Psychiatry*, 21(5):680–5.
- Williams, L., McGovern, E., Kimmich, O., Molloy, A., Beiser, I., Butler, J., Molloy, F., Logan, P., Healy, D., Lynch, T., et al. (2017). Epidemiological, clinical and genetic aspects of adult onset isolated focal dystonia in ireland. *European journal of neurology*, 24(1):73–81.
- Wilson, B. K. and Hess, E. J. (2013). Animal models for dystonia. *Movement Disorders*, 28(7):982–989.
- Wu, L.-Q., Niu, Y.-Q., Yang, J., and Wang, S.-R. (2005). Tectal neurons signal impending collision of looming objects in the pigeon. *European Journal of Neuroscience*, 22(9):2325–2331.
- Wurtz, R. H. and Albano, J. E. (1980). Visual-motor function of the primate superior colliculus. *Annual review of neuroscience*, 3(1):189–226.
- Yan, C.-G. (2010). Dparsi: a matlab toolbox for “pipeline” data analysis of resting-state fmri. *Frontiers in systems neuroscience*, 4.
- Yang, H., Liu, J., Sui, J., Pearlson, G., and Calhoun, V. D. (2010). A hybrid machine learning method for fusing fmri and genetic data: Combining both improves classification of schizophrenia. *Front Hum Neurosci*, 4:192.
- Yang, J., Luo, C., Song, W., Chen, Q., Chen, K., Chen, X., Huang, X., Gong, Q., and Shang, H. (2013). Altered regional spontaneous neuronal activity in blepharospasm: a resting state fmri study. *Journal of neurology*, 260(11):2754–2760.
- Yerys, B. E. and Herrington, J. D. (2014). Multimodal imaging in autism: an early review of comprehensive neural circuit characterization. *Current psychiatry reports*, 16(11):496.
- Yilmaz, M. and Meister, M. (2013). Rapid innate defensive responses of mice to looming visual stimuli. *Current Biology*, 23(20):2011–2015.
- Ylipaavalniemi, J. and Vigario, R. (2008). Analyzing consistency of independent components: An fmri illustration. *NeuroImage*, 39(1):169–180.
- Yoneda, Y., Rome, S., Sagar, H., and Grünewald, R. (2000). Abnormal perception of the tonic vibration reflex in idiopathic focal dystonia. *European journal of neurology*, 7(5):529–533.
- Yoon, J. H., Tamir, D., Minzenberg, M. J., Ragland, J. D., Ursu, S., and Carter, C. S. (2008). Multivariate pattern analysis of functional magnetic resonance imaging data reveals deficits in distributed representations in schizophrenia. *Biol Psychiatry*, 64(12):1035–41.
- Yu-Feng, Z., Yong, H., Chao-Zhe, Z., Qing-Jiu, C., Man-Qiu, S., Meng, L., Li-Xia, T., Tian-Zi, J., and Yu-Feng, W. (2007). Altered baseline brain activity in children with adhd revealed by resting-state functional mri. *Brain and Development*, 29(2):83–91.
- Zang, Y., Jiang, T., Lu, Y., He, Y., and Tian, L. (2004). Regional homogeneity approach to fmri data analysis. *Neuroimage*, 22(1):394–400.
- Zeidman, P., Jafarian, A., Corbin, N., Seghier, M. L., Razi, A., Price, C. J., and Friston, K. J. (2019a). A tutorial on group effective connectivity analysis, part 1: first level analysis with dcm for fmri. *arXiv preprint arXiv:1902.10597*.
- Zeidman, P., Jafarian, A., Seghier, M. L., Litvak, V., Cagnan, H., Price, C. J., and Friston, K. J. (2019b). A tutorial on group effective connectivity analysis, part 2: second level analysis with pbs. *arXiv preprint arXiv:1902.10604*.
- Zeman, W. and Dyken, P. (1967). Dystonia musculorum deformans: clinical, genetic and pathoanatomical studies. *Psychiatra, neurologia, neurochirurgia*.
- Zhang, D., Wang, Y., Zhou, L., Yuan, H., Shen, D., Initiative, A. D. N., et al. (2011). Multimodal classification of alzheimer’s disease and mild cognitive impairment. *Neuroimage*, 55(3):856–867.
- Zhang, X.-Y., Wang, J.-J., and Zhu, J.-N. (2016). Cerebellar fastigial nucleus: from anatomic construction to physiological functions. *Cerebellum and ataxias*, 3(1):9.
- Zhanga, C., Adeli, E., Zhou, T., Chen, X., and Shen, D. (2018). Multi-layer multi-view classification for

- alzheimer's disease diagnosis. *Association for the Advancement of Artificial Intelligence*.
- Zhao, N., Yuan, L.-X., Jia, X.-Z., Zhou, X.-F., Deng, X.-P., He, H.-J., Zhong, J., Wang, J., and Zang, Y.-F. (2018). Intra-and inter-scanner reliability of voxel-wise whole-brain analytic metrics for resting state fmri. *Frontiers in neuroinformatics*, 12:54.
- Zhou, B., Wang, J., Huang, Y., Yang, Y., Gong, Q., and Zhou, D. (2013). A resting state functional magnetic resonance imaging study of patients with benign essential blepharospasm. *Journal of Neuro-Ophthalmology*, 33(3):235–240.
- Zhou, T., Thung, K.-H., Zhu, X., and Shen, D. (2017). Feature learning and fusion of multimodality neuroimaging and genetic data for multi-status dementia diagnosis. In *International Workshop on Machine Learning in Medical Imaging*, pages 132–140. Springer.
- Zhuo, Y., Ni, D., Chen, S., Lei, B., and Wang, T. (2016). Adaptive ensemble manifold learning for neuroimaging retrieval. *IEEE Xplore*, (IEEE 13th International Symposium on Biomedical Imaging (ISBI)):4.
- Zoons, E., Booij, J., Nederveen, A. J., Dijk, J., and Tijssen, M. (2011). Structural, functional and molecular imaging of the brain in primary focal dystonia—a review. *Neuroimage*, 56(3):1011–1020.
- Zuo, X.-N., Xu, T., Jiang, L., Yang, Z., Cao, X.-Y., He, Y., Zang, Y.-F., Castellanos, F. X., and Milham, M. P. (2013). Toward reliable characterization of functional homogeneity in the human brain: preprocessing, scan duration, imaging resolution and computational space. *Neuroimage*, 65:374–386.
- Zweig, R., Hedreen, J., Jankel, W., Casanova, M., Whitehouse, P., and Price, D. (1988). Pathology in brainstem regions of individuals with primary dystonia. *Neurology*, 38(5):702–702.

A Appendix - Ethics

Elm Park
Dublin 4
Tel: +353 1 221 4000
Web: www.stvincents.ie

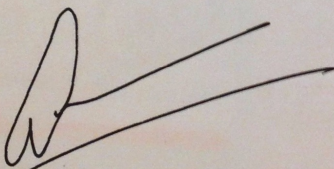
St. Vincent's University Hospital

12/01/2015



To whom it may concern,

This is a letter to confirm that Shruti Narasimham is a full-time PhD Student with the Dystonia Research Group, Department of Neurology, St Vincent's University Hospital and Department of Bioengineering, Trinity College Dublin. Her research project entitled, "A Functional Magnetic Resonance Imaging Study of the Response in the Superior Colliculi to Looming Stimuli", received full ethical approval. Please find attached the supporting documentation.

Yours sincerely,



Professor Michael Hutchinson
Consultant Neurologist
St Vincent's University Hospital
Elm Park, Dublin 4, Ireland
Newman Clinical Research Professor
University College Dublin

  **St. Vincent's Healthcare**
GROUP LIMITED

BOARD OF DIRECTORS: Chairman: Mr. James Menton, Sr. Mary Benton, Dr. David Brophy, Mr. John Compton, Ms. Louise English, Prof. Des Fitzgerald, Mr. Gerard Flood, Ms. Naomi Holland, Prof. Michael Keane, Mr. Myles Lee, Ms. Sharen McCabe, Mr. Michael Meagher, Mr. Frank O'Riordan, Sr. Agnes Reynolds

Elm Park
Dublin 4
Tel: +353 1 221 4000
Web: www.stvincents.ie

St. Vincent's University Hospital

Ethics and Medical Research Committee

ELM PARK, DUBLIN 4
Tel. (01) 2214117 Fax (01) 2214428

email: joan.mcdonnell@ucd.ie or jacinta.mcmanus@ucd.ie

29th October, 2014.

Professor M. Hutchinson,
Consultant Neurologist,
St. Vincent's University Hospital,
Elm Park,
D. 4.

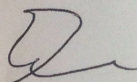
Re: - A functional Magnetic Resonance Imaging Study of the Response in the Superior Colliculi to Looming Stimuli.
Applicant checklist. Application Form revised. Response letter. TCD level of Insurance. Patient Letter vs 1. Detailed Protocol vs 1.1 5/8/14. PIL/Consent: Healthy Controls, Patients, Unaffected relatives vs 1.1 16/10/14

Dear Professor Hutchinson,

We have received the revised documents and clarifications that were requested at the Ethics and Medical Research Committee meeting held on Wednesday 3rd September, 2014 at which the above study was reviewed.

Following review of the revised documents and clarifications, this study is now approved.

Yours sincerely,



Dr. E. McKone,
Chairman,
Ethics & Medical Research Committee

cc Dr. E. McGovern, Dystonia Research Fellow, Dept of Neurology.



St. Vincent's University Hospital
is JCI Accredited 2013 - 2016

St. Vincent's Healthcare
GROUP LIMITED

BOARD OF DIRECTORS: Chairman: Mr. James Menton, Sr. Mary Benton, Dr. David Brophy, Mr. John Compton, Ms. Louise English, Prof. Des Fitzgerald, Mr. Gerard Flood, Ms. Naomi Holland, Prof. Michael Keane, Mr. Myles Lee, Ms. Sharen McCabe, Mr. Michael Meagher, Mr. Frank O'Riordan, Sr. Agnes Reynolds.

Registered in Dublin, Ireland. Company Registration No: 338585 Registered Office: Elm Park, Dublin 4.

B Appendix - Graph Theory Metrics

Table adapted from Rubinov M, Sporns O (2010) *NeuroImage* 52:1059-69.

Measure	Binary and undirected definitions	Weighted and directed definitions
Basic concepts and measures		
Basic concepts and notation	<p>N is the set of all nodes in the network, and n is the number of nodes. L is the set of all links in the network, and l is number of links. (i, j) is a link between nodes i and j ($i, j \in N$). a_{ij} is the connection status between i and j: $a_{ij} = 1$ when link (i, j) exists (when i and j are neighbors); $a_{ij} = 0$ otherwise ($a_{ii} = 0$ for all i). We compute the number of links as $l = \sum_{i,j \in N} a_{ij}$ (to avoid ambiguity with directed links we count each undirected link twice, as a_{ij} and as a_{ji}).</p>	<p>Links (i, j) are associated with connection weights w_{ij}. Henceforth we assume that weights are normalized, such that $0 \leq w_{ij} \leq 1$ for all i and j. l^w is the sum of all weights in the network, computed as $l^w = \sum_{i,j \in N} w_{ij}$.</p> <p>Directed links (i, j) are ordered from i to j. Consequently, in directed networks a_{ij} does not necessarily equal a_{ji}.</p>
Degree: number of links connected to a node	<p>Degree of a node i,</p> $k_i = \sum_{j \in N} a_{ij}.$	<p>Weighted degree of i, $k_i^w = \sum_{j \in N} w_{ij}$.</p> <p>(Directed) out-degree of i, $k_i^{\text{out}} = \sum_{j \in N} a_{ij}$.</p> <p>(Directed) in-degree of i, $k_i^{\text{in}} = \sum_{j \in N} a_{ji}$.</p>
Shortest path length: a basis for measuring integration	<p>Shortest path length (distance), between nodes i and j,</p> $d_{ij} = \sum_{a_{uv} \in g_{i \leftrightarrow j}} a_{uv},$ <p>where $g_{i \leftrightarrow j}$ is the shortest path (geodesic) between i and j. Note that $d_{ij} = \infty$ for all disconnected pairs i, j.</p>	<p>Shortest weighted path length between i and j, $d_{ij}^w = \sum_{a_{uv} \in g_{i \leftrightarrow j}^w} f(w_{uv})$, where f is a map (e.g. an inverse) from weight to length and $g_{i \leftrightarrow j}^w$ is the shortest weighted path between i and j.</p> <p>Shortest directed path length from i to j, $d_{ij}^{\rightarrow} = \sum_{a_{ij} \in g_{i \rightarrow j}} a_{ij}$, where $g_{i \rightarrow j}$ is the directed shortest path from i to j.</p>
Number of triangles: a basis for measuring segregation	<p>Number of triangles around a node i,</p> $t_i = \frac{1}{2} \sum_{j,h \in N} a_{ij} a_{ih} a_{jh}.$	<p>(Weighted) geometric mean of triangles around i,</p> $t_i^w = \frac{1}{2} \sum_{j,h \in N} (w_{ij} w_{ih} w_{jh})^{1/3}.$ <p>Number of directed triangles around i,</p> $t_i^{\rightarrow} = \frac{1}{2} \sum_{j,h \in N} (a_{ij} + a_{ji})(a_{ih} + a_{hi})(a_{jh} + a_{hj}).$
Measures of integration		
Characteristic path length	<p>Characteristic path length of the network (e.g. Watts and Strogatz, 1998),</p> $L = \frac{1}{n} \sum_{i \in N} L_i = \frac{1}{n} \sum_{i \in N} \frac{\sum_{j \in N, j \neq i} d_{ij}}{n-1},$ <p>where L_i is the average distance between node i and all other nodes.</p>	<p>Weighted characteristic path length, $L^w = \frac{1}{n} \sum_{i \in N} \frac{\sum_{j \in N, j \neq i} a_{ij}^w}{n-1}$.</p> <p>Directed characteristic path length, $L^{\rightarrow} = \frac{1}{n} \sum_{i \in N} \frac{\sum_{j \in N, j \neq i} d_{ij}^{\rightarrow}}{n-1}$.</p>

Global efficiency	<p>Global efficiency of the network (Latora and Marchiori, 2001),</p> $E = \frac{1}{n} \sum_{i \in N} E_i = \frac{1}{n} \sum_{i \in N} \frac{\sum_{j \in N, j \neq i} d_{ij}^{-1}}{n-1},$ <p>where E_i is the efficiency of node i.</p>	<p>Weighted global efficiency, $E^w = \frac{1}{n} \sum_{i \in N} \frac{\sum_{j \in N, j \neq i} (d_{ij}^w)^{-1}}{n-1}$.</p> <p>Directed global efficiency, $E^{\rightarrow} = \frac{1}{n} \sum_{i \in N} \frac{\sum_{j \in N, j \neq i} (d_{ij}^{\rightarrow})^{-1}}{n-1}$.</p>
Measures of segregation		
Clustering coefficient	<p>Clustering coefficient of the network (Watts and Strogatz, 1998),</p> $C = \frac{1}{n} \sum_{i \in N} C_i = \frac{1}{n} \sum_{i \in N} \frac{2t_i}{k_i(k_i-1)},$ <p>where C_i is the clustering coefficient of node i ($C_i = 0$ for $k_i < 2$).</p>	<p>Weighted clustering coefficient (Onnela et al., 2005),</p> $C^w = \frac{1}{n} \sum_{i \in N} \frac{2t_i^w}{k_i(k_i-1)}$. See Saramaki et al. (2007) for other variants. <p>Directed clustering coefficient (Fagiolo, 2007),</p> $C^{\rightarrow} = \frac{1}{n} \sum_{i \in N} \frac{t_i^{\rightarrow}}{(k_i^{\text{out}} + k_i^{\text{in}})(k_i^{\text{out}} + k_i^{\text{in}} - 1) - 2 \sum_{j \in N} a_{ij} a_{ji}}$.
Transitivity	<p>Transitivity of the network (e.g. Newman, 2003),</p> $T = \frac{\sum_{i \in N} 2t_i}{\sum_{i \in N} k_i(k_i-1)}$ <p>Note that transitivity is not defined for individual nodes.</p>	<p>Weighted transitivity*, $T^w = \frac{\sum_{i \in N} 2t_i^w}{\sum_{i \in N} k_i(k_i-1)}$.</p> <p>Directed transitivity*, $T^{\rightarrow} = \frac{\sum_{i \in N} t_i^{\rightarrow}}{\sum_{i \in N} [(k_i^{\text{out}} + k_i^{\text{in}})(k_i^{\text{out}} + k_i^{\text{in}} - 1) - 2 \sum_{j \in N} a_{ij} a_{ji}]}$.</p>
Local efficiency	<p>Local efficiency of the network (Latora and Marchiori, 2001),</p> $E_{\text{loc}} = \frac{1}{n} \sum_{i \in N} E_{\text{loc},i} = \frac{1}{n} \sum_{i \in N} \frac{\sum_{j,h \in N, j \neq i} a_{ij} a_{ih} [d_{jh}(N_i)]^{-1}}{k_i(k_i-1)},$ <p>where $E_{\text{loc},i}$ is the local efficiency of node i, and $d_{jh}(N_i)$ is the length of the shortest path between j and h, that contains only neighbors of i.</p>	<p>Weighted local efficiency*, $E_{\text{loc}}^w = \frac{1}{n} \sum_{i \in N} \frac{\sum_{j,h \in N, j \neq i} (w_{ij} w_{ih} [d_{jh}^w(N_i)]^{-1})^{1/3}}{k_i(k_i-1)}$.</p> <p>Directed local efficiency*,</p> $E_{\text{loc}}^{\rightarrow} = \frac{1}{2n} \sum_{i \in N} \frac{\sum_{j,h \in N, j \neq i} (a_{ij} + a_{ji})(a_{ih} + a_{hi}) ([d_{jh}^{\rightarrow}(N_i)]^{-1} + [d_{hj}^{\rightarrow}(N_i)]^{-1})}{(k_i^{\text{out}} + k_i^{\text{in}})(k_i^{\text{out}} + k_i^{\text{in}} - 1) - 2 \sum_{j \in N} a_{ij} a_{ji}}$.
Modularity	<p>Modularity of the network (Newman, 2004b),</p> $Q = \sum_{u \in M} \left[e_{uu} - \left(\sum_{v \in M} e_{uv} \right)^2 \right],$ <p>where the network is fully subdivided into a set of nonoverlapping modules M, and e_{uv} is the proportion of all links that connect nodes in module u with nodes in module v.</p> <p>An equivalent alternative formulation of the modularity (Newman, 2006) is given by $Q = \frac{1}{l} \sum_{i,j \in N} \left(a_{ij} - \frac{k_i k_j}{l} \right) \delta_{m_i, m_j}$, where m_i is the module containing node i, and $\delta_{m_i, m_j} = 1$ if $m_i = m_j$, and 0 otherwise.</p>	<p>Weighted modularity (Newman, 2004),</p> $Q^w = \frac{1}{l^w} \sum_{i,j \in N} \left[w_{ij} - \frac{k_i^w k_j^w}{l^w} \right] \delta_{m_i, m_j}$. <p>Directed modularity (Leicht and Newman, 2008),</p> $Q^{\rightarrow} = \frac{1}{l} \sum_{i,j \in N} \left[a_{ij} - \frac{k_i^{\text{out}} k_j^{\text{in}}}{l} \right] \delta_{m_i, m_j}$.